DIRECT RELIABILITY BASED DESIGN (d-RBD) OF SHALLOW WIND TURBINE FOUNDATIONS

By

Jomâa Ben Hassine

A dissertation submitted to the Faculty and the Board of Trustees of the Colorado School of Mines in partial fulfillment of the requirements for the degree of Doctor of Philosophy (Engineering - Civil).

Golden, Colorado

Date _____

Signed: _____
Jomâa Ben Hassine

Signed: _____
Dr. D.V. Griffiths
Dissertation Advisor

Golden, Colorado

Date_____

Signed: _____
Dr. Terri S. Hogue
Professor and Head
Department of Civil and
Environmental Engineering

ABSTRACT

Wind turbine foundations transfer dynamic and highly eccentric loads to variable soils. The design of such foundations involves the verification of multiple limit states to ensure proper operation of the turbine and avoid catastrophic failures. An optimal foundation design minimizes cost while meeting all relevant limit states at quantifiable and acceptable risks. This dissertation explores three common limit states that are relevant to the design of shallow, gravity based, wind turbine foundations using a fully-probabilistic Monte Carlo Simulation (MCS) method, termed in this work as the direct Reliability Based Design (d-RBD) method. The three limit states are foundation tilt, rotational stiffness and bearing capacity. For each of these limit states, design variables are randomized using predefined probability density functions. The d-RBD method involves running Monte Carlo Simulations to produce realizations covering potential combinations of design decision variables such as foundation dimensions (e.g. width and/or depth). The d-RBD method uses Bayesian conditional probability theory to select the geometry combinations that meet the predefined target probability of failure. With this approach, a single MCS run is needed to identify pools of acceptable designs for each limit state from which an optimal design meeting all limit states can be selected.

This dissertation introduces d-RBD as a direct, fully probabilistic design procedure that offers important advantages over global factor (ASD/WSD) or partial factor (LSD/LRFD) design methods. For each of the limit states under consideration, d-RBD is used to highlight the cost of uncertainty, rank the design variables by their importance and assess the effects of pertinent variability assumptions. The findings from this work are relevant to ongoing efforts to develop international and U.S. standards for the design of wind turbine support structures and their foundations.

TABLE OF CONTENTS

ABSTRACT iii

LIST OF FIGURES ix

LIST OF TABLES xii

LIST OF SYMBOLS xiv

ABBREVIATIONS AND ACRONYMS xvii

ACKNOWLEDGEMENTS xx

CHAPTER 1 INTRODUCTION 1

1.1 Evolution of the Wind Energy Industry 1

1.2 Evolution of Wind Turbine Technology 4

1.3 Evolution of Wind Turbine Foundations 7

1.4 Design Practices within the Wind Energy Industry 9

1.5 Problem Statement and Dissertation Objectives 12

1.6 Dissertation Outline 14

CHAPTER 2 DETERMINISTIC ANALYSIS OF WIND TURBINE FOUNDATIONS 17

2.1 Loading Nature and Levels 17

2.2 Accepted Zero-pressure Allowances 20

2.3 Strain Level Dependence of Elastic Moduli 21

2.3.1 Formulations Based on Shear Strain 22

2.3.2 Formulations Based on Shear Stress 28

2.4 Soil Strain Level Appropriate for Onshore Wind Turbine Foundations 29

2.5 Foundation Tilt 31

2.5.1 Common Tilt Limits 31

2.5.2 Estimating Foundation Tilt 32
2.6 Foundation Stiffness 35
2.6.1 Analysis of Foundation Vibrations 36
2.6.2 Dynamics of Shallow Wind Turbine Foundations 39
2.6.3 Verification of Foundation Stiffness Requirements 40
2.7 Bearing Capacity 42
2.7.1 Basic Bearing Capacity and its Extensions 43
2.7.2 Generalized Bearing Capacity Equations 46
2.7.3 Effective Area Approach 49
2.8 Interaction Curve Approach 51
2.8.1 General VM Interaction Curve Comments 54
2.8.2 VM Curve Comments Relative to Wind Turbine Foundations 55
2.9 Deterministic Finite Element Analysis 57
2.9.1 Contact Pressure Changes under Increasing Load 59
2.9.2 Contact Pressure under Varying Subgrade Stiffness 60
CHAPTER 3 CHARACTERIZATION OF GEOTECHNICAL UNCERTAINTY 65
3.1 Geotechnical Uncertainty 65
3.1.1 Aleatory Uncertainty 66
3.1.2 Epistemic Uncertainty 69
3.2 Geotechnical Uncertainly and Wind Energy Projects 71
3.3 Probabilistic Approaches to Uncertainty 71
3.4 Modeling the Distribution of Random Variables 74
3.4.1 Normal Distribution 75

3.4.2 Lognormal Distribution 78
3.4.3 Bounded tanh Distribution 80
3.4.4 Uniform Distribution 83
3.4.5 Measures of Central Tendency and Variability 84
3.4.6 Selection of Material Property PDF's 84
3.4.7 PDF's for Loads 87
3.5 Cross-correlations of Random Variables 87
3.5.1 Covariance and Correlation Matrices 88
3.5.2 Typical Correlations of Geotechnical Properties 89
3.6 Design Parameters Based on Limited Information 90
3.6.1 Geophysical Methods 91
3.6.2 N-Sigma Procedure 93
3.6.3 Multivariate Correlations and Bayesian Updating 95
3.7 Typical Soil and Rock Property Variability 97
CHAPTER 4 DESIGN METHODS AND RELIABILITY QUANTIFICATION 104
4.1 Characteristic Values and Bias 105
4.2 Global Factor Design 106
4.3 Partial Factor Design 108
4.3.1 Limit States Design 111
4.3.2 Probability of Failure (and Success) 112
4.3.3 Reliability Index 113
4.3.4 Risk and Tolerable Risk Concepts 118
4.3.5 System and Component Reliability 121

4.3.6 Target Reliability Specification 122
4.3.7 Reliability Implied in Various Design Standards 125
4.3.8 Limit States Design of Wind Turbine Foundations 132
CHAPTER 5 RELIABILITY-BASED DESIGN 135
5.1 Reliability Analysis Methods 139
5.2 Direct Reliability Based Design Method (d-RBD) 144
5.2.1 Method Details 145
5.2.2 Hypothesis Testing for Parameter Ranking 151
5.2.3 Method Accuracy 152
5.2.4 d-RBD Advantages 153
5.2.5 d-RBD Limitations 156
5.2.6 Implementation Tools 157
CHAPTER 6 FOUNDATION TILT AND ROTATIONAL STIFFNESS 159
6.1 Foundation Tilt 159
6.1.1 Reliability of Foundation – Tilt Limit State 162
6.1.2 Parameter Ranking – Tilt Limit State 164
6.2 Rotational Stiffness 165
6.2.1 Dynamic Stiffness Verification 166
6.2.2 Static Stiffness Verification 172
CHAPTER 7 BEARING CAPACITY UNDER COMBINED LOADING 179
7.1 Drained Bearing Capacity 179
7.2 Undrained Bearing Capacity 183

CHAPTER 8 CONCLUSIONS AND FUTURE WORK 187
8.1 Conclusions 187
8.1.1 Tilt Limit State 192
8.1.2 Rocking Stiffness Limit State 192
8.1.3 Bearing Capacity Limit State 193
8.1.4 Applications of the d-RBD Method 193
8.2 Future Work 194
8.2.1 Incorporating Spatial Variability 194
8.2.2 Computational Load Reduction 195
8.2.3 Incorporating Design Robustness 196
8.2.4 Considering Other Applications 196
REFERENCES 198
APPENDIX A MathCAD – DETERMINISTIC CALCULATIONS 218
APPENDIX B MATLAB SOURCE CODE AND OUTPUT 225
APPENDIX C SUPPLEMENTAL ELECTRONIC FILES 265

LIST OF FIGURES

Figure 1.1 Cumulative capacity growth (AWEA, 2017; GWEC, 2017) 2

Figure 1.2 Annual added capacity in the U.S. (AWEA, 2017)..... 3

Figure 1.3 Actual and projected U.S. wind penetration..... 5

Figure 1.4 Size of the "average" tubular steel tower 6

Figure 1.5 Gravity based foundation geometries and associated concrete volumes..... 8

Figure 2.1 Combined loading equivalency 18

Figure 2.2 Conventions for loads and displacements 19

Figure 2.3 Sample MKZ curve showing effect of α parameter for $\tau_{\max} = 100kPa$ 24

Figure 2.4 Sample MKZ curve showing effect of β parameter for $\tau_{\max} = 100kPa$ 25

Figure 2.5 Sample shear modulus degradation curves – strain level formulations 28

Figure 2.6 Stress level formulation of shear modulus degradation with m = 1 29

Figure 2.7 Shape influence factor for rectangular footings 35

Figure 2.8 Cross-section of footing and Prandtl's wedge 44

Figure 2.9 Terzaghi's general bearing failure surfaces 45

Figure 2.10 Footing and loading arrangements affecting bearing capacity..... 46

Figure 2.11 Two bearing capacity rupture modes (DNV-GL, 2016b) 47

Figure 2.12 Uniform pressure area centered on load center 50

Figure 2.13 Effective foundation dimensions. Courtesy (DNV-GL, 2016b) 52

Figure 2.14 Normalized VM interaction curves by several researchers..... 55

Figure 2.15 Approximate critical tilt angle (Kourkoulis *et al.*, 2012) 57

Figure 2.16 Finite element models of octagonal and circular WTG foundations..... 58

Figure 2.17 Contact pressure under circular foundation..... 62

Figure 2.18 Contact pressure under octagonal foundation 63

Figure 2.19 Contact pressure for different subgrade stiffness at $DL+1.35LL$ 64

Figure 3.1 Uncertainty in soil property estimates (Kulhawy, 1996)..... 67

Figure 3.2 Sources of geotechnical design uncertainty 67

Figure 3.3 Normally distributed variable $X \sim N(5,4)$ PDF and CDF..... 77

Figure 3.4 Standard normal $Z \sim N(0,1)$ PDF and CDF 77

Figure 3.5 Scaling and shifting of normal PDF's 79

Figure 3.6 Lognormal PDF and CDF 80

Figure 3.7 Bounded tanh PDF and CDF..... 82

Figure 3.8 Location parameter of bounded tanh distributions..... 83

Figure 3.9 Lognormal PDF's for various COV's..... 85

Figure 3.10 N_σ as a function of number of data samples, n (Tippett, 1925) 95

Figure 3.11 Uncertainty reduction using Bayesian approach (Zhang et al., 2004) 97

Figure 4.1 Progression of design philosophies 105

Figure 4.2 PDF of normally distributed resistance, load effects and FS 114

Figure 4.3 Illustration of probability of failure, reliability index and factor of safety 115

Figure 4.4 Probability of failure vs reliability index for normal variables 117

Figure 4.5 Curve fitting of probability of failure vs reliability index relationship 119

Figure 4.6 Customary design acceptance for different reliability levels 123

Figure 4.7 Selection of least cost design meeting multiple limit states..... 134

Figure 5.1 Risk: from concepts to evaluation 139

Figure 5.2 Essential steps in the d-RBD procedure 146

Figure 5.3 d-RBD flowchart 147

Figure 6.1 Tilt failure probability – $B = 17\text{m}$, medium parameter variability 163

Figure 6.2 Tilt failure probability – $B = 17\text{m}$, high parameter variability 163

Figure 6.3 Tilt limit state parameter ranking, $B = 17\text{m}$ 165

Figure 6.4 Dynamic stiffness probability of failure – deep bedrock 169

Figure 6.5 Dynamic stiffness parameter ranking - deep bedrock 169

Figure 6.6 Dynamic stiffness failure probability – bedrock within influence depth 171

Figure 6.7 Dynamic stiffness parameter ranking – bedrock within influence depth 172

Figure 6.8 Static rocking stiffness failure probability - deep bedrock case 175

Figure 6.9 Parameter importance ranking for static rocking stiffness – deep bedrock 176

Figure 6.10 Static stiffness failure probability - bedrock within influence depth 176

Figure 6.11 Parameter importance ranking for static rocking stiffness 177

Figure 7.1 Drained bearing capacity probability of failure 181

Figure 7.2 Importance ranking for drained bearing capacity 182

Figure 7.3 Undrained bearing capacity failure probability 185

Figure 7.4 Parameter importance ranking for undrained bearing capacity 186

Figure 8.1 Main simulation parameters of the d-RBD run 190

Figure 8.2 Foundation geometries generated in the d-RBD program execution 190

LIST OF TABLES

Table 2.1 Shape, depth and load inclination correction factors (DNV-GL, 2016b) 48

Table 2.2 VM interaction curve fitting parameters and maximum moment capacity 54

Table 2.3 Parameters used in the finite element analyses 59

Table 2.4 Load steps considered in the finite element analyses 60

Table 3.1 Example geotechnical properties with known physical bounds 82

Table 3.2 A few parameter distributions recommended in literature 86

Table 3.3 Published correlations between effective friction and effective cohesion 90

Table 3.4 Key geophysical formulas for isotropic materials 93

Table 3.5 Typical COV's of common engineering materials (Ellingwood, 1980) 98

Table 3.6 Typical reported variability of select geotechnical properties 99

Table 3.7 Sample tiered scheme based on site variability (Phoon & Kulhawy, 2008) 102

Table 3.8 Proposed three-tiered COV (%) ranges of select geotechnical properties 103

Table 4.1 Typical global safety factors 108

Table 4.2 Reliability index for normally distributed loads and resistance 116

Table 4.3 Suggested probability of failure vs reliability index relationships 118

Table 4.4 Notional minimum reliability levels in EN 1990 (CEN, 2005) 126

Table 4.5 EN 1990 notional ULS reliability considering costs of safety measures 126

Table 4.6 fib Model Code 2010 reliability indices for ULS/FLS (CEB-FIP, 2013) 127

Table 4.7 fib Model Code 2010 target reliability indices for SLS (CEB-FIP, 2013) 127

Table 4.8 ISO-2394 ULS reliability for 1-year reference period (ISO, 2015) 129

Table 4.9 Target irreversible SLS reliability, 1-year reference period (JCSS, 2001a) 129

Table 4.10 Implied North American annual target reliability indices 129

Table 4.11 Target reliability for onshore WTG foundations adopted in this work 131

Table 5.1 Reliability analysis levels 140

Table 5.2 Summary of quantitative reliability analysis methods..... 141

Table 6.1 Random variables for tilt limit state investigations 161

Table 6.2 Random variable ranking for tilt limit state..... 164

Table 6.3 Random variables for dynamic stiffness investigations 168

Table 6.4 Dynamic stiffness parameter importance ranking – deep bedrock..... 168

Table 6.5 Dynamic stiffness reliability comparisons..... 170

Table 6.6 Dynamic stiffness parameter ranking – bedrock within depth of influence 171

Table 6.7 Random variables for static stiffness investigations..... 174

Table 6.8 Parameter importance ranking for static rocking stiffness - deep bedrock..... 175

Table 6.9 Parameter ranking for static rocking stiffness - shallow bedrock..... 177

Table 6.10 Static stiffness reliability comparisons 178

Table 7.1 Drained bearing capacity random variables..... 180

Table 7.2 Random variable ranking - drained bearing capacity 182

Table 7.3 Undrained bearing capacity random variables..... 184

Table 7.4 Random variable ranking - undrained bearing capacity 185

Table 8.1 Summary of reliability assessments of foundation with $B = 17\text{m}$, $D = 2.8\text{m}$ 189

Table 8.2 Reliability indices for medium variability assumptions, $D = 2.8\text{m}$ 191

Table 8.3 Reliability indices for high variability assumptions, $D = 2.8\text{m}$ 192

LIST OF SYMBOLS

Dimensional frequency ..... a_0

Effective foundation area ..... A_{eff}

Half the foundation width ..... b

Foundation width ..... B

Effective foundation width ..... b_{eff}

Soil cohesion, also damping coefficient used in impedance definition c

Soil effective (drained) cohesion ..... c'

Depth factors for bearing capacity equation ..... d_c, d_q, d_γ

Foundation depth ..... D

Eccentricity (of load) ..... e

Eccentricity (of load) in the x direction ..... e_x

Eccentricity (of load) in the y direction ..... e_y

Young's modulus (modulus of elasticity) ..... E

Drained Young's modulus ..... E'

Small-strain Young's modulus ..... E_0

Undrained Young's modulus ..... E_u

Empirical parameters for defining the stress level factor curve ..... f, g

Shear modulus ..... G

Small-strain shear modulus ..... G_0

Horizontal load acting on foundation ..... H

Distance from bottom of foundation to bedrock or firm stratum ..... H_b

Load inclination factors for bearing capacity equation ..... $i_c, i_q, i_\gamma, i_c^0$

Shape influence factor for foundation tilt ..... I_θ

Dynamic stiffness or stiffness coefficient used in impedance definition ..... k

Dynamic stiffness, static stiffness ..... K_d, K_s

Foundation length L

Overturning moment ..... M

Effective foundation length ..... l_{eff}

Shape factors in bearing capacity equation ..... $s_c, s_q, s_\gamma, s_c^0$

Vertical load acting on foundation V

Number of design decision variables ..... n_{dv}

Number of realizations in a Monte Carlo simulation ..... n_r

Number of random variables ..... n_{rv}

Number of design decision combinations ..... n_{ddc}

Bearing capacity coefficients ..... $N_c, N_q, N_\gamma, N_c^0$

Probability of failure ..... p_f

Target probability of failure ..... p_f^T

Foundation radius ..... R

Stress level factor ..... R_f

Shear wave velocity ..... V_s

Excitation frequency ..... w

A set of n random variables $X = [X_1, X_2, ... X_n]$ X

A set of n random variables $Y = [Y_1, Y_2, ... Y_n]$ ..... Y

Importance index (for parameter ranking) ..... Z_H

Curvature parameter of the shear strain degradation function ..... α

Reliability index ..... β

Target reliability index ..... β_T

Shear strain ..... γ

Resistance partial safety factor ..... γ_M

Reference shear strain ..... γ_{ref}

Maximum tilt angle ..... $\theta_{\max}$

Poisson's ratio ..... ν

Drained Poisson's ratio ..... ν'

Undrained Poisson's ratio ..... ν_u

Soil density, effective soil density ..... ρ, ρ'

Ultimate (maximum) shear stress ..... $\tau_{\max}$

Effective friction angle ..... ϕ'

Standard normal PDF ..... $\phi(z)$

Standard normal CDF ..... $\Phi(z)$

ABBREVIATIONS AND ACRONYMS

AASHTO .....American Association of State Highway and Transportation Officials

ACI..... American Concrete Institute

AHJ .....Authority Having Jurisdiction

AFOSM..... Advanced First Order Second Moment (Hasofer-Lind)

AISC .....American Institute of Steel Construction

ANSI ..... American National Standards Institute

ASCE ..... American Society of Civil Engineers

ASD..... Allowable stress design (same as WSD)

AWEA..... American Wind Energy Association

COV ..... Coefficient of Variation

CDF..... Cumulative Distribution Function

d-RBD .....Direct Reliability Based Design

d-RBDO ..... Direct Reliability Based Design Optimization

FEM ..... Finite Element Method

FLS.....Fatigue Limit State

FORM .....First Order Reliability Method

FOSM.....First Order Second Moment method

FS .....Factor of Safety (typically the global factor of safety)

ICC ..... International Code Council, Installed Capital Cost

IEC .....International Electrotechnical Commission

i.i.d. .....Independent and identically distributed

ISO ..... International Standards Organization

LCOE ..... Levelized Cost of Energy

LPM ..... Lumped parameter model

LQI ..... Life Quality Index

LSD ..... Limit State Design

LRFD ..... Load and Resistance Factor Design

MASW ..... Multi-Channel Analysis of Surface Waves

MCMC ..... Markov Chain Monte Carlo

MCS ..... Monte Carlo Simulation

MCSBD ..... Monte Carlo Simulation Based Design

MRFD ..... Multiple Resistance Factor Design

NREL ..... National Renewable Energy Laboratory

OEM ..... Original Equipment Manufacturer

PBD ..... Performance Based Design

PDF ..... Probability Density Function

PLF ..... Partial Load Factor

QRA ..... Quantitative Risk Analysis

QVM ..... Quantile Value Method

RBD ..... Reliability Based Design

RBDO ..... Reliability Based Design Optimization

RFEM ..... Random Finite Element Method

RGD ..... Robust Geotechnical Design

RNA ..... Rotor-Nacelle Assembly

S1, S2, S3 ..... Three different serviceability load levels

SFEM ..... Stochastic Finite Element Method

SCPT ..... Seismic Cone Penetrometer Test(ing)

SLS ..... Serviceability Limit State

SRA ..... Structural Reliability Analysis

ULS ..... Ultimate Limit State

WSD ..... Working Stress Design (same as ASD)

WEC ..... Wind Energy Converter (same as WTG)

WTG ..... Wind Turbine Generator (same as WEC)

ACKNOWLEDGEMENTS

I am greatly indebted to my advisor, Professor D.V. Griffiths, for the countless weekly meetings during which he provided invaluable guidance, insights and encouragements to help me achieve this work. Dr. Griffiths also showed grace, patience and understanding when this work took more time than usual due to my health challenges. I am grateful also my wife and children for being patient with my reduced attention while I worked on this research. Finally, I dedicate this work to my parents, Ahmed and Fella, for their lifetime sacrifices, for their love and foresight in raising a great family and putting all their children through school. My parents, who were deprived of a formal education in Tunisia, made it their life mission that their children enjoyed the benefits of being literate and educated.

Dedicated to my parents, the love of my life, my four children and my siblings.

CHAPTER 1

INTRODUCTION

A wind energy converter (WEC) consists of moving machinery that exerts large, dynamic and highly variable loads on the support structure and its foundation. Wind energy industry maturity and progress towards competitiveness with traditional electricity sources was made possible through increases in wind turbine size, sophistication of controls and efficiency in power extraction from wind. Design of wind turbine towers and their foundations evolved from classical procedures developed for traditional buildings to scattered design guidelines that attempt to address the load and response characteristics specific to wind turbine support structures. This chapter highlights the remarkable growth of the wind energy industry and describes the associated developments in wind turbine generator support structures and their foundations, as well as the status of design practices. This chapter also presents the problem statement and the objectives of this dissertation.

1.1 Evolution of the Wind Energy Industry

Electrical power generation through wind energy conversion has grown steadily over the past two decades. Installed utility-scale capacity evolved from negligible figures in 2000 to 89 GW in the U.S. and 540 GW globally, as shown in Figure 1.1 (AWEA, 2017; GWEC, 2017). Over the past ten years, cumulative installed capacity experienced a fivefold increase in the United States, going from 16.7 GW in 2007 to 89 GW at the end of 2017 (AWEA, 2017). Globally, as well as domestically, cumulative installed capacity has more than doubled every five years from 2007 to 2017 and is forecast to maintain this pace for at least the next five years, i.e. to 2022 (GWEC, 2017). However, as can be seen from Figure 1.1, the rate of growth of electrical wind power generation in the U.S. has not kept up with global growth. U. S. share of cumulative global capacity

has been on the decline since 2012 and currently stands at about 17%, Figure 1.1. As of 2017, the leading five countries in terms of cumulative installed capacity are China, the United States, Germany, India and Spain with China being the fastest growth market and accounting for 35% of cumulative global capacity and 37% of global yearly added capacity (GWEC, 2017).

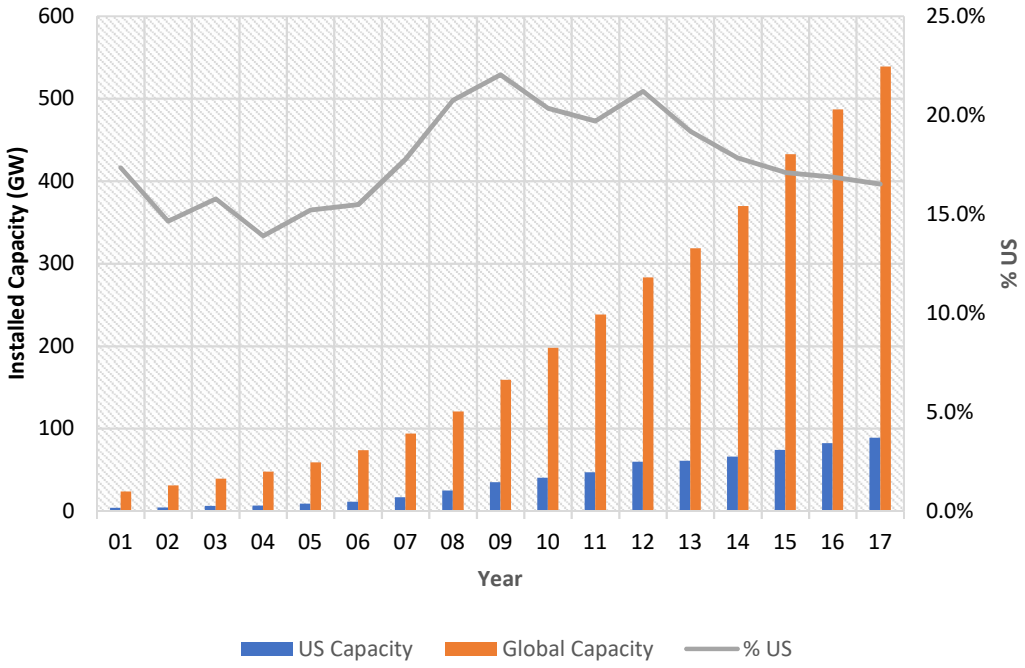

Figure 1.1 Cumulative capacity growth (AWEA, 2017; GWEC, 2017)

The U.S. growth has also been erratic as clearly reflected in the added yearly capacity graph shown in Figure 1.2 (AWEA, 2017). These fluctuations are attributed to uncertain U.S. fiscal policy. The fiscal uncertainty stems primarily from the Production Tax Credit (PTC), a federal production-tied tax incentives program that is put through government extension approval every year. The erratic fluctuations in new capacity carried negative repercussions for the supply chain and the whole industry. In 2015, the U.S. government agreed to a gradual phase out the PTC over a period of five years. The phase out, scheduled to be completed by 2019, offered a stable and

predictable environment that was beneficial to the industry even with declining incentives. After the U.S. wind industry slowdown in 2013 and 2014 and most probably due to the new stable environment, new U.S. installations picked up at a consistent rate of about 8 GW added each year as shown in Figure 1.2. Globally, over 50 GW of capacity was added each year, with China accounting for about half of new global installations. By the end of 2017, global installed capacity stood at about 540 GW and is projected to reach 840 GW by 2022 (GWEC, 2017).

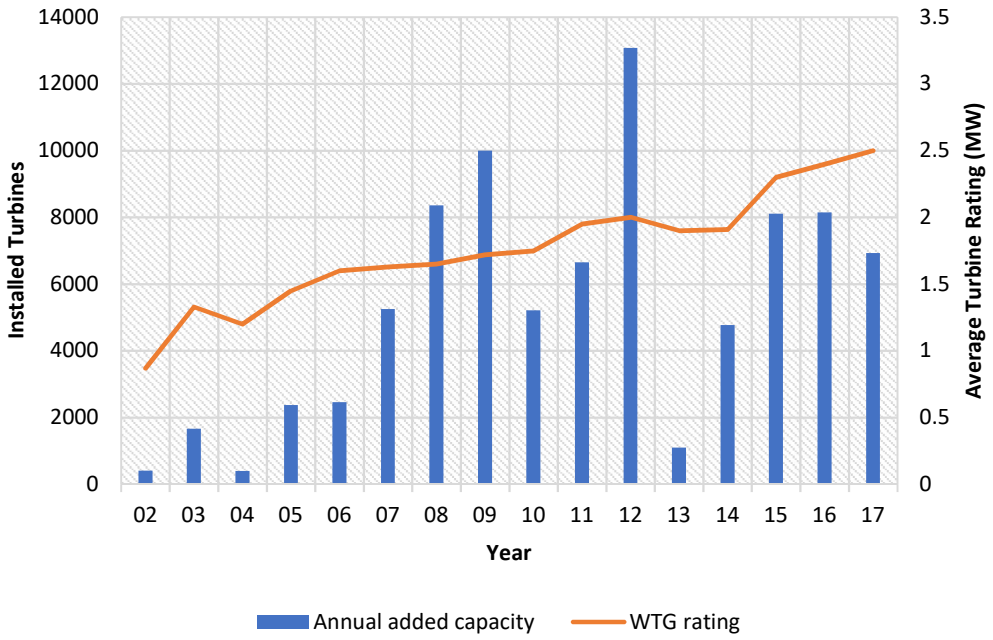

Figure 1.2 Annual added capacity in the U.S. (AWEA, 2017)

In terms of energy mix, renewables are taking up increasingly larger shares of new electrical power generation capacity. The share of renewables varies for different countries. For the U.S., and as of 2016, electricity production from wind accounted for 41% of all new generation. Globally, wind energy accounted for 51% of new generation and the cumulative installed capacity

represented a global wind penetration of about 3.7%. Wind penetration is the fraction of energy produced from wind compared to total generation, expressed as a percentage. The wind technology roadmap developed by the International Energy Agency anticipates a global wind penetration of 15 to 18% by 2050 (IEA, 2013). In the United States, wind penetration was estimated at 4.5% in 2013, 5.5% in 2016 and 6.3% in 2017 (Wiser & Bolinger, 2014; AWEA, 2017). A 2008 study by the U.S. Department of Energy indicated that the rate of penetration could reach 20% by 2030 (DOE, 2008). This study was updated in 2015 as a "wind vision roadmap" to consider various market scenarios and sensitivities and was further updated in 2017 (DOE, 2015; DeMeo, 2017; DOE, 2017). The updated reports and studies indicate that the projected penetration rates shown in Figure 1.3 are possible. The factors driving this growth include increased electricity demand, declining wind energy costs, retiring power generation plants and increasing fuel costs. All these factors point to wind energy becoming increasingly competitive and supplying a more substantial portion of U.S. electricity needs.

1.2 Evolution of Wind Turbine Technology

The remarkable growth of global installed capacity was driven by the ever-increasing demand for electricity. This growth has been maintained through wind turbine technological advances, siting improvements and capital cost reductions. Turbines feature larger rotor diameters, higher hub heights, improved energy extraction efficiency and more sophisticated controls. Technological advances resulted in turbines that had rated capacities eight times greater than those for typical turbines in the nineties and produced seventeen times more energy (AWEA, 2013).

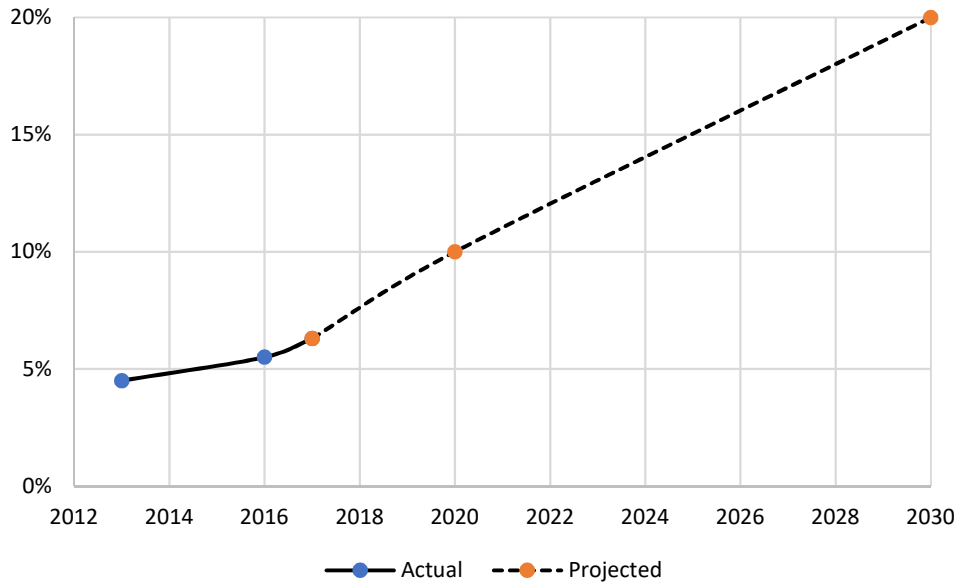

Figure 1.3 Actual and projected U.S. wind penetration

Additionally, capacity factors, i.e. the ratios of average power produced by a turbine to its maximum rated power, increased from less than 30% to over 40%. In 2013, the average wind turbine had a hub height of 80 meters and a rotor diameter of 97 meters. In that year, the industry experienced a significant shift towards higher hub heights and especially larger rotors. Tubular steel towers for multi-megawatt machines continue to dominate but there is ongoing development of concrete towers and increasing adoption of concrete for even higher hub heights (Kaldellis & Zafirakis, 2011). Common hub heights for contemporary steel tube towers range from 80 to 115 meters with rotor diameter typically between 100 and 140 meters. As shown in Figure 1.4 for the "average" tubular steel wind turbine, increases in rotor diameter outpaced hub height increases. A larger rotor diameter translates into greater swept area and more extracted energy. However, transportation limitations for the steel tube create an upper bound on the section diameter. This limitation on tube diameter limits the tower height because slender steel towers would be too

flexible. Slender steel tube towers would also cause bearing limits of grout and concrete to be reached. It is generally accepted that concrete towers are likely more attractive economically for hub heights greater than 120 meters (Engström *et al.*, 2010; ACI, 2016). With increased turbine size, support structures needed to adapt to keep up with larger loads and address transportation challenges. In general, a larger wind turbine size translates into larger loads for the support structures and foundations, although more sophisticated controls have helped stem the load increases and hold significant promise for further reductions (Bossanyi, 2003; Selvam, 2007; Njiri & Soffker, 2016; Vali *et al.*, 2016; Menezes *et al.*, 2018).

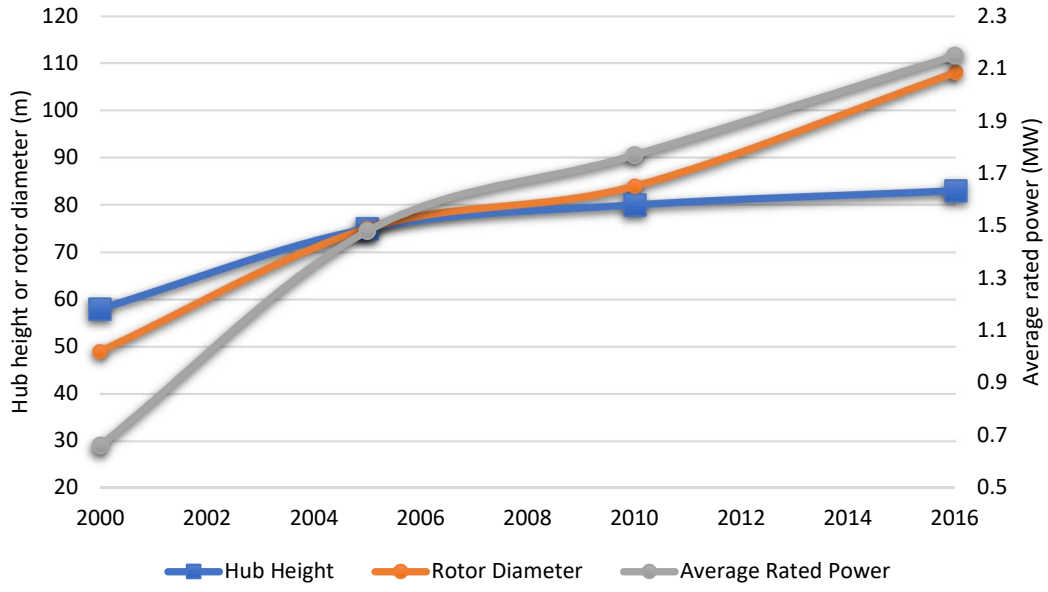

Figure 1.4 Size of the "average" tubular steel tower

Cost-wise, Installed Capital Cost (ICC) per kilowatt for onshore wind decreased by more than two thirds from the early eighties to around 2004 while Levelized Cost of Energy (LCOE),

i.e., the net present value of the unit-cost of electricity over the lifetime of the generating asset, decreased by an approximate factor of three (Lantz *et al.*, 2012). However, from around 2004 to 2009, LCOE experienced a slight increase with China being the only exception due mostly to the emergence of several strong domestic original equipment manufacturers. The overall decreasing cost trend is expected to continue globally with the most recent estimates putting the LCOE decline between 20 and 30% over the next two decades (Lantz *et al.*, 2012). This estimate is in line with the wind technology roadmap developed by the International Energy Agency which projects a 25% LCOE decline of land-based installations (IEA, 2013).

1.3 Evolution of Wind Turbine Foundations

The selection of a foundation system for a wind turbine support structure depends on the loads and the geotechnical conditions at the turbine location. With bigger turbines and larger loads, foundation systems had to evolve to address the challenges specific to dynamic and eccentric wind turbine loads while containing costs. Possible foundation systems include shallow gravity-based foundations, deep foundations, and proprietary systems. Some geotechnical conditions might require specific foundation systems, such as rock anchored foundations at sites with competent shallow bedrock or extensive ground modification where the site has very poor/soft soils. In the latter case, a shallow gravity-based foundation would typically be placed on ground that has been improved. In general, the gravity-based foundation is very common. This foundation is a shallow concrete slab that relies on gravity to resist overturning. Gravity forces are the foundation self-weight, the weight of soil overburden over the foundation and the self-weight of the turbine and the support structure. To reduce the volume of foundation concrete, the slab is typically tapered from the center towards the edges. The foundation plane geometry has also gone through evolutions within the industry, progressing from square, to octagonal or hexagonal to circular

shapes as shown in Figure 1.5. As an illustrative example, for a foundation with a width of $B = 20m$, and with all other dimensions kept unchanged, the total volume of concrete can be reduced from 1271m^3 for a non-tapered square foundation to 445m^3 for the optimal tapered circular foundation (Figure 1.5). Nowadays, the tapered octagon geometry is common in the industry with the optimal circular shape becoming increasingly popular. Typical foundation widths (or diameters) for contemporary turbines range from 15 to 25 meters and the foundation concrete volume typically ranges from 250 to over 550 m^3. The foundation would normally bear on a competent native stratum or structural fill at depths greater than the depth of frost penetration but not less than 2 to 3.5 meters. Reliability based design of this shallow foundation system is the focus of this dissertation.

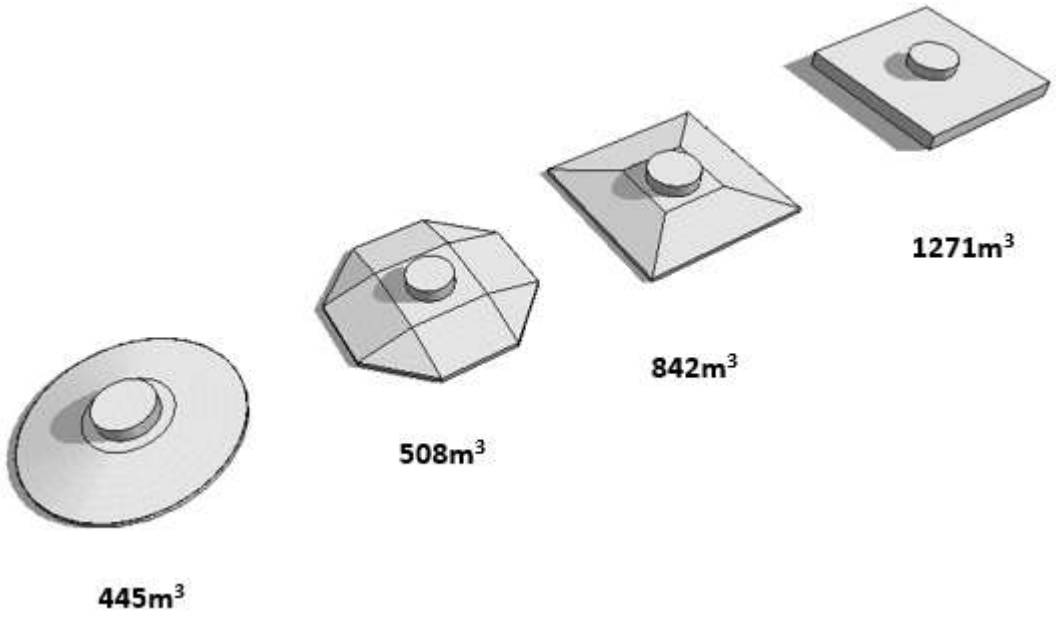

Figure 1.5 Gravity based foundation geometries and associated concrete volumes

The typical breakdown of the Installed Capital Cost (ICC) for land-based wind energy assigns the lion's share to the turbine (drivetrain, rotor and tower) with the foundation being a

distant third or fourth cost item. For instance, in 2011, the turbine accounted for about 68% of the ICC while the foundation accounted for about 4% for a "representative" 1.5MW land-based turbine in the U.S. "heartland", (Tegen *et al.*, 2011). In 2017, the cost share of a land-based turbine foundation is estimated at 3.5% while the cost of foundation and substructure for an offshore turbine is estimated at 14.7% of ICC (Mone *et al.*, 2017). In Europe, and according to the European Wind Energy Association, foundation cost is about 6.5% of ICC for onshore projects and 34% for offshore installations (Horgan, 2013). As would be expected, the foundation share of ICC is much higher for offshore installations. Whether for land-based or offshore installations, the foundation share of the ICC is considerable. It is obvious that optimization of the foundation design and construction methods can have a significant contribution to the competitiveness of wind energy, particularly for offshore wind. Reducing the foundation cost share shall be achieved while ensuring design reliability level is maintained. Reducing foundation cost share and ensuring design reliability are conflicting objectives. Reliability-based design can be a rational framework for optimizing engineering designs while ensuring that the target reliability is met.

1.4 Design Practices within the Wind Energy Industry

Wind energy converters are type-certified per accepted industry standards (IEC, 2008). This means that a turbine design is selected or verified for a range of site conditions grouped under a "site class." This approach means that a turbine at a given location is not designed for the exact external environmental conditions at that specific site but is adequate for a range of conditions including the conditions at that site. The direct consequence of this approach is that most turbines already have some "hidden" safety because the external environmental conditions at locations where turbines are placed are within a site class but very rarely at the upper bound of that class.

Compared to the rapid growth of the wind energy industry and the associated fast-paced research and development, civil engineering design standards appropriate for these structures have been lagging. Investors, owners and developers rely on certification agencies to reduce risks through type certification of WTG's. Certification agencies have served the industry well by publishing standards and design guidelines, (DNV/Riso, 2002; GL, 2003; DNV/Risø, 2004; DNV-GL, 2016b). While type certification of wind energy converters to IEC specifications resulted in global acceptance of the "IEC61400-1 Wind turbines - Part 1: Design Requirements" loads standard (IEC, 2008), there are considerable differences in structural and geotechnical design practices in different parts of the world. Frequently, differences between North American, European, Japanese and Chinese practices are natural extensions of differences in structural and material design codes in these markets. On the loads side, current design practice relies on load cases and partial load factors prepared per IEC61400-1. This standard defines external condition classes, design load cases and associated partial load factors for designing wind turbine support structures. However, this standard reverts to national design codes for material resistance factors with the understanding that a "coherent set of standards" for materials, design and construction is used. The IEC61400-1 standard specifies that when partial safety factors for material resistance are based on national codes, the resulting safety level should be greater than that intended or implied by the IEC standard. Furthermore, since the division and factorization of partial safety factors for loads and materials adopted by the IEC are consistent with the methodology defined in ISO 2394 (ISO, 2015), the IEC standard cautions that adjustments may be necessary if the factorizations or formulations adopted in the national standard are different. This IEC guidance is insufficient and such requirements are difficult to appreciate by design engineers. Clearer guidance is necessary especially for designers entering the industry from traditional geotechnical and

structural engineering practice. Consequently, design reliability varies depending on the national standard, the choice of material resistance factors and the designer's interpretation of a "coherent set of standards." Designs, even those produced by experienced practitioners within the industry, tend to have varying levels of reliability due to at least the following reasons:

a) lack of properly calibrated partial safety factors for the various limit states,
b) lack of uniform guidance on partial safety factors,
c) varying interpretations of existing national standards which are mostly concerned with buildings and classical infrastructure, and
d) varying calculation models and assumptions.

The wind energy industry has much to gain from harmonized, properly calibrated and globally accepted standards. In addition to promoting trade, such standards would improve competitiveness of wind energy relative to other sources of energy. There are several attempts to achieve consistent reliability in design practice. In the US market, the author of this dissertation participated in the development of a joint ASCE/AWEA guideline document, the "ASCE/AWEA RP2011 – Recommended Practice for Compliance of Large Land-based Wind Turbine Support Structures," with the main objective of providing guidance in code interpretations and assumptions to achieve a token of consistency in design reliability (AWEA & ASCE, 2011). There is additional guidance with similar objectives by certification agencies such as Germanischer Lloyd's "Guideline for the Certification of Wind Turbines," (GL, 2010), DNV-GL's "Support Structures for Wind Turbines," (DNV-GL, 2016b) and DNV/Riso's "Guidelines for Design of Wind Turbines," (DNV/Risø, 2002), as well as national standards such as the "Guideline for Wind Turbines" in Germany (DIBt, 2012) and the "Guideline for Design of Wind Turbine Support Structure and Foundation" in Japan (JSCE, 2010). At the global level, there is an on-going effort

to develop the "IEC61400-6 Wind Turbines – Part 6: Tower and Foundation Design Requirements," an international standard currently in Final Draft International Standard (FDIS) status, (IEC, 2016). This standard is aimed at reducing differences in global design practice and harmonizing wind energy design standards. The author of this dissertation has been helping coordinate U.S. involvement in the development of this standard.

1.5 Problem Statement and Dissertation Objectives

Ideally, the design of wind turbine foundations should ensure, to a pre-determined reliability level and for the design lifetime of the installation, that the foundation is safe against catastrophic failures as well as performance deficiencies that can hinder the proper operation of the wind turbine. Current design practice is based on limit states design principles with load cases and partial load factors determined per IEC61400-1 but with partial material resistance factors per various national or regional material codes. The reliability levels achieved through this design practice are only of implied nature because of reliance on interpretations relative to the coherence of the selected set of standards. The resulting implied reliability levels are those that would be anticipated from the coherent set of standards. Furthermore, material design codes are normally prepared for traditional building structures where the safety, performance, cost and longevity considerations differ from those for wind turbines. Therefore, it is not possible to say that the set of standards is coherent unless wind turbines are treated as regular building structures. Currently, there are no actual calibrations prepared to estimate the material safety factors that are appropriate for use in wind turbine support structure or foundation design. The IEC6100-6, a draft international standard, recommends partial resistance factors based on expert judgement and adopted target reliability deemed appropriate for wind turbine structures (IEC, 2008; Sorensen & Toft, 2014; IEC, 2016). Thus, a primary objective of this dissertation is to propose and demonstrate a fully

probabilistic, reliability-based design procedure that achieves the target reliability intended in these documents without the need to specify any partial safety factors. The method is a Monte Carlo Simulation procedure termed the "direct Reliability Based Design (d-RBD)" method: an efficient process that is suggested as a practical and versatile design tool (Ben-Hassine & Griffiths, 2012).

To demonstrate the d-RBD method, this dissertation considers a foundation design developed through state-of-practice procedures and investigates three limit states that are commonly considered in the design of wind turbine support structure foundations. The three limit states are: a) foundation tilt as a serviceability limit state, b) foundation rotational stiffness as a serviceability limit state, and c) bearing capacity as an ultimate limit state. The aims of this exercise are to identify design variables with most influence on these limit states and to compare results obtained through this tool to current design practices which are based on industry guidelines and extensions and interpretations of existing building design standards (e.g. AWEA & ASCE, 2011; DNV-GL, 2016b; IEC, 2016). Finally, an important objective of this dissertation is to show that the d-RBD method can serve as a design tool for the various foundation limit states. These results are of direct relevance to the on-going international effort to develop IEC 61400-6 as a harmonized standard for the design of WTG support structures and their foundations (IEC, 2016). In this regard, the desired outcome is either to include the d-RBD as an acceptable design tool or to base recommended partial safety factors on actual calibrations using d-RBD or similar higher order reliability analysis methods.

1.6 Dissertation Outline

This dissertation contains several introductory and literature review chapters followed by research contributions consisting of novel implementations of a probabilistic method to extend the state of knowledge relative to shallow WTG foundation design and design reliability:

- Chapter 1 (this chapter) contains background information on the growth of the wind energy industry, common WTG foundation systems and a state of practice summary relative to the design of shallow wind turbine foundations; it also presents the problem statement and objectives of this dissertation.
- Chapter 2 describes deterministic computations for estimating elastic tilt, rotational stiffness and bearing capacity of shallow wind turbine foundations. These computations involve closed form and empirical formulations as well as numerical solutions such as the finite element method. This chapter contains a summary of bearing capacity formulations starting from vertical bearing capacity of a rigid disk on undrained clay, to general foundations on drained soils, and to foundations subjected to highly eccentric loads. Based on this literature survey, select computational models are identified as most suitable for use for shallow wind turbine foundations.
- Chapter 3 focuses on uncertainly that is prevalent in geotechnical design and describes its various sources, types and ways to quantify it. This chapter describes several probability density functions that are particularly suitable for modeling geotechnical design parameters as random variables. The chapter also reviews practical methods for estimating geotechnical variability based on limited geotechnical data, contains a literature review of reported variability ranges and proposes a tiered format with associated variability ranges for common geotechnical properties.

- Chapter 4 is a literature review of engineering design methods and the progression of these methods from the global factor of safety approach to partial factor reliability-motivated formats. This chapter also describes risk and reliability concepts and summarizes notional reliability targets embedded in leading design standards. Finally, this chapter presents ULS and SLS target reliability deemed appropriate for use with wind turbine support structures and their foundations.
- Chapter 5 discusses reliability analysis and reliability-based design methods and presents the details of an efficient Monte Carlo Simulation method called direct Reliability Based Design (d-RBD) and suggests this approach as a practical, fully probabilistic engineering design tool.
- Chapter 6 presents the results of using the d-RBD method to investigate tilt and rotational stiffness as two serviceability limit states of great interest in the design of shallow wind turbine foundations. For the stiffness limit state, dynamic and static stiffness are investigated per industry guidelines and considered the cases where bedrock is deep and where it is within a depth of influence. The investigation includes calculating the reliability indices of the design for such scenarios for medium and high variability assumptions, identifying the main driving variables and highlighting the cost of uncertainty associated with these variables.
- Chapter 7 investigates the use of the d-RBD method in the assessment of bearing capacity of shallow wind turbine foundations as an ultimate limit state for drained and undrained conditions. The investigation adopts the classical effective area approach for modeling shallow foundations subjected to combined loading. Like the earlier limit states, the chapter

presents the results for medium and high variability assumptions and identifies the driving variables for drained and undrained bearing capacity limit states.

- Chapter 8 contains a summary of the original contributions of this work in relation to the results detailed in Chapters 6 and 7 for the three limit states under consideration. These results are also compared to those obtained based on current practice to identify areas of potential design optimization or areas where current practice may be too risky. This chapter also outlines recommendations for future work.

CHAPTER 2

DETERMINISTIC ANALYSIS OF WIND TURBINE FOUNDATIONS

This chapter describes common assumptions, analysis models and equations that designers of shallow wind turbine foundations perform to compute foundation tilt, rotational stiffness and bearing pressure; i.e., the foundation responses of relevance to three limit states considered in this dissertation. Covering these calculation models is useful in understanding the state-of-the-practice within the industry and in identifying some of the uncertain design variables that these models invoke. However, before describing these calculations, it is important to understand the nature of the loading that these foundations are subjected to.

2.1 Loading Nature and Levels

Wind turbine foundations are subjected to highly variable loads where the overturning moment is the predominant component. Such a loading scenario is described in the literature as a "combined loading." Combined loading includes vertical (V), moment (M) and horizontal (H) components. One approach to modeling a foundation subjected to combined loading is to replace the VMH loads by an equivalent inclined loading acting at an eccentricity e as shown in Figure 1.1. The horizontal and vertical components of the equivalent load are equal to the original applied horizontal and vertical loads while the moment is replaced by the fact that vertical load is applied at the "load center" which is at eccentricity, e. When moment loading is present in two orthogonal directions such as M_x and M_y, the equivalent load would be eccentric in two directions and the load center would be at eccentricities $e_x = M_x / V$ and $e_y = M_y / V$.

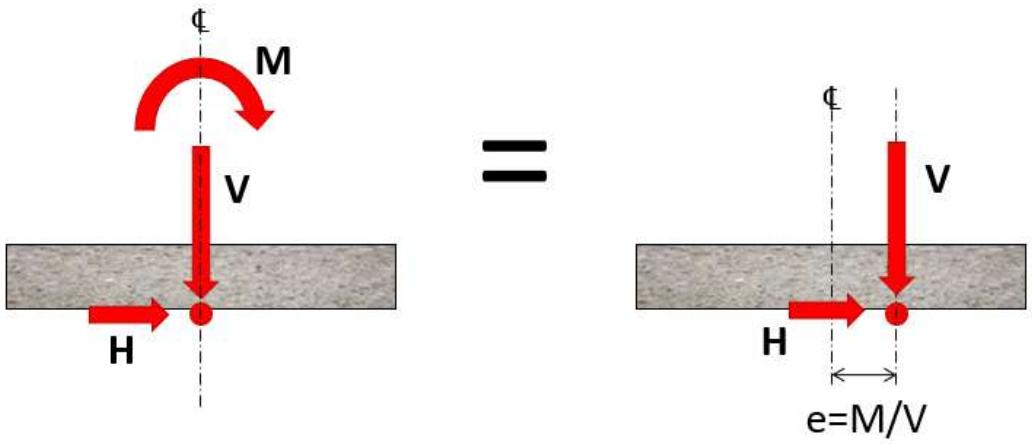

Figure 2.1 Combined loading equivalency

In order to simplify interpretations from experimental and numerical analyses of foundations subjected to combined loading, some researchers proposed the standard convention for loads and displacements shown in Figure 2.2 (Butterfield *et al.*, 1997). In this convention, loads are proposed to be listed in the $V-M-H$ order, are applied at the geometrical center of the foundation and are attached to a coordinate system which translates with the foundation but does not rotate with it. Figure 2.2 illustrates this convention for a foundation subjected to $V-M-H$ loading and undergoing vertical and horizontal displacements w and u and tilt θ.

Loads are evaluated per IEC61400-1 procedures for the various design load cases outlined in that standard (IEC, 2008). The latest edition of this standard, Edition 3, was published in 2008. Edition 4 is in final national balloting and is anticipated to be released in November 2018. A certification agency loads standard that is coherent with the IEC 61400-1 is the "DNVGL-ST-0437: Loads and Site Conditions for Wind Turbines," first published in 2016 (DNV-GL, 2016a). Load cases in these standards cover many design situations such as power production, power production plus occurrence of fault, start up, normal shutdown, emergency shutdown, parked

condition (standing still or idling), transport, assembly, maintenance and repair. These standards outline statistical procedures and acceptable experimental and numerical modeling methods for evaluating loads. Load cases are categorized into normal (N) extreme cases, abnormal (A) extreme cases and fatigue (F) cases and are assigned different partial safety factors.

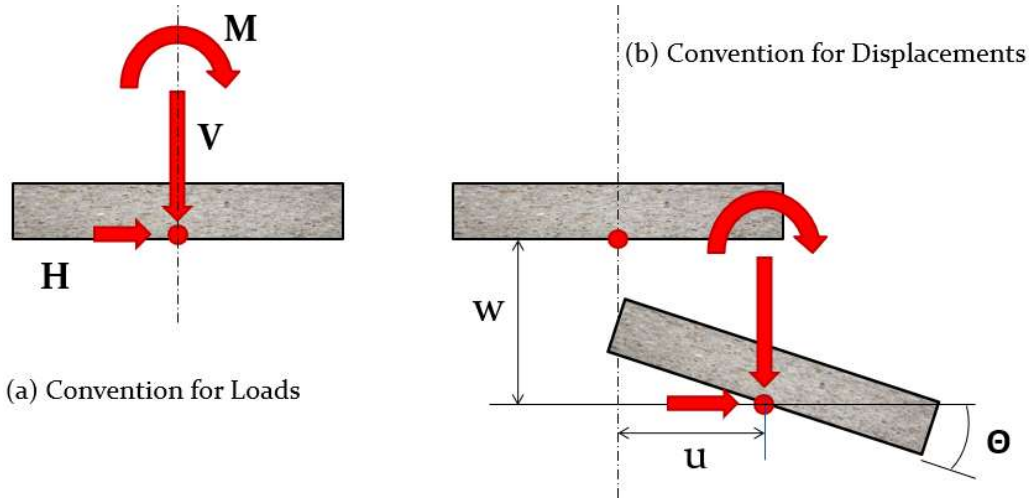

Figure 2.2 Conventions for loads and displacements

The predominance of the overturning component in wind turbine loads invites specific challenges in the design of shallow wind turbine foundations. A primary challenge is the development, as the moment loading is increased, of a zero-pressure or no-contact zone under the foundation. The presence of a zero-pressure or no-contact area reduces the foundation area that engages the subgrade in providing stiffness, resisting tilt, and/or mobilizing bearing resistance. Stiffness and tilt responses vary as a function of the applied and the resulting reduced area, while bearing capacity mobilization may or may not occur as the foundation can overturn without a bearing capacity failure. To facilitate the treatment of different limit states which are invoked at

different load levels, industry standards introduced three serviceability load levels (DNV-GL, 2016b; IEC, 2016):

1. S1 - Governing "normal extreme" loading: this is an extreme normal operational loading corresponding to a return period (or average recurrence interval) of 50 years; i.e., a load level that, on average, will be exceeded once every 50 years. The 50-year return period for the S1 load level was selected by the wind energy industry to provide a design basis that is, at least in terms of design life, comparable to that adopted by building codes for common structures. Another reason could have been to provide an additional cushion of safety that would be useful if a wind project is at the end of the 20-year design life and is being considered for repowering or extension of life. This is a growing interest within the wind energy industry in design life extension as projects commissioned around the turn of the millennium are nearing their original design life and are still performing well.
2. S2 – "Frequent" load level: this load level corresponds to an annual probability of exceedance of 10^{-4}; i.e., a load level that will be exceeded 0.01% of the time. This is equivalent to a period of exposure to higher loads of 0.87 hour per year (17.5 hours over a 20-year design life), and
3. S3 – "Quasi-permanent" load level: this load level corresponds to an annual probability of exceedance of 10^{-2}; i.e., a load level that will be exceeded 1% of the time. This is equivalent to a period of exposure to higher loads of 87 hours per year (or a total of 1752 hours over a design life of 20 years).

2.2 Accepted Zero-pressure Allowances

Designers of most traditional civil engineering structures would avoid zero-pressure conditions under footings for the extreme characteristic load case. They achieve this by ensuring

that the footing is large enough to keep the resultant force acting within the Kern; i.e., within middle third of a rectangular foundation. Even though this limit is a typical requirement of ASD design codes, it is not necessary to maintain equilibrium of the foundation or for any other performance consideration so long as the consequences, such as reduced bearing area and increased bearing pressure, are addressed in the design. In foundation design, it is common practice to allow zero pressure under factored loads, i.e., the "strength limit state." Some recent standards, especially those that are based on limit states design principles, are allowing for limited zero-pressure to develop under characteristic (unfactored) normal extreme loads, especially for foundations bearing on rock (AASHTO, 2012). For wind turbine foundations, certification agencies and the wind industry at-large have adopted even less onerous limits such as allowing zero pressure over no more than half the foundation width under the characteristic extreme loading (S1 load level) and requiring compressive pressure over the entire foundation area for the S3 serviceability level loading (DNV/Risø, 2002; GL, 2003; DNV-GL, 2016b; IEC, 2016). Some certification agency guidelines allow for minor exceedances of these limits provided that the designer can show through testing or calculation that the negative effects of cyclic gapping can be mitigated or are negligible.

2.3 Strain Level Dependence of Elastic Moduli

Geomaterials are nonlinear and their elastic moduli are known to be a function of strain level. Small strain elastic moduli are estimated from shear wave velocity measurements collected in the field through geophysical surveys such as Multi-Analysis of Shear Waves (MASW) campaigns and seismic cone penetrometer testing (SCPT). The following theoretical equation expresses the small strain shear modulus, G_0, in terms of in-situ density, ρ, and shear wave velocity, V_s :

$$G_0 = \rho V_s^2 \tag{2.1}$$

The small strain Young's modulus, E_0, can then be calculated from the following theory of elasticity equation in which ν is Poisson's ratio:

$$E_0 = 2(1+\nu)G_0 \tag{2.2}$$

The degradation of shear modulus with shear strain is a fundamental characteristic of nonlinear soil behavior. However, experimental studies on this degradation indicate that it depends on many factors including soil type, plasticity index, void ratio, over-consolidation ratio, cyclic loading and degree of saturation. Shear modulus degradation in commonly formulated as a function of shear strain. Formulations based on shear stress are not as popular.

2.3.1 Formulations Based on Shear Strain

Hyperbolic relationships of varying forms and number of required parameters have been used to obtain better fits to experimental data of the shear stress-strain curve (Kondner, 1963b, 1963a; Kondner & Zelasko, 1963; Hardin & Drnevich, 1972; Borden & Gupta, 1996; Darendeli, 2001). The original hyperbolic models, also known as KZ models, were simple because they required only two physical parameters, k and z, to define the shear stress-shear strain curve in the following format:

$$\tau(\gamma) = \frac{\gamma}{\frac{1}{k} + \frac{\gamma}{z}} \tag{2.3}$$

The parameters a and b have physical meanings because:

i) at $\gamma = 0$, the tangent to the curve is equal to k which is equal to the zero-strain shear modulus; i.e., $k = G_0$, and

ii) when $\gamma \to \infty$, the curve converges asymptotically to parameter z which is equal to the shear strength, $\tau_{\max}$; i.e., $z = \tau_{\max}$.`

Thus, Equation (2.3) can be re-written using meaningful parameters as follows:

$$\tau(\gamma) = \frac{\gamma}{\frac{1}{G_0} + \frac{\gamma}{\tau_{\max}}} = \frac{G_0 \gamma}{1 + \frac{G_0}{\tau_{\max}} \gamma} \tag{2.4}$$

The above equation is simple, has meaningful parameters and properly models behavior at both ends of the strain spectrum. However, it lacks geometric flexibility to model test data at intermediate strain ranges. A modified hyperbolic model, described as a modified KZ or MKZ model, was proposed by Matasovic & Vucetic (1993) to improve the ability of the curve to fit test data. The model introduces two curvature parameters, α and β:

$$\tau_{MKZ}(\gamma) = \frac{G_0 \gamma}{1 + \beta \left(\frac{G_0}{\tau_{\max}} \gamma \right)^{\alpha}} \tag{2.5}$$

Defining an auxiliary reference strain $\gamma_{ref} = \tau_{\max} / G_0$, the above equation can be re-written as:

$$\tau_{MKZ}(\gamma) = \frac{G_0 \gamma}{1 + \beta \left(\frac{\gamma}{\gamma_{ref}} \right)^{\alpha}} \tag{2.6}$$

Sample plots of this relationship are shown in Figure 2.3 and Figure 2.4 to illustrate the effects of the curvature parameters on the shear stress – shear strain curve for the case where the ultimate shear strength is $\tau_{max} = 100kPa$. As can be seen in the figures, the curve maintains the asymptotic tendency to τ_{max} only for the case where the original hyperbolic equation is recovered; i.e., for $\alpha = 1.0$ and $\beta = 1.0$. For other cases, the ultimate shear stress either exceeds τ_{max} in an unbounded fashion or the material softens causing the curve to tend towards a lower ultimate shear stress.

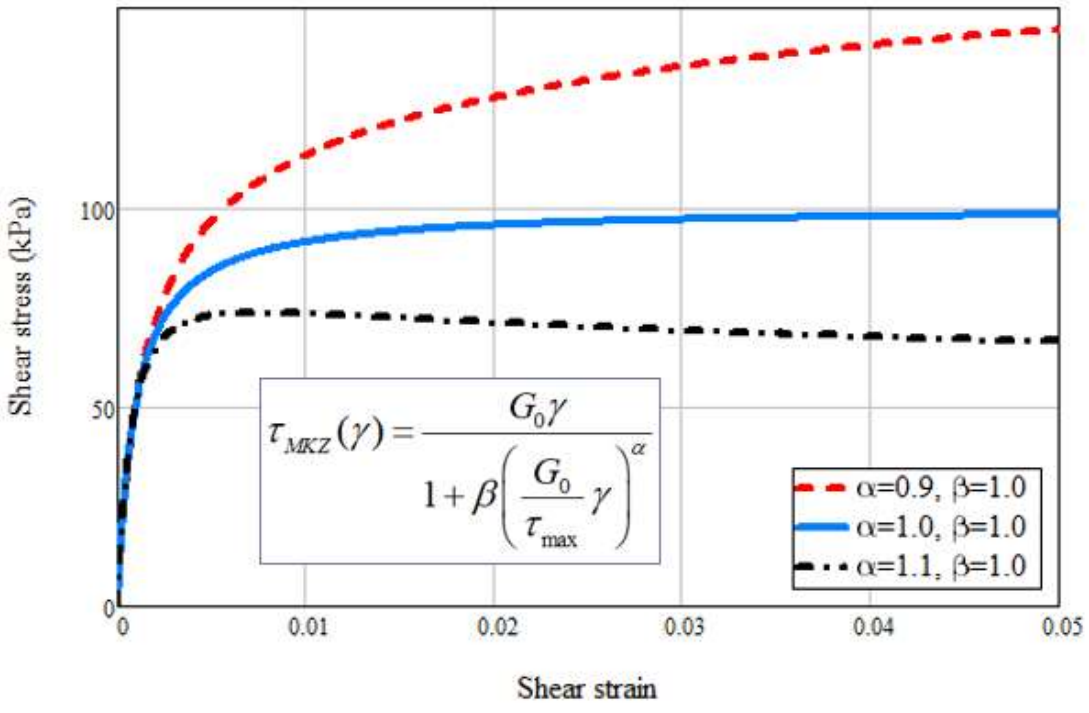

Figure 2.3 Sample MKZ curve showing effect of α parameter for $\tau_{max} = 100kPa$

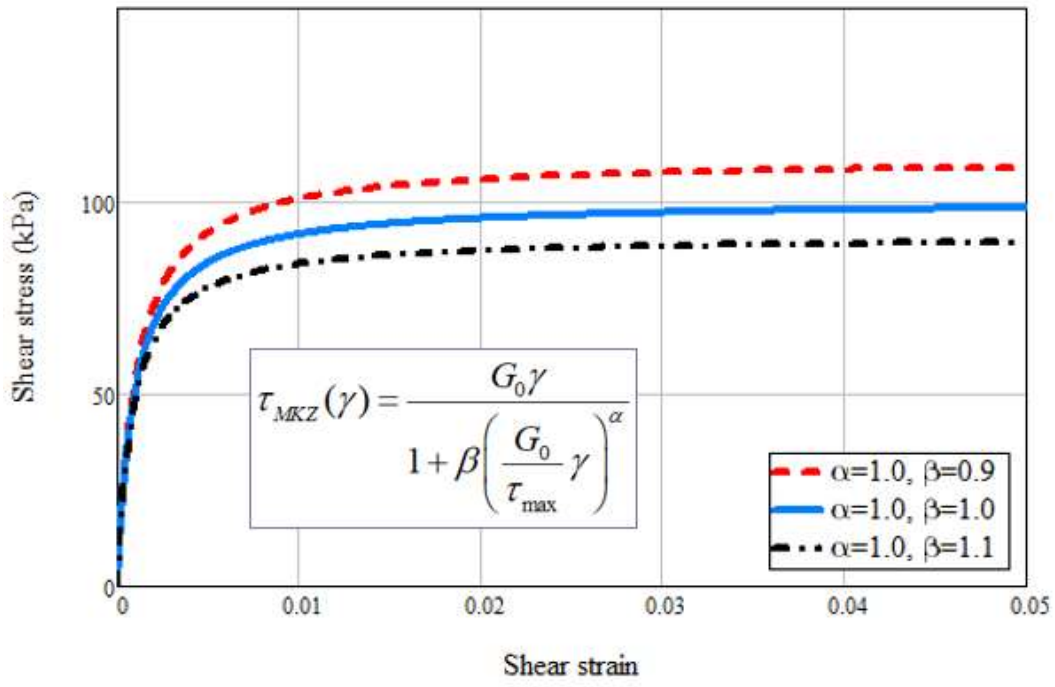

Figure 2.4 Sample MKZ curve showing effect of β parameter for $\tau_{max} = 100kPa$

The loss of fidelity of MKZ models at higher strains may not be important for low to medium strain levels prior to mobilization of the soil's shear strength; i.e., for strains levels of about 10^{-3}. However, at higher strain levels, this loss of fidelity can be problematic as the predicted shear strength is unbounded. For this reason, Shi & Asimaki (2017) proposed a flexible "hybrid hyperbolic or HH" formulation that extends the MKZ model to higher strain levels. The proposed formulation, termed "FKZ" model, requires a transition function, $w(\gamma)$, to transition the stress-strain curve from small to large strain regimes. The hybrid relationship is defined as:

$$\tau_{HH}(\gamma) = w(\gamma)\tau_{MKZ}(\gamma) + \left[1 - w(\gamma)\right]\tau_{FKZ}(\gamma) \tag{2.7}$$

where the $\tau_{MKZ}(\gamma)$ is as defined in Equation (2.6) and $\tau_{FKZ}(\gamma)$ is the hyperbolic model applicable at large strains and is expressed as:

$$\tau_{FKZ}(\gamma) = \frac{\gamma^d \mu}{\frac{1}{G_0} + \frac{\gamma^d \mu}{\tau_{\max}}} \tag{2.8}$$

in which d and μ are new model parameters. The transition function is a modification of an S-shape function to transition from the point where the MKZ formulation starts to deviate from being a reliable representation of soil behavior, judged by Shi & Asimaki (2017) to be between a shear strain of 10^{-4} and $3 \cdot 10^{-2}$. Shi & Asimaki (2017) suggested the following expression for the transition function:

$$w(\gamma) = 1 - \frac{1}{1 + 10^{a\left[\log_{10}\left(\frac{\gamma}{\gamma_t}\right) - 4.039a^{-1.036}\right]}} \tag{2.9}$$

in which parameter γ_t is the transition strain level when the MKZ model stops to be a reliable representation of soil behavior and parameter a is the rate of transition. With the preceding flexible formulation, Shi & Asimaki (2017) have proposed a nine-parameter model that covers shear modulus degradation over the full range of shear strains. Furthermore, the authors outlined a procedure for estimating all nine model parameters based solely on shear wave velocity profiles.

Dong *et al.* (2018) provided a review of these existing shear modulus degradation models and Vardanega & Bolton (2011) summarized practical methods for modeling the nonlinear dependence of shear modulus on shear strain for fine grained soils. A comparative study of modulus reduction methods conducted by Guerreiro *et al.* (2012) found that the family of normalized curves proposed by Darendeli (2001) are able to capture the influence of plasticity index, over-consolidation and confining pressure and for a larger strain range (Darendeli, 2001; Guerreiro *et al.*, 2012). Per Shi & Asimaki (2017), the Darendeli model is verified for strains up

to $5 \cdot 10^{-3}$, the typical limit for resonant column tests. In the Darendeli (2001) method, the modulus ratio is expressed as a function of shear strain, γ, as follows:

$$\frac{G}{G_0} = \frac{1}{1 + \left(\frac{\gamma}{\gamma_{ref}} \right)^{\alpha}} \tag{2.10}$$

where α is a curvature parameter and γ_{ref} is a reference shear strain used to normalize shear strain. This model is an MKZ formulation where $\beta = 1$ and $\alpha = 0.9190$. In the Darendeli model, the reference strain, γ_{ref}, is the strain corresponding to a modulus equal to half the small strain modulus; i.e., the shear modulus drops to half its initial value at the reference shear strain ($G = G_0/2$ at $\gamma = \gamma_{ref}$). In the original Hardin and Drnvich model, the reference strain is defined as the ratio of ultimate shear stress, τ_u, to the initial shear modulus; i.e., $\gamma_{ref} = \tau_u / G_0$. Sample plots of shear modulus degradation curves for different curvature parameter α are shown in Figure 2.5. The shear modulus ratio or stress level factor (G/G_0) varies between 0 and 1 and is sometimes referred to as the normalized shear modulus because the ratio normalizes the shear modulus at a given strain level to that at zero strain. It is reported to depend greatly on shear strain amplitude, mean effective confining stress, soil type and plasticity index. The modulus ratio is reported to depend to a lesser extent on over-consolidation ratio, void ratio, degree of saturation, loading frequency, number of load cycles, and grain characteristics such as shape, size, gradation and minerology (Darendeli, 2001).

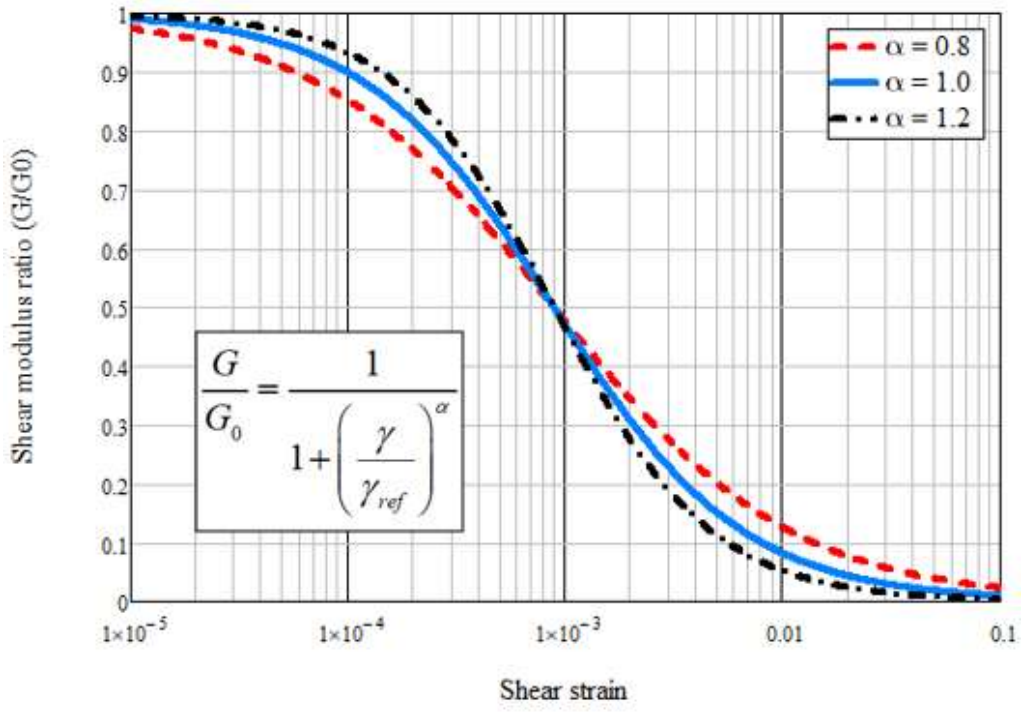

Figure 2.5 Sample shear modulus degradation curves – strain level formulations

2.3.2 Formulations Based on Shear Stress

Most formulations of the shear modulus ratio are as a function of shear strain. However, there are some formulations as a function of shear stress that are potentially equally valid (Fahey & Carter, 1993; Mayne, 2001). In these formulations, the shear modulus ratio is called the stress level factor, R_f, and is expressed as follows:

$$R_f = \frac{G}{G_0} = 1 - m\left(\frac{\tau}{\tau_u}\right)^n \tag{2.11}$$

where τ is shear stress, τ_u is the ultimate shear stress, and where m and n are empirical parameters with typical values of $m = 1.0$ and $n = 0.3$ for most soils (Poulos, 2018). Sample shear modulus degradation curves formulated as a function of shear stress are shown in Figure 2.6.

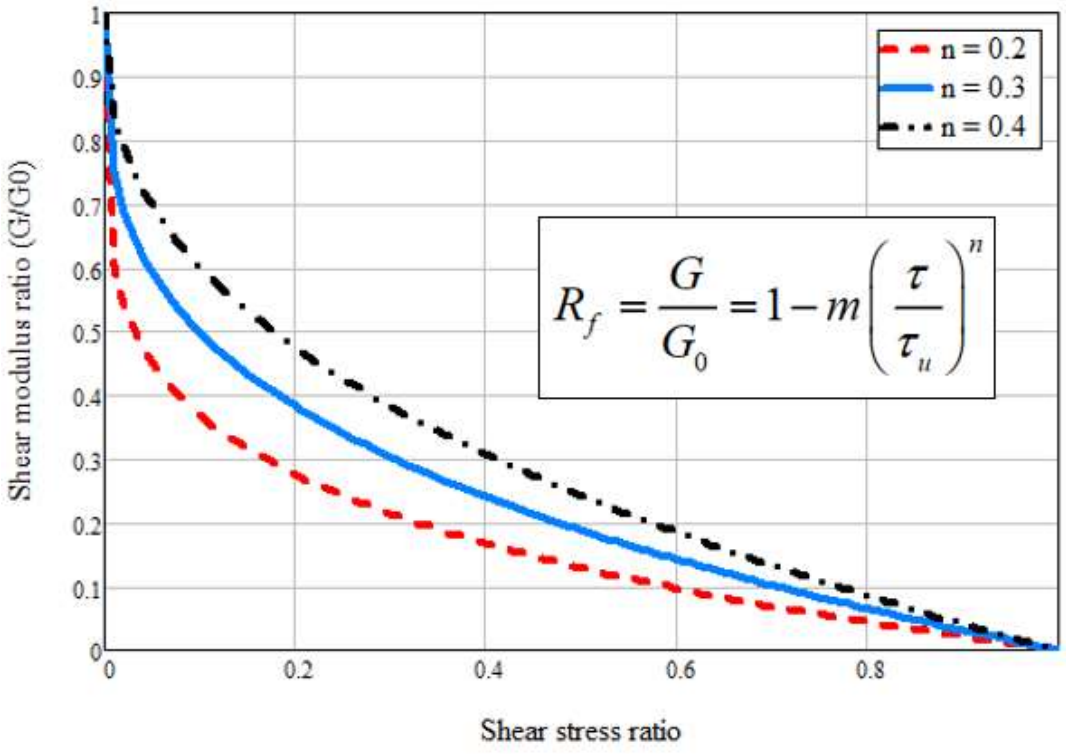

Figure 2.6 Stress level formulation of shear modulus degradation with m = 1

2.4 Soil Strain Level Appropriate for Onshore Wind Turbine Foundations

The goal of the preceding discussion on shear strain and shear modulus degradation is to assess the appropriate modulus reductions to adopt for wind turbine foundation design. Since most formulations are in terms of shear strain, the primary question is relative to strain levels expected for the soils supporting the foundation. For the most part, the wind energy industry has followed the 2002 DNV guidance on this subject (DNV/Risø, 2002). Per this guidance, the suggested subgrade shear strain level for extreme onshore wind turbine load cases is around 10^{-3}. Some recent instrumented foundations showed that cyclic shear strain level immediately under the wind turbine foundation was 2×10^{-4} and that it dropped rapidly with depth under the foundation (Yilmaz *et al.*, 2014). This appears to suggest that the 10^{-3} to 10^{-2} strain range proposed by DNV is

conservative and may be more appropriate for ocean waves. For reference, the IEC61400-6 draft standard estimates that the soil shear strain should be in the range of 10^{-4} to 10^{-3} during normal operation and up to characteristic extreme loads (IEC, 2016).

Diaz-Rodriguez & Lopez-Molina (2008) reviewed published data on strain and stress thresholds that mark changes in soil behavior and suggested four shear strain thresholds separating different behavior regimes: linear, volumetric, degradation and flow. The five regimes separated by these thresholds are:

1. Very small strain (up to around 5×10^{-5}): practically linear behavior and no degradation of moduli.
2. Small strain (between 5×10^{-5} and 6×10^{-4}): behavior is nonlinear but is fully recoverable (elastic); no degradation of moduli.
3. Medium strain (up to 10^{-3}): behavior is nonlinear with start of minor strength degradation; moduli degradation between 0.6 and 0.85.
4. Large strain (greater than 10^{-3}, dependence on number of cycles): behavior is nonlinear, and moduli are degradable with start of flow behavior
5. Residual strains (dependence on number cycles): nonlinear behavior, degradable moduli and large residual strains.

Based on the regimes identified above and strain levels between 10^{-4} and 10^{-3}, wind turbine foundation soils would generally fall into the small to medium strain regimes where soil behavior is typically nonlinear with minor strength degradation. The MKZ-type shear modulus degradation model proposed by Darendeli (2001), which has been verified to strains up to $5 \cdot 10^{-3}$ (Shi & Asimaki, 2017), is therefore appropriate for onshore wind turbine foundations.

2.5 Foundation Tilt

Foundation settlement and tilt are important serviceability design considerations. Issues associated with uniform settlement can often be addressed through regrading of the ground around the foundation. However, tower tilt due to differential settlement, tower installation imperfections and solar irradiation (uneven heating of the tower) can be more detrimental to turbine operation. Normally, differential settlement is caused by moment loading and varying subgrade support under the foundation.

2.5.1 Common Tilt Limits

Turbine manufacturers either specify the limit on tilt caused by differential settlement and an additional load to account for the total tower tilt, or they simply specify the limit on differential settlement tilt and include the additional load caused by total tower tilt in the specified loads. A typical limit on differential settlement tilt is 3mm/m, or 0.17 degree. This limit is also recommended in the ASCE/AWEA recommended practices document (AWEA & ASCE, 2011). To maintain the validity of the loads specified by the manufacturer, the foundation designer must keep tilt caused by differential settlement under the specified limit. For a rough idea on scale, a 3 mm/m tilt limit corresponds to 60 mm (2.5 in) of differential settlement across a 20 m (65 ft) foundation.

To put this common tilt limit of 0.17 degree in context, we can look at some lessons learned from pushover analysis of a tall slender structure with a mass at its top. For a rigid slender structure of height, H, rigidly connected to a rigid base of width, B, resting on infinitely stiff subgrade, the critical inclination angle before collapse is (Gazetas, 2013, 2015):

$$\theta_{cr,\infty} = \arctan\left(\frac{0.5B}{H}\right) \approx \frac{0.5B}{H} \tag{2.12}$$

For wind turbines with typical contemporary hub height of 90 m and foundation width of 20 m, this critical tilt angle is around 6 degrees. This critical tilt angle is overly optimistic since neither the turbine nor the foundation is truly rigid, the supporting soils could also under undergo plastic deformations and $P-\delta$ effects could hasten the toppling of the tower. Furthermore, the applied wind turbine loads are dynamic and do not increase monotonically as is the case for a pushover analysis. Nevertheless, comparing 0.17 to 6 degrees is a useful exercise. The so-called $P-\delta$ effect is the moment added to the applied moment when a structure deflects and is equal to vertical load P times the horizontal deflection δ. Many times, when a structure nears its load carrying capacity, this additional moment is what precipitates the collapse.

2.5.2 Estimating Foundation Tilt

Foundation settlement and tilt due to soil compressibility can be caused by immediate elastic deformation of the supporting soils within the depth of influence as well as longer term consolidation and creep settlement if fine grained soils are present. However, due to the dynamic nature of the applied loads, it is difficult to select a sustained load level that is applied long enough for pore water pressure to dissipate and consolidation settlement to occur. This load level is the subject of debate within the industry, such as within the committee working on the development of the IEC61400-6 international design standard (IEC, 2016). The FDIS version of this document requires that settlement and tilt be evaluated at the S3 load level both for short term (elastic) and long term (consolidation) deformations.

For consolidation settlement estimates, adopting the S3 load level may be conservative since the total duration of this level being exceeded (about 1750 hours or 73 days in 20 years) is not applied continuously, but in short-lived exceedances over the design life of the project which are not long enough to cause porewater pressure dissipation and soil consolidation. On the other

hand, it could be argued that the governing normal extreme load level (S1) should be selected for estimating elastic deformations since all it takes is one load exceedance to cause an immediate deformation that exceeds the limit. However, the 50-year return period for the S1 load level is significantly longer than the typical 20 to 25-year design life of a wind project. Thus, an appropriate load level to use in estimating elastic deformations ought to be lower. Therefore, the adoption of the S3 load level for both elastic and long-term deformations appears to be a reasonable compromise. It should be noted that in design practice, consolidation settlement is only considered when the soil profile within the depth of influence contains saturated, fine grained soils. Furthermore, it is typical to include the consolidation settlement in the total, i.e., uniform settlement estimate based on an equivalent uniform pressure. To account for the moment loading which gives rise to non-uniform soil pressure and for variability of the soils under the foundation, many designers find it prudent to assume a consolidation tilt magnitude based on a portion of the uniform consolidation settlement. In this work, we limit our focus to elastic tilt.

A common theoretical formula for calculating elastic rotation of a surface foundation under an overturning moment with the base in full contact is as follows (Poulos & Davis, 1974; Madhav & Poorooshasb, 2001):

$$\tan(\theta) = M \frac{1-\nu^2}{EB^2L} I_\theta \tag{2.13}$$

where E is the elastic modulus of the subgrade soils, M is the applied moment at the S3 load level, L is footing length, B is footing width and I_θ is a shape and rigidity influence factor that is a function of foundation aspect ratio, Figure 2.7 (Bowles, 1996). For a rigid, square foundation, the influence factor is $I_\theta = 4.17$. This influence factor agrees very well with results published by Gazetas & Hatzikonstantinou (1988) which were based on extensive parametric boundary element

analyses and which yielded $I_\theta = 4.26$. These analyses also investigated the effect of embedment (trench effects) and sidewalls and found that trench effects were negligible compared to the effects of sidewalls. Wind turbine foundations are buried without sidewalls. Thus, it is convenient, reasonable and conservative to ignore any beneficial trench and sidewall effects.

For circular foundations with diameter B, the above equation becomes:

$$\tan(\theta) = M \frac{1-\nu^2}{EB^3} I_\theta \tag{2.14}$$

in which the influence factor I_θ varies between 3.0 for flexible foundations and 5.5 for rigid foundations (Tettinek & Matl, 1953; Taylor, 1967; Poulos & Davis, 1974). The above expressions assume the foundation to be bearing at ground surface without embedment and ignore the effects of vertical loads such as the self-weights of the turbine, foundation and the foundation backfill. Influence factors are tabulated in Bowles (1996) and were based on Taylor (1967) for rigid foundations and Tettinek & Matl (1953) for flexible foundation, Figure 2.7. Generally, industry practice treats the gravity-based foundation as rigid; i.e., $I_\theta = 5.5$. This assumption can be challenged for the larger foundations needed to support bigger wind turbines, especially if such foundations are bearing on hard or rock subgrades. However, this assumption has not been questioned probably because it is on the safe side. For polygonal foundation shapes such as a hexagon or an octagon, it would be logical to adopt a shape influence factor for a rigid foundation that varies between that for a square foundation, i.e., 4.2, and a circular foundation, i.e., 5.5.

Recalling that industry practice and guidelines do not allow gapping or zero pressure under the foundation for the S3 load level, the plan dimensions in these equations are the full foundation dimensions. Furthermore, per the draft IEC61400-6 standard, the elastic modulus used in this

estimate should be the static modulus which accounts for degradation associated with strain level. The tilt check is a simple pass/fail verification without any safety factors beyond the conservatism built into these assumptions.

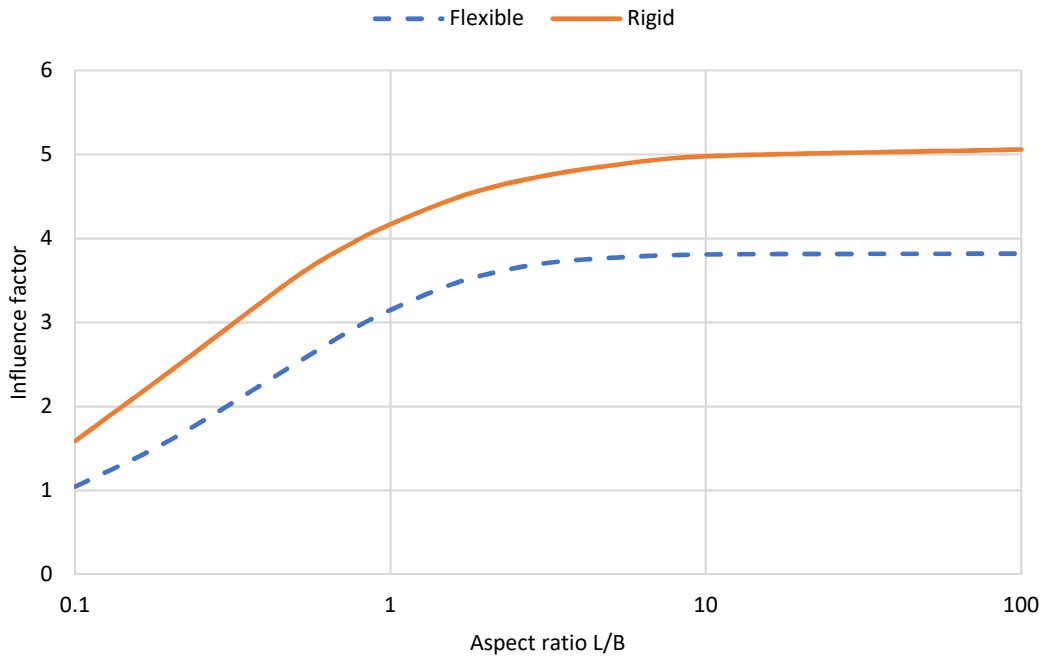

Figure 2.7 Shape influence factor for rectangular footings

2.6 Foundation Stiffness

Foundation stiffness is another serviceability limit state of great relevance to WTG foundation design. This section provides a literature review of foundation vibration modeling and describes how these methods are applied to the design of wind turbine foundations.

2.6.1 Analysis of Foundation Vibrations

In a 1983 state-of-the-art paper, Gazetas reviewed the progress of methods for analyzing the dynamic response of foundations subjected to machine-type loadings (Gazetas, 1983). The review covered the major milestones of this progress starting with the "dynamic Boussinesq" problem (Lamb, 1904), to the first attempted engineering application of "elastodynamic theory" (Reissner, 1936), and to the now widely accepted lumped-parameter inertia-spring-dashpot model for all modes of vibration (Richart & Whitman, 1967). In this model, four modes of vibration are considered: vertical, torsional, horizontal (lateral translation) and rocking (rotational). The vertical and torsional oscillation modes are axisymmetric and may be modeled independently of each other (uncoupled) using a single degree of freedom system for each mode:

$$m_x\ddot{x} + C_x\dot{x} + K_x x = P_x(t) \tag{2.15}$$

where x, $\dot{x}$ and $\ddot{x}$ are the vertical displacement (or angle of rotation around the vertical axis; i.e., twist), vertical velocity (or angular velocity) and vertical acceleration (or angular acceleration), respectively. Parameters m_x, C_x and K_x are equivalent mass (or the effective mass polar moment of inertia, I_z), effective damping and effective stiffness in the two different oscillation modes, respectively; while $P_x(t)$ is the dynamic loading applied by the vibrating machinery in the vertical or angular twist directions.

The other two modes; i.e., lateral translation and rocking, are antisymmetric and are therefore coupled. Theoretically, a two-degree of freedom system is necessary to represent such modes. In this case, the displacement, velocity and acceleration terms in the above equation of motion are 2×1 vectors to represent the horizontal and rocking degrees of freedom and the C and K parameters are 2×2 matrices with the off-diagonal terms representing the coupling terms. For

surface or shallow foundations, the coupling terms are small and are normally neglected for all practical purposes. However, for deep foundations and stubby piles, the coupling terms are as important as the diagonal terms and cannot be neglected.

The lumped-parameter model (LPM) proposed by Whitman & Richart (1967) adopted frequency-independent parameters m, C and K. However, since stiffness is known to be a function of frequency, Richart & Whitman (1967) introduced a fictitious mass to keep the resonant frequency constant and to obtain good agreement between the resonant frequency of the LPM predictions and the actual system response. In a more recent review of foundation vibration analysis methods, Dobry suggested that assuming frequency-independent stiffness and damping is not unreasonable for the vertical and horizontal vibration modes of circular or square foundations (Dobry, 2014). However, Dobry suggested that for foundations with higher aspect ratios and for the rocking and torsional vibration modes, assuming frequency independent parameters is not reasonable.

A solution that has proven effective in modeling the dependence of stiffness and damping on frequency is through complex numbers and the concept of impedance function or dynamic stiffness. The complex-valued impedance function is used to model stiffness and damping characteristics of foundations under dynamic loads and has a real part and an imaginary part as follows (Veletsos & Wei, 1971; Gazetas, 1975, 1991):

$$\bar{Z}_j = k_j + iwc_j \tag{2.16}$$

in which j denotes the degree of freedom in which vibration is occurring, i is the imaginary number, w is the angular frequency of the excitation in ($^{rad}/_{s}$), k_j is stiffness and c_j is damping.

This expression is sometimes written in the following form where β_j is interpreted as percent of critical damping:

$$\bar{Z}_j = k_j(1 + 2i\beta_j) \quad \text{where} \quad \beta_j = \frac{wc_j}{2k_j} \tag{2.17}$$

Based on a literature review of available impedance solutions, Pais & Kausel (1988) proposed that a simpler form of the impedance function as a product of static stiffness, K_j, and a complex, frequency-dependent, dynamic modifier, S_j:

$$\bar{Z}_j = K_j S_j(a_0) \quad \text{where} \quad S_j(a_0) = k_j + ia_0c_j \tag{2.18}$$

In the above equation, a_0 is the dimensional frequency defined as $a_0 = {wb}/{V_s}$ where b is half the foundation width, i.e., $b = {B}/{2}$, and V_s is the shear wave velocity of the soil.

For lumped-parameter models with multi-degrees of freedom, an impedance matrix $\mathbf{Z}$ is defined such that its terms, for example for a two-degree of freedom system, Z_{ij} can be expressed, as a function of dimensional frequency, a_0, as follows (Andersen, 2010):

$$Z_{ij}(a_0) = K_{ij}S_{ij}(a_0) \tag{2.19}$$

where K_{ij} is the static stiffness and $S_{ij}(a_0)$ is a frequency-dependent dynamic stiffness coefficient. The frequency-dependent stiffness coefficient , $S(a_0)$, had been suggested to be made up of two parts: a singular part, $S_s(a_0)$, and a regular part, $S_r(a_0)$ (Wolf, 1994):

$$S(a_0) = S_s(a_0) + S_r(a_0) \tag{2.20}$$

The singular part is of the form:

$$S_s(a_0) = k^\infty + ia_0c^\infty \tag{2.21}$$

where k^∞ and c^∞ are stiffness and damping constants selected such that $KS_s(a_0)$ is equal to the total stiffness in the high frequency limit, i.e., as $a_0 \to \infty$. The regular part, $S_r(a_0)$ is the remaining part of the dynamic stiffness; i.e.:

$$S_r(a_0) = \frac{Z(a_0)}{K} - S_s(a_0) \tag{2.22}$$

and is calculated by fitting a rational filter to the above result using domain transformation methods (Andersen, 2010). Some key features of the foregoing formulation are:

1. It is exact for the static limit since $S(a_0) \to 1$ as $a_0 \to 0$; hence $Z(0) = K$, and
2. It is exact in the high frequency limit since $S_r(a_0) \to 0$ and $S(a_0) \to S_s(a_0)$ as $a_0 \to \infty$.

2.6.2 Dynamics of Shallow Wind Turbine Foundations

The foregoing vibration analysis review is applicable to general machine foundations with multiple modes of vibration and where excitation frequency can be high. This review is equally valid for wind turbine foundation dynamics. However, some simplifications are possible for wind turbine foundations. For example, the excitation frequency under normal and extreme operational conditions is typically less than 1 Hz; i.e., in the low frequency range. Thus, the frequency dependence can be ignored. Furthermore, theoretically there are three rotational and three translational degrees of freedom. The rotational degrees of freedom consist of two rocking freedoms about the two orthogonal horizontal axes and one torsional freedom about the vertical axis. The three translational degrees of freedom are in the three orthogonal axis directions. Due to

symmetry and due to the nature of the loading where the overturning moment is the predominant load component, the torsional and vertical vibrations are negligible and are normally ignored. In common practice, only the coupled rocking and horizonal modes are considered. For shallow foundations, the coupling terms are also negligible and the rocking and horizontal modes can be verified independently. For deep and short pile foundations, the coupling terms are significant and must be considered.

2.6.3 Verification of Foundation Stiffness Requirements

To ensure that quoted loads remain valid, turbine manufacturers specify the minimum required rocking and lateral impedances (dynamic stiffnesses). More recently, some turbine manufacturers started to also specify the minimum static stiffnesses, typically as fractions of the dynamic stiffnesses. In addition to validity of loads, an important reason for minimum stiffness requirements is to avoid amplification of movements due to resonance of the tower-foundation system with applied excitations. In designing wind turbine support structures, it is important to ensure safe separation of the different eigen-mode frequencies of the tower-foundation system and excitation frequencies. For example, DNV/Risø recommends a minimum 10% frequency separation the first natural frequency of the system and the rotor and blade passing frequencies (DNV/Risø, 2002). Sometimes, when separation is not possible, wind turbine operational controls are designed to ensure a "safe pass through."

Due to the simplifications that can be assumed for wind turbine foundations, only the rocking stiffness is investigated in this dissertation. Based on elastic theory, the rocking stiffness of a surface circular foundation supported on an elastic half space can be calculated as (Arya *et al.*, 1979):

$$K_r = \frac{8GR^3}{3(1-\nu)} \tag{2.23}$$

where R is the radius of the foundation ($R = B/2$), ν is Poisson's ratio and G is the shear modulus. Wind turbine foundations are typically embedded and have backfill over them. Furthermore, bedrock or a hard stratum is not too deep below the bearing depth of the foundation. These factors improve the foundation stiffness and damping. It is common for designers to multiply the stiffness by an enhancement factor, η_ψ For embedded foundations where bedrock or a hard stratum is within a depth of influence, the rocking stiffness as calculated above is multiplied by an enhancement factor, η_ψ (DNV-GL, 2016b):

$$\eta_\psi = \left(1+2\frac{D}{R}\right)\left(1+0.7\frac{D}{H_b}\right)\left(1+\frac{R}{6H_b}\right) \tag{2.24}$$

In the above equation, D is the foundation depth and H_b is the distance from the bottom of the foundation to bedrock or hard stratum. The rocking stiffness equation then becomes:

$$K_r = \frac{8GR^3}{3(1-\nu)}\left(1+2\frac{D}{R}\right)\left(1+0.7\frac{D}{H_b}\right)\left(1+\frac{R}{6H_b}\right) \tag{2.25}$$

Dynamic and static stiffnesses are checked at different strain levels and with due consideration of zero-pressure conditions if they are present at the different serviceability load levels (as allowed in common industry practice). Ntambakwa *et al.* (2016) surmised that the dynamic stiffness should be evaluated using strain-corrected dynamic shear modulus. The zero-strain shear modulus is commonly obtained from shear wave velocity measurements and corrected for strain level. Ntambakwa et al. suggested that the strain-level correction for the dynamic stiffness estimate should be for operational level loads. On the other hand, they suggested that the

static stiffness should be based on a shear modulus corresponding to higher strain levels appropriate for the extreme load cases. They reference the 2002 DNV guidance on this subject (DNV/Risø, 2002). Per this guidance, the strain levels to be expected for wind and ocean waves in up to 10^{-2}, typically around 10^{-3}. In Section 2.4, it was suggested that this DNV guidance may be conservative and that a more appropriate shear strain range is 10^{-4} to 10^{-3}. We will adopt this strain level range for the analyses in this dissertation. For reference, the draft IEC6400-6 standards makes the following requirements (IEC, 2016):

1. Dynamic stiffness is to be verified using small strain shear modulus at the S3 load level and accounting for reduced contact area if this is present at this load level
2. Static stiffness is to be verified using a shear modulus that is reduced for the appropriate strain at the S1 load level and considering reduced contact area under this load level. This dissertation investigates rocking stiffness at the S1 load level following this recommendation. However, it would be interesting to compare results from this procedure to the findings of Gazetas *et al.* (2013) which included rocking stiffness of foundations in the nonlinear range and with loss of contact.

2.7 Bearing Capacity

The built environment contains structures that are supported on foundations and that have performed adequately for centuries. It is evident that the design of such foundations had ample safety margins above the ultimate loads that they could withstand. However, to this day, there is no general exact analytical solution for computing the ultimate vertical load that a foundation can carry even though there are several rigorous equations or coefficients for specific geometry, loading and/or geotechnical conditions. It is difficult to develop broader analytical solutions because geomaterials are highly variable and exhibit complex behavior that is dependent on stress

history, loading rates, presence of groundwater, and many more factors. This section contains a brief historical literature review of bearing capacity formulations and concludes with select equations that are in common use within the wind energy industry.

2.7.1 Basic Bearing Capacity and its Extensions

Early attempts to analyze ultimate bearing capacity of shallow foundations were based on Rankine's classical earth pressure theory developed in the late 19th century. Among those attempts were those by Pauker in 1889 and Bell in 1915 (Murthy, 2002). Later, the approach to this problem shifted to applications of plasticity theory. Prandtl investigated punching penetration of metals by subdividing the bearing material under and around the area under pressure into five zones: one centered triangular zone immediately under area and two wedges on either side. Failure would be equally likely to occur to the left or right by pushing out of the central zone and two zones, with all three zones forming what has been known as Prandtl's wedge. Prandtl applied Mohr's stress theory to arrive at a simple analytical equation for computing the ultimate punching resistance based on the material's shear strength in plain strain, c (Prandtl, 1920, 1921):

$$q_{ult} = (\pi + 2)c = 5.14c \tag{2.26}$$

The solution provided by Prandtl was quickly adapted to shallow foundations and was recognized as a valid solution for a strip footing subjected to a vertical load and bearing at the surface of a half space undrained clay medium, Figure 2.8. Prandtl's solution was later proven to be exact for these assumptions using the lower and upper bound theorems of the theory of plasticity.

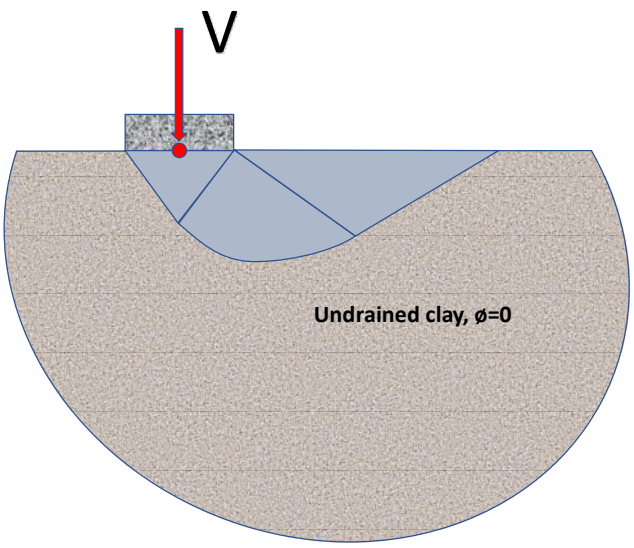

Figure 2.8 Cross-section of footing and Prandtl's wedge

In the early 1940's, Buisman, Caquot and Terzaghi extended Prandtl's equation to include the effects of overburden and width of the foundation (Terzaghi, 1943). The resulting equation for a strip footing of width B, depth D and undergoing the general shear failure mode shown in Figure 2.9 is elaborated assuming superposition principle as follows:

$$q_{ult} = c'N_c + q'_0 N_q + \frac{1}{2}\gamma B N_\gamma \tag{2.27}$$

where $q'_0 = \gamma D$ is the effective overburden pressure at foundation bearing depth and N_c , N_q and N_γ are bearing capacity coefficients. The N_c and N_q coefficients have their origins in Prandtl's work and are expressed rigorously as follows:

$$N_q = e^{\pi \tan\phi'} \frac{1+\sin\phi'}{1-\sin\phi'} \quad and \quad N_c = (N_q - 1)\cot\phi' \tag{2.28}$$

However, the N_γ term has several published approximations but the version produced by Martin assuming an associative flow rule is rigorous (Hansen, 1970; Martin, 2005):

$$N_\gamma = \frac{3}{2}(N_q - 1)\tan\phi' \tag{2.29}$$

Equation (2.27) is the most general expression for strip footing bearing capacity that can possibly be argued to be rigorous or "exact." Subsequent extensions obtained by various researchers to account for differing conditions such as foundation shape, load inclination, ground slope and base inclination are approximate and are typically in the form of correction factors applied to the terms of the basic bearing capacity equation, Figure 2.10 (e.g. Meyerhof, 1953; Hansen, 1970; Vesic, 1975).

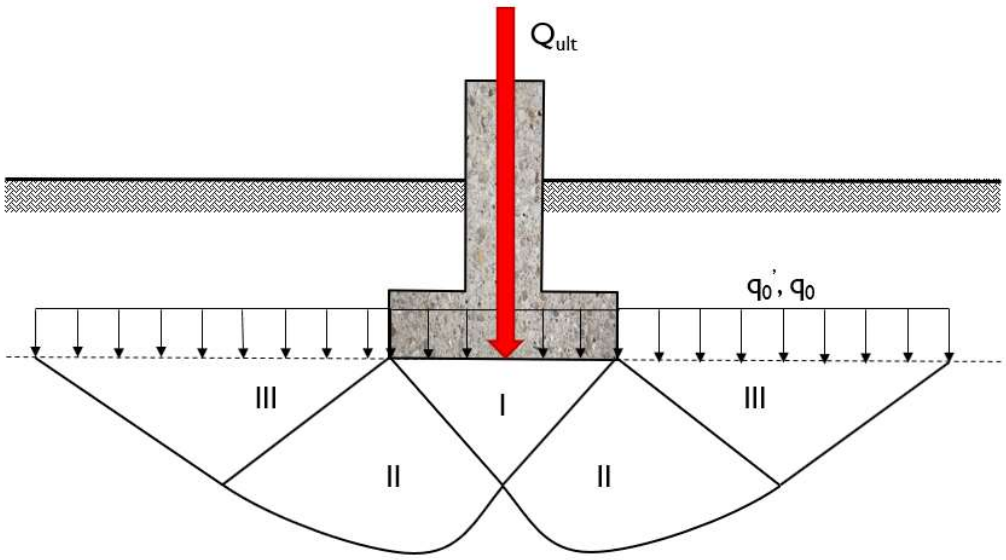

Figure 2.9 Terzaghi's general bearing failure surfaces

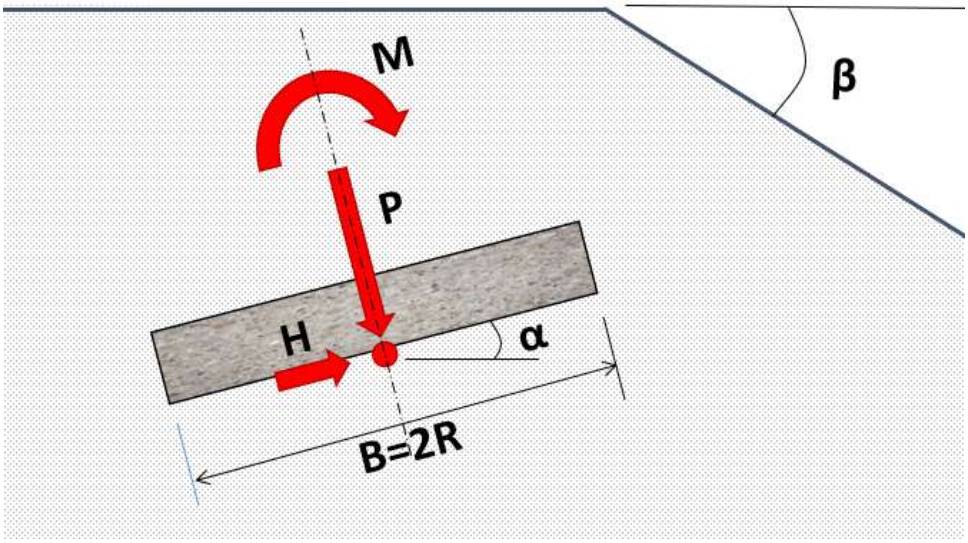

Figure 2.10 Footing and loading arrangements affecting bearing capacity

2.7.2 Generalized Bearing Capacity Equations

For problems treated in this dissertation, the foundation is always assumed to be flat (no base inclination). The ground is also assumed to be flat, even though it is common for a wind turbine to be located on top of mountains and close to the edge of mesas. The generalized bearing capacity equations adopted in this dissertation are in agreement with the forms recommended by DNV GL, a leading certification agency in the wind energy industry (DNV, 1992; DNV-GL, 2016b). Per DNV GL guidance, bearing capacity should be verified for undrained and/or drained conditions as appropriate for the project conditions. Furthermore, this guidance recommends the verification of two bearing capacity rupture modes: Rupture 1 for "normal" eccentricity cases and Rupture 2 for "extreme" eccentricity cases (Figure 2.11).

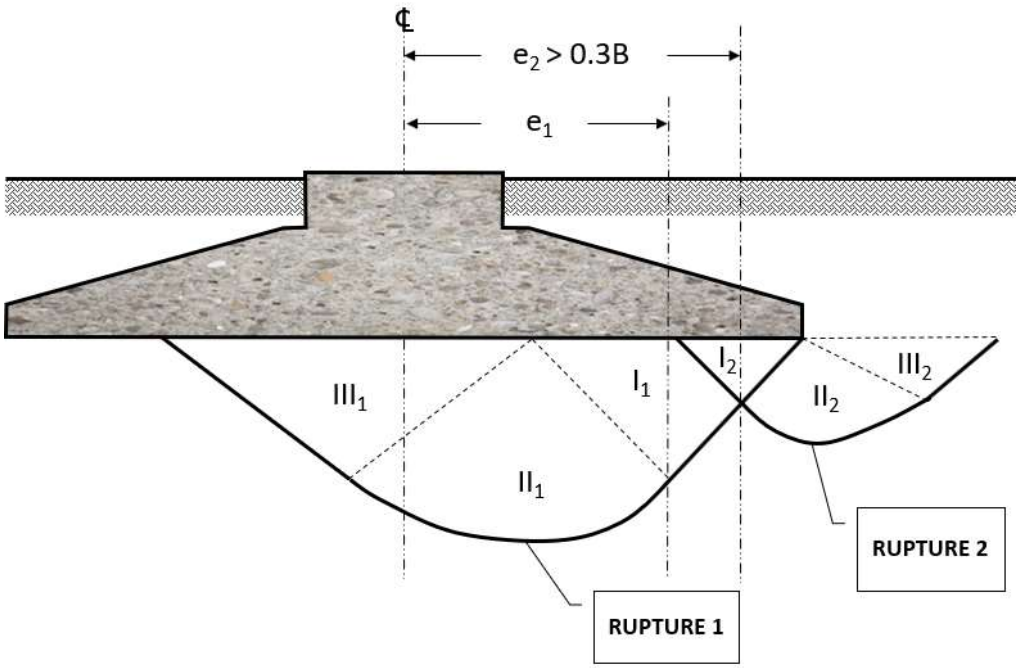

Figure 2.11 Two bearing capacity rupture modes (DNV-GL, 2016b)

2.7.2.1 Drained Conditions

For drained conditions, the "generalized" bearing capacity equation for a $c'-\phi'$ soil (effective stress analysis) is expressed as follows:

$$q_{ult} = c'N_c s_c d_c i_c + q_0' N_q s_q d_q i_q + \frac{1}{2}\gamma' b_{eff} N_\gamma s_\gamma d_\gamma i_\gamma \tag{2.30}$$

Where (i) N_c , N_q and N_γ are bearing capacity coefficients as defined in equations (2.28) and (2.29), (ii) s_c , s_q and s_γ are shape correction factors (Table 2.1), (iii) d_c , d_q and d_γ are depth correction factors (Table 2.1), (iv) i_c , i_q and i_γ are load inclination correction factors (Table 2.1), (v) b_{eff} is effective foundation width, and (vi) γ' is effective unit weight of the soil.

Table 2.1 Shape, depth and load inclination correction factors (DNV-GL, 2016b)

Term Affected	Foundation Shape	Foundation Depth	Load Inclination
N_c	$s_c = 1 + 0.2\frac{b_{eff}}{l_{eff}}$	$d_c = 1 + 0.4\frac{D}{b_{eff}}$	$i_c = \left(1 - \frac{H}{V + A_{eff}c'\cot\phi'}\right)^2$
N_q	$s_q = 1 + 0.2\frac{b_{eff}}{l_{eff}}$	$d_q = 1 + 1.2\frac{D}{b_{eff}}(1-\sin\phi')^2\tan\phi'$	$i_q = \left(1 - \frac{H}{V + A_{eff}c'\cot\phi'}\right)^2$
N_γ	$s_\gamma = 1 - 0.4\frac{b_{eff}}{l_{eff}}$	$d_\gamma = 1.0$	$i_\gamma = \left(1 - \frac{H}{V + A_{eff}c'\cot\phi'}\right)^4$

2.7.2.2 Undrained Conditions

For undrained conditions (constant volume response of bearing soils and $\phi = 0$), the bearing capacity equation reduces to:

$$q_u = s_u N_c^0 s_c^0 d_c^0 i_c^0 + q_0 \tag{2.31}$$

where $N_c^0 = \pi + 2 = 5.14$, $s_c^0 = s_c = 1 + 0.2\frac{b_{eff}}{l_{eff}}$ and $i_c^0 = \frac{1}{2} + \frac{1}{2}\sqrt{1 - \frac{H}{A_{eff}s_u}}$. The depth correction factor can conservatively be taken as unity, i.e., $d_c^0 = 1.0$.

2.7.2.3 Extreme Eccentricity

Under extreme eccentricity, defined by DNV GL as a load eccentricity greater than $0.3B$, DNV GL recommend that an additional rupture mode, i.e. Rupture 2 in Figure 2.11, be verified and provide a different bearing capacity equation for this check. This dissertation will not consider this rupture mode since current practice for designing onshore wind turbine foundations does not generally approach this eccentricity.

2.7.3 Effective Area Approach

Eccentric loads produce a non-uniform pressure distribution under the foundation. If the load center is outside the middle third of the foundation dimension (in either the B or L directions, or both), part of the foundation either loses contact or has zero contact pressure with the soil. In this case, bearing resistance is provided only by the part of the foundation area where the soil is providing support. As overturning loads increase, the contact area that is providing resistance decreases. Therefore, the bearing capacity of a foundation that is subjected to combined loading is a function of not only the foundation shape, embedment depth and the strength of the bearing materials, but also of the applied loading. For combined loading, the nature of the loading changes some of the basic geometric parameters that go into the bearing capacity equations. Moreover, for certain combinations of moment, horizontal load and vertical load, the failure mode may change. For example, the critical failure mode can change from a general shear failure for predominantly vertical loading to a sliding failure for predominantly horizontal loading. Combined loadings introduce complex soil-structure interactions dependent on foundation-soil relative stiffnesses and the relative magnitudes of the loading components. The limitations of the generalized bearing capacity equation are therefore apparent, especially for highly eccentric loading. Generalized bearing capacity equations found in the literature may work well for common foundations with reasonable load eccentricity but are not adequate for foundations subjected to large overturning moments such as wind turbine foundations.

A classic approach to deal with the reduced area caused by eccentric loading is to base bearing capacity on the effective dimensions of the foundation. This approach seemed reasonable and worked well for traditional structures. For lack of a better alternative, or probably because of its familiarity, this approach is also widely used for designing wind turbine foundations.

Assumptions and derivations of effective area dimensions for common foundation shapes such rectangular, octagonal or circular, are published widely. A common approximation of the effective area for circular or octagonal foundation is a uniform pressure rectangular area centered on the load center (Figure 2.12), (DNV-GL, 2016b).

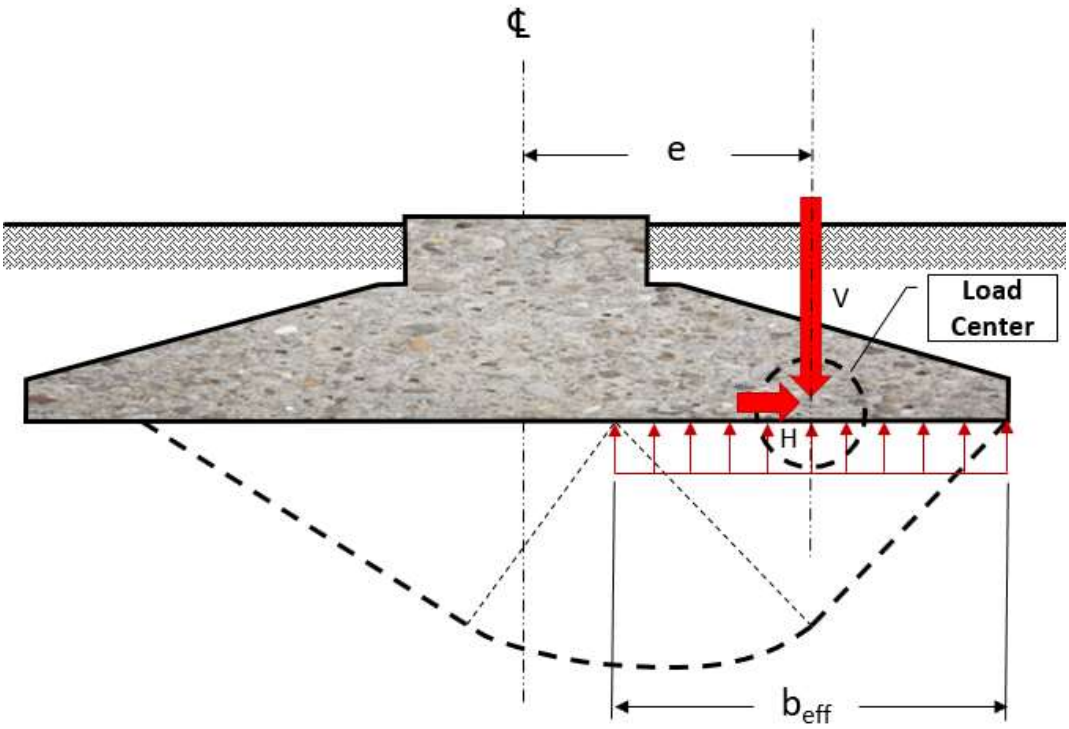

Figure 2.12 Uniform pressure area centered on load center

The uniform pressure effective area is constructed such that its geometrical center coincides with the load center while adhering as much as possible to the true geometry of the foundation. For a circular foundation of radius R and resultant load eccentricity e, the contact area is bounded by two circular segments with common secant midpoints located at the load center Figure 2.13. The area of this shape is equal to:

$$A_{eff} = 2\left[R^2 \operatorname{acos}\left(\frac{e}{R}\right) - e\sqrt{R^2 - e^2} \right] \tag{2.32}$$

and its major axis dimensions of this shape are:

$$b_e = 2(R - e) \quad \text{and} \quad l_e = 2R\sqrt{1 - \left(1 - \frac{b_e}{2R}\right)^2} \tag{2.33}$$

This contact shape is further simplified as an equivalent rectangular area with the following effective dimensions:

$$l_{eff} = \sqrt{A_{eff}\frac{l_e}{b_e}} \quad \text{and} \quad b_{eff} = \frac{l_{eff}}{l_e} b_e \tag{2.34}$$

The effective rectangular area dimensions given by equations (2.34) are used in the generalized bearing equations and the corrections factors described in Section 2.7.2.

2.8 Interaction Curve Approach

Researchers are drawing on plasticity theory, numerical methods and experimental testing to study the modes of failure and nonlinear soil-structure interactions of rocking foundations. Houlsby & Purzin (1999) investigated the extension of Prandtl's theory to a strip footing subjected to combined loading. They found that while Prandtl's equation can be proven to be exact using the lower- and upper- bound theorems of the theory of plasticity for a strip footing under vertical loading, the same cannot be said for the case involving combined loading. In fact, the existence of a unique or exact solution could not be proven. Houlsby & Purzin (1999) described a method that is based partly on the bound theorems of plasticity and on additional necessary ad-hoc assumptions to arrive at various solutions that bracket a "working" solution.

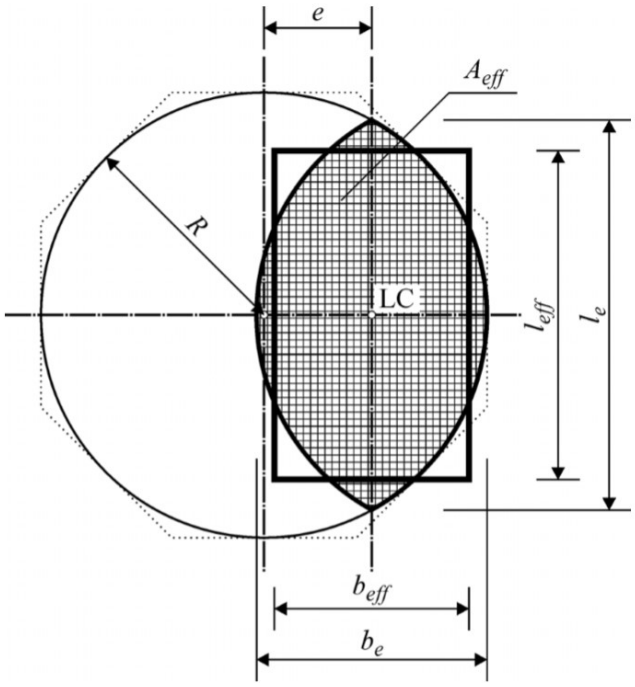

Figure 2.13 Effective foundation dimensions. Courtesy (DNV-GL, 2016b)

Many other researchers tackled the problem of foundations subjected to combined loading using sophisticated finite element formulations to study the various failure mechanisms under different loading scenarios. Researchers found that it was convenient and insightful to present results of such investigations in the form normalized failure envelopes which are interaction curves, similar in concept to moment-axial load interaction curves for axial column capacity. For a column capacity curve, VM combinations that plot within the curve are safe, while for those that plot outside indicate inadequate column load carrying capacity. The failure envelope concept was used for foundation stability assessment by Roscoe & Schofield (1957) and the method was elaborated further by Murff (1994). It is widely used for offshore structure foundations where loading is highly eccentric due to seafloor depth and considerable horizontal loads caused by wind and wave actions. For offshore structures, failure envelopes are often expressed as three-

dimensional yield surfaces in normalized VMH space. Combinations of VMH within this surface are acceptable while those outside of it are unsafe. Another form to present VMH interactions is through a tilted ellipsoid in two-dimensional space. There is considerable research describing the development and applications of the failure envelope approach (Griffiths, 1980; Bell, 1991; Butterfield & Gottardi, 1994; Bransby & Randolph, 1997; Gottardi *et al.*, 1997; Houlsby & Purzin, 1999; Bransby, 2001; Cassidy *et al.*, 2005; Zhang, 2008; Cassidy *et al.*, 2013; Shen *et al.*, 2016). For onshore structures (wind or otherwise), foundation sliding is not a common failure mode. Therefore, the horizontal load component is often combined with the moment component as an additional moment (H times the moment arm) and the interaction curves are elaborated in normalized VM space. Based on literature review, the following parabolic equation is found to be a good fit for published VM interaction curves (Gottardi & Butterfield, 1993; Tang *et al.*, 2015):

$$m = \frac{\eta_1}{FS}\left[1-\left(\frac{1}{FS}\right)^{\eta_2}\right] \tag{2.35}$$

In the above equation, η_1 and η_2 are curve fitting parameters, $FS = {V_{u0}}/{V}$ is the bearing capacity factor of safety (under pure axial loading), and $m = {M}/{BV_{u0}}$ is normalized rocking moment. Fitting parameters from several published studies are shown in Table 2.2 below. These interaction curves are plotted on Figure 2.14. There are a few important notes to make based on this table and figure, as discussed in the next subsections.

Table 2.2 VM interaction curve fitting parameters and maximum moment capacity

Reference	Parameter η_1	Parameter η_2	Moment Capacity	FS at Maximum Moment Capacity
Meyerhof (1953)	0.50	0.50	$0.074V_{u0}B$	2.25
Loukidis *et al.* (2008)	0.44	0.625	$0.078V_{u0}B$	2.2
Gottardi & Butterfield (1993)	0.36	1.0	$0.09V_{u0}B$	2.0
Gazetas (2015)	0.55	1.0	$0.138V_{u0}B$	2.0

2.8.1 General VM Interaction Curve Comments

The interaction curve developed by Meyerhof which is based on the effective area approach discussed in the earlier section as the method in use by the wind energy industry, this curve yields the lowest maximum moment capacity and is therefore the most conservative. Furthermore, it should be noted that all curves yield a maximum moment capacity at $FS \approx 2$ with the Meyerhof maximum moment capacity at $FS = 2.25$. Incidentally, this is also the bearing capacity factor of safety adopted by the wind energy industry but the reasoning used to arrive at this number is not based on interaction curves (AWEA & ASCE, 2011). If we accept that the maximum moment capacity is around $0.10V_{u0}B$, a load equal to the vertical bearing capacity V_{u0} that is placed at an eccentricity of $M_u / V_{u0} = 0.10B$ would cause bearing capacity failure.

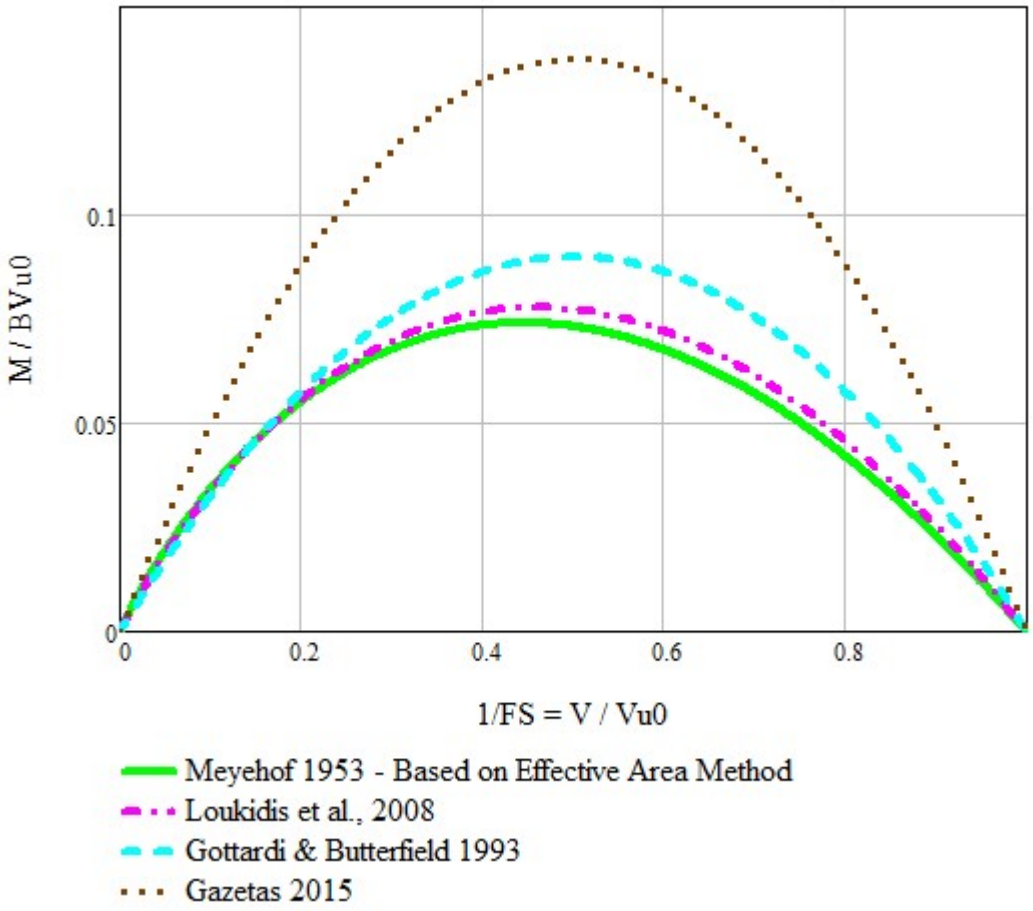

Figure 2.14 Normalized VM interaction curves by several researchers

2.8.2 VM Curve Comments Relative to Wind Turbine Foundations

Wind turbine foundations are lightly loaded in the downward vertical direction; i.e., gravity loads are low. However, they are subjected to large overturning moments. Under these circumstances, uplift behavior of the foundation will almost always prevail, Figure 2.14 (Gazetas, 2015). Per commonly accepted industry practice, they are sized to maintain positive contact with the subgrade at S3 level loads and not to lose contact for more than half the foundation width at the S1 level loading. This means that for loads between the S3 and S1 levels, zero pressure or no contact conditions exist over a length ranging from zero to half the foundation width. Gazetas *et*

al. (2013) investigated nonlinear rocking stiffness of surface foundations bearing on undrained half-space. Their investigation used advanced finite element modeling involving a tensionless contact algorithm to model loss of contact with the subgrade, as well as shear modulus degradation with strain level. They describe the foundation-soil system response to increasing overturning moment as going from elastic and fully bonded response at low load levels, to nearly-elastic but nonlinear response when part of the foundation loses contact with the subgrade and, finally, to full mobilization of overturning failure mechanisms or full mobilization of bearing capacity mechanisms under very extreme eccentricity. Due to the low vertical loading, wind turbine foundations are likely to fail by overturning mechanisms rather than by bearing capacity mobilization. In fact, based on finite element analyses, Kourkoulis *et al.* (2012) proposed the following approximation of the overturning angle as a function of factor of safety:

$$\frac{\theta_c}{\theta_{c,\infty}} \approx \left(1-\frac{1}{FS}\right)+\frac{1}{3\sqrt{FS}}\left(1-\log\frac{h}{0.5B}\right) \tag{2.36}$$

The tilt angle is plotted for several wind turbine hub height and foundation width combinations, starting with a common combination of 80 m hub height and 17 m base and considering two more unusually slender combinations. For a 20 m wide foundation supporting a 90m hub height turbine and designed for a bearing capacity factor of safety $FS = 2.25$, the approximate critical tilt angle that would cause toppling is about 3.6 degrees. Recall that we estimated the critical angle of rigid system and subgrade ($FS \approx \infty$) to be around 6 degrees in Section 2.5.1. Both estimates are still optimistic due to load dynamics. However, it is still useful to compare these critical tilt limits to the common limit of 0.17 degree.

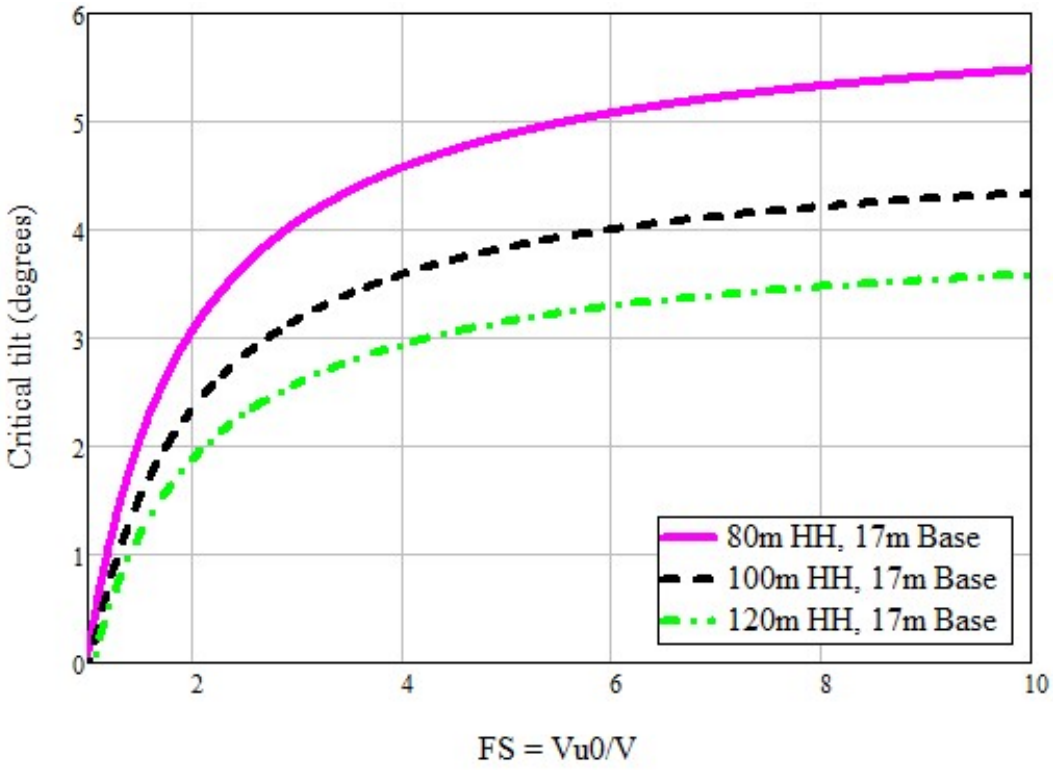

Figure 2.15 Approximate critical tilt angle (Kourkoulis *et al.*, 2012)

2.9 Deterministic Finite Element Analysis

The finite element method is a powerful numerical modeling tool that is widely used in structural and geotechnical analysis and design. Soil-structure interactions can be captured in detail and the results can be readily used for design purposes. In this section, we illustrate an example implementation of the finite element method to study wind turbine foundation soil-structure interactions and obtain the response quantities necessary for foundation geotechnical as well structural (reinforced concrete) design. Figure 2.16 shows finite element models of circular and octagonal footings produced using STAAD.Pro, a commercial general purpose finite element program (Bentley, 2018). The footings are modeled using plate elements. The subgrade is represented using compression only springs with spring coefficients computed at every node based

on an assumed modulus of subgrade reaction and on the tributary area for the node (Terzaghi, 1955). Typically, plate element models with compression only springs are enough to reproduce the basic soil-structure interaction features and provide the main response quantities (bearing pressure, moments, etc.) needed for design. If more detailed response features are of interest, solid models are normally required.

To investigate the influence of the subgrade stiffness, three modulus of subgrade reactions values are considered, representing soft, medium and hard subgrades. The selected values are based on typical ranges (e.g.Das, 2007). The overturning moment is applied at the center and is distributed around the tower base through an assemblage of stiff columns and beams. Foundation dimensions and loading are representative of a typical foundation for an 80-meter hub height WTG. The width or diameter of the octagonal and circular foundations have been selected so that two foundations have the same area. All other dimensions and unit weights are identical for both foundations and are summarized in Table 2.3.

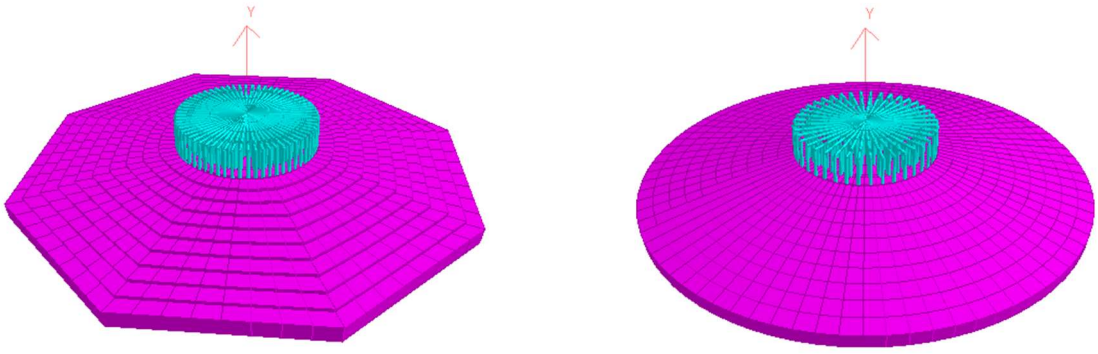

Figure 2.16 Finite element models of octagonal and circular WTG foundations

Table 2.3 Parameters used in the finite element analyses

Foundation dimensions		**Unit weights and moduli**	
Diameter or width	Circle: 17.0 m Octagon: 16.5 m	Concrete unit weight	23.5 kN/m^3
Edge thickness	0.5 m	Backfill unit weight	17.5 kN/m^3
Middle thickness	1.7 m	Modulus of subgrade reaction	Soft: 25 MN/m^3 Medium: 80 MN/m^3 Hard: 250 MN/m^3
Pedestal height	1.0 m	Elasticity modulus (concrete)	28.3 GPa
Foundation depth	2.5 m	Poisson's ratio (concrete)	0.17

Base pressure is an important design parameter as it is used to verify soil bearing capacity, to perform concrete design and to estimate tilt and settlement. For this reason, base pressure is evaluated at eight load steps. Table 2.4 lists the eight load steps and the practical motivation of their selection.

2.9.1 Contact Pressure Changes under Increasing Load

The contours shown on Figure 2.17 and Figure 2.18 correspond to increasing levels of overturning moment with the first step limited to self-weight of the footing, the soil backfill and the turbine dead load and the last step corresponding to the factored design moment. As can be seen from these series of plots, the foundation starts off by being under concentric pressure contours. The contours then shift under the effect of the increasing overturning moment. Similar pressure contour patterns are noted for circular and octagonal foundations.

Table 2.4 Load steps considered in the finite element analyses

Step	Description and significance
DL	Dead loads: self-weight of WTG, backfill and concrete. Contact pressure at the footing/subgrade interface is a baseline pressure in the absence of other operational loads.
$DL+0.2LL$	An intermediate low-pressure step with no special significance. LL represents the unfactored (characteristic) extreme loading case.
$DL+0.4LL$	SLS load levels typically range between 0.4 to 0.8 the extreme loading
$DL+0.6LL$	SLS load levels typically range between 0.4 to 0.8 the extreme loading
$DL+0.8LL$	SLS load levels typically range between 0.4 to 0.8 the extreme loading
$DL+1.0LL$	This level is of special interest at it represents the characteristic extreme loading
$DL+1.1LL$	Typical PLF for ULS checks
$DL+1.35LL$	Typical PLF for ULS checks
Note: For the example problem described in this section, the loads are: • WTG self-weight: 2275 kN • LL Moment: 51600 kNm • LL horizontal load: 660 kN	

2.9.2 Contact Pressure under Varying Subgrade Stiffness

Contours shown on Figure 2.19 illustrate the response for foundations that are identical except for the modulus of subgrade reaction. Three modulus values investigated:

1. A value representative of a "soft" subgrade such as soft and firm clays: 25 MN/m^3
2. A value representative of a "medium" subgrade such as sands and stiff to hard clays: 80 MN/m^3
3. A value representative of a "hard" subgrade such as cemented soils and rock of varying quality: 250 MN/m^3

The contours highlight the significant impact of footing/soil relative rigidity, whereby a footing supported on soft soils behaves as a rigid footing and one supported on rock behaves as a flexible foundation. In general, rigid footings (footings over softer subgrades) tend to have the maximum base pressure at the edge, while flexible footings (or footings over hard subgrades) have the highest pressure away from the edge. However, in terms of magnitude, with all other parameters being equal, the maximum base pressure tends to be lower for footings resting on softer subgrade. In the example, as shown in Figure 2.19, maximum base pressure for the "soft subgrade" case is about 30% lower than that for the "hard subgrade" case.

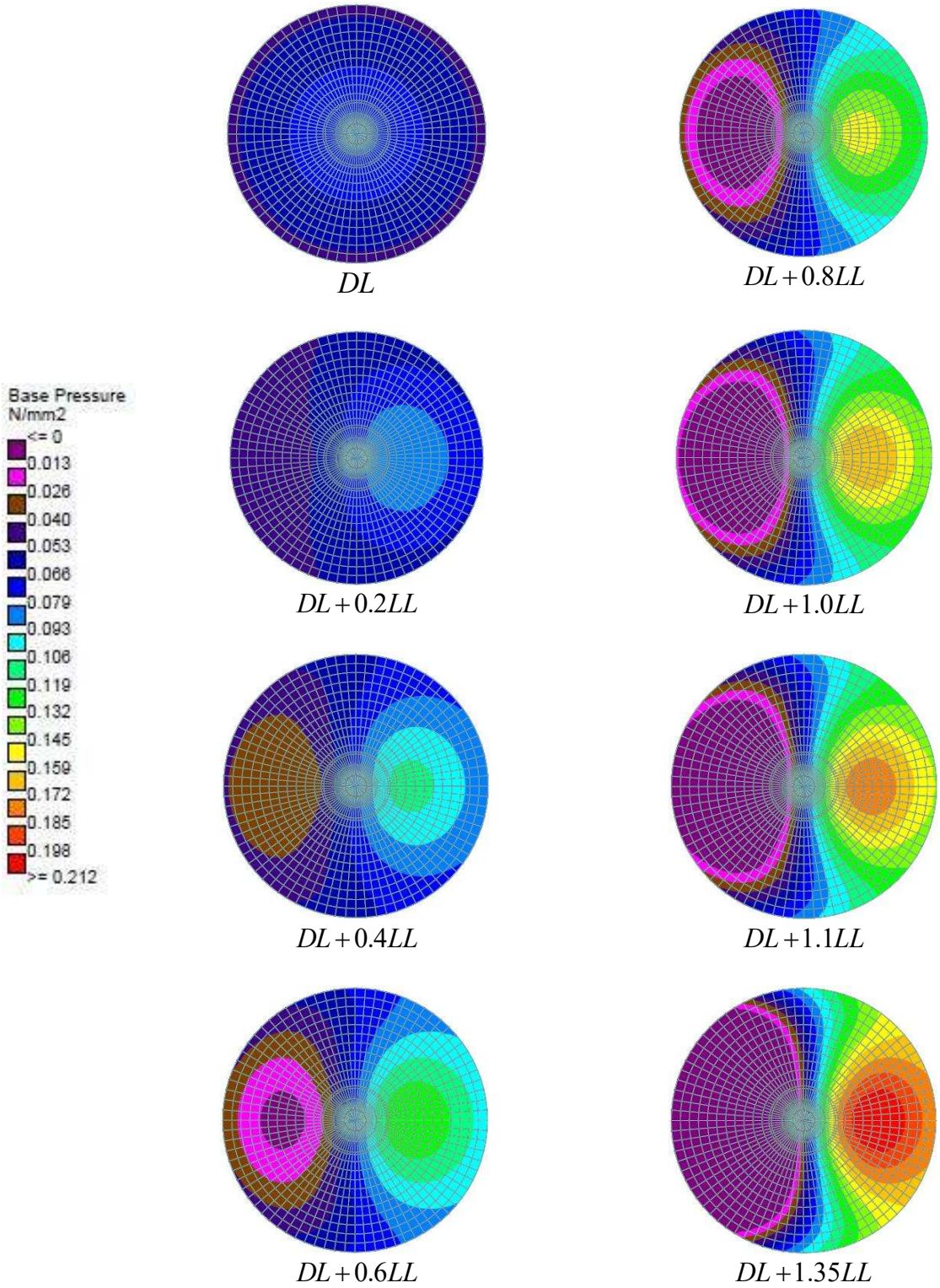

Figure 2.17 Contact pressure under circular foundation

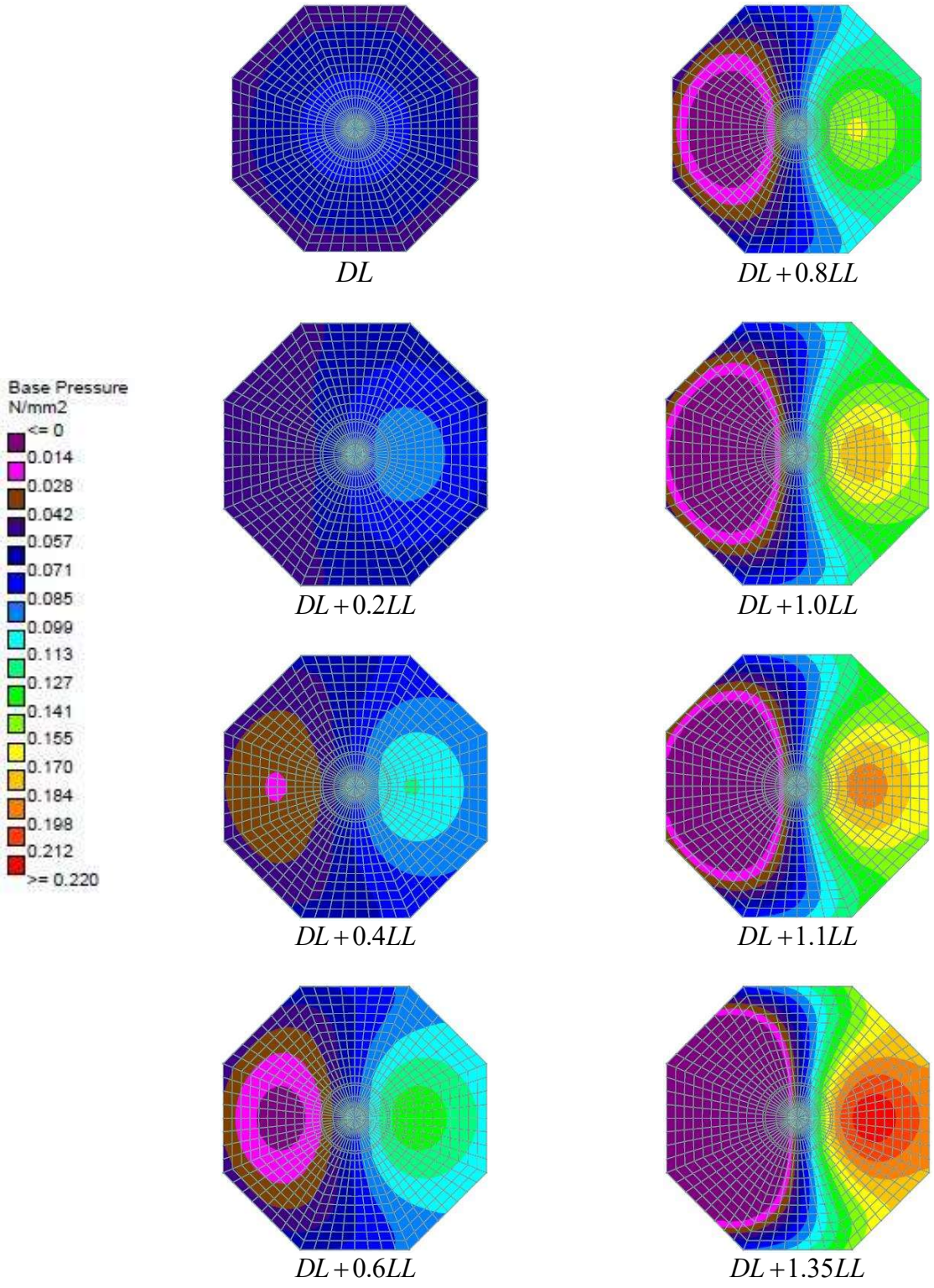

Figure 2.18 Contact pressure under octagonal foundation

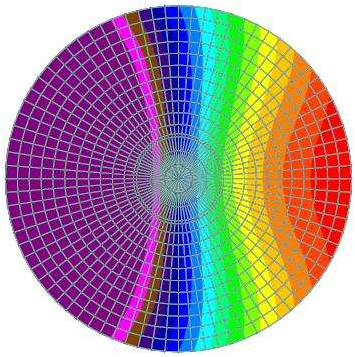

Soft subgrade
Maximum pressure = 214 kPa

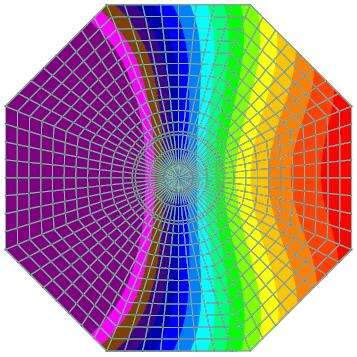

Soft subgrade
Maximum pressure = 226 kPa

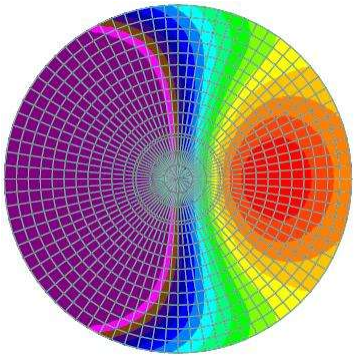

Medium subgrade
Maximum pressure = 212 kPa

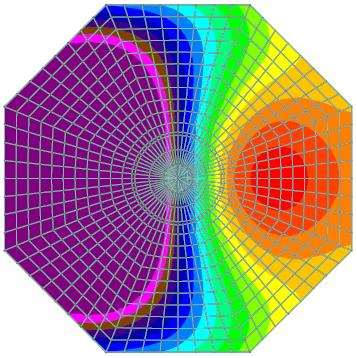

Medium pressure
Maximum pressure = 220 kPa

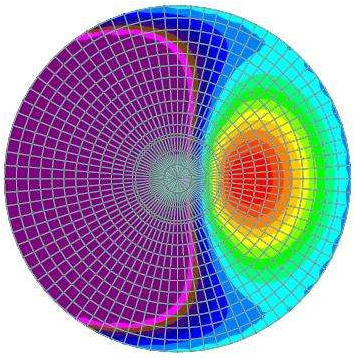

Hard subgrade
Maximum pressure = 294 kPa

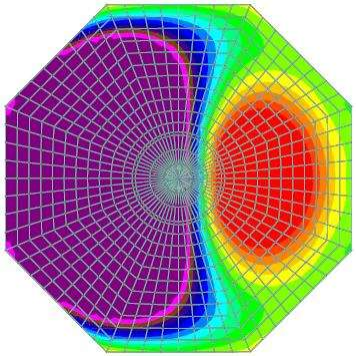

Hard subgrade
Maximum pressure = 304 kPa

Figure 2.19 Contact pressure for different subgrade stiffness at $DL + 1.35LL$

CHAPTER 3

CHARACTERIZATION OF GEOTECHNICAL UNCERTAINTY

Uncertainty is present in all kinds of environments, processes and phenomena. It is accepted that there is always some level of uncertainty in engineering practice. However, uncertainty is particularly more pervasive in geotechnical engineering. The deterministic computations described in Chapter 2 use representative values of geotechnical properties that are known to be uncertain. This chapter discusses the sources of uncertainty in such parameters, techniques to characterize their variability for a given project, different probability density functions used to model these parameters as random variables, and published literature on their typical ranges of variability. These topics are critical to the proper implementation of reliability-based design methods discussed in subsequent chapters. Understanding and assessing geotechnical design uncertainty is essential to proper use of reliability-based design methods and producing designs with quantifiable levels of reliability.

3.1 Geotechnical Uncertainty

Geotechnical design involves many uncertain sources. Uncertainties exist in the applied loads as well as in all the geotechnical parameters used to compute geotechnical resistance. Geotechnical materials are also heterogenous and design parameters are generally variable in space, even though natural processes such as tectonics, geology, erosion and deposition are governed by physical laws which can be understood, and which tend to render some level of predictability at differing scales. Uncertainties exist even in the historical data upon which event recurrence statistics and trends in natural phenomena are based, e.g., the effects of climate change, even though such uncertainties are rarely considered in design practice.

Many authors have written to describe different types and sources of uncertainty. The wealth of literature and the associated broad taxonomy resulted in much confusion on the types and sources of uncertainty and on whether some of these types need to be explicitly accounted for in design methods or have already been accounted for as part of the design process. One way to categorize uncertainties is to group them into three sources: inherent soil variability, uncertainties due to measurements and uncertainties due to transformation models, Figure 3.1. Many authors have also found it convenient to categorize uncertainty into two types: Type 1 - aleatory uncertainty arising from the natural variability and Type 2 - epistemic uncertainty arising from insufficient knowledge, Figure 3.2 (e.g. Apostolakis, 1990; Ferson & Ginzburg, 1996; Phoon & Kulhawy, 1999a; Whitman, 2000; Baecher & Christian, 2003). Since natural processes are governed by physical laws, it can be argued that all uncertainty is epistemic; i.e., caused by lack of understanding/knowledge of the physical laws and the settings upon which these laws act. Nevertheless, such categorizations are useful because they break up uncertainty sources (the known unknowns) into a few primary areas of focus. It should be mentioned that uncertainty modeling does not typically include gross or human errors since these are considered as deviations from established processes and are normally reduced via quality control measures. In this section, the common types of uncertainties identified in the literature are discussed in more detail.

3.1.1 Aleatory Uncertainty

Aleatory uncertainties represent sources that are naturally random and out of the designer's control; i.e., they cannot be reduced through more knowledge or data. A commonly accepted understanding of aleatory uncertainty is that it has an inherent as well as a spatial component. Several sources of aleatory uncertainty are described below with comments on how they relate to wind energy projects.

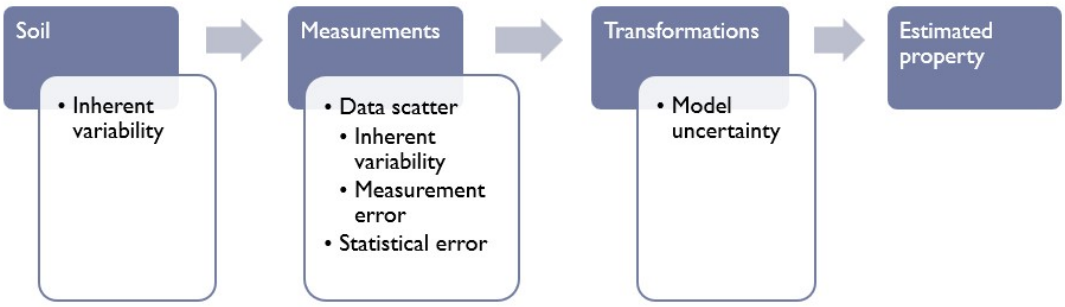

Figure 3.1 Uncertainty in soil property estimates (Kulhawy, 1996)

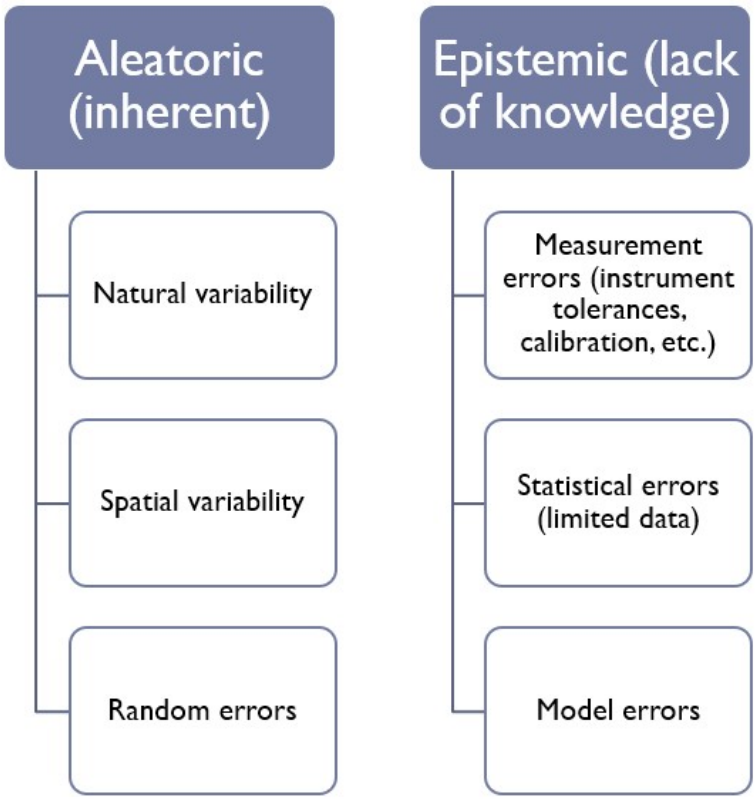

Figure 3.2 Sources of geotechnical design uncertainty

3.1.1.1 Inherent Variability

Inherent soil variability is related to natural randomness and does not include the influence of physical trends (e.g., shear strength or density increases with depth), predictable mixing of soils from different geologic units, or measurement errors. Inherent soil variability is present between any two points, no matter how close they are to each other or whether they belong to similar or the same soil layer.

3.1.1.2 Spatial Variability

Another source of uncertainty is due to spatial variability extending vertically and horizontally within influence distances from the foundation. An efficient method of modeling spatial variability is through random field theory, typically implemented using the Random Finite Element Method (RFEM) (e.g. Griffiths *et al.*, 2006; Griffiths *et al.*, 2013). In this theory, an important parameter used to quantify spatial variability is the spatial correlation length which is loosely defined as the distance within which the values of a given parameter are significantly correlated (Fenton & Griffiths, 2008). The larger the spatial correlation length, the more uniform is the random field and the lower is the rate of spatial variation. The reverse is also true: the smaller the spatial correlation length, the "choppier" is the field. Soil deposits are found typically in horizontal or near horizontal layers; therefore, spatial variability is anisotropic, and the spatial correlation length is generally larger in the horizontal direction than it is in the vertical direction. Based on a literature review, Huber (2013) provided a useful compilation of typical values of spatial correlation length for different soils.

3.1.1.3 Random Errors

Random or data scatter errors include those due to measurement errors from equipment, procedural, operator and random test effects.

3.1.2 Epistemic Uncertainty

Epistemic uncertainty represents sources that can be reduced through, among other things, better quality measurements (more accurate instruments), more data collection and improved procedures (better models).

3.1.2.1 Measurement Uncertainty

Measurement uncertainty is related to the equipment being used (tolerances and calibration), in-situ or laboratory test procedures, operator errors, and random scatter in the measured data. Naturally, measurement error is different for different test procedures. Reported measurement error data have been summarized for various laboratory and field tests by various investigators (e.g. Phoon & Kulhawy, 1999b). It is worthwhile to note that the highest variability attributed to in-situ test measurement error is that corresponding to the Standard Penetration Test (SPT). The error introduced by sample size is sometimes considered as a measurement error.

3.1.2.2 Statistical Uncertainty

Statistical uncertainty is associated with insufficient data being collected or insufficient sample size. Normally, the greater the number of data points or sample size, the smaller the error. However, beyond a rather low number of samples, it is more important to capture the full range of variability than to obtain more data points. For this reason, the effort to capture the full range of variability as early as possible in the life of a project is very important to the early assessment of risks. There are numerous simplified rules of thumb to estimate standard deviation and variability based on the range and number of samples (Tippett, 1925; Whitman, 2000; Foye *et al.*, 2006).

3.1.2.3 Model Uncertainty

In the literature, model uncertainty is described as that which is associated with the choice of the idealizations, assumptions, computational models as well as transformations performed on measured data to obtain design parameters. This uncertainty is meant to reflect current imperfect knowledge of the "real" behaviors or processes. This logic assumes that there is an "absolute truth" which we need to measure things against. A computational model is supposed to be the best available for a specific situation or application short of an absolute truth. Absolute truth will always remain as unknown or not completely understood. Thus, it is difficult to conceive of a way to measure progress towards an absolute truth or an end goal when that end goal is not completely understood. Furthermore, engineering design has long been performed per the state-of-the-art in human modeling of natural physical phenomena. When better models are developed, their merits are verified and then they are adopted; it does not seem rational to invoke this uncertainly only when reliability-based design is concerned.

Appendix D of ISO-2394 defines model uncertainty as that "emanating from imperfections of analytical models for predicting engineering behavior" (ISO, 2015). This ISO standard characterizes model uncertainty through a model factor applicable to each specific set of conditions which include failure mode, calculation models and local conditions. Furthermore, there are typically many geotechnical calculation models in a single design problem. For these reasons, this ISO standard anticipates a proliferation of model factors. The model factor is defined as the ratio of measured performance to predicted performance. However, it is not clear how such a ratio can be linked to calculation models or to a specific calculation model.

3.2 Geotechnical Uncertainly and Wind Energy Projects

Wind energy projects differ from most traditional projects in that they cover large terrains. Wind turbines are typically placed 5 to 10 rotor diameters apart to optimize energy extraction (Denholm *et al.*, 2009). Nowadays, common rotor diameter for utility-scale wind turbine generators is around 130 meters, signifying turbine typical spacing of 0.6 to 1.3 kilometers just for energy extraction efficiency. Therefore, wind turbines are too far apart to consider possible relationships or correlations between ground conditions from one turbine location to another. This is separate from regional or larger scale characteristics which may be applicable to the project area or portions of it, such as those related to different geologic settings or terrains.

Engineering design practice, including that within the wind energy industry, considers single representative value of geotechnical properties to represent an entire soil mass or a soil layer. With exploratory borings drilled in the vertical direction, focus is limited to variations in the vertical direction because a geotechnical exploration rarely goes beyond one boring at the center of the foundation unless there is strong reason to believe conditions are non-uniform. Knowledge of the vertical spatial variation is often limited to the line of the boring. On the other hand, knowledge in the horizontal direction is limited to observations of outcrops and the exposed foundation bearing surface. In general, this is very limited information but is standard industry practice. This is also why at least two forms of exploration should be carried out at each turbine location: a traditional boring and a geophysical survey such as Multi-channel Analysis of Surface Waves (MASW) survey.

3.3 Probabilistic Approaches to Uncertainty

As discussed in the previous section, geotechnical properties are uncertain; and the uncertainty could be attributed to many sources. Two schools of thought exist in the understanding

of probabilities associated with uncertain properties or variables: 1) a frequentist approach based on dry statistics and 2) a Bayesian approach based on "degree of belief."

The classical frequentist definition of probability is that which has been taught in engineering curricula and is based on dry, un-nuanced statistics. For example, if an experiment can yield a total number of equally likely outcomes, n_{total}, among which there are n_A equally likely outcomes of type A, then the probability of getting an outcome of type A is:

$$P(A) = \frac{n_A}{n_{total}} \tag{3.1}$$

The above definition of probability is useful in experiments that can be repeated with great fidelity and in large numbers; i.e., in production settings where thousands of "identical items" are manufactured following the same process. This setting is hardly relevant to civil engineering design where structures that are often unique are built on unique geotechnical conditions and are subjected to site specific environmental loads.

The Bayesian definition of probability is based on "degree of belief" and the probability of Event A, $P(A)$, is simply the degree of belief that Event A will occur. By definition, degree of belief is subjective. For the experiment example above, even when there are some statistics that indicate that the probability of event A could be n_A / n_{total}, the person providing the probability of Event A may give a different estimate based on his/her degree of belief which could be emanating from prior and/or personal experience, observations of other events, etc. Bayesian probability is also described as prior probability because a degree of belief has to be assumed prior to obtaining any new information or estimates of probability. The new information serves to update the prior

probability estimate or the degree of belief. Updating of the prior probability; i.e., obtaining the posterior, can be formulated using the conditional probability and the total probability theorems.

The conditional probability theorem expresses the probability of an Event A given an Event B has occurred, $P(A|B)$ as:

$$P(A|B) = \frac{P(A \cap B)}{P(B)} \tag{3.2}$$

In the above equation, $P(A \cap B)$ is the probability of both Events A and B occurring; i.e., the joint probability of Events A and B, and $P(B)$ is the probability of Event B. Since joint probability operation is commutative; i.e., $P(A \cap B) = P(B \cap A)$, the following equivalency is obtained:

$$P(A|B)P(B) = P(B|A)P(A) \tag{3.3}$$

The total probability theorem gives the probability of Event A, $P(A)$, in terms of prior probabilities of other events E_i for all events $i \ldots n$ in events space Ω:

$$P(A) = \sum_{i=1}^{n} P(A|E_i)P(E_i) \tag{3.4}$$

Equation (3.3) can be written for Events A and E_i as:

$$P(A|E_i)P(E_i) = P(E_i|A)P(A) \tag{3.5}$$

Therefore:

$$P(E_i|A) = \frac{P(A|E_i)P(E_i)}{P(A)} \tag{3.6}$$

Substituting $P(A)$ with the expression from the total probability theorem; i.e., Equation (3.4), we obtain Bayes' rule which gives the posterior probability of Events E_i as:

$$P(E_i \mid A) = \frac{P(A \mid E_i)P(E_i)}{\sum_{j=1}^{n} P(A \mid E_j)P(E_j)} \tag{3.7}$$

In Equation (3.7), $P(A \mid E_i)$ is called the likelihood and can be described as the probability of obtaining a certain Event A given the observation of Event E_i and $P(E_i)$ are the prior probabilities of Events E_i. Bayes' rule provides a theoretically rigorous format for dealing with design situations where knowledge is limited or comes from different streams. Such situations fit the usual design setting in civil, and particularly geotechnical, design practice. The approach is probabilistic where statistics plays an important role. However, the format provides a mechanism for dealing with uncertainty through accumulation of knowledge and a learning loop for continuous improvement and reduction of uncertainty.

3.4 Modeling the Distribution of Random Variables

Modeling distributions of random variables is achieved through probability density functions. A probability density function (PDF) of a random variable X is a function, $f_X(x)$, which gives the likelihood of the random variable X taking on the value of x. The sum of the likelihoods of all possible values of X is equal to one. Therefore, the area under the PDF curve is equal to one:

$$\int_{-\infty}^{\infty} f_X(x)dx = 1.0 \tag{3.8}$$

The cumulative distribution function (CDF), $F_X(x)$, is the area under the PDF from the lower bound of the domain of X to x, and is also expressed as the probability the random variable X takes on a value less than x; i.e. $P[X < x]$:

$$F_X(x) = \int_{-\infty}^{x} f_X(x)dx = P[X < x] \tag{3.9}$$

Usually, there is only a limited set of data points, but theoretically, the variable could take on any value between the data points if more measurements are taken. Thus, random variables are suitably modeled using continuous PDF's. There are many continuous PDF's to choose from to represent random variables, each with its advantages and disadvantages for different applications (e.g. Fenton & Griffiths, 2008). This section describes three PDF's selected for the work in this dissertation and discusses their distinctive features: normal, lognormal and bounded $\tanh$ PDF's.

3.4.1 Normal Distribution

The symmetric, bell-shaped normal (Gaussian) distribution, Figure 3.3, is widely used in statistical fields and is a basic assumption of the great majority of statistical research to date. One reason for its prominence is that many random variables can be adequately represented through this shape. Another reason is that even if the PDF of a single random variable is not symmetric, the combined effect of many variables with non-symmetric distributions tends to drift back to the symmetric bell-shaped curve. This fact can be demonstrated through the central limit theorem (e.g. Fenton & Griffiths, 2008). The normal probability density function of a random variable X with mean μ_X and variance of σ_X^2 , denoted as $X \sim N(\mu_X, \sigma_X^2)$, is expressed as:

$$f_X(x) = \frac{1}{\sigma_X\sqrt{2\pi}} e^{\frac{1}{2}\left(\frac{x-\mu_X}{\sigma_X}\right)^2} \quad \text{for} \quad -\infty < x < \infty \tag{3.10}$$

There is no closed form solution to the integral of the normal probability density function above. Therefore, the normal cumulative density function (CDF) is obtained through numerical integration. The PDF and CDF of a random variable X with mean $\mu_X = 5$ and standard deviation $\sigma_X = 2$; i.e., $X \sim N(5,4)$, are shown in Figure 3.3. While the normal PDF is a common choice for many naturally occurring random variables. it inevitably includes the possibility of predicting negative numbers that may be physically meaningless. This presents a difficulty for many engineering properties where a negative value has no physical significance. Examples of such properties include cohesion, friction angle, compressibility, permeability, etc.

One special normal PDF with a mean of zero $(\mu = 0)$ and variance of one $(\sigma^2 = 1)$ is called the standard normal PDF, $Z \sim N(0,1)$, Figure 3.4. The PDF of the standard normal distribution is expressed as:

$$\phi(z) = \frac{1}{\sqrt{2\pi}} e^{\frac{1}{2}z^2} \quad \text{for} \quad -\infty < z < \infty \tag{3.11}$$

and the standard normal CDF is denoted as:

$$\Phi(z) = \int_{-\infty}^{z} \phi(z) dz \tag{3.12}$$

Any normally distributed variable, $X \sim N(\mu_X, \sigma_X^2)$, can be standardized; i.e., turned into the standard normal distribution, $Z \sim N(0,1)$, by subtracting the mean from its variate and dividing the result by the standard deviation:

$$z = \frac{x - \mu_X}{\sigma_X} \tag{3.13}$$

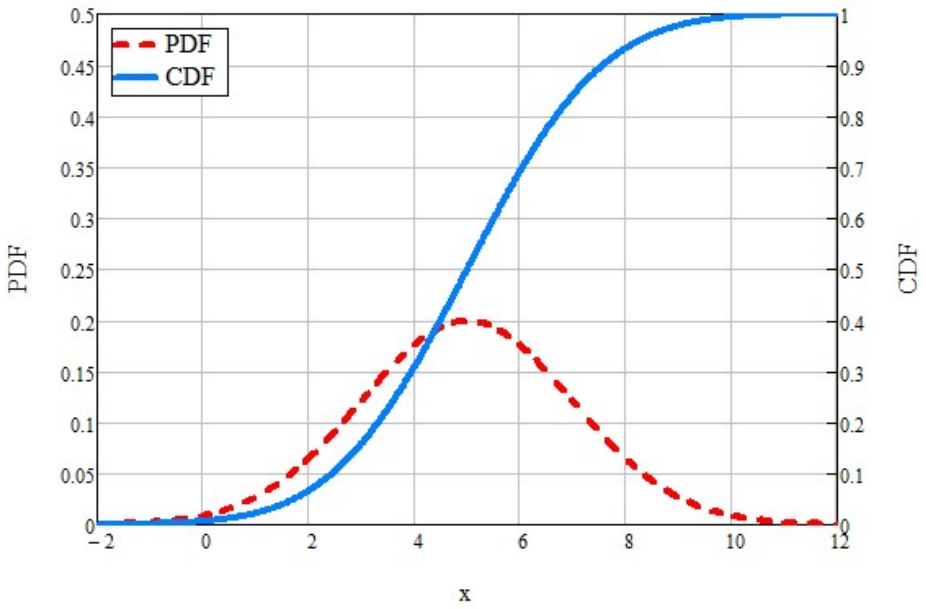

Figure 3.3 Normally distributed variable $X \sim N(5,4)$ PDF and CDF

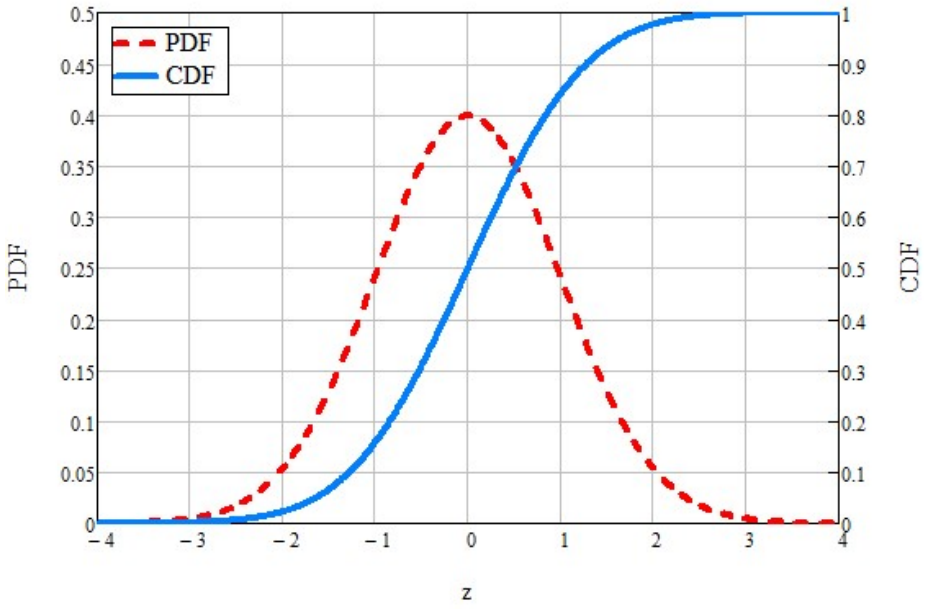

Figure 3.4 Standard normal $Z \sim N(0,1)$ PDF and CDF

The shifting and scaling back and forth between a normal PDF and a standard normal PDF are illustrated in Figure 3.5 which shows the PDF for a normally distributed random variable $X \sim N(5,4)$, as well as the PDF of the standard normal PDF, $Z \sim N(0,1)$. This shifting and scaling is used to calculate the probabilities of any normally distributed random variable, $P[X < x]$, by converting the normal variate into a standard normal variate and consulting published tables for the standard normal CDF, $\Phi(z)$:

$$P[X < x] = P\left[\frac{X-\mu_X}{\sigma_X} < \frac{x-\mu_X}{\sigma_X}\right] = P\left[Z < \frac{x-\mu_X}{\sigma_X}\right] = \Phi\left(\frac{x-\mu_X}{\sigma_X}\right) \tag{3.14}$$

The standard normal PDF is also useful in calculating the probability for non-standard PDF's and is used extensively in random variable generation for simulation purposes. In the case of a normal PDF, $X \sim N(\mu_X, \sigma_X^2)$, the standard normal PDF value is generated randomly in the standard normal space and then scaled and shifted back to the original normal PDF using this equation:

$$X = \sigma_X Z + \mu_X \tag{3.15}$$

3.4.2 Lognormal Distribution

A random variable X is said to be lognormally distributed with mean μ_X and variance σ_X^2 ; i.e., $X \sim LN(\mu_X, \sigma_X^2)$, if the logarithm of X is normally distributed, i.e., $\ln(X) \sim N(\mu_{\ln X}, \sigma_{\ln X}^2)$, Figure 3.6. In this sense, a lognormal PDF is an exponential transformation of a normal PDF and the normal PDF being transformed is called the underlying normal PDF:

$$f_X(x) = \frac{1}{x\sigma_{\ln X}\sqrt{2\pi}} e^{-\frac{1}{2}\left(\frac{\ln(x)-\mu_{\ln X}}{\sigma_{\ln X}}\right)^2} \quad \text{for} \quad 0 \le x < \infty \tag{3.16}$$

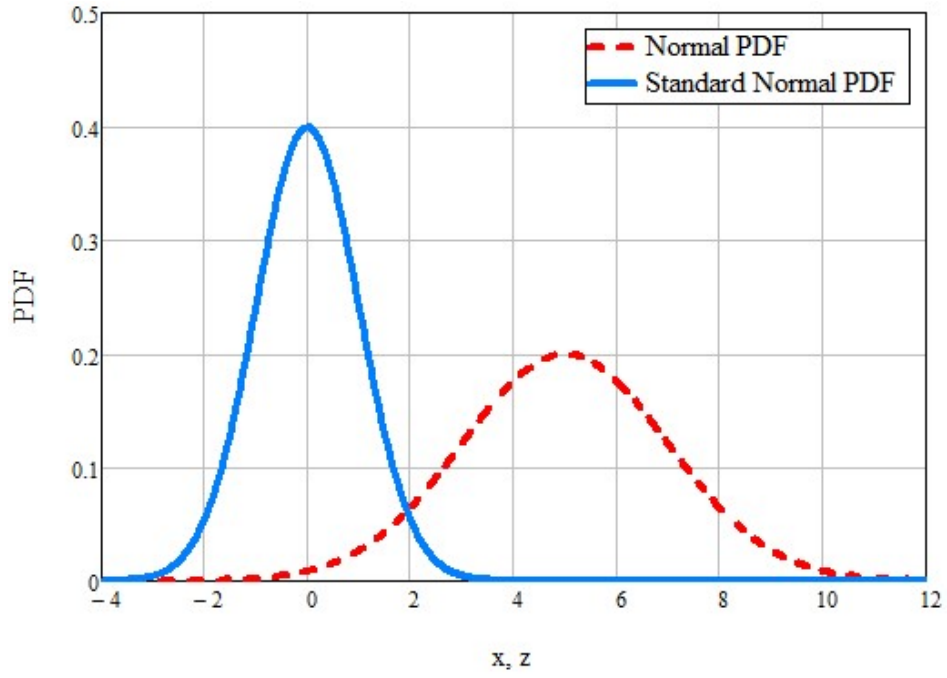

Figure 3.5 Scaling and shifting of normal PDF's

In the above equation, the mean and standard deviation of the lognormal PDF are related to the mean and standard deviation of the underlying normal PDF as follows:

$$\sigma_{\ln X} = \sqrt{\ln\left(1+\frac{\sigma_X^2}{\mu_X^2}\right)} \quad \text{and} \quad \mu_{\ln X} = \ln\left(\mu_X\right) - \frac{1}{2}\sigma_{\ln X}^2 \tag{3.17}$$

A noteworthy characteristic of the lognormal PDF is that it is positively skewed whereby its right tail is longer than its left one, and both its mode and median are to the left of the mean. Another useful feature of the lognormal PDF is that it is always positive; hence, it does not produce meaningless negative values for many engineering design parameters such as elasticity moduli, shear strength parameters, shear wave velocity, etc. Therefore, the lognormal PDF is a popular substitute for the normal PDF. Furthermore, there is field data to support that many geotechnical parameters approximately follow lognormal distributions (Jones *et al.*, 2002). The two-parameter

lognormal distribution discussed here is a special case of the general three-parameter lognormal distribution where the third parameter is a skewness parameter and is equal to zero (Holicky, 2009). The general three-parameter formulation may be useful if there is a lower, non-zero bound for the geotechnical property being modeled.

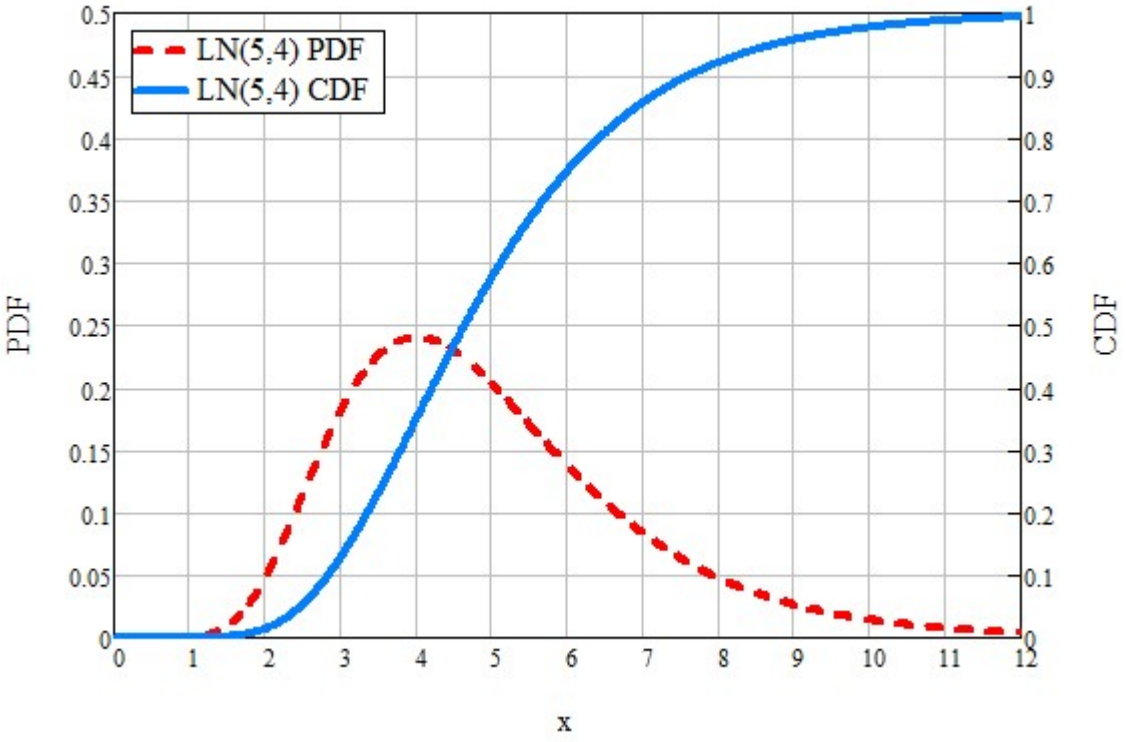

Figure 3.6 Lognormal PDF and CDF

3.4.3 Bounded tanh Distribution

The bounded tanh PDF, $X \sim BT(\mu_X, \sigma_X^2, a, b, m)$, results in a distribution that is bounded by two variate values a and b:

$$f_X(x) = \frac{\sqrt{\pi}(b-a)}{s\sqrt{2}(x-a)(b-x)} e^{-\frac{1}{2s^2}\left[\pi \ln\left(\frac{x-a}{b-x}\right)-m\right]^2} \tag{3.18}$$

where s and m are scale and location parameters, respectively. The bounded tanh PDF is a transformation of the standard normal PDF, $G \sim N(0,1)$, obtained as follows:

$$X = a + \frac{1}{2}(b-a)\left[1 + \tanh\left(\frac{m + sG}{2\pi}\right)\right] \tag{3.19}$$

in which the tanh function is defined as:

$$\tanh(z) = \frac{e^{z} - e^{-z}}{e^{z} + e^{-z}} \tag{3.20}$$

The location parameter m is equal to zero for symmetrical bounded tanh PDF's. The scale parameter s is a measure of variability. Fenton & Griffiths (2008) used a third-order Taylor series expansion for tanh and a first-order approximation for the expectation to express the scale parameter s in terms of the standard deviation of the underlying normal distribution. They also applied an empirical correction and suggested the following approximation of the scale parameter:

$$s \approx \frac{2\pi\sigma_X}{\sqrt{0.46^2(b-a)^2 - \sigma_X^2}} \tag{3.21}$$

Figure 3.7 shows the PDF and CDF of a bounded tanh variable $X \sim BT(5,4,0,10,0)$. In this example, the mean value is $\mu_X = 5$, the variance is $\sigma_X^2 = 4$, the lower bound is $a = 0$, the upper bound is $b = 10$ and location parameter is $m = 0$ (symmetric). As can be seen in this figure, the bounded tanh PDF would be attractive for parameters with known physical or practical bounds such as those listed in Table 3.1.

Even though a symmetric PDF is often adequate for geotechnical parameters, non-symmetric distributions can also be modeled by the bounded tanh PDF by adjusting the location

parameter, m. This parameter is equal to zero for a symmetrical PDF's, positive when the peak is to the right of the mean, and negative when the peak is to the left of mean, Figure 3.8.

Table 3.1 Example geotechnical properties with known physical bounds

Geotechnical Property	Physical Bounds
Elastic moduli, shear wave velocity, undrained shear strength, etc..	≥ 0
Theoretical limits on angle of internal friction	0 to 90 degrees
Practical limits on angle of internal friction	0 to 45 degrees
Porosity, degree of saturation, relative density	0 to 1
Poisson's ratio of common materials	0 to 0.5
Poisson's ratio for isotropic linear elasticity (Mott & Roland, 2013)	0.2 to 0.5

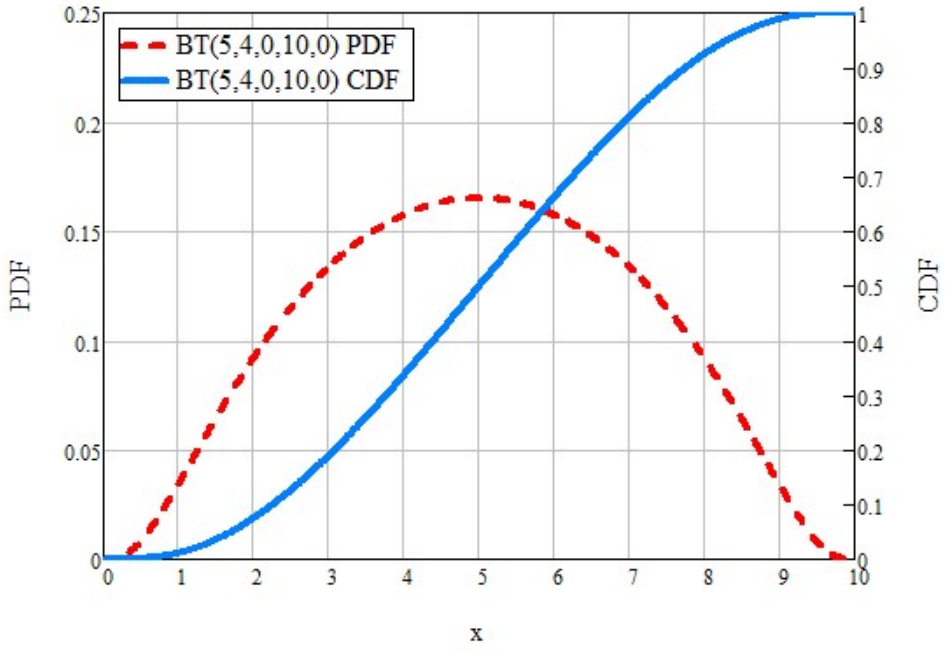

Figure 3.7 Bounded tanh PDF and CDF

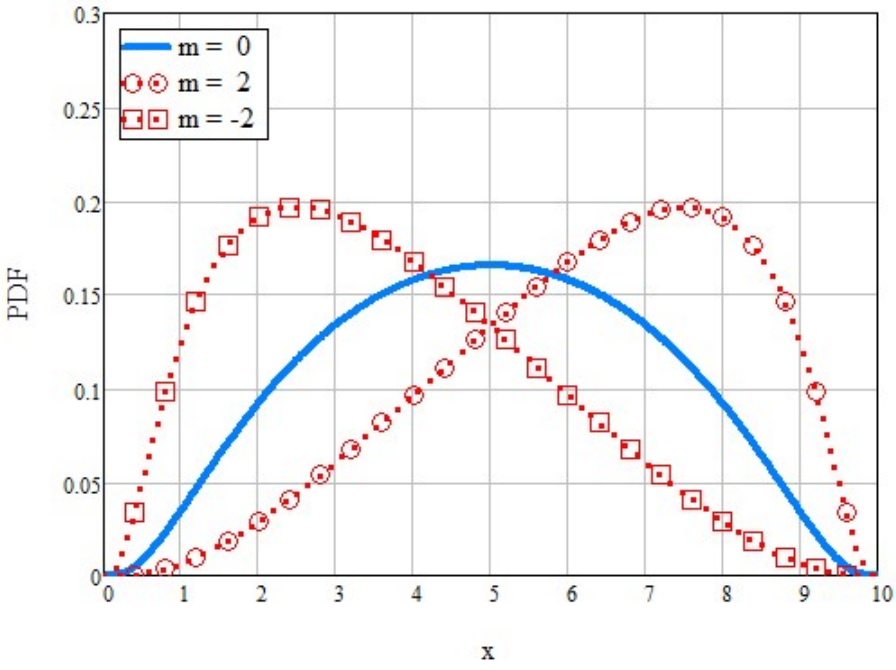

Figure 3.8 Location parameter of bounded tanh distributions

3.4.4 Uniform Distribution

The uniform distribution $X \sim U(a,b)$ is a noninformative distribution where the random variable X is equally likely to take on any value between a lower bound a and an upper bound b . Thus, its PDF and CDF are as follows:

$$f(x) = \begin{cases} \dfrac{1}{b-a} & \text{for} \quad a \le x \le b \\ 0 & \text{otherwise} \end{cases} \tag{3.22}$$

$$F(x) = P\left[X \le x\right] = \begin{cases} 0 & \text{for} \quad x \le a \\ \dfrac{x-a}{b-a} & \text{for} \quad a < x < b \\ 1 & \text{for} \quad x \ge b \end{cases} \tag{3.23}$$

One particular uniform distribution is $U(0,1)$ which generates random numbers between 0 and 1. This particular distribution is useful for randomly selecting an element from a set without preference or bias.

3.4.5 Measures of Central Tendency and Variability

The two most important parameters defining the central tendency and variability of a random variable, X, are the mean, μ_X, (a measure of central tendency) and the variance, σ_X^2, (a measure of variability), Figure 3.9. The square root of the variance is the standard deviation and is usually used as a measure of variability because it has the same units as the random variable. Another useful measure of variability is the standard deviation divided by the mean, or coefficient of variation (COV). The COV is an attractive variability measure because it is dimensionless and, therefore, scale independent as it is normalized with the respect to the mean. The COV is often expressed as a percent (of the mean). As can be noted from Figure 3.9, the spread of the PDF curve is narrower for smaller COV's; i.e., for random variables with lower variability; and vice versa.

3.4.6 Selection of Material Property PDF's

For use in RBD methods, Fenton & Griffiths (2008) detail a logical process for distribution selection given a data set, starting with fitting several reasonable probability density functions to the data and then comparing the goodness of fit to select the best distribution. The normal

distribution is very popular in statistics and could be a good fit for many geotechnical design variables, Table 3.2. However, unless the mean value of the normal distribution is far from zero and its variance is low, this distribution would inevitably predict negative values which would be physically meaningless for many geotechnical properties. There are also geotechnical parameters that are bounded at the low and high ends. In these cases, good alternate distributions to the normal distribution are the lognormal and the bounded (tanh) distributions.

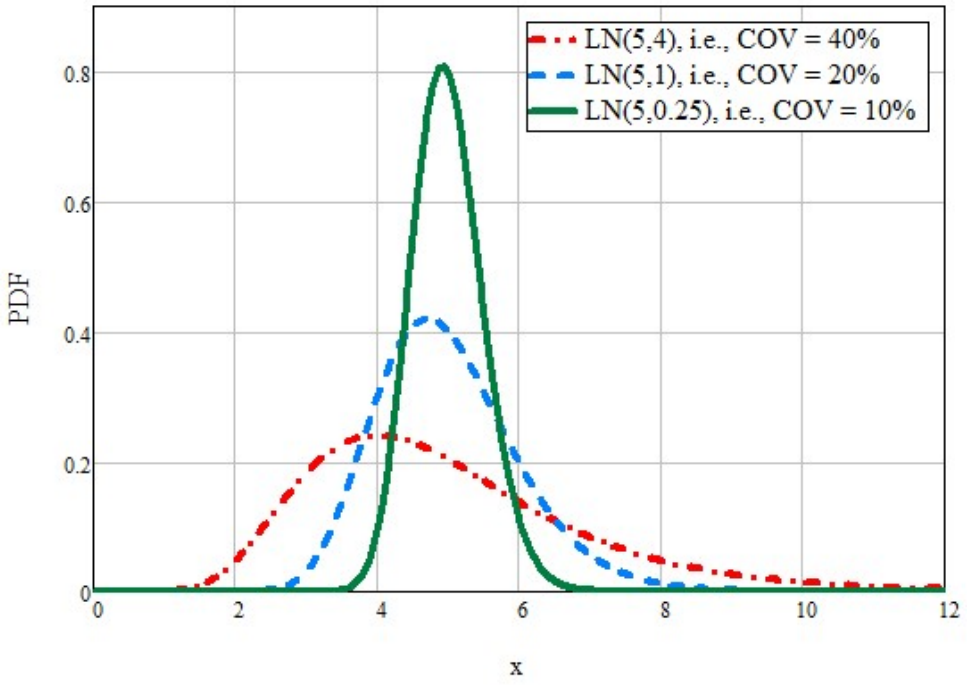

Figure 3.9 Lognormal PDF's for various COV's

Another consideration to keep in mind in selecting the distribution is the number of parameters required in its definition. Many basic (but adequate) distributions of a random variable, X, require only two parameters: its mean, $\mu_X$and its standard deviation, σ_X. Bounded

distributions would also need the two bounds but those can be obvious and intuitive physical or practical limits such as the limits on Poisson's ratio or friction angle, Table 3.1. Therefore, the specification of these bounds can be an added benefit of such distributions. All analyses performed as part of this dissertation are limited to the normal, lognormal and bounded tanh distributions. The selection of the probability model can be challenging when only limited data is available. In this case, a starting choice would be to refer to recommendations in the literature such as those shown in Table 3.2. Zhang *et al.* (2014) also describe a selection procedure based on copula theory and Bayesian updating.

Table 3.2 A few parameter distributions recommended in literature

Soil Type	Parameter	Distribution(s)	Reference(s)
All soil types	Submerged unit weight	NR	3
	Void ratio, initial void ratio and porosity	NR	3
	Shear wave velocity	LN	2
Sands	Friction angle	NR	3, 1
Clays	Initial void ratio	NR	3
	Liquid limit	NR	3
	Over-consolidation ratio	NR/LN	3
	Plastic limit	NR	3
	Undrained shear strength	LN	3
Clayey silts	Undrained shear strength	NR	3
References: 1. Wolff *et al.* (1996) 2. Toro (1996) 3. Lacasse & Nadim (1997)		Notes: • NR: Normal • LN: Lognormal	

3.4.7 PDF's for Loads

Loads are often variable in time. What is important in modeling variability in loads is not the instantaneous values of the load but the extreme values that occur during a predefined reference period. The extreme values are modeled as random variables with specified PDF and PDF parameters. Example suitable PDF's for wind turbine loads are the Weibull and Gumbel distributions used for DLC 1.1 and DLC 6.1, respectively (Sorensen & Toft, 2014). DLC 1.1 is a power production load case corresponding to annual maximum load effect obtained by load extrapolation has a COV of 15%, while DLC 6.1 load case corresponds to parked (standing still or idling) condition and has a 50-year recurrence period and a COV of 20%, (IEC, 2008; Sorensen & Toft, 2014). Even though the Weibull and Gumbel PDF's were used to model the distributions of the above load cases for the purposes of partial factor calibration in IEC61400-1, this dissertation uses the lognormal distribution for both load cases and for all limit states considered in these analyses. This choice is made because the objective is not calibration of partial factors but the illustration of the d-RBD methodology. Furthermore, Sorensen & Toft (2014) found that the use of a normal or lognormal PDF for the loads caused negligible changes in the partial factors.

3.5 Cross-correlations of Random Variables

Geotechnical design parameters may occasionally be cross-correlated, and it is important to consider such cross-correlations and to understand how they impact design reliability. The impact can be positive or negative depending on the situation. Not only may geotechnical parameters be cross-correlated, they may also be correlated to the applied load as implied by Coulomb's equation in which shear strength (resistance) is a function of applied stress (load).

3.5.1 Covariance and Correlation Matrices

The relationship between two random variables X and Y can be described using joint moments. Covariance of X and Y measures the interdependence of these two random variables and is defined as:

$$\mathrm{cov}(X,Y) = E\left[(X-\mu_X)(Y-\mu_Y)\right] = E(XY) - \mu_X\mu_Y \tag{3.24}$$

In the above equation, E for a random variable X is $E(X)$ and is the expected value, or mean, of X:

$$E(X) = \mu_X = \int_{-\infty}^{\infty} xf(x)dx \tag{3.25}$$

When $\mathrm{cov}(X,Y) = 0$, the two random variables X and Y are statistically independent. When the covariance is negative, the two random variables are said to be negatively correlated which means that when of the variables increases, the other also decreases, and vice versa. When the covariance is positive, the two variables are positively correlated and they both tend to increase or decrease together. When there are n random variables $X_{i=1,..n}$, the covariances between the random variables is conveniently expressed as a covariance matrix:

$$\mathbf{C} = \begin{bmatrix} c_{11} & c_{12} & .. & c_{1n} \\ c_{21} & c_{22} & .. & c_{2n} \\ .. & .. & .. & .. \\ c_{n1} & c_{n2} & .. & c_{nn} \end{bmatrix} \tag{3.26}$$

where $c_{ij} = \mathrm{cov}(X_i, X_j)$ and $c_{ii} = \mathrm{cov}(X_i, X_i) = \sigma_i^2$.

Covariances are normalized with respect to variances to obtain dimensionless coefficients for correlation varying from -1 to 1:

$$\rho_{ij} = \frac{\mathrm{cov}\left(X_i, X_j\right)}{\sigma_i \sigma_j} \quad \text{for} \quad i \neq j \quad \text{and} \quad \rho_{ii} = \rho_{jj} = 1 \quad \text{for} \quad i = j \tag{3.27}$$

and a correlation matrix is obtained as:

$$\boldsymbol{\rho} = \begin{bmatrix} 1 & \rho_{12} & .. & \rho_{1n} \\ \rho_{12} & 1 & .. & \rho_{2n} \\ .. & .. & 1 & .. \\ \rho_{1n} & \rho_{2n} & .. & 1 \end{bmatrix} \tag{3.28}$$

Correlation coefficients measure the strength of association between random variables. The diagonal terms of the correlation matrix measure the association of a random variable with itself. A random variable is perfectly associated with itself; thus, the diagonals are all equal to 1. For the off-diagonal terms, if the term is positive, the variables are positively correlated and vice versa. The closer the coefficient is to 1, the stronger the positive association; and the closer the coefficient is to -1, the stronger is the negative association. Finally, the correlation matrix is symmetric; i.e., if X is negatively correlated with Y, then Y is also negatively correlated with X and by the same strength of association.

3.5.2 Typical Correlations of Geotechnical Properties

One of the widely debated association between geotechnical properties is the correlation of the two components of shear strength; i.e., friction and cohesion. Most published information points to a negative correlation between effective friction angle and effective cohesion of a $c' - \phi'$ soil. Several reported negative correlations are shown in Table 3.3. Greco (2016) provides a much more extensive literature review on this issue and included the mention of a few researchers

reporting positive correlations. Fenton & Griffiths (2003) commented on the lack of consensus on this issue and investigated the implications of extreme cases of negative and positive correlation between cohesion and friction for bearing capacity of a shallow foundation on random soil. Fenton & Griffiths (2003) found that the impact was minimal. The reason could be that the assumption of negative correlation between friction and cohesion leads to two counteracting tendencies: on one hand, it leads to a reduction of shear strength (negative impact) and on the other, it leads to a reduction in the shear strength variance (positive impact). In general, it is acceptable to treat effective friction and cohesion as independent properties. For other geotechnical parameters, Uzielli *et al.* (2006) summarize many other reported correlations, many of which have clear and undisputed correlations.

Table 3.3 Published correlations between effective friction and effective cohesion

Reference	Coefficient of Correlation Range
Yucemen *et al.* (1973)	$-0.49 \leq \rho \leq -0.24$
Lumb (1970)	$-0.70 \leq \rho \leq -0.37$
Cherubini (1997)	$\rho = -0.61$
Uzielli *et al.* (2006)	$-0.75 \leq \rho \leq -0.25$

3.6 Design Parameters Based on Limited Information

Geotechnical investigations, even when they may be deemed exhaustive, will certainly not provide a full characterization of a project site. The reality is that geotechnical investigations are limited in scope for most civil engineering projects, and they are particularly so for wind energy projects which cover large terrains. Fortunately, what is important in reliability-based design is not

an exact value of a design parameter, but the uncertainty associated with it. Therefore, the objective of geotechnical explorations and data collection from various sources should be to establish the bounds on the variability of design parameters; i.e., to assess their uncertainties. Such assessment should be the focus of geotechnical explorations even when they are deemed exhaustive. Uncertainty assessment is beneficial whether it results in lower or higher variability because the resulting design would be reflective of the better knowledge of the uncertainties. There are many strategies for conducting effective geotechnical investigations with the aim of identifying geotechnical hazards and optimizing the often-limited resources dedicated to investigations (e.g. Barnes, 1993; Halim & Tang, 1993; Zhang *et al.*, 2004; Jaksa *et al.*, 2005; Goldsworthy *et al.*, 2007; Ben-Hassine & Griffiths, 2013). This section contains a brief description of some cost-effective techniques that are useful in assessing uncertainty and establishing reasonable bounds on parameter variability, as well as developing a feel for site variability.

3.6.1 Geophysical Methods

Geophysical methods used in geotechnical site characterization are primarily of three types: methods based on analysis of surface waves such as Spectral Analysis of Surface Waves (SASW) and Multichannel Analysis of Surface Waves (MASW) (e.g. Xia *et al.*, 1999; Stokoe & Santamarina, 2000; Nazarian, 2012; Taipodia *et al.*, 2013; Hutchinson & Beird, 2016b), methods based on analysis of cross-hole or down-hole waves such as the Seismic Cone Penetrometer Test (SCPT) (Stokoe & Woods, 1972; Stokoe & Hoar, 1981; Robertson *et al.*, 1986) and refraction micrometer (ReMi) arrays (Louie, 2001). MASW is a more accurate extension of Spectral Analysis of Surface Waves (SASW) as it achieves higher resolution and higher consistency and repeatability through the use of multiple data channels to isolate noise (Park *et al.*, 1999).

Geophysical methods have found success in site characterization due to several key advantages:

i) They are cost-effective typically adding only a small fee to the cost of a geotechnical exploration,

ii) They are non-intrusive: MASW is completely non-intrusive and SCPT does not require a probe beyond the CPT probe.

iii) They are considered to be the best methods for measuring undisturbed, zero strain shear modulus,

iv) Their accuracy is acceptable with MASW highly ranked in terms of cost and overall utility (Anderson *et al.*, 2006);

v) They characterize near surface geomaterials delivering profiles showing variation of shear and compression wave velocities with depth; 1D profiles can be combined to create a 3D model of local soil stratigraphy (Hutchinson & Beird, 2016a).

vi) Shear and compression wave profiles can be converted to profiles of geotechnical parameters based on elasticity formulas; see Table 3.4 for the key formulas for linear elastic, isotropic materials.

vii) They provide additional insights such as depth to bedrock, potentially detecting anomalies, etc.

Because of the above advantages, geophysical surveys, particularly the MASW technique, are a logical undertaking when geotechnical data is limited such as during the preliminary phase of projects.

Table 3.4 Key geophysical formulas for isotropic materials

Parameter	Formula	Measured/Computed/Notes
Compression wave velocity, V_p	$V_p = \sqrt{\frac{K + \frac{4}{3}G}{\rho}}$	Measured. For granite, $V_p \approx 4.8\, {km}/{\text{sec}}$ For water, $V_p = 1.5\, {km}/{\text{sec}}$
Shear wave velocity, V_s	$V_s = \sqrt{\frac{G}{\rho}}$	Measured. For granite, $V_s \approx 3.0\, {km}/{\text{sec}}$ For water, $V_s = 0\, {km}/{\text{sec}}$
Shear modulus, G	$G = \rho V_s^2$	Computed zero-strain modulus.
Young's modulus, E	$E = 2\rho V_s^2 (1+\nu)$	Computed zero-strain modulus.
Bulk modulus, K	$K = \rho\left(V_p^2 - \frac{4}{3}V_s^2\right)$	Computed zero-strain modulus.
Poisson's ratio, ν	$\nu = \frac{\frac{1}{2}V_p^2 - V_s^2}{V_p^2 - V_s^2}$	Computed zero-strain Poisson's ratio.

3.6.2 N-Sigma Procedure

The "N-sigma" procedure is an extension to the "Six-sigma" rule (also called the "Three-sigma rule") which suggests that the standard deviation of a normally distributed random variable can be approximated as the estimated range of the variable; i.e., the difference between the highest and lowest conceivable variable values, divided by six (Dai & Wang, 1992; Duncan, 2000):

$$\sigma_X \approx \frac{Range_X}{6} \tag{3.29}$$

This suggestion is based on the fact that 99.74% of the area under the normal PDF is contained within $\pm 3\sigma_X$. For the common case where there is a small number of data points, judgment is crucial in estimating the range of the variable. Thus, the accuracy of the six-sigma procedure is dependent on the judgment in estimating the range and the strong likelihood that the available data do not cover the range of the variable. The N-sigma procedure is conceived to account for this deficiency (Duncan, 2000; Foye *et al.*, 2006):

$$\sigma_X \approx \frac{Range_X}{N_\sigma} \tag{3.30}$$

In the equation above, N_σ is typically less than 6. Tippett (1925) suggested a relationship between N_σ and the number of available data points, n, for a normally distributed variable. Based on tabulated data for this relationship attributed to Tippett (1925) and republished by Foye *et al.* (2006), a logarithmic regression on this relationship, with $R^2 = 0.9867$ yields the following relationship, Figure 3.10:

$$N_\sigma = 0.7991 \ln(n) + 1.161 \tag{3.31}$$

It should be noted that this method is equivalent to shortcut estimates of the standard deviation as the range of the available data points multiplied by a coefficient that is a function of number of samples (Snedecor & Cochran, 1964; Krumbein & Grayhill, 1965).

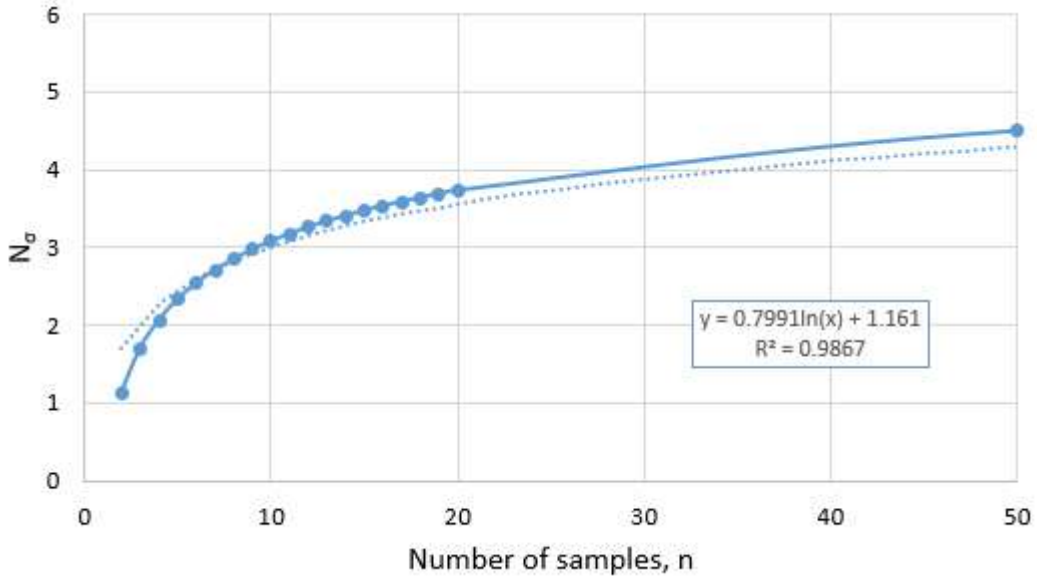

Figure 3.10 N_σ as a function of number of data samples, n (Tippett, 1925)

3.6.3 Multivariate Correlations and Bayesian Updating

Bayesian updating or learning is a formal expression of an activity that geotechnical engineers do all the time without attaching Bayes' name to it: they make inferences based on observations (Baecher, 2017). For example, the approach is recognized, without a formal expression of how it can be accomplished, by the Eurocode in the determination of characteristic values of geotechnical parameters (CEN, 2004):

> *"If statistical methods are employed in the selection of characteristic values for ground properties, such methods should differentiate between local and regional sampling and should allow the use of a priori knowledge of comparable ground properties."*

The formal expression of this approach is widely documented in the literature and is based on Bayes' conditional probability rule where new information is used to update "prior" information to "posterior" information (e.g. Denver & Ovesen, 1994; Cao *et al.*, 2016; Wang *et al.*, 2016; Papaioannou & Straub, 2017; Zhang, 2017; Li *et al.*, 2018; Zhang *et al.*, 2018). "Bayesian thinking" represents a shift from the "frequentist" methods of statistics covered in formal engineering education (Lumb, 1974; Zhang, 2017). Zhang et al. (2004) describe Bayesian updating procedures for reducing uncertainty based on empirical correlations, regional data and site-specific observations and propose three levels of uncertainty reduction depending on the available data, Figure 3.11. Zhang et al. (2004) show that uncertainty reduction increases with each level and can be significant, reaching one half to three fourth reductions in the coefficient of variation (COV). Wang *et al.* (2016) also used Bayesian updating and the Bayesian Equivalent Sample Method for probabilistic characterization of geotechnical properties based on limited site investigation data to gain better assessment of uncertainty. It should be noted that uncertainty reduction means a better assessment of the variability of geotechnical properties; i.e., reduction of uncertainty about uncertainty. This reduction usually means a reduction in the assumed variability because when little information is available, it is typical to start with conservative assumptions of large variability and the variability is reduced as more information becomes available. The additional information could be in the form of more data points on the same property or more data from field or laboratory tests on related information that can be used to reduce the variability through Bayesian updating and multivariate correlations (Kulhawy & Mayne, 1990; Cao & Zhang, 2012; Ching *et al.*, 2012; Huang *et al.*, 2013). Neural networks also have been used with Bayesian-based learning and databases of test results to establish relationships between parameters and estimating soil properties (e.g. Neal, 1992; Goh *et al.*, 2005; Goh & Kulhawy, 2006; Giovanis *et al.*, 2010).

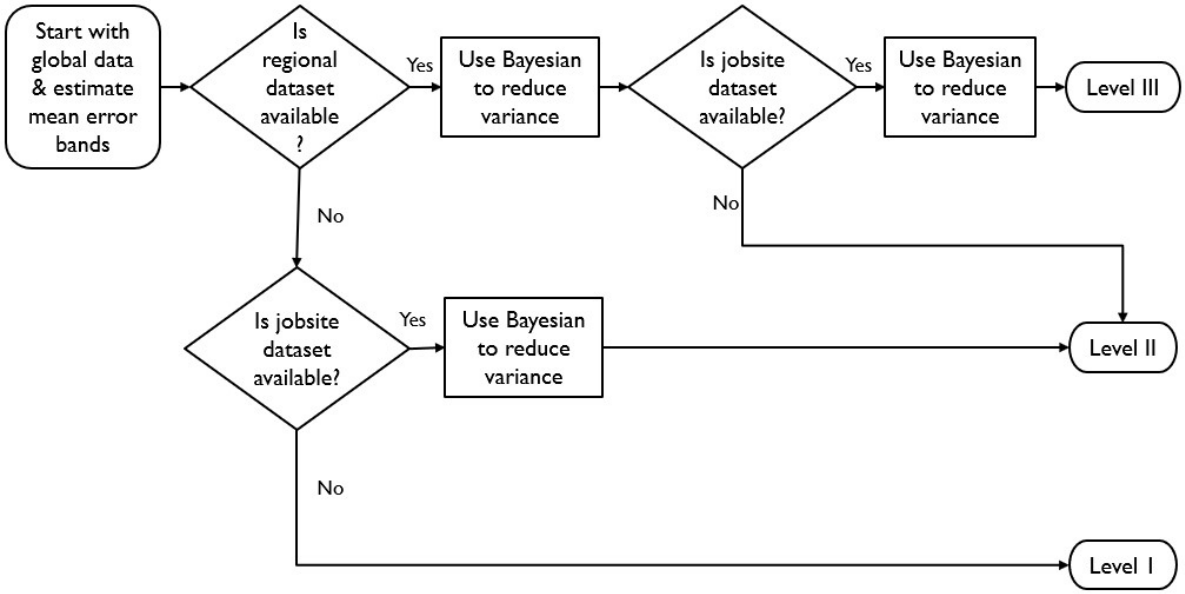

Figure 3.11 Uncertainty reduction using Bayesian approach (Zhang et al., 2004)

3.7 Typical Soil and Rock Property Variability

Well planned geotechnical investigations are necessary for a better understanding of the uncertainty in design parameters for a given project. However, during the early planning stages, it is often useful to consult published data on typical soil property variability. It is important to note that the variability of geotechnical design properties is significantly higher than that of other engineering materials. For example, while the resistance of most engineering materials has a COV of less than 20%, Table 3.5 (Ellingwood, 1980), the COV of some geotechnical properties can be as high as 300%, Table 3.6. In reliability-based design, reduction in parameter uncertainty translates directly into more optimal designs. Therefore, it is of great interest to assess uncertainty to produce designs that are reflective of that uncertainty. This section contains some typical COV ranges for common geotechnical design parameters and soil types suggested in the literature (e.g.

Schultze, 1971; Lee *et al.*, 1983; Harr, 1987; Kulhawy, 1992; Lacasse & Nadim, 1997; Jones *et al.*, 2002; Uzielli *et al.*, 2006). A summary of soil property variability gleaned from some of these references is contained in Table 3.6. For rock, Aladejare & Wang (2017) provide a good collection of typical rock property variability for different types of rock. Highlights from Aladejare & Wang (2017) are not reproduced here.

Table 3.5 Typical COV's of common engineering materials (Ellingwood, 1980)

Material	Member Type	Typical Resistance COV (%)
Concrete	Flexure beams	8-14
	Short columns	12-16
	Slender columns	12-17
	Shear beams	17-21
Steel	Tension members	11
	Compact beams	13
	Axially loaded columns	14
	Beam-columns	15
Aluminium	Tension members	8
	Beams	8-13
	Columns	8-14
Glue-laminated timber beams		18

Table 3.6 Typical reported variability of select geotechnical properties

Soil Type	Parameter	Test Type	COV (%)	Reference(s)
Sands	Tangent of friction angle $\tan\phi'$	NS	5-15	1
	Angle of internal friction ϕ'	NS	5-15	2
		NS	2-13	3, 4
	Undrained shear strength s_u	NS	20-50	2
	Relative density D_r	Direct	10-40	6
	Relative density D_r based on SPT	Indirect	50-70	6
Clays	Angle of internal friction ϕ'	NS	12-56	2
	Liquid limit w_L	Lab	20-48	2
	Liquid limit, clay & silt w_L	Lab	6-30	6
	Plastic limit w_P	Lab	9-29	2
	Plastic limit, clay & silt w_P	Lab	6-30	6
	Plasticity index	Lab	7-79	2
	Unconfined compressive strength	NS	6-100	2
	Undrained shear strength s_u	NS	20-50	1
		NS	25-30	2
		NS	13-40	3, 4, 5
		UC	20-55	6
		UU	10-30	6
		CIUC	20-40	6
	Undrained strength ratio s_u/σ_v'	NS	5-15	5
	Unit weight, clays and silts	NS	<10	6
	Permeability, partly saturated clays	NS	130-240	3, 6
	Permeability, saturated clays	NS	68-90	3, 6

Table 3.6 Continued

Soil Type	Parameter	Test Type	COV (%)	Reference(s)
NS	Effective friction angle ϕ'	NS	5-15	6
	Coefficient of consolidation c_v	NS	25-50	1
		NS	33-68	6
	Compression index C_c	NS	10-37	3, 4, 6
	Unit weight	NS	5-10	1
		NS	1-10	2
		NS	3-7	3, 4
	Buoyant unit weight	NS	0-10	5
	Young's modulus	NS	2-12	2
	Shear wave velocity	NS	25-55	7, 8, *
	Over-consolidation ratio OCR	NS	10-35	6
	Coefficient of permeability	NS	200-300	1, 2
	Pre-consolidation pressure	NS	10-35	3, 5, 6
	Void ratio	NS	15-30	1
		NS	13-42	2
	Void ratio & porosity all soil types	NS	7-30	6
	Standard penetration test blow count	Field	15-45	3, 4
		Field	25-50	6

References:

1. Schultze (1971)
2. Lee *et al.* (1983)
3. Harr (1987)
4. Kulhawy (1992)
5. Lacasse & Nadim (1997)
6. Uzielli *et al.* (2006)
7. Toro (1996)

Abbreviations:

1. NS: Not Specified
2. CIUC: Consolidated-isotropically undrained compression
3. UC: Unconfined compression
4. UU: Unconfined Undrained
5. *: Range assumed by author

8. Jones *et al.* (2002)	

As can be deduced from published typical variability of select geotechnical properties, unit weight seems to be one of the least variable soil properties ($COV < 10\%$), followed by effective friction angle ($5\% \leq COV \leq 15\%$), while the most variable property is the coefficient of permeability with a COV as high as 300%. The variability noted in several key geotechnical design parameters is one of the reasons that a tiered approach is typically adopted for specifying variability in LSD/LRFD geotechnical design standards. One such tiered specification is that by the 2014 CHBDC which assigns different geotechnical resistance safety factors based on the "degree understanding" of site conditions and prediction model. The 2014 CHBDC specifies a three-tiered approach consisting of "Low," "Typical" and "High" degrees of understanding (Fenton *et al.*, 2016). Another tiered approach is based on the anticipated level of site geotechnical variability as shown in Table 3.7, (Phoon & Kulhawy, 2008). Based on the literature review presented in Table 3.6, a three-tiered summary is proposed in Table 3.8. These proposed ranges are adopted in the analyses presented in this dissertation.

Table 3.7 Sample tiered scheme based on site variability (Phoon & Kulhawy, 2008)

Property	Variability	COV (%)
Undrained shear strength, s_u	Low	10-30
	Medium	30-50
	High	50-70
Effective friction angle, ϕ'	Low	5-10
	Medium	10-15
	High	15-20
Lateral earth pressure coefficient, K_a or K_p	Low	30-50
	Medium	50-70
	High	70-90

Notes:

- "Low" variability is typical of good quality direct lab or field measurements
- "Medium" variability is typical of indirect correlations with good field data, except for the standard penetration test (SPT)
- "High" variability is typical of indirect correlations with SPT data and strictly empirical correlations

Table 3.8 Proposed three-tiered COV (%) ranges of select geotechnical properties

Soil Type	Property	Test Type	Low	Medium	High
All Types	Unit weight	NS	1-4	4-7	7-10
	SPT blow count	Field	15-26	26-38	38-50
	Young's modulus	NS	2-5	5-8	8-12
	Shear wave velocity	NS	25-35	35-45	45-55
Sands	Friction angle	NS	2-6	6-10	10-15
	Relative density	Direct	10-20	20-30	30-40
	Relative density	SPT-based	50-56	56-63	63-70
Clays and Silts	Friction angle	NS	12-26	26-41	41-56
	Unconfined compressive strength	NS	5-35	35-65	65-100
	Undrained shear strength	NS	13-25	25-37	37-50
	Undrained shear strength	UC	20-31	31-43	43-55
	Undrained shear strength	UU	10-16	16-23	23-30
	Undrained shear strength	CIUC	20-26	26-33	33-40
	Undrained shear strength ratio	NS	5-8	8-11	11-15
	Permeability of unsaturated clays	NS	130-165	165-200	200-240
	Permeability of saturated clays	NS	68-75	75-82	82-90
	Coefficient of consolidation	NS	25-39	39-53	53-68
	Compression index	NS	10-19	19-28	28-37
	Over-consolidation ratio	NS	6-15	15-25	25-35
	Pre-consolidation pressure	NS	10-18	18-26	26-35
	Void ratio and porosity	NS	7-18	18-30	30-42

Abbreviations:

- NS: Not Specified
- CIUC: Consolidated-isotropically undrained compression
- UC: Unconfined compression
- UU: Unconfined Undrained

CHAPTER 4

DESIGN METHODS AND RELIABILITY QUANTIFICATION

The deterministic computations described in Chapter 2 involve the use of assumed values for design variables that are known to be uncertain. Deterministic computations use representative values for design variables. Such computations provide an idea on the expected response without much information on the variability or the uncertainty of the response thus computed. Classical ASD or LRFD/LSD design schemes involve deterministic computations with safety factors applied to the demand and/or resistance sides of equations to embed some measure of safety in the design. In the case of the ASD approach, i.e., the global factor approach where a single safety factor is applied, all uncertainty is lumped into a single factor and the level of reliability is difficult to quantify and is only approximated based on judgement and historical performance. In the case of the LRFD/LSD approach, i.e., the partial factor approach, achievement of an intended level of reliability is only possible when the assumptions adopted in the development of the partial factors are also applicable to the design at hand. Most current design codes adopt this partial factor approach.

In this chapter, the chronological progression of engineering design thought is described, Figure 4.1. This progression is presented as a transition from the "single factor" format based on accepted practice, historical performance and engineering judgement to the contemporary semi-probabilistic "multiple factor" or "partial factor" approach that targets quantifiable reliability and risk levels through calibrated factors. The discussion sets the stage for "factor-free" reliability-based design methods discussed in Chapter 5.

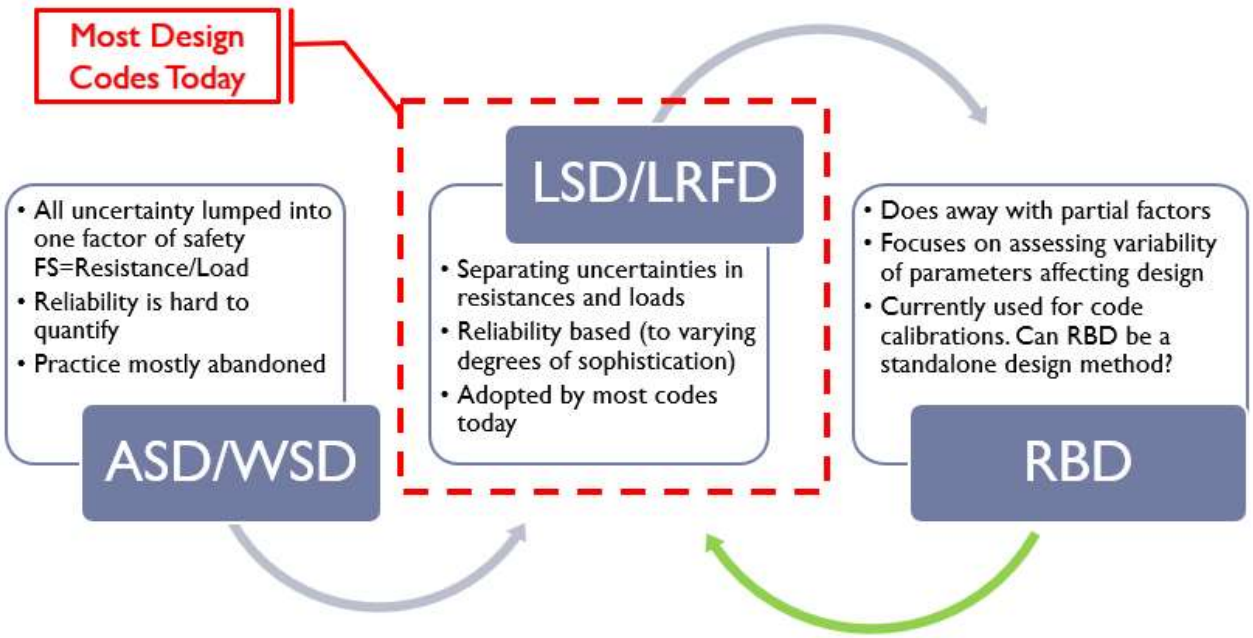

Figure 4.1 Progression of design philosophies

4.1 Characteristic Values and Bias

A basic decision in a deterministic computation of resistance or load involves the selection of characteristic values to use in the computational model. The selection which is often based on limited data or empirical correlations introduces bias. Contemporary design codes require the use of a "characteristic" or a "nominal" value of a design variable. This value is sometimes described as a prudent or cautious estimate of the mean; i.e., due to the limited size of the data set, the real mean of the variable is not the arithmetic mean from the data set but a lower or higher value depending on which side is more conservative. Schneider (1999) provides a suggested step-by-step procedure for calculating the characteristic value for different data availability scenarios. Orr (2017) provides the historical background for characteristic value definitions, describes how it should be selected per Eurocode 7 and suggests an alternate equation that reduces subjective judgement in its selection. Below are some descriptions of this value from leading codes:

1. Prudent estimate: Model Code 2010 defines a prudent estimate as "a value which, compared to the estimate, is provided with an adequate margin to meet the required reliability," (CEB-FIP, 2013).
2. Characteristic value: ISO 2394 defines the characteristic value of a material property as a "priori specified fractile of the statistical distribution of the material property in the relevant supply," (ISO, 2015). European design standards typically adopt the 5% fractile, i.e. for resistance, the value corresponding to a 95% confidence level (CEN, 2004). Eurocode 7 describes the characteristic value of a geotechnical parameter as a "cautious estimate of the value affecting the occurrence of the limit state" (CEN, 2004).
3. Nominal value: NCHRP 651 defines nominal values (e.g., the nominal resistance, R_n or nominal load, Q_n) as "those calculated by the specific calibrated design method and the loading conditions, respectively, and are not necessarily the means" (Paikowsky *et al.*, 2010).

4.2 Global Factor Design

In recent history, safety margins in engineering designs have been achieved through the conscious decision to separate the load effects, $\sum_i Q_i$, and the nominal resistance, R_n, by a certain safety margin. The practice of applying a global factor of safety in geotechnical stability computations dates back to the eighteenth century (Belidor, 1729; Coulomb, 1773). The approach was formalized in the early 1900's in steel design practice through the allowable (working) stress design (ASD or WSD) method where the applied stresses are not permitted to exceed an allowable (working) stress equal to yield stress divided by (or multiplied by) a global factor of safety. In

terms of loads, the applied loads, $\sum_i Q_i$, are not permitted to exceed an allowable load, R_{all} equal to the nominal capacity divided by a global factor of safety, FS:

$$\sum_i Q_i \le R_{all} = \frac{R_n}{FS} \tag{4.1}$$

The global factor of safety is typically applied to the resistance side to obtain an "allowable" resistance as shown in the equation above by dividing a nominal resistance by a number greater than 1, or by multiplying it by a number smaller than 1 as done in steel working stress design where the steel yield strength is multiplied by 0.6, i.e., $FS = 1/0.6 = 1.67$.

For foundation bearing capacity, the conventional global factor of safety is based on load increase; $FS = q_{ult}/q_{all}$, i.e., a factor relating the ultimate load (or ultimate bearing capacity) to the allowable load (or allowable bearing capacity). It is intuitive to think of bearing capacity as the load required to cause failure; i.e., the load is increased to the point of failure. In geotechnical design, alternate expressions of the global factor of safety can be devised based on shear strength reduction, i.e., based on reduction, under constant load, of effective cohesion, c' and effective friction, $\tan\phi'$, to the point of failure (Griffiths, 2015). This approach is counter-intuitive but it can serve to illustrate the sensitivity of geotechnical problems to variations in resistance. Griffiths found that the conventional bearing capacity factor of safety (based on load increase) is about twice that based on strength reduction; e.g., the typical conventional factor of safety of 3 would be approximately equivalent to a strength reduction safety of factor of 1.5. Griffiths (2015) noted that this finding illustrates the fact that geotechnical problems are more sensitive to strength reduction than they are to load increase.

The value of the global factor of safety accepted in practice is different depending on the industry, historical performance, the design problem formulation, material providing resistance, local/regional preferences and the designer's judgement, Table 4.1. For geotechnical designs where soil resistance is typically highly variable, global safety factor values vary widely between 1.3 for slope stability and 3.0 for bearing capacity (Terzaghi & Peck, 1948, 1967). For geotechnical problems, these common factor of safety values correspond to differing levels of reliability; e.g. slopes designed to a factor of safety of 1.3 are a lot less reliable that foundations designed to bearing capacity factor of safety of 3.0 (e.g. Lumb, 1970). These factor of safety ranges have been established through practice and historical performance without the benefit of a robust scientific/probabilistic basis. There is overwhelming agreement in literature that the traditional global factor of safety is not a reliable measure of reliability.

Table 4.1 Typical global safety factors

Application	Failure Mode	Typical Factor of Safety
Shallow foundations and retaining walls	Bearing capacity	2.0-3.0
	Sliding	2.0-3.0
	Overturning or overall stability	1.25-2.0
	Settlement or tilt	1.0
Slope stability	Slope failure	> 1.1 seismic > 1.5 static

4.3 Partial Factor Design

The idea of assigning different safety factors to loads and resistance appears to have been first introduced in Denmark. Danish structural engineer A. J. Moe reportedly proposed the concept as early as 1927, (Krebs Ovesen, 1981). Moe (1936) recognized the many inconsistencies caused by the use of a single factor of safety and proposed using separate factors of safety for dead load,

live load and material resistance in the design of concrete structures. The concept was partly introduced in the Danish Code of Practice for Concrete Design in 1949 and was further detailed for the design of retaining structures by Hansen (1953). By the mid-1950's, partial factor design became the norm in Denmark through Danish Standard DS-415 and was widely accepted by engineers. It is worthwhile to note that the introduction of partial factors was not motivated by uncertainties but by inconsistencies associated with different behavior at serviceability and collapse scenarios and different nature of loads; e.g., dead vs live loads (Bolton, 1993).

In the mid-1950's, strength-based formulations were introduced in the United States by the concrete industry; first in ACI 318-56 as a recognized and permitted methodology, then in ACI 318-63 where working stress and strength design methods were covered equally and finally in ACI 318-71 which was based fully on strength design. The strength design approach is also referred to as ultimate strength design because loads are factored, and members are sized to provide a code mandated design strength (or resistance), R_d, approaching ultimate resistance. The de facto result of the methodology is to factor loads and resistance separately. The approach was promoted by the concrete industry because working stress design, performed at working load levels and assuming linear elasticity, is not adequate in capturing the inelastic concrete behavior at higher loads. Thus, the principal original motivation was not the separation of uncertainties in loads and resistances but the capture of a more realistic concrete capacity in the inelastic range. Code mandated design resistance, R_d is obtained by multiplying the nominal ultimate resistance, R_n, by a resistance reduction factor, ϕ .

$$R_d = \phi R_n \tag{4.2}$$

The strength design method is thus formulated as ensuring that the code mandated design resistance, R_d, is greater than the factored (design) loads, $\sum_i (Q_d)_i$:

$$R_d = \phi R_n \geq \sum_i (Q_d)_i \tag{4.3}$$

Prompted by the Danish practice and energized by reconstruction effort following World Word II, many European technical organizations and national committees spent the 70's and 80's on the development of model codes for various materials. Among the early deliverables of this effort were British Standard CP110 on the Structural Use of Concrete published in 1972 and NKB Report No. 36 published in 1978 by the Nordic Committee on Building Regulations (BSI, 1972). British Standard CP110 used "limit states" terminology to consider limiting states such as those related to collapse, deformation and cracking. CP110 was also a pioneer in the explicit use of probability theory and statistics in the selection of a "characteristic" value of strength; e.g., the 95% fractile (or the 5% quantile) where 95% of samples have higher values. NKB Report No. 36 outlined the basic principles of Limit States Design (LSD).

In the US, the steel industry introduced load and resistance factor design (LRFD) methodology in 1986 where the explicit purpose of partial factors was the separation of uncertainties in loads and resistance so that they can be assigned different safety factors reflective of those uncertainties. In 1989, in anticipation of a smooth transition to LRFD, AISC released what was supposed to be the last revision of the allowable stress (ASD) design manual (AISC, 1989). However, primarily due to the low variability in steel resistance, the ASD methodology had been working well since its inception in the early 1900's. This fact combined with the ensuing confusion with the partial factor approach resulted in the steel design community resisting the move to LRFD and AISC releasing a combined ASD/LRFD design manual in 2006. While the US steel industry

struggled with the transition to LRFD, transportation departments across North America embraced the new methodology, spearheaded its application to bridge design and extended it to geotechnical and foundation design. In 1983, the Ontario Highway Bridge Design Code introduced partial factors and geotechnical limit states design to Canadian engineering practice (Becker, 1996b, 1996a, 2003; Fenton *et al.*, 2016). In 1994, AASHTO released the first LRFD based design specifications (AASHTO, 1994). By the turn of the millennium, all European and most North American design codes, as well as many codes around the world, have adopted the LRFD/LSD format with a few exceptions in U.S. geotechnical design practice. Current geotechnical design standards assign partial factors to resistances and such factors are calibrated to work with specific partial load factors typically outlined in loads standards such as ASCE 7 (ASCE, 2017). The calibration of the partial factors reflected some newer knowledge based on uncertainties but was mostly carried out with the aim of recovering, as much as possible, reliability levels understood to be present in classical ASD design. As Christian (2007) pointed out, such an objective would be misguided as it nullifies the benefits of new, fundamentally sound methods.

4.3.1 Limit States Design

Limit states design is predicated on ensuring, to a predefined level of reliability, that a certain "limit" state of a structure or foundation is not reached. Reliability of a structure or foundation is its ability to fulfil its design purpose for a specified design lifetime. IEC 61400-1 defines a limit state as the "state of a structure and the loads acting upon it, beyond which the structure no longer satisfies the design requirement" (IEC, 2008). For example, if for a given failure mode, the effect of the applied loads, $Q = \sum_i Q_i$, exceeds resistance, R , then that limit state is violated, and failure is said to have occurred. A limit state is often expressed as a performance

function g being equal to zero; i.e., $g = 0$, with the unacceptable domain being $g < 0$. A common form of the limit state (or performance) function, g, is presented as the case where the factor of safety, $FS = R/Q$, is equal to 1:

$$g = \frac{R}{Q} - 1 = FS - 1 = 0 \tag{4.4}$$

Other equally valid forms of the limit state function include:

$$g = R - Q = 0 \quad \text{or} \quad g = \log\left(\frac{R}{Q}\right) = \log\left(FS\right) = 0 \tag{4.5}$$

Resistance is a function of many variables that are uncertain; i.e. random variables, and so are the load effects. Thus, resistance, load effects and the factor of safety are themselves uncertain random variables. Figure 4.2 (a) and Figure 4.2 (b) show sample PDF's of resistance, load effects and factor of safety.

4.3.2 Probability of Failure (and Success)

Designs performed using LSD/LRFD and reliability-based methods have a target probability of failure, p_f^T, as the main design criterion for each limit state. The probability of failure is defined as the probability that resistance is less than the load effects:

$$p_f = P\left[R < Q\right] = P\left[g < 0\right] \tag{4.6}$$

Referring to Figure 4.2 (a) and assuming that resistance and loads are independent random variables, the infinitesimal contribution to probability of failure from each infinitesimally small increment dx of the variate is:

$$P\left[x \le Q \le x + dx\right] \cdot P\left[R < x\right] = f_Q(x) F_R(x) dx \tag{4.7}$$

where $f_Q(x)$ is the loads effects PDF and $F_R(x)$ is the resistance CDF. When this contribution is integrated over all possible variates of the loads effect, the total probability of failure is obtained as:

$$p_f = \int f_Q(x) \cdot P\left[R < x\right] dx = \int f_Q(x) \cdot F_R(x) dx \tag{4.8}$$

Safety is the complementary event of failure; i.e., if the probability of success, also called reliability, is p_s then $p_f + p_s = 1$. Both probabilities (p_f and p_s) vary between 0 and 1. If the probability of failure is known, reliability (or the probability of success) can be calculated as:

$$p_s = 1 - p_f = 1 - \int f_Q(x) \cdot F_R(x) dx \tag{4.9}$$

4.3.3 Reliability Index

An alternative approach of calculating the probability of failure is through the factor of safety PDF. It is difficult to characterize the factor of safety distribution if loads and resistance are not normally distributed. However, since loads effect and resistance are typically the product of other random variables of varying probability distributions, they tend to be normally distributed.

Therefore, it is common to assume that the factor of safety is normally distributed as shown in Figure 4.2 (b); i.e., $FS \sim N(\mu_{FS}, \sigma_{FS}^2)$. If $F_{FS}(x)$ is the factor of safety CDF, the probability of failure is the shaded area in Figure 4.2 (b) and is calculated as:

$$p_f = F_{FS}(1) = \Phi\left(\frac{1 - \mu_{FS}}{\sigma_{FS}}\right) = \Phi(-\beta) = 1 - \Phi(\beta) \tag{4.10}$$

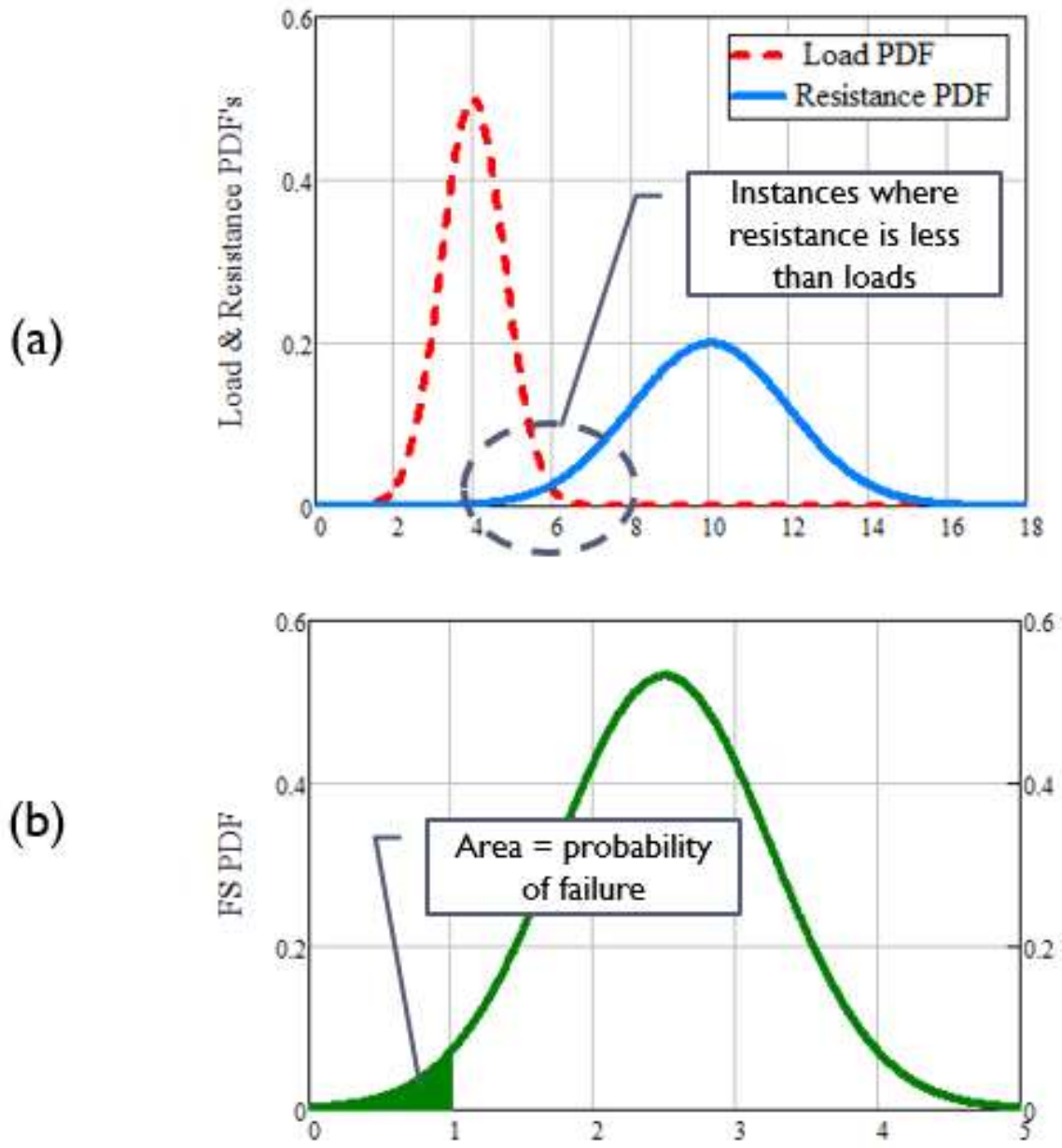

Figure 4.2 PDF of normally distributed resistance, load effects and FS

In the above equation, where Φ is the standard normal CDF and β is commonly called the reliability index and is calculated as:

$$\beta = \frac{\mu_{FS} - 1}{\sigma_{FS}} = -\Phi^{-1}\left(p_f\right) \tag{4.11}$$

The reliability index is a measure of reliability or safety of the design. In fact, the reliability index was referred to as the safety index in the 80's and 90's (Nowak, 1983; Reddy *et al.*, 1994; Wang & Grandhi, 1994):

$$\beta = \Phi^{-1}\left(p_s\right) = \Phi^{-1}\left(1 - p_f\right) \tag{4.12}$$

The reliability index measures the shortest distance, in units of performance function standard deviations, between the most probable point (calculated at the mean values of random variables) and the failure point. Figure 4.3 illustrates these relationships for a normally distributed FS with mean of 2.5 and standard deviation of 0.75. As indicated by Equation (4.11), there is a one-to-one relationship between probability of failure and reliability index. Therefore, the use of a reliability index as a design target is equivalent to using a probability of failure.

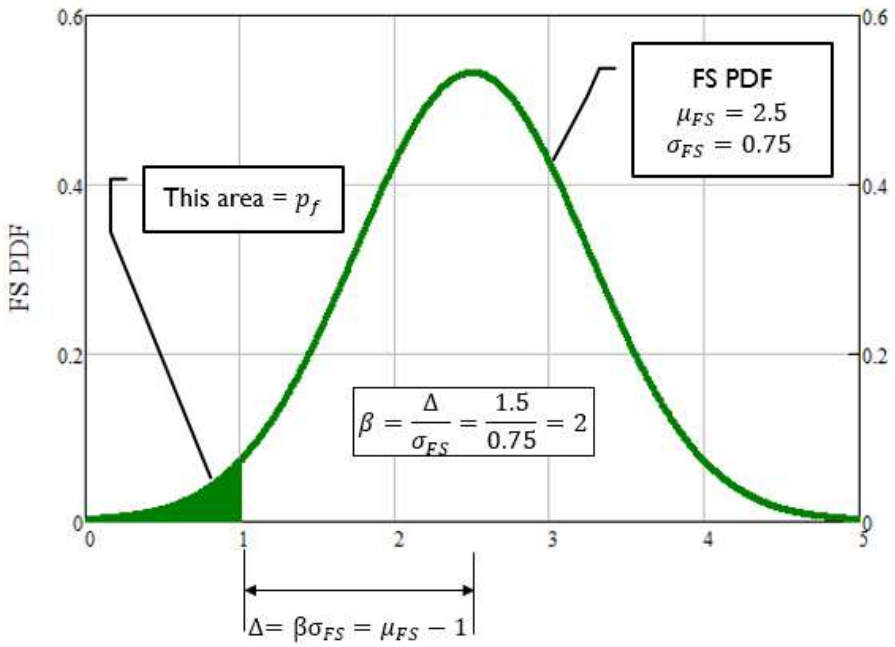

Figure 4.3 Illustration of probability of failure, reliability index and factor of safety

The reliability index can also be computed rigorously for normally distributed resistance and load effects as a function of the mean factor of safety, $\overline{FS} = \mu_R / \mu_Q$, and coefficients of variation of resistance and load effects, COV_R and COV_Q, respectively. The expression depends on the specific form adopted for the limit state function as shown in Table 4.2 (Li & Lumb, 1987). When loads effect and resistance are both lognormally distributed, the reliability index can be calculated as follows (Whitman, 1984):

$$\beta = \frac{\ln\left(\overline{FS}\sqrt{\frac{1+COV_Q^2}{1+COV_R^2}}\right)}{\sqrt{\ln\left[\left(1+COV_Q^2\right)\left(1+COV_R^2\right)\right]}} \tag{4.13}$$

Table 4.2 Reliability index for normally distributed loads and resistance

Limit State Function Format	Reliability Index
$g = FS - 1 = 0$	$\beta = \frac{\overline{FS} - 1}{\overline{FS}\sqrt{COV_R^2 + COV_Q^2}}$
$g = R - Q = 0$	$\beta = \frac{\overline{FS} - 1}{\sqrt{\overline{FS}^2 COV_R^2 + COV_Q^2}}$
$g = \ln(FS) = 0$	$\beta = \frac{\ln\left(\overline{FS}\right)}{\sqrt{COV_R^2 + COV_Q^2}}$

As evidently clear from these expressions, the relationship between the reliability index and the factor of safety depends of the coefficients of variation of loads and resistance; i.e., the variability of loads and resistance. This fact illustrates why a global factor of safety is not a good measure of reliability.

For normal variables, the relationship between probability of failure and reliability index is shown in Figure 4.4. An approximate expression is provided by Baecher & Christian (2003) and is plotted on the same graph shown in Figure 4.4:

$$p_f = 460e^{-4.3\beta} \quad for\ 2 \le \beta \le 6 \tag{4.14}$$

and

$$\beta = \frac{\ln\left(\frac{460}{p_f}\right)}{4.3} \quad for\ 10^{-9} \le p_f \le 10^{-1} \tag{4.15}$$

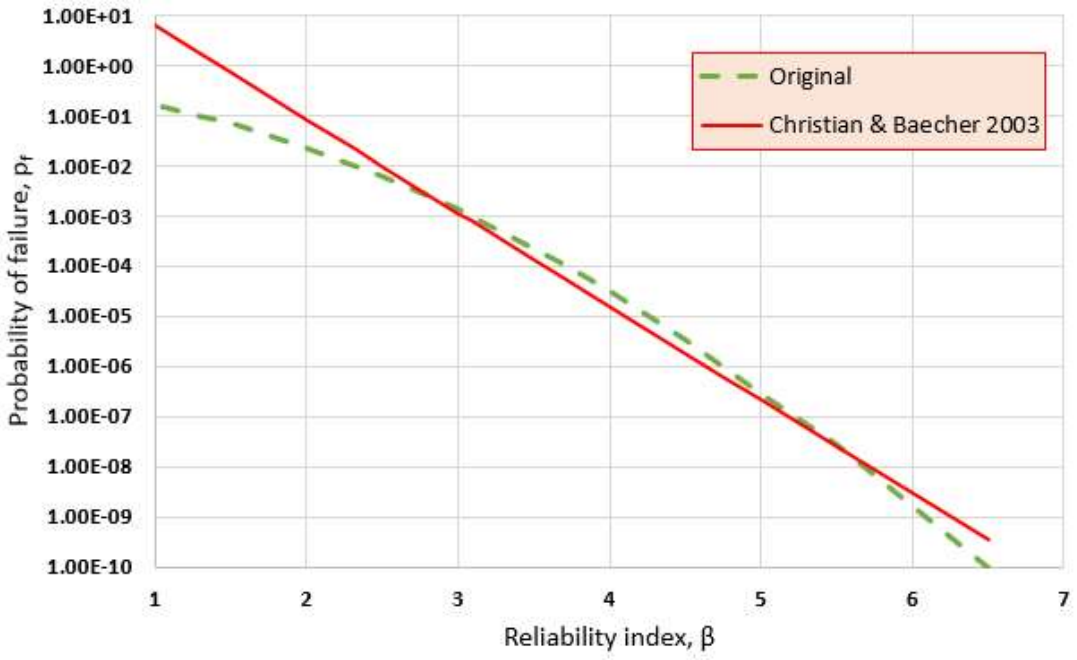

Figure 4.4 Probability of failure vs reliability index for normal variables

The relationship proposed by Baecher & Christian (2003) was provided with validity limits on reliability ($2 \le \beta \le 6$). To obtain better accuracy for a wider range of reliability levels, the relationships shown in Table 4.3 are suggested in this dissertation. Figure 4.5 illustrates the goodness of fit of the proposed relationships. The improved relationships are especially important for low reliability levels such as encountered in serviceability limit states or high reliability levels such as those required when probability of failure must be very low.

Table 4.3 Suggested probability of failure vs reliability index relationships

Range	$p_f = f(\beta)$	$\beta = f(p_f)$	R^2
$p_f > 6 \cdot 10^{-3}, \beta < 2.6$	$p_f \approx 1.2e^{-2.06\beta}$	$\beta \approx \frac{1}{2.06} \ln\left(\frac{1.2}{p_f}\right)$	0.98
$10^{-6} \le p_f \le 6 \cdot 10^{-3}$ $2.6 \le \beta \le 4.8$	$p_f \approx 196e^{-4.0\beta}$	$\beta \approx \frac{1}{4.0} \ln\left(\frac{196}{p_f}\right)$	0.99
$p_f < 10^{-6}, \beta > 4.8$	$p_f \approx 10^6 e^{-5.8\beta}$	$\beta \approx \frac{1}{5.8} \ln\left(\frac{10^6}{p_f}\right)$	1.00

4.3.4 Risk and Tolerable Risk Concepts

ISO-2394 defines risk as the *"effect of uncertainty on the objectives"* and clarifies this definition with a note that *"risk is the expected value of all undesirable consequences, i.e. the sum of all the products of the possible consequences of an event and the corresponding probabilities"* (ISO, 2015). It is obvious from this definition that risk is not equivalent to the likelihood or probability of failure, p_f. In other words, if the occurrence of a failure does not carry consequences, the risk represented by that failure is zero.

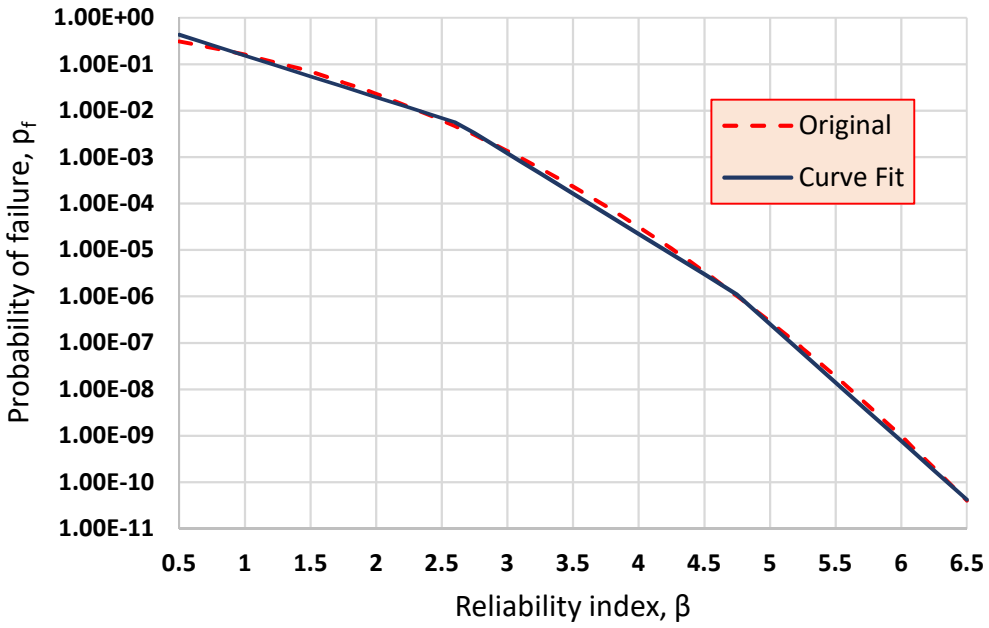

Figure 4.5 Curve fitting of probability of failure vs reliability index relationship

Probability of failure is a real number that varies between 0 (impossibility of failure) and 1 (certainty of failure) and that can be calculated using probability theory. Risk is also not equivalent to hazard. While hazard is the probability that a threat or danger occurs and causes failure within a given time period, risk measures the exposure to damages resulting from that occurrence and is defined as hazard multiplied by potential worth of loss (Lacasse *et al.*, 2012). Risk involves quantification of the damage or the consequence of failure. When the consequence of failure is low, a higher probability of failure can be tolerated. The opposite is also true; i.e., when the consequence of failure is high, a lower probability of failure needs to be sought to achieve a similarly tolerable risk. Therefore, a more accurate expression of risk should incorporate the probability of the hazard materializing, the probability of failure when exposed to the hazard and the consequence of failure. The probability of the hazard and the probability of failure when

exposed to the hazard can be combined into a probability of failure conditioned on a hazard magnitude or a return period for the hazard. An accepted formula for risk is to express it as a product of the probability of failure, p_f, and the consequence of failure, c_f:

$$Risk = p_f c_f \tag{4.16}$$

As can be deduced from the above equation, the risk associated with a high probability of failure and low consequence may represent the same risk as the case of a low probability of failure but high consequence of failure.

It is important to note that while the probability of failure can be computed mathematically and is within the scope of engineers, the consequence of failure is a measure of human and economic impacts and often includes considerations that are difficult to evaluate or put in monetary terms, such as human life or environmental/ecological damage. The value given to such considerations is subjective and is typically a function of evolving societal norms (Vick, 2002; Trbojevic, 2005; Bea, 2006; Trbojevic, 2009). Standards are starting to include rational methods for quantifying such consequences; e.g., through the Marginal Lifesaving Cost (MLSC) principle and the concept of Life Quality Index (LQI) as *"an indicator of the societal preference and capacity for investments into life safety"* (Nathwani *et al.*, 1997; ISO, 2015). Many of these methods classify risk as negligible, tolerable or non-acceptable, with risks falling in the tolerable category requiring an analysis to show that they are As Low As Reasonably Possible/Practicable (ALARP) (Bowles, 2013). In the United States, ALARP principles and risk-informed decision making are adopted extensively by the US Army Corps of Engineers (USCOE, 2014).

Geotechnical and structural design standards attempt to capture the consequence component of risk by assigning different building class categories, risk categories, or importance

factors to structures and facilities with different consequences of failure (ASCE, 2017; ICC, 2018). Perhaps a classic example where more thorough consideration of consequence of failure could have yielded different results is the extensive damage caused by Hurricane Katrina in 2005. In a "lessons learned" paper, the need for a risk-based planning and design approach was identified (Sills *et al.*, 2008).

4.3.5 System and Component Reliability

Most structures consist of many components and the reliability of such structures depends on the reliabilities of the different components and on how such components are assembled; i.e., on the load paths and the degree of redundancy present in such assemblages. For wind turbine foundations, particularly gravity-based foundations, there is no redundancy. Reliability depends on verifying different limit states representing different failure modes. This is equivalent to thinking of the foundation as a single component of a system or as a system consisting of a single component which can fail in different modes. Such a system can be modeled as being in series where the occurrence of failure in any of the failure modes causes the failure of the entire system. Note that failure here includes violation of any limit state and does not necessarily mean collapse. If all failure modes are statistically independent, the reliability of the system is equal to the product of reliabilities of all possible failure modes; i.e., if there are n possible failure modes, the reliability of failure in mode i would be ps_i and the reliability of the full system would be (Nadim, 2007):

$$PS = \prod_{i=1}^{n} ps_i = \prod_{i=1}^{n} \left(1 - pf_i\right) \tag{4.17}$$

For low probabilities of failure, the probability of failure of the system would then be:

$$PF = 1 - PS = 1 - \prod_{i=1}^{n} \left(1 - pf_i\right) \approx \sum_{i=1}^{n} pf_i \tag{4.18}$$

If probabilities of failure of all components in series are perfectly correlated, the probability of failure of the system is simply the probability of failure of the most unreliable component; i.e., $PF = \max\left(pf_i\right)$. In all cases, the probability of failure of the foundation system is bounded as follows:

$$\max\left[pf_i\right] \le PF \le 1 - \prod_{i=1}^{n} \left(1 - pf_i\right) \tag{4.19}$$

Except for unusual proportions, a foundation that is likely to fail in one mode is also likely to fail in at least a few other modes. Thus, foundation failure modes are typically strongly correlated. The usual assumption in foundation design is to assume that failure modes are perfectly correlated and to use the failure probability of the least unreliable mode as that for the foundation system, i.e., $PF = \max\left(pf_i\right)$.

The risk can then be calculated by multiplying the probability of failure of the system (foundation) by the consequences of failure. This dissertation is limiting the analyses to the determination of the probability of failure for a few modes or limit states; i.e., there are no risk evaluations.

4.3.6 Target Reliability Specification

As mentioned in earlier sections, there is a one-to-one relationship between probability of failure and reliability index. Thus, specifying a target reliability index is equivalent to specifying a target probability of failure. Figure 4.6 shows this one-to-one relationship and points on the curve indicating approximate ranges of typical levels of design reliability common in design standards.

Selecting the target reliability index (or probability of failure) for a design needs to consider at least the following three aspects: cost of safety measures, failure consequences and time of exposure as reflected in a reference period (Holický *et al.*, 2015). The first two aspects are cost related, while the third is an integral input to the determination of the probability of failure as the reference period needs to be mentioned whenever the probability of failure is specified.

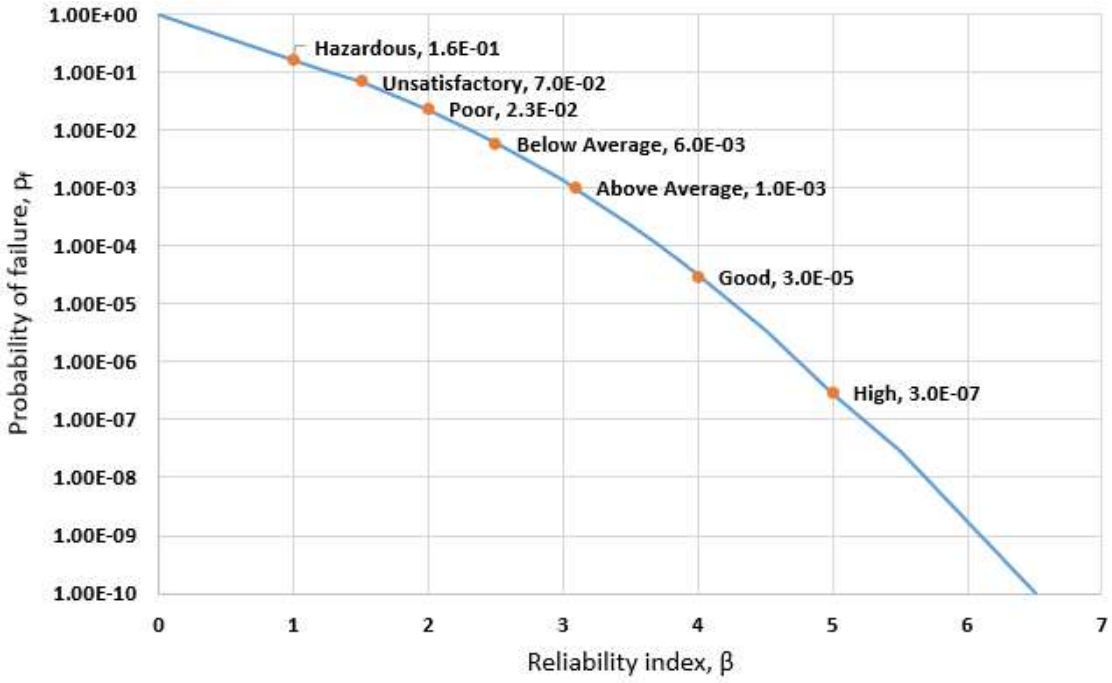

Figure 4.6 Customary design acceptance for different reliability levels

4.3.6.1 Failure Consequences

Failure consequences include potential losses in human lives, injuries and material damages. Failure consequences should also include direct damage caused by the failure and indirect damage caused to the surrounding environment and to society at large.

4.3.6.2 Cost of Safety Measures

These are the costs associated with incorporating certain safety measures in the design to achieve the desired reliability level. Theoretically, a structure can be made so stout and a foundation can be made so large that failure is impossible or extremely rare. However, such safety measures come at costs that need to be balanced against the benefits through a cost-benefit analysis. This is typically achieved through an assessment of the marginal cost of reliability; i.e., the ratio of additional costs to reduction in risk. The point of diminishing returns indicates that an optimal design has been reached.

4.3.6.3 Reference Period

For most civil, structural and geotechnical design standards where failure can involve loss of human lives, the implied reliability levels are specified based on annual probabilities; i.e. 1-year reference period. Another common reference period is 50 years. Reliability levels for another arbitrary reference period, t_{ref}, can be estimated, assuming reference period independence, based on the reliability for annual probabilities, β_1 (CEN, 2005):

$$\beta_{tref} = \Phi^{-1}\left(\left[\Phi\left(\beta_1\right)\right]^{tref}\right) \tag{4.20}$$

The assumption of reference period independence is common for ULS and SLS limit states. However, it is obvious that such an assumption cannot be expected to be valid for fatigue limit states as such states are concerned with fatigue life where the annual probability of fatigue failure is time dependent; i.e. dependent the current age of the element and the associated accumulated damage.

4.3.7 Reliability Implied in Various Design Standards

According to Baecher and Christian (2003), a reliability index of 2 to 3 is common in modern (circa 2003) design codes, while typical values for ASD methods ranged from 2.5 to 3.5 corresponding to probabilities of failure of 10^{-4} to 10^{-2}. However, in a critical review of safety acceptance criteria, Diamantidis (2008) found a much larger scatter in annual reliability implied by current (circa 2008) design codes and standards, varying between a reliability index of $\beta \approx 3 \quad (p_f \approx 10^{-3})$ to $\beta > 7 \quad (p_f = 10^{-12})$. This wide range could be attributed to conflicting objectives in the selection of the target reliability in the various codes. For examples, standards for critical and significant structures prioritize human safety, while the majority of standards for common buildings are mere calibrations to match previous codes, and yet a smaller percentage of codes are based on cost-benefit optimizations. It is also important to mention that target reliability is typically applied to components or dominant failure modes rather than to whole systems or structures. Designers should be cognizant of any dependencies in component reliabilities; e.g. parallel or series dependencies and how they impact the reliability of whole systems.

4.3.7.1 Eurocode 1990

The objective of reliability differentiation in the EN 1990 is the socio-economic optimization of resources considering the cost of construction and the consequences of failures. Reliability differentiation is achieved through the following three Reliability Classes (RC's) that are directly associated with three Consequence Classes (CC's) (CEN, 2005):

- RC1: High consequence for loss of human life, or very great economic, social or environmental consequences

- RC2: Medium consequence for loss of human life, or considerable economic, social or environmental consequences
- RC1: Low consequences for loss of human life, and small/negligible economic, social or environmental consequences

Implicit minimum reliability levels for 1 and 50 reference periods are summarized in Table 4.4 for the three reliability classes and low relative cost of safety measures. For reference, residential and office buildings are typically classified as RC2 structures with notional reliability index of 3.8 for a 50-year reference period. More detailed notional reliability levels that consider the relative cost of safety measures are shown in Table 4.5.

Table 4.4 Notional minimum reliability levels in EN 1990 (CEN, 2005)

Reliability Class	Minimum reliability index β_{min}					
	1-year reference period			50-year reference period		
	ULS	FLS	SLS	ULS	FLS	SLS
RC3	5.2	NA	NA	4.3	NA	NA
RC2	4.7	NA	2.9	3.8	1.5 to 3.8	1.5
RC1	4.2	NA	NA	3.3	NA	NA

Table 4.5 EN 1990 notional ULS reliability considering costs of safety measures

Relative costs of safety measures	1-year reference period				50-year reference period			
	Consequence of failure				Consequence of failure			
	Small	Some	Moderate	Great	Small	Some	Moderate	Great
High	2.3	3.0	3.5	4.1	0.0	1.5	2.3	3.1
Moderate	2.9	3.5	**4.1**	4.7	1.3	2.3	3.1	3.8
Low	3.5	4.1	4.7	5.1	2.3	3.1	3.8	4.3

4.3.7.2 fib Model Code for Concrete Structures 2010

The fib Model Code for Concrete Structures 2010 provides codification guidance that can serve as basis for concrete design codes (CEB-FIP, 2013). It is published by the International Federation for Structural Concrete which serves as a "pre-normative" organization with global participation. Target reliability indices recommended by this guidance are shown in Table 4.6 and Table 4.7. Per this guidance, three consequence levels are considered for ULS: low, medium and high. Also, this guidance considers FLS as part of ULS. For SLS, this guidance considers whether the serviceability issue is reversible or irreversible, Table 4.7.

Table 4.6 fib Model Code 2010 reliability indices for ULS/FLS (CEB-FIP, 2013)

Consequence level	50-year reference period	1-year reference period
Low	3.1	**4.1**
Medium	3.8	4.7
High	4.3	5.1

Table 4.7 fib Model Code 2010 target reliability indices for SLS (CEB-FIP, 2013)

Serviceability nature	Reference period	β_T
Reversible	Life	0.0
Irreversible	50-year	1.5
Irreversible	1-year	3.0

4.3.7.3 ISO 2394 General Principles on Reliability for Structures

ISO-2394 is an international standard that outlines general principles of reliability-based design of structures (ISO, 2015). This document is commonly included by reference in other

international standards such as the IEC61400 series developed by the International Electrotechnical Commission for utility scale wind turbines (IEC, 2008, 2016). The methodical basis for ISO-2394 is outlined in the Probabilistic Model Code (JCSS, 2000, 2001a, 2001b) and in Risk Assessment in Engineering Principles, System Representation & Risk Criteria (JCSS, 2008). ISO-2394 (2015) identifies five consequence classes (Class 1 through Class 5) with increasing consequence from Class 1 characterized as "predominantly insignificant material damages" to Class 5 described as "catastrophic events causing losses of societal services and disruptions and delays beyond national scale over periods in the order of years." Large wind turbines and unmanned offshore facilities fall into Class 2 which is described as "material damages and functionality losses of significance for owners and operators but with little or no societal impact; less than five fatalities." Intended reliability levels for ULS and 1-year reference period are shown in Table 4.8. The level of reliability indicated in bold font in this table; Class 3 with normal cost of safety measures, agrees with the 1-year level adopted by EN 1990 for moderate consequence of failure and relative cost of safety measure (Table 4.5) and the 1-year level adopted by fib Model Code 2010 for low consequence level (Table 4.6).

For serviceability limit states, JCSS (2001a) distinguishes between reversible and irreversible limit states and recommends the tentative target reliability indexes shown in Table 4.9 for irreversible limit states and 1-year reference period. As can be noted, there is a large discrepancy with the recommendations of the fib Model Code 2010.

4.3.7.4 Reliability Implied in North American Standards

Target reliability indices for geotechnical design per several North American design codes and guidelines are listed in Table 4.10 (Canadian Geotechnical Society, 2006). As can be seen, the

ranges are comparable to European and International standards, but the guidance is not so granular as to delineate between the limit state categories and consequence of failure classes.

Table 4.8 ISO-2394 ULS reliability for 1-year reference period (ISO, 2015)

Relative cost of safety measure	Consequence of failure class					
	Class 2: Minor		Class 3: Moderate		Class 4: Large	
	β_T	p_f	β_T	p_f	β_T	p_f
Large	3.1	$\approx 10^{-3}$	3.3	$\approx 5 \cdot 10^{-4}$	3.7	$\approx 10^{-4}$
Normal	3.7	$\approx 10^{-4}$	**4.2**	$\mathbf{\approx 10^{-5}}$	4.4	$\approx 5 \cdot 10^{-6}$
Small	4.2	$\approx 10^{-5}$	4.4	$\approx 5 \cdot 10^{-6}$	4.7	$\approx 10^{-6}$

Table 4.9 Target irreversible SLS reliability, 1-year reference period (JCSS, 2001a)

Relative Cost of Safety Measure	Target reliability index & probability of failure
High	$\beta_T = 1.3 \quad p_f^T \approx 10^{-1}$
Normal	$\beta_T = 1.7 \quad p_f^T \approx 5 \cdot 10^{-2}$
Low	$\beta_T = 2.3 \quad p_f^T \approx 10^{-2}$

Table 4.10 Implied North American annual target reliability indices

Design code or guide	SLS	ULS	FLS
Electric Power Research Institute (EPRI)	2.6	3.2	NA
National Building Code of Canada (NBCC)	NA	3.5	NA
AASHTO	2.0 to 3.5		
Canadian Foundation Engineering Manual 2006	2.8 to 3.5		

4.3.7.5 Reliability Levels for Wind Turbine Structures

Sorensen & Toft (2014) provide background information and assumptions made in the recommendations of partial safety factors included in IEC61400-1 and IEC61400-6 ((IEC, 2008, 2016). Based on this background document, the following assumptions and observations are relevant to wind turbines:

1. In case of failure or at the end of its lifetime, a new wind turbine is erected
2. Failures only cause economic damage; i.e., failures do not result in fatalities or pollution
3. A key driver of design is the reduction of cost of energy; this means that the relative cost of safety measures is high.
4. The fact that wind turbines are type-certified means that most turbines have hidden safety since each turbine is designed to the higher limits of its class but will operate at conditions that are less severe than the higher limits.

With the above assumptions in mind, the notional target annual probability of failure is selected as $p_f^T = 5 \cdot 10^{-4}$ which corresponds to a target reliability index of $\beta_T = 3.3$. As shown in Table 4.5, this reliability level corresponds to a high cost of safety measures and to a consequence of failure between "some" and "moderate" per EN 1990. With regards to ISO-2394, this suggested reliability level corresponds to consequence of failure Class 3 and large relative cost of safety measures, Table 4.8. This appears to be more conservative than the classification of large wind turbines into Class 2 per ISO 2394. If the ISO 2394 classification were adopted, the annual probability of failure would be $p_f \approx 10^{-3}$ and the reliability index would be $\beta = 3.1$. This discrepancy could be due to the recommendation made by JCSS (2001a) to overestimate the target

reliability index by no more than 5% to account for uncertainty caused by the use of approximate calculation methods; thus the higher target is obtained from: $\beta_T = 3.1 \cdot 1.05 = 3.3$. This reliability target; i.e. $\beta_T = 3.3$ and $p_f^T \approx 5 \cdot 10^{-4}$, is also specified by ISO 19902 for fixed steel offshore structures that are unmanned or that are evacuated during severe storms (ISO, 2007).

4.3.7.6 Reliability Levels Adopted in this Dissertation

Target reliability levels adopted in this dissertation for the design of onshore wind turbine foundations are indicated in Table 4.11. These levels are based on the aforementioned discussion of notional reliability targets in various standards and particularly in Sorensen & Toft (2014) background document to IEC61400-1. The ULS reliability level is as recommended by Sorensen & Toft (2014) and corresponds to the EN1990 level for structures with high relative cost of safety measures and some-to-moderate consequences of failure. Target reliability for serviceability limit states is based on the assumption of normal costs of safety measures as recommended in (JCSS, 2001a). The SLS reliability level adopted here is higher than would be if costs of safety measures were considered high as done for the ULS case and is comparable to a level between either of the following EN1990 scenarios: (i) high cost of safety measures with some to moderate consequence of failure, or (ii) moderate cost of safety measures with small to some consequence of failure.

Table 4.11 Target reliability for onshore WTG foundations adopted in this work

Limit State	Reference Period	Reliability Index	Probability of Failure
ULS	1-year	3.3	$\approx 5 \cdot 10^{-4}$
	50-year	2.0	$\approx 2 \cdot 10^{-2}$
SLS	1-year	1.7	$\approx 3.5 \cdot 10^{-2}$
	50-year	1.0	≈ 0.165

4.3.8 Limit States Design of Wind Turbine Foundations

Under combined loading, failure of a shallow foundation can be in the form of excessive settlement, tilt, overturning, sliding or failing in any one of several bearing modes. For wind turbine foundations, a low stiffness of the foundation can also affect the performance of the tower structure. Each of these outcomes can be described in terms of a limit state where the foundation is either failing to perform as required and is thus affecting the performance of the plant; i.e. has violated a serviceability limit state, or has totally collapsed; i.e., has violated an ultimate limit state. There are at least three types of limit state categories that are relevant to the design of wind turbine foundations: 1) Ultimate Limit States (ULS), 2) Serviceability Limit States (SLS) and 3) Fatigue Limit States (FLS).

4.3.8.1 Ultimate limit states (ULS)

Violation of an ultimate limit state is typically associated with a catastrophic failure. Examples include soil bearing capacity failure, foundation overturning, foundation sliding and concrete flexure, shear or punching failures. Catastrophic failures are total failures that cause collapse of the turbine or render it unsafe to operate or approach.

4.3.8.2 Serviceability limit states (SLS)

Violation of a serviceability limit state results in a plant that may operate outside specified tolerances and limits. Continued operation outside tolerances typically leads to distressed components, break downs and/or reduced life. Example serviceability limit states include unacceptable foundation tilt, settlement, stiffness and excessive concrete cracks.

4.3.8.3 Fatigue limit states (FLS)

Fatigue limit states involve material failures caused by repeated application of variable loads and are typically unpredictable and catastrophic. Some designers and design standards, such as the fib Model Code (CEB-FIP, 2013), classify fatigue limit states as ultimate limit states. However, methods for evaluating fatigue are very different from those of the common ultimate limit states and are dependent on the material fatigue characteristics and the loading spectra. Because of the cyclic and highly variable nature of the loading, the fatigue life of practically all components and materials making up the foundation is normally verified.

4.3.8.4 Semi-probabilistic Design Optimization

Wind turbine foundation design practice involves verification of multiple limit states and selection of the least cost design that is valid for all limit states under consideration, Figure 4.7. This dissertation is focused on three common limit states: one ultimate limit state; i.e., bearing capacity, and two serviceability limits; i.e., tilt and rotational stiffness. Experience indicates that serviceability limit states often govern the design of WTG foundations. For instance, foundation stiffness is likely to govern most foundations supported on soft subgrades. Fatigue limit states of structural materials (steel, concrete, grout, etc) may also govern the design, however, their treatment is beyond the scope of this dissertation.

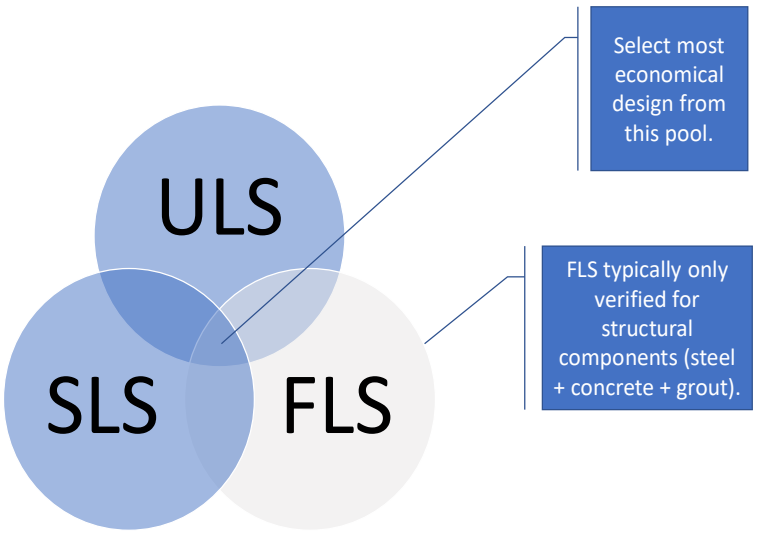

Figure 4.7 Selection of least cost design meeting multiple limit states

CHAPTER 5

RELIABILITY-BASED DESIGN

At the second Karl Terzaghi Lecture delivered in 1964, Casagrande spoke of Terzaghi's accomplishments in reducing "unknown risks" through rational methods of soil mechanics (Casagrande, 1965). Casagrande emphasized the need for careful consideration of risks and for the exercise of judgment to achieve "calculated risk." Casagrande described "calculated risks" as:

> *"(a) The use of imperfect knowledge, guided by judgment and experience, to estimate the probable ranges for all pertinent quantities that enter into the solution of the problem.*
>
> *(b) The decision on an appropriate margin of safety, or degree of risk, taking into consideration economic factors and the magnitude of losses that would result from failure."*

While Casagrande gave a well-formulated definition of calculated risks, he did not specify how risk could be calculated. In fact, Casagrande acknowledged that calculated risk was a problem which, at the time, "defied quantitative analysis." The practical takeaway from Casagrande's hopeful definition was that "calculation of risk" consisted of the careful consideration of risk relying most likely on local/regional experience, professional experience and judgement, but without a clear and systematic process for how this objective could be achieved.

Whitman (1984) revisited the topic at the 17th Karl Terzaghi Lecture by reviewing advances in reliability analysis and applications of probability theory over the two decades since Casagrande's lecture and attempted to answer the question of whether risk can (or should) be calculated. One of Whitman's concluding remarks was the recommendation that reliability theory may only be used to guide the selection of a safety factor if the problem was well understood and there was an adequate related database. Whitman also acknowledged a reigning perception of

doubt among geotechnical engineers that risk could or even should be calculated. However, Whitman still argued that the need for reliability analysis in geotechnical engineering would continue to exist and that such studies must be pursued further.

Two decades later, at the Sixth Arthur Casagrande Memorial Lecture in 1996, Kulhawy presented on reliability-based design in foundation engineering and acknowledged a state of complacency within the geotechnical engineering community and a sense that existing (and "proven") methods were adequate for carrying out optimal designs (NRC, 1995; Kulhawy, 1996). Kulhawy argued for a Reliability-Based Design (RBD) alternative which he described as any method that used reliability analysis, explicitly or otherwise. The version Kulhawy advanced at this lecture was the calibrated multiple/partial factor format such as the LSD/LRFD design approach described in Chapter 4. In 2000, Whitman discussed organizing and evaluating uncertainty in geotechnical engineering and identified four potential uses of probabilistic methods: site characterization, design evaluation, decision making, and construction control (Whitman, 2000); i.e., he did not include direct design as a potential use but he did include design evaluation.

The perception that current geotechnical design practice produces optimal designs appears inconsistent with historical facts. Christian & Baecher (2011) noted the discrepancy, usually by two orders of magnitude, between the observed and computed failure rates in geotechnical design and identified this discrepancy as the No. 1 unresolved problem in geotechnical risk and reliability. The perception of doubt and reluctance described by Whitman and Kulhawy is also present in the wider engineering design community as illustrated in the debate of whether "probabilistic design should replace safety factors" by Doorn & Hansson (2011). The outcome of this debate was that probabilistic risk assessment and safety factor approaches were complementary, rather than mutually exclusive. The authors claimed that that "in most applications, uncertainties prevent

probabilistic risk assessments from providing an objective probability of failure" as if safety factors had objective bases other than historical performance and as if uncertainties were not the real basis for probabilistic design. The authors concluded that safety factors were "indispensable for dealing with dangers that cannot be assigned meaningful probabilities;" an argument that seems to prefer an arbitrary safety factor over assigning some form of probability to poorly understood dangers. It seems from these arguments that the main stumbling block is the unfamiliarity of engineers with probabilistic concepts and methods.

Currently and probably for a few decades to come, geotechnical design practice will continue to be based on the semi-probabilistic LSD/LRFD format. It is interesting to recall that when Moe (1936) argued against the global factor of safety approach and in favor of using separate factors of safety for dead load, live load and material resistance, he pointed out that the single factor of safety was not adequate because it had *"gradually been found necessary to supplement it by statements of special requirements."* Ironically, this is also a prime limitation of current LSD/LRFD design methods; i.e., the use of the calibrated partial factors has to be supplemented by conditions on assumed target reliability, variabilities of design inputs, methods by which inputs have been estimated, computational models used, etc. In fact, the traditional ASD format offered more flexibility as the designer was free to select a global factor of safety, within a relatively wide range, to reflect familiarity with the site and his/her judgment. The LSD/LRFD format specifies code-mandated partial factors and takes away most flexibility from the designer.

For similar reasons, Phoon & Ching (2015) wondered if there was "*anything better than LRFD for simplified geotechnical RBD.*" They proposed the Quantile Value Method (QVM) as a potential answer to that question (Ching & Phoon, 2011b, 2013). The basic idea of the QVM method is to reduce stabilizing random variables, such as shear strength, to a quantile value η and

to increase destabilizing random variables, such as load, to a quantile value $1-\eta$ to reach design values for both stabilizing and destabilizing random variables. Parameter η is called a probability threshold and is assumed to be constant for both stabilizing and destabilizing variables. Because the probability threshold is a quantile value, the procedure is equivalent to applying partial factors that are functions of the variable COV's. However, Ching, Phoon*, et al.* (2015) showed that the QVM method was not robust against variable redundancy and came up with the concept of an Equivalent Random Dimension (ERD) whose equation is determined by the code developer through a calibration process. Thus, it appears this method is not much better than the LRFD framework in terms of designer flexibility and the need to perform calibrations.

In light of the constraints placed by all of the above methods and the confusion caused by multiple factors for different scenarios, applications and industries, breaking free of any such factors or calibrations would be a great advantage and a welcome relief. Many favorable developments have taken place since 1964 or 1996 such that it is now possible and far simpler to use full probabilistic methods, such as direct Monte Carlo or a Monte Carlo version with improved sampling and/or Bayesian updating, directly in geotechnical design, Figure 5.1. These developments include better understanding of typical ranges and effects of soil variability, advances in Bayesian probability methods and the abundant and portable availability of computing power. Probabilistic methods calculate risk, complement judgement and provide new insights into the design and its critical parameters. They afford the designer great flexibility in design assumptions and the opportunity to focus on assessing design input variability. This chapter reviews various reliability-based design methods and covers in more detail the direct reliability-based design (d-RBD) method which is used in this dissertation.

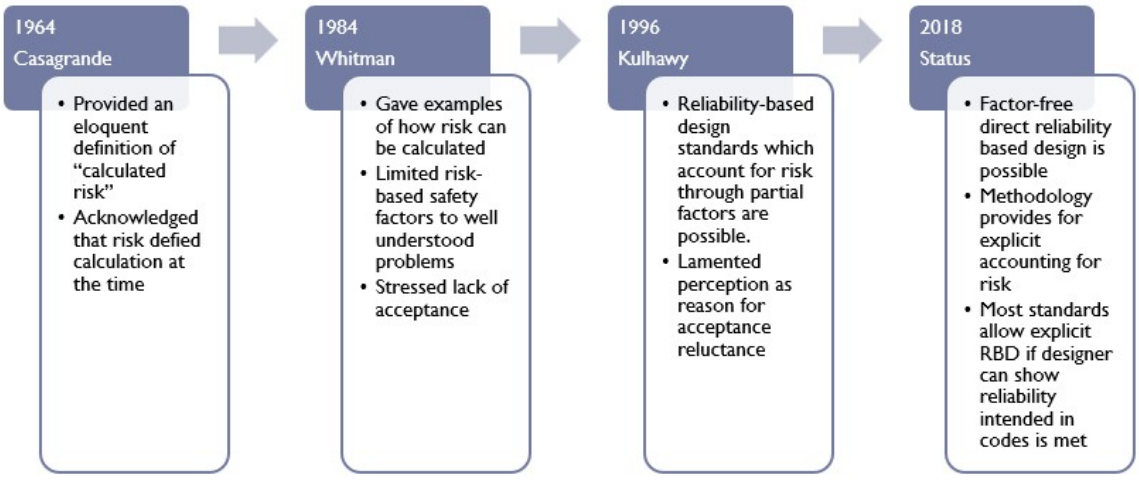

Figure 5.1 Risk: from concepts to evaluation

5.1 Reliability Analysis Methods

Design methods based on reliability analysis come in various forms and levels of complexity and accuracy (Jonkman *et al.*, 2015). There are at least five levels of reliability method sophistication where each higher level can be used to calibrate or develop guidance for the levels below it. In general, reliability methods leverage, to varying degrees, available knowledge and information about the problem or design situation to infer information on design reliability. Thus, probability and statistics are the primary tools used in these methods. Many of these methods are based on the frequentist's approach to probability but the Bayesian definition of probability is making inroads and has the biggest potential of advancing the field, especially for geotechnical design. Leimeister & Kolios (2018) reviewed reliability-based methods for risk analysis as applied in the offshore wind industry. They classified these methods into three broad categories: qualitative, semi-quantitative and quantitative. Quantitative methods include analytical methods which calculate the reliability index (or probability of failure) via analytical estimates such as Tayler Series expansion. Stochastic methods achieve the same goals through sampling techniques

such as Monte Carlo Simulation. Both analytical and stochastic methods are based on the idea of limit states and limit state functions and their primary objective is the calculation of the probability of failure and hence the reliability index. Compared to stochastic methods, analytical methods such as FORM and FOSM have the advantage of light computational effort. However, they are not as accurate because they are based on first order Taylor series expansion approximations of the limit state function; in effect, they are based on a linearization, at the mean values of variables, of the limit state function which is often nonlinear. Table 5.2 contains a summary of quantitative reliability analysis methods.

Table 5.1 Reliability analysis levels

Level	Description	Where/how used
0 – Deterministic	Deterministic values of loads & resistance	Classical ASD/WSD
I - Semi-probabilistic	Characteristic values of loads & resistance	LSD/LRFD, current codes
II – Approximation	Uncertain parameters modeled as random variables possibly including cross-correlations. Moments up to second order are used (mean and variance).	Used to calibrate current codes. FORM and FOSM are sample Level II methods.
III – Numerical	Uncertain parameters modeled through joint probability density functions & probability of failure determined exactly (analytical formulations, numerical integration or Monte Carlo simulations).	RFEM and d-RBD are a sample Level III method
IV- Risk-based	Consider Level II or III probability of failure and consequence of failure.	Risk-based: consider probability and consequences of failure

Table 5.2 Summary of quantitative reliability analysis methods

No.	Method name	Category	Descriptions, pros and cons	Example References
1	Taylor Series Methods	Analytical	• FOSM • Simple, easy to understand & apply • Requires an assumption on the FS PDF • Requires 2N+1 calculations of the factor of safety (if an equation cannot be derived) • Only good for rough estimate; can give non-unique solutions.	• Cornell (1969) • Harr (1987) • Duncan (2000) • Baecher & Christian (2003)
2	Point Estimate Methods (PEM)	Analytical	• FOSM • Requires an assumption on the FS PDF • Requires 2^N calculations of the FS	• Rosenblueth (1975) • Rosenblueth (1981) • Zhao & Ono (2000) • Christian & Baecher (2002)
3	Hasofer-Lind Methods	Analytical	• FORM, SORM, AFOSM • Allows modeling of random variable cross-correlations • More accurate than Methods 1 and 2	• Hasofer & Lind (1974) • (Li & Lumb, 1987) • Baecher & Christian (2003) • Low (2006)

Table 5.2 Continued

No.	Method name	Category	Descriptions, pros and cons	Example References
4	Direct MCS Method	Stochastic	• Computationally intensive • No assumptions needed other than those related to random variables. • Robust, unbiased method where the accuracy of probability of failure can be improved by more sampling. • Almost sure convergence (strong law of large numbers)	• (Baecher & Ingra, 1981) • Kalos & Whitlock (2008) • Au & Wang (2014)
5	Kriging	Stochastic	• More computationally efficient than direct MCS • Used effectively for sensitivity analyses	• Zhang *et al.* (2015) • Wang *et al.* (2013)
6	Subset simulation, MCMC Methods, Gibbs Sampling, etc.	Stochastic	• Methods are more computationally efficient than direct MCS as they make use of Importance Sampling (IS) or other sampling schemes, but are less robust; i.e., may not converge. • Used effectively for sensitivity analyses • Subset simulation can be combined with Markov chain Monte Carlo (MCMC) methods and neural networks.	• Au & Wang (2014) • Robert & Casella (2011) • Giovanis *et al.* (2010)

Table 5.2 Continued

No.	Method name	Category	Descriptions, pros and cons	Example References
7	Random Finite Element Method (RFEM)	Stochastic	• Combines the finite element method and random fields for proper modeling of spatial variability • Can be combined with direct MCS or any of the other sampling schemes that improve computational efficiency • Computationally intensive • State-of-the-art in computational probabilistic geotechnical analysis	• Fenton & Griffiths (1993) • Fenton & Griffiths (2003) • Griffiths & Fenton (2007a) • Fenton & Griffiths (2008) • Huang *et al.* (2010)
8	Bayesian Updating & Inference	Analytical & Stochastic	• Reduction of parameter variability resulting in uncertainty reduction in all methods above (analytical or stochastic).	• Caspeele (2014) • Baecher & Christian (2015) • Ering & Babu (2017) • Wang *et al.* (2017)
FORM: First Order Reliability Method, FOSM: First Order Second Moment reliability method. N is the number of random variables.				

5.2 Direct Reliability Based Design Method (d-RBD)

Monte Carlo Simulation (MCS) is a measurement process that involves sampling from a population that is described through statistical parameters with pre-defined underlying distributions (e.g. Fishman, 1995; Morgan & Henrion, 1999; Kalos & Whitlock, 2008; Kroese *et al.*, 2011). The process of sampling is described as simulation or the generation of scenarios. Each generation instance or scenario is termed a realization. Data collected through sampling are analyzed using different statistical methods. However, to gain useful knowledge from sampled data, the number of realizations needs to be sufficiently high. Methods involving MCS are used in diverse fields such as financial markets as well as risk assessment and management in practically any field.

The Direct Reliability Based Design (d-RBD) method presented in this dissertation is a direct MCS process used to obtain, through a single MCS run for each limit state, designs meeting predefined reliability criteria for that limit state (Ben-Hassine & Griffiths, 2012). The method is general and can be applied to various limit states with different target reliabilities, in which case the method can be used as a Direct Reliability Based Design Optimization (d-RBDO) tool. The d-RBD method is a Level III reliability analysis method (Table 5.1), and as such, it can be used for code calibration or development of other semi-probabilistic design procedures. As outlined in Chapter 4, target reliability would be different for different limit states and reference periods and the method allows the setting of a different reliability target for each limit state. The method is versatile and, similar to other probabilistic methods, has the critical feature of enabling the design engineer to focus effort on assessing the variability of the key design inputs and to exercise judgment in employing different computational models and analysis techniques.

5.2.1 Method Details

In the d-RBD method, design parameters are treated as random variables with predefined probability density functions. MCS is used to generate realizations of a performance function corresponding to the limit state under consideration, assumed to be represented as follows:

$$g\left[b \cdot \delta \cdot R(\mathbf{X}, \mathbf{A}), \mathbf{Q}\right] = 0 \tag{5.1}$$

where:

- $R(\,)$ is the computational model or equation for calculating resistance
- $\mathbf{X}$ is a vector of random variables that make up the equation for calculating resistance
- $\mathbf{Q}$ is a vector representing random load components; note that for the case of wind turbine foundations, the predominant component is the overturning moment.
- $\mathbf{A}$ is a vector of uniformly distributed discrete random variables representing the potential values of the important design decision section dimensions; e.g., foundation diameter and/or depth,
- δ is model uncertainty which can be modeled as a lognormal random variable with mean of 1 and a COV of COV_δ, but is assumed to be deterministic and equal to 1 in these analyses, and
- b is bias in the resistance model $R(\,)$ and is also assumed to be deterministic and equal to 1 in these analyses with mean values of resistance random variables taken as the characteristic values.

The realizations of the performance function are obtained by using the generated values of the random variables and checking whether failure occurred or not. Failure corresponds to the

performance function taking on a value that is less or equal to zero; i.e., $g\left[b\cdot\delta\cdot R(\mathbf{X},\mathbf{A}),\mathbf{Q}\right]\le 0$. Depending on the limit state under consideration, failure could mean collapse, due for example to bearing capacity failure, or the development of an operational issue such as excessive tilt or low foundation stiffness. Statistical analysis of the realization results is carried out using Bayes' theorem to determine the probability of failure conditioned on the design decision parameters for each combination of design decision dimensions. The ensuing procedure is effectively a design tool that identifies the pool of combinations of design decision dimensions that have acceptable probabilities of failure. Different limit states can be considered through multiple implementations of this process, with each implementation resulting in a pool of acceptable designs for that limit state. The optimal design for all considered limit states is the lowest cost design that is common to all the pools of acceptable designs. The essential steps of the d-RBD procedure are shown in Figure 5.2. A flow chart for multiple limit states is shown in Figure 5.3, in which nr is the number of realizations and ir is a realization counter.

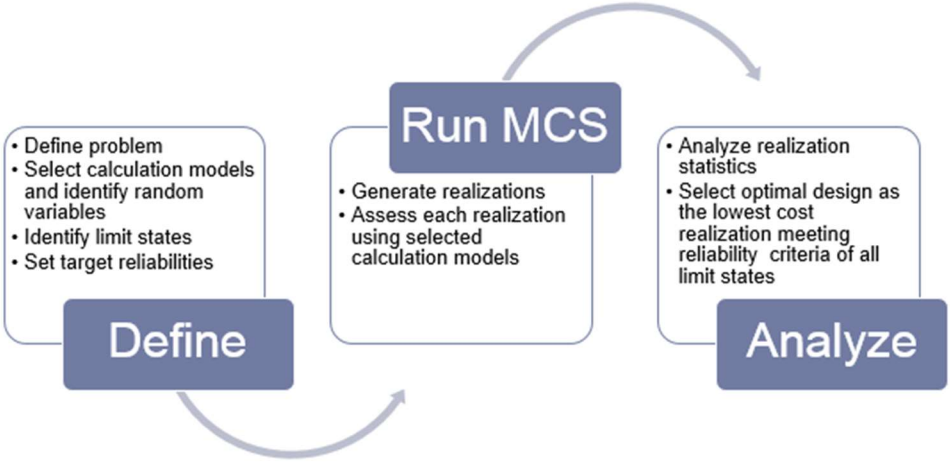

Figure 5.2 Essential steps in the d-RBD procedure

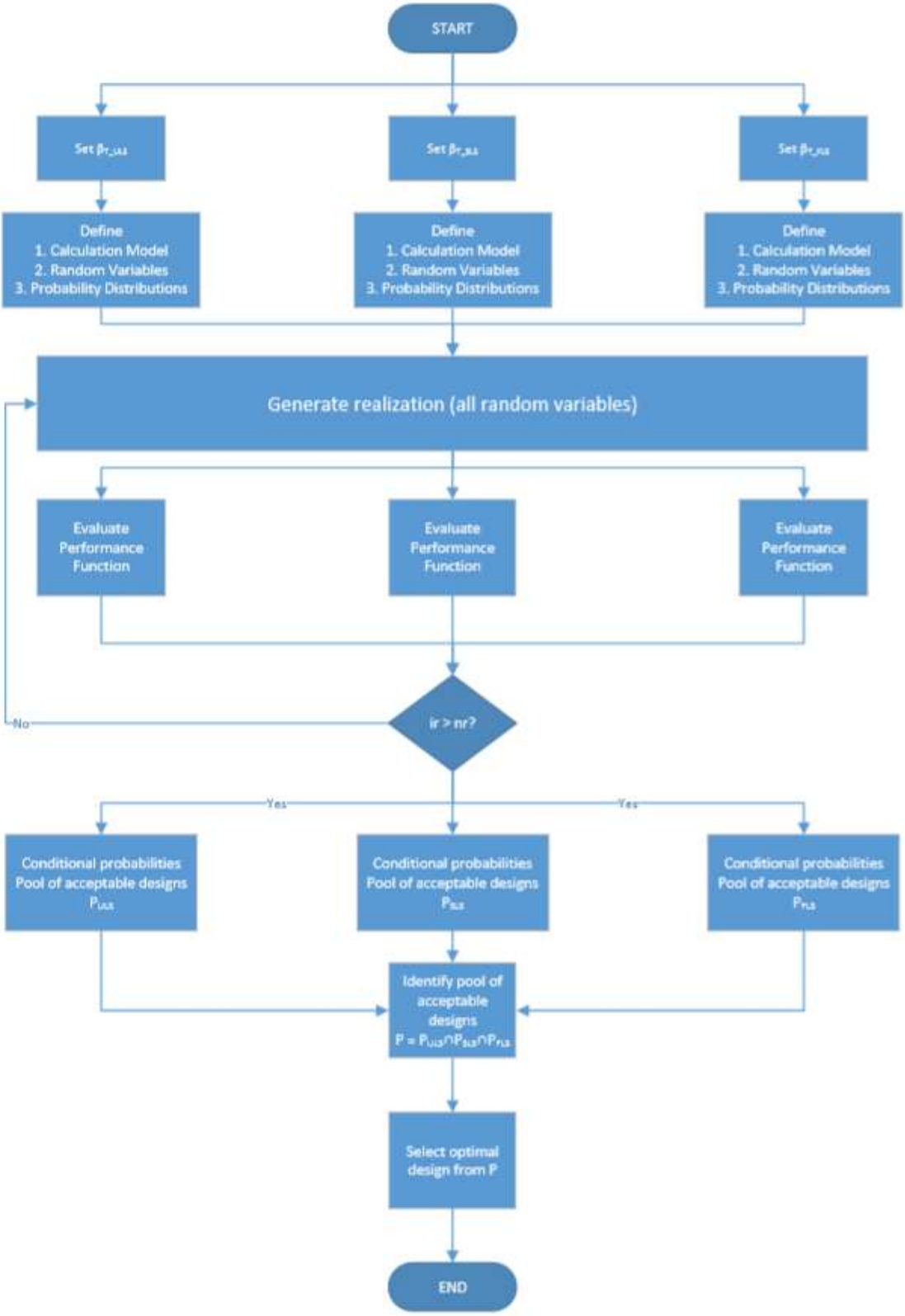

Figure 5.3 d-RBD flowchart

5.2.1.1 Problem Definition

The problem definition step is required for each limit state and it includes:

- Identification of the failure mode and performance function
- Selection of the resistance and loading random variables and definition of their probability density functions and any cross-correlations
- Selection of the cross-section dimension values to be considered. These would cover the anticipated practical ranges considering construction and cost aspects.
- Selection of the target reliability index, β_T, or target probability of failure, p_f^T, for the limit states under consideration. This choice needs to reflect the consequence of failure and the reference period.

5.2.1.2 Generation of Realizations

MCS consists of generating a large number of realizations, n_r, and evaluating each realization using the selected computation model to decide whether the limit state is violated. The total number of failure simulations, n_f is determined. The probability of failure for the MCS run is:

$$p_f = \frac{n_f}{n_r} \tag{5.2}$$

The generation of realizations involves generating uniform random samples and using the inversion principle to obtain independent and identically distributed (i.i.d.) samples of any distribution. The inversion principle provides that a random sample from any CDF $F(x) = P\left[X \le x\right]$ can be generated by transforming a uniform random sample. This is because if

U is uniformly distributed between 0 and 1; i.e. $U \sim U(0,1)$ then the CDF of $X = F^{-1}(U)$ is equal to $F(x)$.

This step also includes incorporating random variable cross-correlations in the generation process. This is achieved through Cholesky factorization of the correlation matrix.

5.2.1.3 Analysis of MCS Results

For each combination of design decision parameters, in this case for each combination of foundation width and depth, the number of violations (failures) is also counted as n_{fBD} . An acceptable combination of design decision parameters is a combination that has an acceptable conditional failure probability; namely, its conditional failure probability must be less than the target failure probability, p_t

$$p(Failure \mid B, D) \leq p_t \tag{5.3}$$

The conditional probability $p(Failure \mid B, D)$ is calculated using Bayes' Theorem as:

$$p(Failure \mid B, D) = \frac{p(B, D \mid Failure)}{p(B, D)} p_f \tag{5.4}$$

In the above equation, the conditional joint probability of B and D given failure, $p(B, D \mid Failure)$, and the probability of the uniformly distributed design decision parameters, $p(B, D)$, are calculated as follows:

$$p(B, D \mid Failure) = \frac{n_{fBD}}{n_f} \tag{5.5}$$

and

$$p(B,D) = \frac{1}{n_B n_D} \tag{5.6}$$

In the above equation, n_B and n_D are the numbers of discrete B and D values.

Combining the above definitions into Equation (7.4), the n_f term drops out and the conditional probability of failure, $p(Failure \mid B,D)$, can be calculated using:

$$p(Failure \mid B,D) = \frac{n_{fBD}}{n_r} n_B n_D \tag{5.7}$$

5.2.1.4 Why the d-RBD Name?

Because uncertainty is represented explicitly through random variables to use in a computational model, without the need for partial factors, and because the method uses a direct Monte Carlo process, the procedure is called a direct Reliability-Based Design (d-RBD) method. The outlines of the d-RBD approach, whether in regards to its intent or mechanics, have been described and used in the literature (e.g. Honjo, 2011; Wang, 2011; Wang *et al.*, 2011; Fan & Liang, 2012; Wang & Cao, 2015). However, it was given different names by different authors. For example, Wang (2011) called it the "Expanded RBD" or RBD^E and used it for bearing capacity design of foundations, while Fan & Liang (2012) labelled it the MCS Based Design (MCSBD) method and used it the design of laterally loaded piles.

One aim of this dissertation is to formalize the d-RBD method and to provide examples of its practical applications. The method also lends itself to Performance Based Design (PBD) as the target reliability index, β_T , or the target probability of failure, p_f^T can be selected to design to any target performance.

5.2.2 Hypothesis Testing for Parameter Ranking

Many uncertain load and resistance design parameters form the input to the d-RBD method, each with predefined uncertainty parameters. A valuable insight would be to know which uncertain parameter has the most or least effect on the probability of failure. Such insight can be obtained by statistically comparing, for each parameter, the mean of the parameter for the failed realizations, μ_F , to the mean of the same parameter for the unconditional realizations, μ . The statistical difference is computed through hypothesis testing where the null hypothesis is $H_0 : \mu = \mu_F$ and the alternate hypothesis is $H_A : \mu \neq \mu_F$. A measure of the difference is given by a hypothesis test statistic, the absolute value of which is Z_H , where n_f is the number of failures and σ is the standard deviation of the parameter for the unconditioned realizations:

$$Z_H = \frac{|\mu - \mu_F|}{\frac{\sigma}{\sqrt{n_f}}} \tag{5.8}$$

This index, which could be described as an "importance index", has a range of $(0, +\infty)$ and is computed for each of the random variables. The vector of indices serves to rank all uncertain parameters per their effect on the probability of failure. In the resulting ranking, the magnitude of the index is not important but what is important is how it compares to indices of the other parameters. Thus, it is useful to normalize the vector of indices. Knowing the parameters that have a larger impact on probability of failure can serve to focus the uncertainty assessment or geotechnical exploration efforts on those parameters. On the other end of the spectrum, parameters with the least impact on probability of failure can be treated as deterministic without appreciable loss of method accuracy.

5.2.3 Method Accuracy

Increasing the number of realizations is the obvious method for reducing the error of the d-RBD MCS process. The improvement of accuracy can be observed through a plot of probability of failure versus the number of realizations where large fluctuations of the probability of failure converge to a more defined value as the number of realizations increases. Such plots are shown for all the limit states considered in this dissertation in subsequent chapters. An important feature of the Monte Carlo method is that it has "linear complexity" (Morgan & Henrion, 1999). This means that the number of uncertain variables has no bearing on the required number of samples to reach a certain output precision or confidence level. The primary factor affecting this precision is the sample size; i.e., the number of MC runs. There are many recommendations relative to the minimum number of realizations or the required number of realizations as a function of the desired accuracy of the probability of failure (Fishman, 1995; Morgan & Henrion, 1999; Fenton & Griffiths, 2008).

As a rough indicator, the required number of realizations should be at least one order of magnitude greater than the reciprocal of the target probability level, p_f^T (Robert & Casella, 1999). Thus, if there are N_{ddc} design decision combinations, i.e., possible combinations of design decision parameter values, the recommended lowest number of realizations per Robert & Casella (1999), $n_{r\min}$, is:

$$n_{r\min} = \frac{10N_{ddc}}{p_f^T} \tag{5.9}$$

Another estimate of the minimum number of realizations is proposed by Ang & Tang (2007) as:

$$n_{r\min} = \frac{\left(\frac{1}{p_f^T} - 1\right) N_{ddc}}{COV_T^2} \tag{5.10}$$

where COV_T is the target coefficient of variation of the target probability of failure. In both of the above two equations, if there are no design decision variables; i.e., if the reliability of a particular design is being assessed, the suggested number of realizations is as indicated in the equations with $N_{ddc} = 1$.

While increasing the number of realizations is the obvious means for reducing the error, it comes at additional computational cost. There are more efficient alternatives such as the Markov Chain Monte Carlo (MCMC) algorithms (Robert & Casella, 2011), subset simulation (Au & Wang, 2014) and Bayesian updating. These alternatives keep the computational cost at manageable levels and deliver improved accuracy. These alternatives are beyond the scope of this dissertation.

5.2.4 d-RBD Advantages

In the d-RBD design method, uncertainty is modeled separately for each load and/or material parameter and the designer has full flexibility to select an appropriate computational model, random and deterministic parameters, variable probability density functions, variable uncertainties and variable cross-correlations. Therefore, engineering judgment can be applied at any step of the process. Duncan & Sleep (2017) emphasize the importance of judgement by stating that *"judgement and experience are essential prerequisites for meaningful assessment of geotechnical reliability."* This section enumerates the different ways the d-RBD method retains flexibility and provides room for the engineer to exercise judgement.

5.2.4.1 Freedom to Adjust Target Reliability

The target reliability index is selected based on tolerable risk associated with a failure event. In LSD/LRFD codes, notional target reliability is hard coded through a process of partial factor calibration, making such codes limited in application to the limit states covered in the codes and to conditions assumed in the calibration process. With the d-RBD method, the designer can set the target reliability to match reliability levels intended by any of these LSD/LRFD standards. In addition, the designer can verify additional limit states not included in standards and, if desired, can select a different target reliability index; e.g., in a performance-based design (PBD) context.

5.2.4.2 Factor-free Approach

With the d-RBD method, there are no partial factors on loads or resistances and no factors to account for consequence of failure, or any other design consideration. All such considerations can be embedded in adjusting the probability of failure which produces the desired target reliability.

5.2.4.3 Characteristic Value Free Approach

Today's standards define characteristic values of loads and resistances differently. Some define the characteristic value as the mean, others specify a particular "cautious estimate of the mean" be used, while others call for the use of lower or higher fractile whichever is more conservative. Such basic differences make it difficult to navigate codes and are partly responsible for the differences in calibrated partial factors and the ensuing confusion. With the d-RBD approach, there is no need to define characteristic values.

5.2.4.4 Freedom to Select an Appropriate Computational Model

Some design standards specify different partial resistance factors for different assumptions made in computational and transformation models, sometimes leaving out specific models and

always neglecting models that are yet to come (future models). With the d-RBD method, the computational model can be arbitrary and is part of the problem definition. Furthermore, the computation model can be as complex as necessary without adding complexity to the d-RBD process, except possibly additional computational cost.

5.2.4.5 Freedom to Define Random Variable Distribution and Uncertainty

The d-RBD method allows designers to select the random variables, their probability distributions and their uncertainties; in fact, these are the basic inputs of the method. This affords the designer the opportunity to account for local knowledge and site-specific uncertainty which is often ignored by pre-packaged LSD/LRFD based design standards.

5.2.4.6 Ability to Account for Variable Cross-correlations

Variable cross-correlations, such as the positive correlation between soil unit weight and shear modulus or potential correlation between friction and cohesion, can be accounted for through a covariance matrix. This feature is an opportunity to exercise judgement and reap benefits based on rational analysis.

5.2.4.7 Ability to Compare Results Using Different Computational Models

In Section 3.1.2.3, model uncertainty was presented as a potentially frivolous concern. The designer is supposed to be able to choose the computational model that is appropriate for the limit state and its assumptions. However, if necessary or in doubt, the d-RBD procedure enables the designer to investigate different computational models and select the more onerous results. This is also applicable if there are multiple equally valid computational models for a given limit state. An obvious example is bearing capacity of foundations over fine grained soils which is typically evaluated for drained and undrained conditions, hence the two different computational models. The range of designs for the various computational models can also serve to bound the uncertainty

associated with the selection of the computational model, if one admits the existence of model uncertainty.

5.2.4.8 Manageable Computational Effort

The computational effort depends on the number of random variables and the magnitude of probability of failure. For rare events; i.e., where the probability of failure is very low, the required number of realizations is often in the millions. Even though many MCS realizations are often needed to compute probability of failure with acceptable accuracy, the calculations are manageable on everyday personal computers. For typical limit state equations involving about half a dozen randomized design decision variables and target probability of failure of 10^{-3}, each MCS takes at most a few minutes. However, this number can be drastically reduced through Bayesian updating, subset simulation, neural networks and other techniques described in Section 5.2.3. Thus, adopting d-RBD as an everyday design tool is computationally possible and can be very beneficial since designers would spend most of their effort focusing on understanding and assessing the variability of the parameters impacting their designs.

5.2.4.9 Reliability-based Design Optimization (RBDO)

When multiple limit states are verified, and the optimal design is selected from the intersection of all pools of acceptable designs, the d-RBD method turns into a reliability-based design optimization tool.

5.2.5 d-RBD Limitations

Even though d-RBD has many advantages, it does have a few challenges and limitations. The main challenge is that many designers only have a basic appreciation of probabilistic concepts or understanding of design parameter variability. Without these critical skills, the method may not

be adopted as a routine design tool soon. Engineering curricula, especially in geotechnical engineering where designers deal with high material variability, should include a stronger focus on probabilistic tools and uncertainty assessments to better equip future engineers with the proper knowledge.

Another limitation, which is also common to almost all other methods, is the inability to model spatial variability. The most rigorous method for modeling spatial variability is through random fields and stochastic finite element methods such as the random finite element method (RFEM) (Fenton & Griffiths, 2007; Griffiths & Fenton, 2007b). However, there are ongoing efforts to incorporate the effects of special variability, at least approximately, through "spatially averaged" or "equivalent" parameters for soil masses in a process called homogenization (Ching & Phoon, 2011a, 2012; Griffiths *et al.*, 2013; Ching, Hu*, et al.*, 2015).

5.2.6 Implementation Tools

There are numerous computational tools that can be used to implement the d-RBD procedure. Almost any computer programming language can be used. However, popular calculation and data processing packages such as Microsoft Excel (Microsoft, 2018), MATLAB (MathWorks, 2016) or Mathcad (PTC, 2018) would be practical and readily accessible choices that do not require much programming. Even though the investigations carried out in this dissertation are performed using MATLAB, Microsoft Excel would be a more accessible choice since it resides on almost every personal computer, laptop or tablet. Microsoft Excel has many built-in tools for data analysis, manipulation and rendering. Excel also comes equipped with Visual Basic for Applications (VBA), a Basic programming language enhanced over the years with countless built-in functions and object-oriented tools. An efficient approach to implementing d-RBD in Excel is to use datasheets to enter inputs and Excel VBA to generate Monte Carlo

Simulations and perform the statistical analysis of the results associated with d-RBD. Modern day applications can also be developed for tablets and smart phones for ultimate portability.

CHAPTER 6

FOUNDATION TILT AND ROTATIONAL STIFFNESS

This chapter illustrates use of the d-RBD method for verifying the tilt and rotational stiffness serviceability limit states of shallow wind turbine foundations. The method is also used to investigate effects of uncertainty as reflected in random variable COV's and effects of random variable cross-correlations. The deterministic models or equations for tilt and stiffness presented in Chapter 2 are used in this chapter where parameters are randomized.

6.1 Foundation Tilt

The tilt limit state is verified using theoretical equation (2.14) and by defining the performance function as:

$$g = \tan\left(\theta_{\max}\right) - M\frac{1-\upsilon^2}{EB^3}I_\theta = 0 \tag{6.1}$$

where:

- $\theta_{\max}$ is the maximum tilt angle, taken equal to $0.17\,\text{deg}$
- υ is Poisson's ratio
- E is strain-level corrected Young's modulus, computed as $E = 2\left(1+\upsilon\right)G$
- G is strain-level corrected shear modulus computed as $G = \lambda G_0$
- G_0 is the zero-strain shear modulus computed from $G_0 = \rho V_s^2$ in which ρ is the in-situ soil density and V_s is shear wave velocity

- λ is the shear modulus ratio $\lambda = \dfrac{G}{G_0} = \dfrac{1}{1+\left(\dfrac{\gamma}{\gamma_{ref}}\right)^{\alpha}}$ in which α is the curvature parameter,

  γ is the shear strain level and γ_{ref} is the reference shear strain computed as $\gamma_{ref} = \dfrac{\tau_{\max}}{G_0}$

  where $\tau_{\max}$ is the maximum shear stress or the shear strength of the soil

- B is foundation diameter
- M is the applied load, selected at the S3 level per IEC61400-6 recommendation (IEC, 2016), and
- I_θ is a correction factor

In the computation of the performance function, the intermediate quantities can be calculated using the relationships mentioned above and then plugged into Equation (6.1) or, alternatively, it can be computed directly as:

$$g = \tan\left(\theta_{\max}\right) - M\frac{\left(1-\upsilon\right)\left[1+\left(\dfrac{\gamma\rho V_s^2}{\tau_{\max}}\right)^{\alpha}\right]}{2\rho V_s^2 B^3} I_\theta = 0 \tag{6.2}$$

Any or all of the parameters in the above equation can be assumed to be deterministic or random with assumed PDF's. In this analysis, loads and material properties are selected to match those of the example foundation analyzed in Section 2.9 using STAAD finite element program. That example foundation is a realistic scenario for an 80-meter hub height wind turbine. COV values are selected based on medium variability suggested in Table 3.8. The adopted parameter assumptions are shown in Table 6.1.

Table 6.1 Random variables for tilt limit state investigations

Parameter		Variable PDF's				Notes
		Dist.	Mean	COV		
				Med.	High	
Applied moment (Nm)	M	LN	S3: $2 \cdot 10^7$	0.20	0.25	Annual maximum load effect at S3 level.
In-situ soil density ($\frac{\text{kg}}{\text{m}^3}$)	ρ	NR	1750	0.05	0.10	
Poisson's ratio	υ	NR	0.35	0.05	0.10	
Shear wave velocity ($\frac{\text{m}}{\text{s}}$)	V_s	LN	200	0.40	0.60	
Shear strain level	γ	LN	$5 \cdot 10^{-4}$	0.20	0.30	The shear modulus ratio (at mean values) is 0.70, which is in line with current practice.
Shear strength (Pa)	$\tau_{\max}$	LN	10^5	0.25	0.50	
Shear modulus degradation curvature parameter	α	NR	0.90	0.10	0.20	$\alpha = 0.9$ is close to the (Darendeli, 2001) value.
Correction factor	I_θ	NR	4.16	0.05	0.10	
Foundation diameter (m)	B	NA	17.0	NA	NA	Design decision variable.
Probability of failure	p_f			$7 \cdot 10^{-6}$	$2 \cdot 10^{-3}$	
Reliability index	β			4.4	2.9	

Notes:

- Maximum allowed tilt is $\theta_{\max} = 0.17\,\text{deg}$
- Target reliability is as outlined in Table 4.11; i.e. $\beta_T = 1.7$ ($p_f^T = 0.035$) for 1-year reference period and $\beta_T = 1.0$ ($p_f^T = 0.165$) for 50-year reference period.

6.1.1 Reliability of Foundation – Tilt Limit State

Adopting the random variables and their associated PDF's listed in Table 6.1, the probability of failure; i.e., probability of exceeding the tilt limit of $0.17\,\text{deg}$ is computed using MCS for a foundation diameter of $B = 17m$. The tilt angle calculated deterministically using mean values of random variables is 0.0063 degree, which is much smaller than the limit of 0.17 degree. As shown in Figure 6.1 and Figure 6.2, the probability of failure converges, as the number of realizations is increased, to about $p_f = 7 \cdot 10^{-6}$ $(\beta = 4.4)$ for the medium variability case and $p_f = 2 \cdot 10^{-3}$ $(\beta = 2.9)$ for the high variability case. The probability of failure for either case is much lower than the target probability of failure of $p_f^T = 0.035$ $(\beta_T = 1.7)$ for 1-year reference period serviceability limit states.

Apparently, other design requirements such as requiring positive contact pressure under the S3 level loading or other more onerous limit states make the tilt limit state unlikely to govern. The formulation used in this exercise is for a surface foundation and it ignores any potential beneficial effects of embedment or vertical loads. The formulation is based on elasticity theory and ignores other sources of potential deformation. Furthermore, it is reasonable to expect non-uniform ground conditions under the foundation which add to tilt from elastic deformation. Therefore, some level of conservatism is warranted. However, this reliability based exercise shows that either the tilt limit is conservative, as inferred from the discussion in Sections 2.5.1 and 2.8.2, or the current guidance recommendations are conservative.

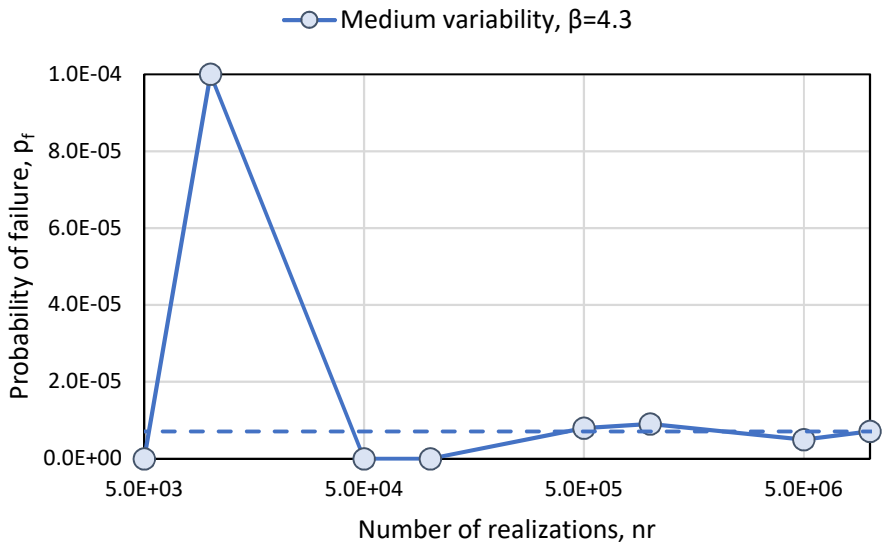

Figure 6.1 Tilt failure probability – $B = 17\text{m}$, medium parameter variability

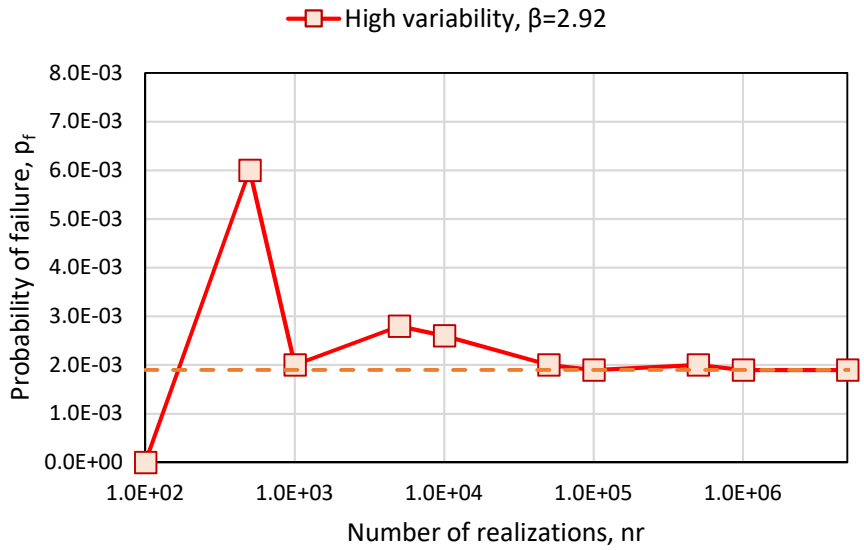

Figure 6.2 Tilt failure probability – $B = 17\text{m}$, high parameter variability

6.1.2 Parameter Ranking – Tilt Limit State

Even though the reliability analysis described in the previous section shows that the tilt limit state is not governing, it is useful to know how the random variables in the adopted limit state function rank in terms of importance. The hypothesis testing procedure described in Section 5.2.2 is used for this purpose and the resulting normalized importance indices are shown in Table 6.2 and shown as a pie chart in Figure 6.3**Error! Reference source not found.**. As can be noted from this table and chart, shear wave velocity and applied moment have the greatest impact followed to much lesser extent by the rest of the parameters where the shear strain level seems to have the least impact. Such information can be useful in deciding where effort should be focused to reduce uncertainty. Such a decision would be particularly important if this limit state were governing the design.

Table 6.2 Random variable ranking for tilt limit state

Variability		V_s	M	ν	I_θ	ρ	$\tau_{\max}$	α	γ
Medium	Rank	1	2	3	4	5	6	7	8
	Index	0.838	0.509	0.114	0.106	0.099	0.059	0.029	0.009
High	Rank	1	2	5	3	4	7	6	8
	Index	0.853	0.456	0.167	0.163	0.085	0.040	0.030	0.019

(a) Medium variability

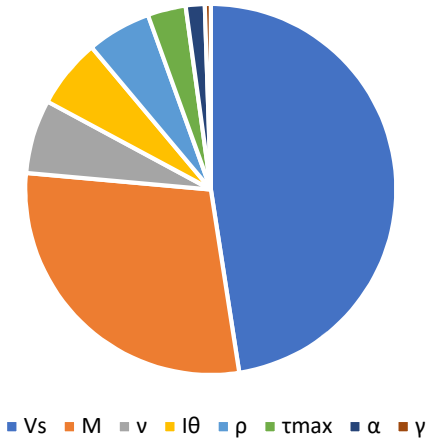

(b) High variability

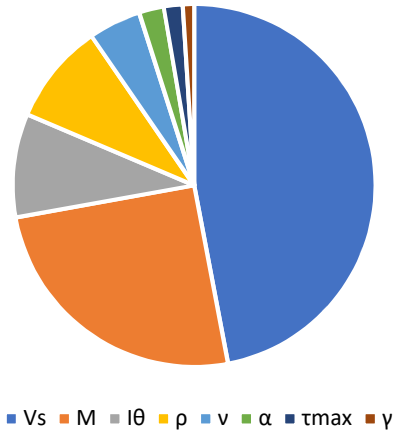

Figure 6.3 Tilt limit state parameter ranking, $B = 17\text{m}$

6.2 Rotational Stiffness

For the rotational stiffness limit state, both the dynamic and static stiffness should be verified as recommended in IEC61400-6 (IEC, 2016). Recall that this draft guidance recommends the following two verifications be performed:

1. Dynamic stiffness should be verified using zero strain moduli at the S3 load level, and
2. Static stiffness should be verified at the S1 load level using moduli that are adjusted for strain level and accounting for any reduction in bearing area if that occurs at this load level (which is likely to occur).

Making use of Equation (2.25), the performance function for both of these verifications is of the form:

$$g = K_r - K_{\min} = \frac{8GR^3}{3(1-\nu)}\left(1+2\frac{D}{R}\right)\left(1+0.7\frac{D}{H_b}\right)\left(1+\frac{R}{6H_b}\right) - K_{\min} = 0 \tag{6.3}$$

where:

- $K_{\min}$ is the minimum dynamic or static rotational (rocking) stiffness, as the case may be, specified by the wind turbine manufacturer,
- R and D are foundation radius and depth, respectively, where R is a reduced dimension to account for gapping for the static stiffness verification, in which case it can be taken as $R = {b_{eff}}/{2}$ (IEC, 2016),
- G is the shear modulus equal to G_0 for the dynamic stiffness check and reduced for the appropriate strain level for the static stiffness check, and
- H_b is distance from bottom of foundation to firm bedrock, if applicable.

In these investigations, we consider the case where H_b is too large to influence stiffness (deep bedrock taken at around 200m) and the case where bedrock is at a depth of half foundation width ($H_b \approx R = 8.5\text{m}$) to investigate the effect of uncertainty in bedrock depth. As in the tilt limit state, we also consider the cases of medium and high parameter uncertainty.

6.2.1 Dynamic Stiffness Verification

At the S3 load level, positive contact pressure is maintained at the foundation-subgrade interface. Assuming the foundation is sized to ensure positive contact is maintained considering

the uncertainty of the load, the performance function is rewritten in terms of all the applicable random variables listed in Table 6.3 as follows:

$$g = \frac{8\rho V_s^2 R^3}{3(1-\nu)}\left(1+2\frac{D}{R}\right)\left(1+0.7\frac{D}{H_b}\right)\left(1+\frac{R}{6H_b}\right) - K_{\text{dmin}} = 0 \tag{6.4}$$

6.2.1.1 Case of Deep Bedrock

Monte Carlo simulations were performed for the case of deep or non-existent bedrock, and for the cases of medium and high variability. As shown in Figure 6.4, for the medium variability case, probability of failure converges to $p_f = 0.018, \beta \approx 2.1$ which is comfortably more reliable than the target of $p_f^T = 0.165, \beta_T = 1.0$. The same is true but not by as large of a margin for the high variability case. For the high variability case, the probability of failure converges to $p_f = 0.096$. The corresponding reliability is $\beta = 1.27$ and only slightly larger than the target of 1.0. In this case, a design that is largely acceptable for medium variability is barely acceptable when variability is high. This finding illustrates how risk can be reduced either through reducing uncertainty or through adopting a more robust design if the high parameter variability is confirmed. Both of these outcomes can be confirmed through improved certainty relating to parameter variability. Parameter importance ranking is a useful tool to focus uncertainty reduction efforts on the important variables. The resulting parameter rankings is shown in Figure 6.5 for both the medium and high variability cases. It is no surprise that the design is most sensitive to shear wave velocity.

Table 6.3 Random variables for dynamic stiffness investigations

Variable		Dist.	Mean	*COV*		Notes
				Medium	High	
Density $\left(\mathrm{kg}/\mathrm{m}^3\right)$	ρ	NR	1750	0.05	0.10	
Poisson's ratio	ν	LN	0.35	0.05	0.10	
Shear wave velocity $\left(\mathrm{m}/\mathrm{s}\right)$	V_s	LN	200	0.40	0.60	
Depth to bedrock (m)	H_b	LN	200, 8.5	0.30	0.70	
Foundation radius (m)	R	NA	8.5	NA	NA	Design decision variable
Foundation depth (m)	D	NA	2.8	NA	NA	Design decision variable
Probability of failure	p_f			0.018	0.097	
Reliability index	β			2.1	1.3	

Notes:

- Minimum dynamic stiffness is $K_{\mathrm{dmin}} = 5 \cdot 10^{10}\ \mathrm{J}/\mathrm{rad}$
- Target probability of failure (and reliability index) as outlined in Table 4.11; i.e. $\beta_T = 1.7$ ($p_f^T = 0.035$) for 1-year reference period and $\beta_T = 1.0$ ($p_f^T = 0.165$) for 50-year reference period

Table 6.4 Dynamic stiffness parameter importance ranking – deep bedrock

Variable	V_s	ρ	ν
Rank	1	2	3
Index – Medium Variability	0.9935	0.0969	0.0604
Index – High Variability	0.9868	0.1440	0.0739

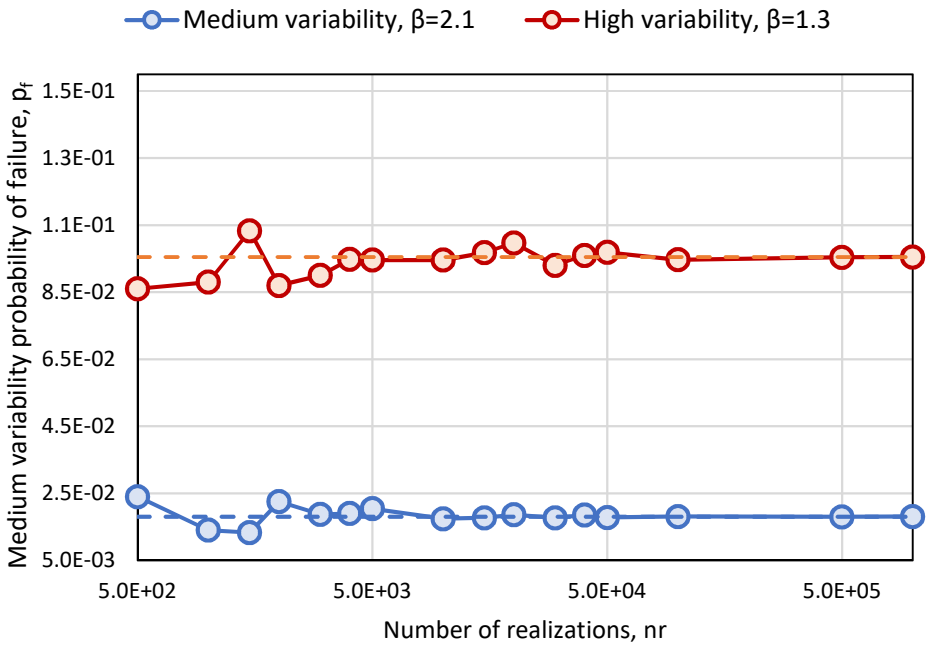

Figure 6.4 Dynamic stiffness probability of failure – deep bedrock

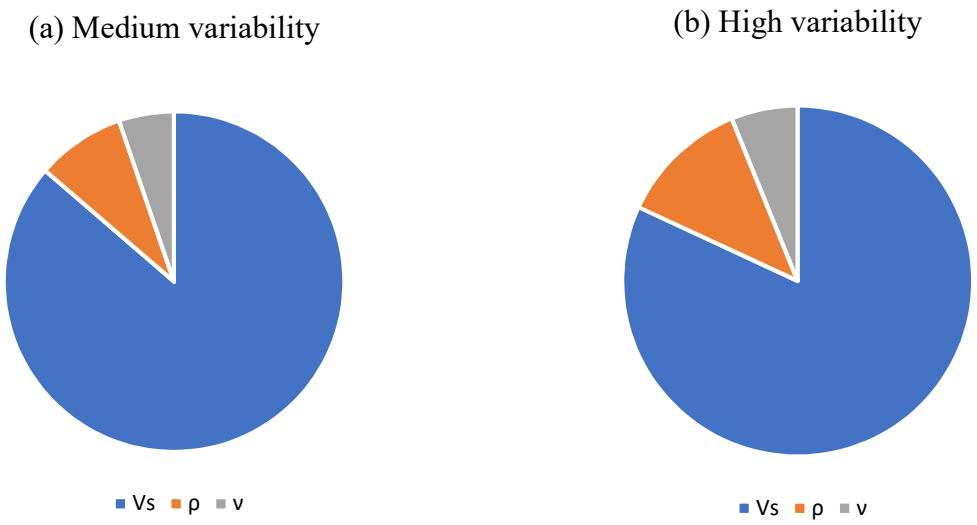

Figure 6.5 Dynamic stiffness parameter ranking - deep bedrock

6.2.1.2 Case of Bedrock within Zone of Influence

The case of bedrock within a depth of influence is investigated to assess the importance of accurate bedrock depth characterization when bedrock or a significantly stiffer stratum exists within a depth that may affect foundation stiffness. Fortunately, depth to bedrock is not too difficult to ascertain using geophysical or drilling explorations. During preliminary stages of a project, the depth to such a stratum may need to be established to a high level of confidence at every turbine location. To investigate this question, an arbitrary mean depth of one half the foundation width (or diameter) is selected and is treated as a random variable. The results for medium and high variability cases are shown in Figure 6.6. Table 6.5 shows reliability comparisons for the different scenarios. It should be noted that, as might be expected, having a firm stratum or bedrock within the depth of influence lowers the probability of foundation stiffness failure. This is true for the medium variability case. However, for the high variability case, uncertainty in the depth to bedrock actually lowers reliability when bedrock is within zone of influence. This result makes the case for establishing depth to bedrock with a high degree of certainty. Cost-effective geophysical surveys should ideally be conducted at every turbine location as early as possible during the project development phase.

Table 6.5 Dynamic stiffness reliability comparisons

	Medium Variability	High Variability
Deep bedrock	$p_f = 0.018, \beta \approx 2.1$	$p_f = 0.096, \beta \approx 1.3$
Bedrock within depth of influence	$p_f = 0.005, \beta \approx 2.7$	$p_f = 0.045, \beta \approx 1.6$

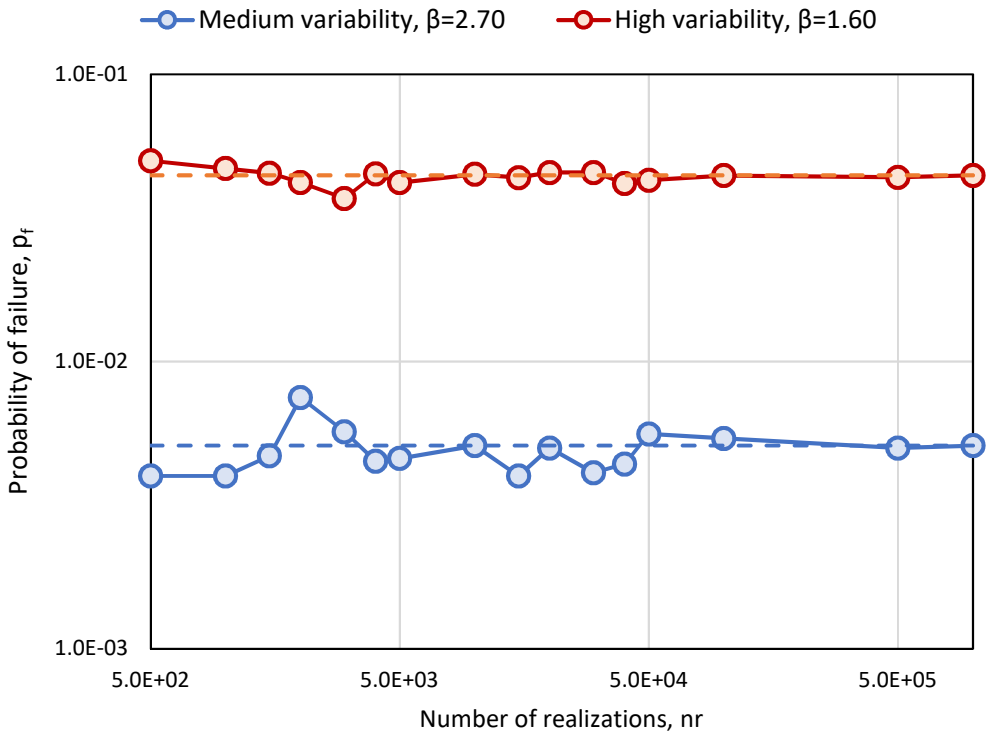

Figure 6.6 Dynamic stiffness failure probability – bedrock within influence depth

Parameter rankings for the case where bedrock is within depth of influence are shown in Table 6.6 and Figure 6.7. It is telling to notice that while shear wave velocity is still the most important parameter, the variability in depth to bedrock is more important than that of soil density or Poisson's ratio.

Table 6.6 Dynamic stiffness parameter ranking – bedrock within depth of influence

Variable	V_s	H_b	ρ	ν
Rank	1	2	3	4
Index – Medium Variability	0.9711	0.2062	0.1075	0.0537
Index – High Variability	0.9443	0.2803	0.1512	0.0832

(a) Medium variability

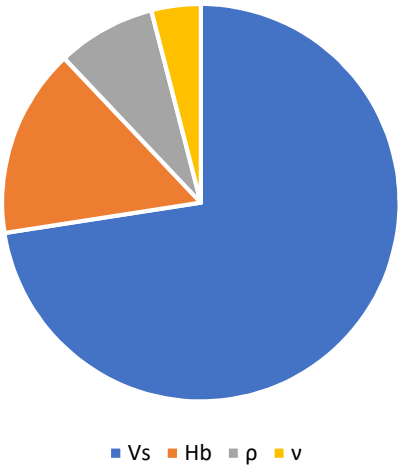

(b) High variability

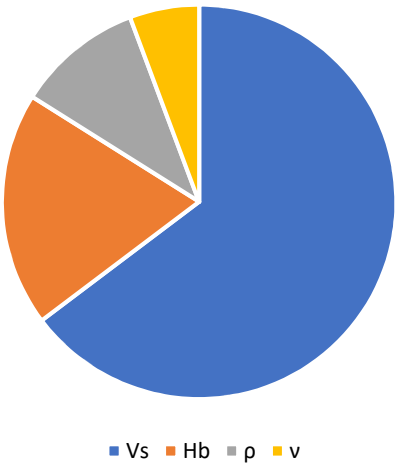

Figure 6.7 Dynamic stiffness parameter ranking – bedrock within influence depth

6.2.2 Static Stiffness Verification

For the static stiffness, after substituting into Equation (6.3) the relationships for shear modulus reduction, shear wave velocity and $b_{eff}/2$ for R, the following performance function can be obtained:

$$g = \frac{\rho V_s^2 b_{eff}^3}{3(1-\nu)\left[1+\left(\frac{\gamma\rho V_s^2}{\tau_{\max}}\right)^{\alpha}\right]}\left(1+4\frac{D}{b_{eff}}\right)\left(1+0.7\frac{D}{H_b}\right)\left(1+\frac{b_{eff}}{12H_b}\right)-K_{\text{smin}}=0 \qquad (6.5)$$

Table 6.7 lists all the random variables and the associated PDF assumptions for medium and high variability. The effective dimension, b_{eff}, is obtained using the DNV effective area approach described in Section 2.7.3 based on the applied moment M, modeled as a random

variable, corresponding to the S1 loading level. The computation of the effective dimension involves computing the equivalent vertical loading which includes the weight of turbine, foundation backfill and foundation concrete. Deterministic quantities provided in Table 2.3 are assumed in the computation of the total vertical loading. As in the dynamic stiffness case, the effect of bedrock within the depth of influence on static stiffness is investigated, in addition to the case of deep bedrock.

6.2.2.1 Case of Deep Bedrock

For the case of deep bedrock, the static rocking stiffness MCS converges to a probability of failure of 0.046 ($\beta = 1.61$) for medium variability and 0.150 ($\beta = 1.06$) for high variability, Figure 6.8. Both are acceptable, but the high variability case is right at the target reliability of 1.0. As in the case of dynamic stiffness, shear wave velocity and the moment loading are the driving parameters for design reliability, see Table 6.8 and Figure 6.8.

6.2.2.2 Case of Bedrock within Zone of Influence

MCS results for the case of bedrock within a depth of influence, taken here as random variable with a mean equal to foundation radius, are shown in Figure 6.10. Parameter importance ranking is shown in Table 6.9 and Figure 6.11. It should be noted here that depth to bedrock comes in third place, ranking higher than all other parameters with the exception of shear wave velocity and overturning moment. As expected, when bedrock is within a depth of influence, we obtain better reliabilities than for the case of deep bedrock, Table 6.10. However, the reliability improvement is more pronounced for the case of medium variability (compared to high variability case).

Table 6.7 Random variables for static stiffness investigations

Variable		Dist.	Mean	*COV*		Notes
				Medium	High	
Moment (J)	M	LN	$5{\cdot}10^{7}$	0.20	0.25	S1 load level, typically 50-year reference period
Density $\left(\mathrm{kg}/\mathrm{m}^{3}\right)$	ρ	NR	1750	0.05	0.10	
Poisson's ratio	ν	NR	0.35	0.05	0.10	
Shear strength (Pa)	$\tau_{\max}$	LN	$1{\cdot}10^{5}$	0.25	0.50	
Shear wave velocity $\left(\mathrm{m}/\mathrm{s}\right)$	V_s	LN	200	0.40	0.60	
Shear strain	γ	LN	$5{\cdot}10^{-4}$	0.20	0.30	
Curvature parameter	α	NR	0.90	0.10	0.20	Per MKZ formulation
Depth to bedrock (m)	H	LN	200, 8.5	0.30	0.60	
Foundation diameter (m)	B	NA	17.0	NA	NA	Design decision variable
Foundation depth (m)	D	NA	2.8	NA	NA	Design decision variable

Notes:

- Minimum dynamic stiffness is $K_{\mathrm{smin}} = 1{\cdot}10^{10}\ \mathrm{J}/\mathrm{rad}$
- Target probability of failure (and reliability index) as outlined in Table 4.11; i.e. $\beta_T = 1.7$ ($p_f^T = 0.035$) for 1-year reference period and $\beta_T = 1.0$ ($p_f^T = 0.165$) for 50-year reference period.

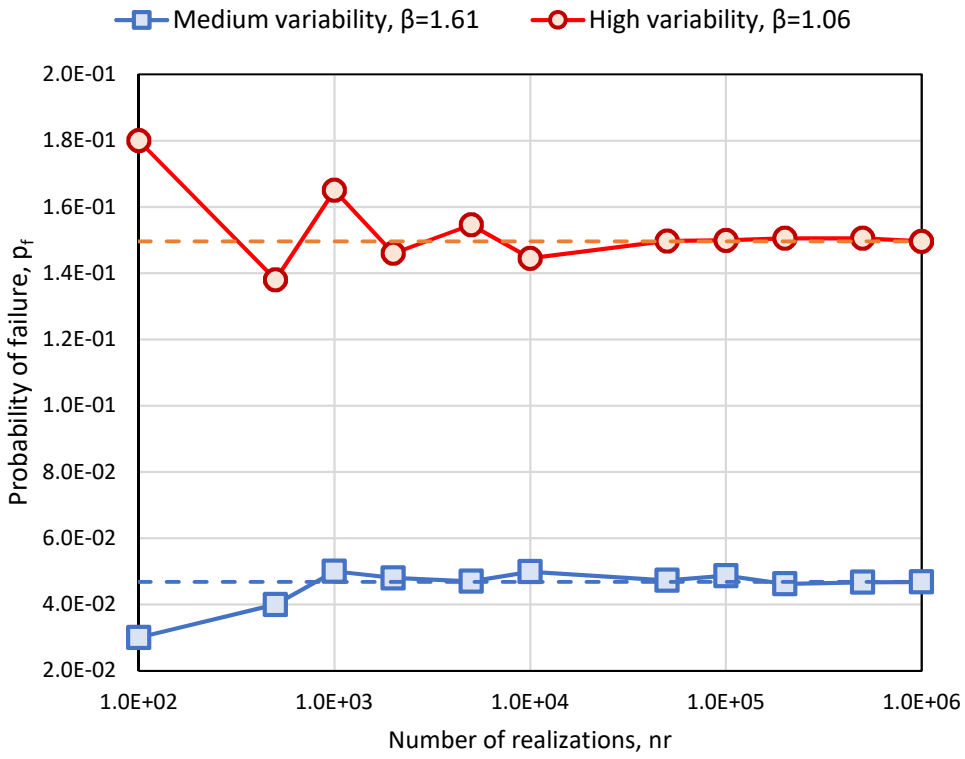

Figure 6.8 Static rocking stiffness failure probability - deep bedrock case

Table 6.8 Parameter importance ranking for static rocking stiffness - deep bedrock

Variability		V_s	M	ρ	τ_{max}	ν	α	γ
Medium	Rank	1	2	3	4	5	6	7
	Index	0.707	0.710	0.063	0.043	0.039	0.034	0.032
High	Rank	1	2	3	5	4	6	7
	Index	0.766	0.627	0.099	0.056	0.058	0.048	0.044

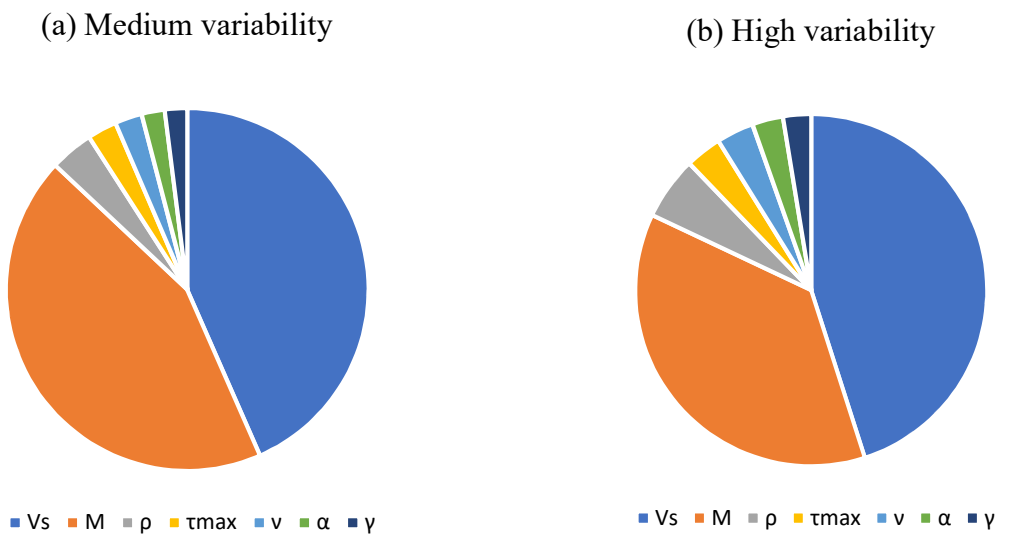

Figure 6.9 Parameter importance ranking for static rocking stiffness – deep bedrock

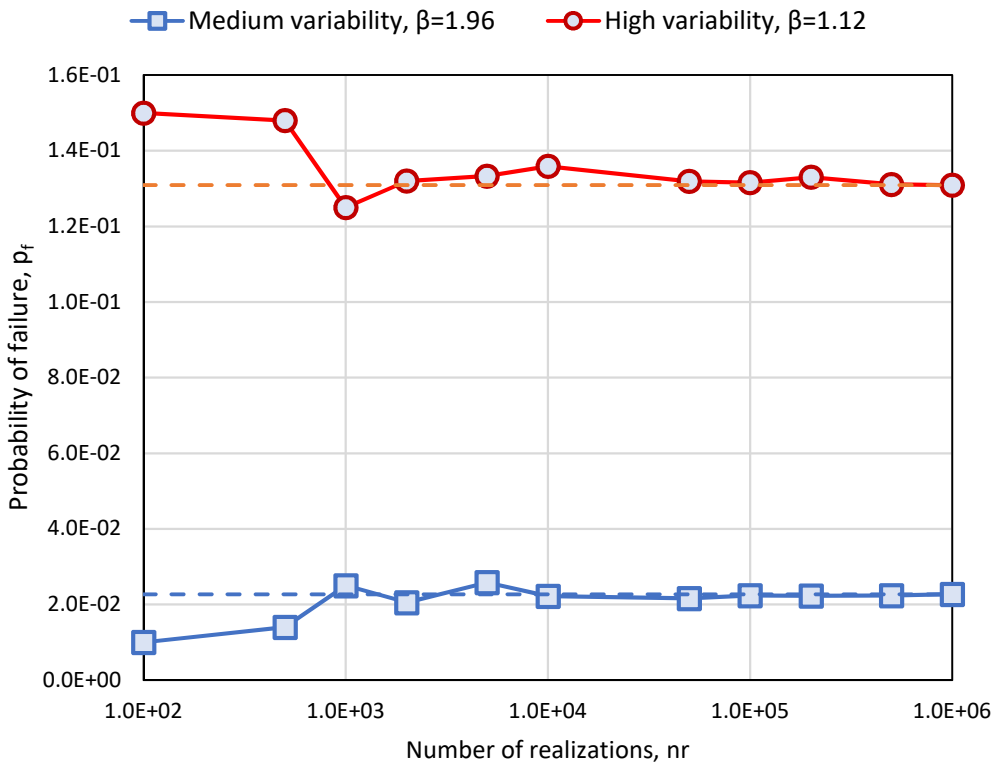

Figure 6.10 Static stiffness failure probability - bedrock within influence depth

Table 6.9 Parameter ranking for static rocking stiffness - shallow bedrock

Variability		V_s	M	H_b	ρ	ν	α	τ_{max}	γ
Medium	Rank	2	1	3	4	6	7	5	8
	Index	0.647	0.750	0.104	0.060	0.035	0.026	0.037	0.024
High	Rank	1	2	3	5	4	6	7	8
	Index	0.689	0.633	0.326	0.091	0.061	0.046	0.044	0.039

(a) Medium variability

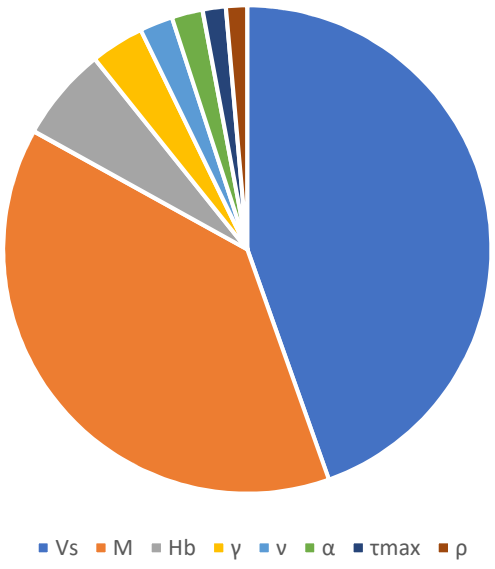

(b) High variability

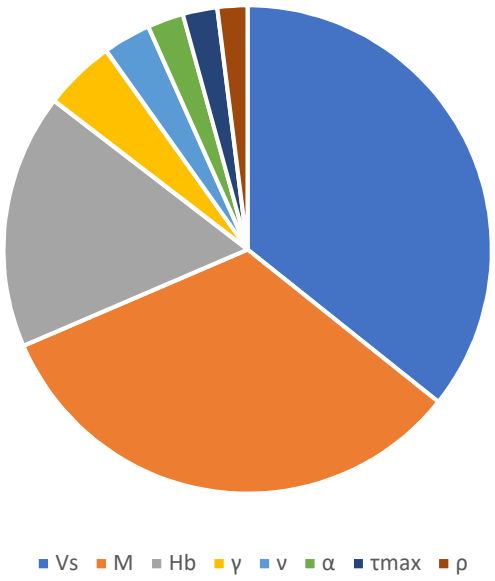

Figure 6.11 Parameter importance ranking for static rocking stiffness

Table 6.10 Static stiffness reliability comparisons

	Medium Variability	High Variability
Deep bedrock	$p_f = 0.047, \beta \approx 1.6$	$p_f = 0.150, \beta \approx 1.06$
Bedrock within depth of influence	$p_f = 0.023, \beta \approx 1.96$	$p_f = 0.131, \beta \approx 1.12$

Note:

- Target probability of failure (and reliability index) as outlined in Table 4.11; i.e. $\beta_T = 1.7$ ($p_f^T = 0.035$) for 1-year reference period and $\beta_T = 1.0$ ($p_f^T = 0.165$) for 50-year reference period.

CHAPTER 7

BEARING CAPACITY UNDER COMBINED LOADING

In this chapter, the bearing capacity ultimate limit state is investigated for drained conditions, per Equation (2.30), and for undrained conditions, per Equation (2.31), both using the effective area approach. The investigation adopts the generally accepted formulation for effective dimensions for circular foundations recommended by DNV (DNV/Risø, 2002). The generalized equation for computing ultimate bearing capacity, q_{ult} ; i.e., Equation (2.30) for drained conditions or Equation (2.31) for undrained conditions, is used to define the performance function as follows:

$$g = q_{ult} - \frac{V}{A_{eff}} = 0 \tag{7.1}$$

7.1 Drained Bearing Capacity

Classical effective stress analysis assumptions apply when the effects of porewater pressure can be measured such as for granular soil deposits or when the loading rate allows for pore water pressure dissipation. For wind turbine foundations, loading rate is such that undrained conditions should be considered for bearing capacity verification whenever fine-grained soils are within the depth of influence under the foundation. For drained conditions, the generalized bearing capacity equation; Equation (2.30), is used to define the performance function:

$$g = c'N_c s_c d_c i_c + q'_0 N_q s_q d_q i_q + \frac{1}{2}\gamma' b_{eff} N_\gamma s_\gamma d_\gamma i_\gamma - \frac{V}{A_{eff}} = 0 \tag{7.2}$$

Variables that can be randomized and their associated PDF's are listed in Table 7.1 for "medium" and "high" variability assumptions. Effective area dimensions and bearing capacity

correction factors are computed using the DNV method described in Section. 2.7.2. The resulting probability of failure and reliability index for each variability level are also listed in Table 7.1.

Table 7.1 Drained bearing capacity random variables

Variable		Dist.	Mean	COV		Notes
				Medium	High	
Moment (J)	M	LN	$5.0{\cdot}10^{7}$	0.20	0.25	Governing S1-level loading. Typically, annual probability.
Horizontal (N)	H	LN	$6.6{\cdot}10^{5}$	0.20	0.25	
Effective friction angle (deg)	ϕ'	NR	30.0	0.08	0.12	Sands
		LN	25.0	0.30	0.45	Clays and silts
Effective cohesion (Pa)	c'	LN	0.0	NA	NA	Sands
		LN	$5.0{\cdot}10^{4}$	0.20	0.30	Clays and silts
Effective soil unit weight $\left(\mathrm{N}/\mathrm{m}^3\right)$	γ_e	NR	17000	0.05	0.10	
Foundation diameter (m)	B	NA	17.0	NA	NA	Design decision variable
Foundation depth (m)	D	NA	2.8	NA	NA	Design decision variable
Probability of failure	p_f			$8.4{\cdot}10^{-6}$	$3.3{\cdot}10^{-4}$	
Reliability index	β			4.25	3.34	

Notes:

Target reliability as adopted in this dissertation per Table 4.11 considering the reference period of the load case:

- For 50-year reference period: $\beta_T = 2.0$ or $p_f^T \approx 2{\cdot}10^{-2}$
- For 1-year reference period: $\beta_T = 3.3$ or $p_f^T \approx 5{\cdot}10^{-4}$

Probability of failure convergence plots are shown in Figure 7.1. As can be noted, the design meets the target reliability index of 3.3 even with the assumption of high variability. If variability can be reduced to the "medium" level, the design reliability index is 4.24 which far exceeds the target reliability.

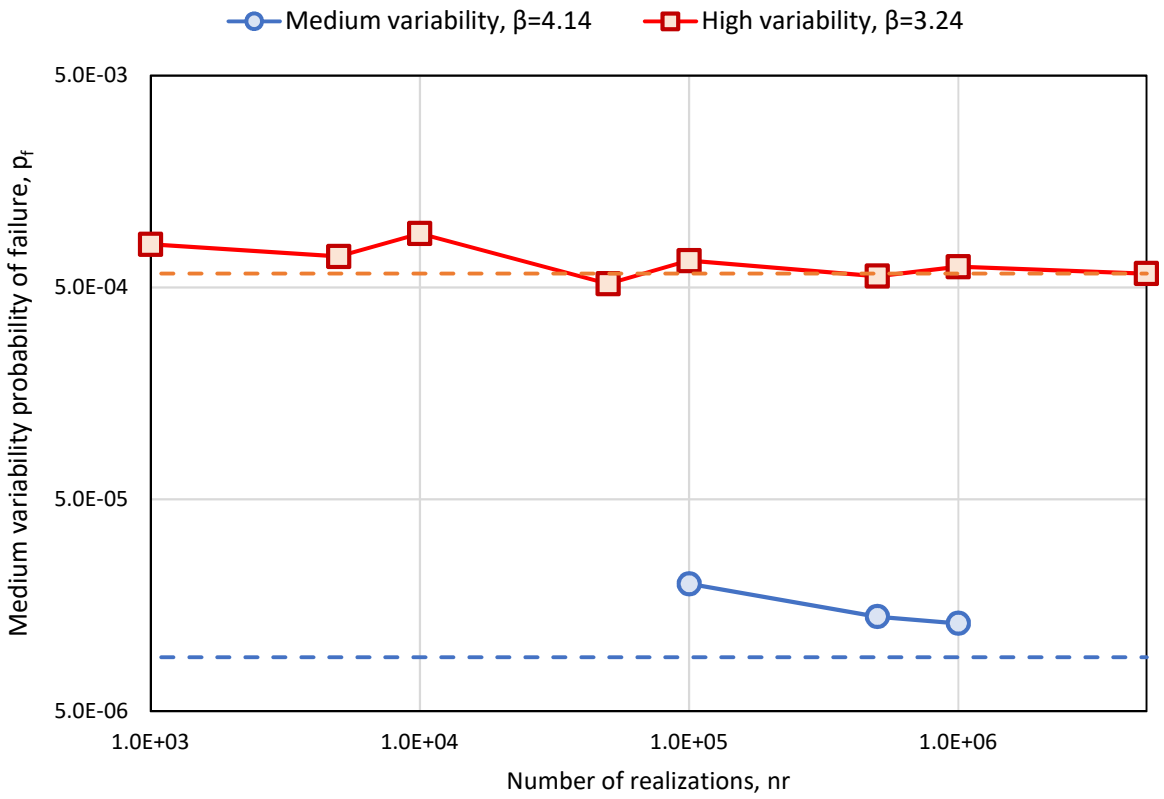

Figure 7.1 Drained bearing capacity probability of failure

Parameter importance ranking is shown in Table 7.2 in the form normalized importance indices for both medium and high variability cases. The same information is illustrated in Figure 7.2. The pie charts show that there are essentially three important variables governing the undrained bearing capacity limit state: overturning moment, effective friction angle and effective

cohesion. They also show that when uncertainty is high, the variability of the governing parameters can "drown out" the less important parameters and alter their cross-parameter importance proportions as a function of their relative variabilities. Thus, driving parameters with higher variability are more important than similar parameters with lower variability.

.

Table 7.2 Random variable ranking - drained bearing capacity

Variability	Variable	M	H	γ_e	ϕ'	c'
Medium	Rank	1	2	3	5	4
	Index	0.9848	0.0165	0.0178	0.1578	0.0686
High	Rank	1	4	2	3	5
	Index	0.8668	0.0011	0.0093	0.4732	0.1573

(a) Medium variability

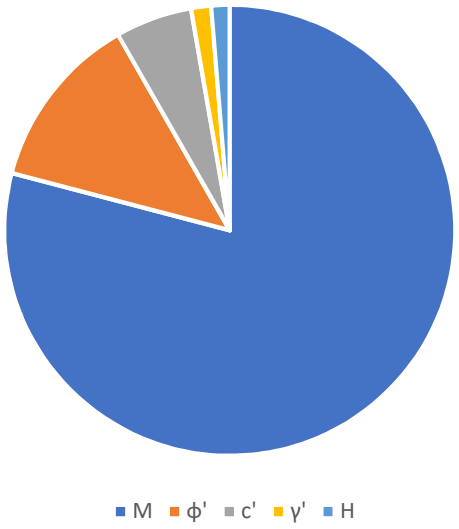

(b) High variability

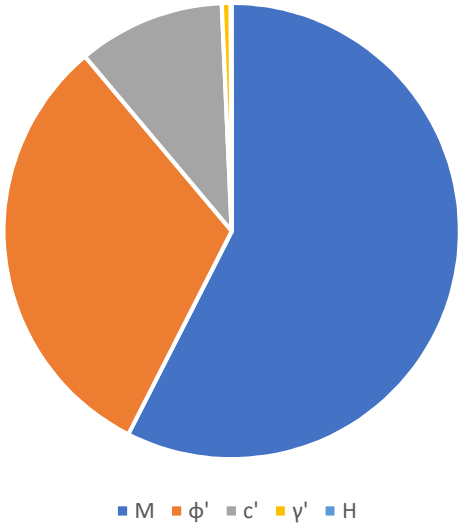

Figure 7.2 Importance ranking for drained bearing capacity

7.2 Undrained Bearing Capacity

The performance function makes use of the generalized bearing capacity equation for undrained conditions given in Equation (2.31), namely:

$$g = s_u N_c^0 s_c^0 d_c^0 i_c^0 + q_0 - \frac{V}{A_{eff}} = 0 \tag{7.3}$$

Effective dimensions per the DNV method are used in the evaluation as before. Substituting these effective dimensions and the expressions for the other terms, the following expression for the undrained bearing capacity performance function is obtained:

$$g = 2.57\left(1 + 0.2\frac{b_{eff}}{l_{eff}}\right)\left(1 + \sqrt{1 - \frac{H}{A_{eff} s_u}}\right)s_u + \gamma_t D - \frac{V}{A_{eff}} = 0 \tag{7.4}$$

In the undrained $(\phi' = 0)$ case, three levels of variability are assumed (low, medium and high). The random variables and their associated variability assumptions are shown in Table 7.3. Figure 7.3 shows probability of failure convergence for the three variability cases. The resulting probabilities of failures indicate that only the low and medium variability cases meet the target reliability index of 3.3. This example illustrates the great impact of design parameter variability on the reliability of a design. This is especially true when there are only a few driving parameters such as in this case where parameter importance ranking, shown in Table 7.4 indicates very strong dominance of the undrained bearing capacity limit state by the applied moment followed by followed by the undrained shear strength. The pie charts in Figure 7.4 illustrate the proportions and highlight the "drowning out" effect of the least important parameters by the more important ones. In fact, in this case, the total unit weight and the horizontal load component could be treated as deterministic variables without changing the results of the reliability analysis.

Table 7.3 Undrained bearing capacity random variables

Variable		Dist.	Mean	COV			Notes
				Low	Medium	High	
Moment (J)	M	LN	$5.0 \cdot 10^7$	0.15	0.20	0.25	Governing S1-level loading. Typically, annual probability.
Horizontal (N)	H	LN	$6.6 \cdot 10^5$	0.15	0.20	0.25	
Undrained shear strength (Pa)	s_u	LN	$1.0 \cdot 10^5$	0.15	0.25	0.40	
Total unit of soil $\left(\mathrm{N}/\mathrm{m}^3\right)$	γ_t	NR	17000	0.03	0.05	0.10	
Foundation diameter (m)	B	NA	17.0	NA	NA	NA	Design decision variable
Foundation depth (m)	D	NA	2.8	NA	NA	NA	Design decision variable
Probability of failure	p_f			$2.5 \cdot 10^{-5}$	0.0035	0.022	
Reliability index,	β			3.98	2.76	1.97	

Notes:

Target reliability as adopted in this dissertation per Table 4.11 considering the reference period of the load case:

- For 50-year reference period: $\beta_T = 2.0$ or $p_f^T \approx 2 \cdot 10^{-2}$
- For 1-year reference period: $\beta_T = 3.3$ or $p_f^T \approx 5 \cdot 10^{-4}$

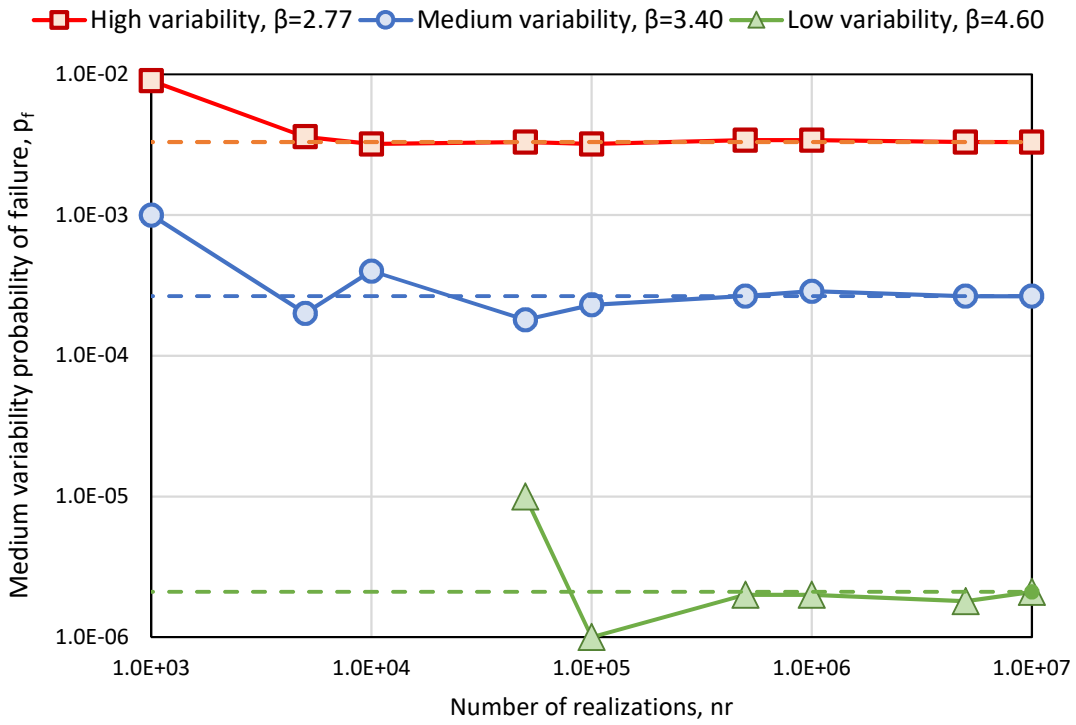

Figure 7.3 Undrained bearing capacity failure probability

Table 7.4 Random variable ranking - undrained bearing capacity

Variability	Variable	M	s_u	H	γ_t
Low	Rank	1	2	3	4
	Index	0.9911	0.1311	0.0196	0.0082
Medium	Rank	1	2	3	4
	Index	0.9872	0.1593	0.0060	0.0044
High	Rank	1	2	3	4
	Index	0.9761	0.2168	0.0113	0.0108

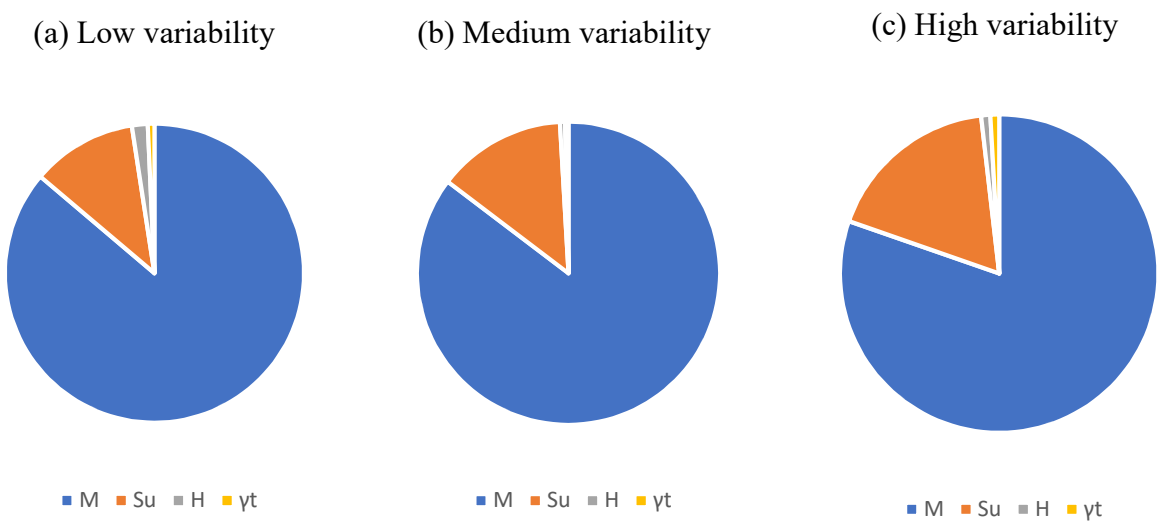

Figure 7.4 Parameter importance ranking for undrained bearing capacity

CHAPTER 8

CONCLUSIONS AND FUTURE WORK

A novel probabilistic design methodology, called d-RBD, is presented in this dissertation. The methodology is free of partial safety factors and is well-suited to geotechnical design problems where design inputs are characteristically more variable and partial safety factors typically fail to cover the common ranges of variability of design inputs. Compared to state-of-practice procedures, the d-RBD method is shown in this dissertation to result in safe yet more economical designs and to produce designs meeting target reliability and optimized for site conditions. The d-RBD method was used in this dissertation to verify several wind turbine foundation design limit states and to identify the important design variables affecting those limit states. Knowledge of the important design variables is useful for optimal allocation of geotechnical investigation funds. When the most cost-effective design is selected from the intersection of the pools of acceptable designs obtained for the different limit states under consideration, the d-RBD becomes a direct reliability-based design optimization (d-RBDO) tool. This chapter summarizes the conclusions of the d-RBD application to the three limit states that were investigated and discusses opportunities to improve the scope and efficiency of the d-RBD process. The implementation of the d-RBD method is achieved using MATLAB. The source code of this implementation is included as Appendix B.

8.1 Conclusions

In this dissertation, the reliability associated with three limit states pertinent to the design of shallow wind turbine foundations was assessed. The three limit states are: tilt, rocking stiffness and bearing capacity. A gravity-base foundation, sized per common industry practice for a typical 80-meter hub height turbine, was used as a reference example. The foundation was first analyzed using a finite element package that is able to model subgrade stiffness and development of zero-

pressure zone in response to combined loading. Industry guidelines were followed in sizing the foundation. These methods resulted in a foundation that is 17 meters in diameter and 2.8 meters deep. The d-RBD method was then used to assess the reliability of the design assuming different levels of design parameter variability. The COV levels (low, medium and high) were estimated based on published ranges. The results of this assessment, as well as the most influential design parameters, are summarized in Table 8.1 and show that the design has acceptable reliability for low and medium design input variability but has inadequate reliability for the high input variability case. Thus, the design is optimal for medium or better variability.

This result can be obtained in one single run of the d-RBD method as implemented in the MATLAB code shown in Appendix B and provided in Appendix C. In this run, we instruct the program to consider all five limits states and to evaluate six foundation diameters (15, 16, 17, 18, 19 and 20 meters) and four foundation depths (2.8, 2.9, 3.0 and 3.1 meters); i.e., twenty-four combinations of foundation diameter and depth. The main simulation parameters are shown in Figure 8.1 and the generated possible geometries are shown in Figure 8.2. Foundation depths are obtained by maintaining the middle thickness constant and varying the pedestal height. The main simulation parameters specified at the start of the program include the diameter and depth ranges, the target SLS and ULS reliability indices, and the desired COV for the target probability of failure. A high probability of failure COV; e.g., 0.30 to 0.4, should be specified for preliminary runs as it is used to determine the number of realizations. The PDF's for the various random variables are specified as part of the code specific to each limit state.

The results for the medium variability case, given in Table 8.2, show that if foundation depth is maintained at 2.8 meters, the optimal diameter is 17 meters. In this example, we have shown that the optimal design determined through the straight forward d-RBD process for the

medium variability case is the same as the design obtained through industry practice which involves various partial factors, many conflicting standards, guidelines and certification agency requirements. Such a practice would be a hit-and-miss process while the d-RBD process is straight forward and only needs the computational models and the best assessment of input variability.

Table 8.1 Summary of reliability assessments of foundation with $B = 17\text{m}$, $D = 2.8\text{m}$

Limit state	Design parameter variability			Target reliability, β_T	Most important variables
	Low	Medium	High		
Tilt	NP	4.3	2.9	1.7	V_s with M a close second.
Dynamic stiffness, deep bedrock	NP	2.1	1.3	1.7	V_s with ρ distant second.
Dynamic stiffness, shallow bedrock	NP	2.7	1.6	1.7	V_s, H_b with ρ distant third.
Static stiffness, deep bedrock	NP	1.6	1.1	1.7	V_s, M with γ distant third.
Static stiffness, shallow bedrock	NP	2.0	1.1	1.7	V_s, M, H_b with γ distant fourth.
Drained bearing capacity	NP	4.1	3.2	3.3	M, ϕ', c'
Undrained bearing capacity	4.0	3.4	2.0	3.3	s_u, M
Notes: • NP: Not Performed					

```
%% Main simulation parameters
fileID = fopen('dRBD_MV.txt','w');
Title="All Limit States - Medium Variability"; % Descriptive design tiltle
PLS=["TLT" "DYS" "STS" "DBC" "UBC"]; % Possible limit states
LSO=[    1     1     1     1     1]; % 1=verify, 0=do not verify
LST=[    1     1     1     2     2]; % Limit state type: 1=SLS,2=ULS,3-FLS
nrvmax=10;              % Maximum number of random variables in any limit state
B=15:1:20;              % Foundation diameter(s)
D=2.8:0.1:3.1;          % Foundation depth(s)
btsls=1.7;              % Target reliabilty index for SLS
btuls=3.3;              % Target reliability index for ULS
pfCOV=0.15;             % Desired COV of probability of failure
```

Figure 8.1 Main simulation parameters of the d-RBD run

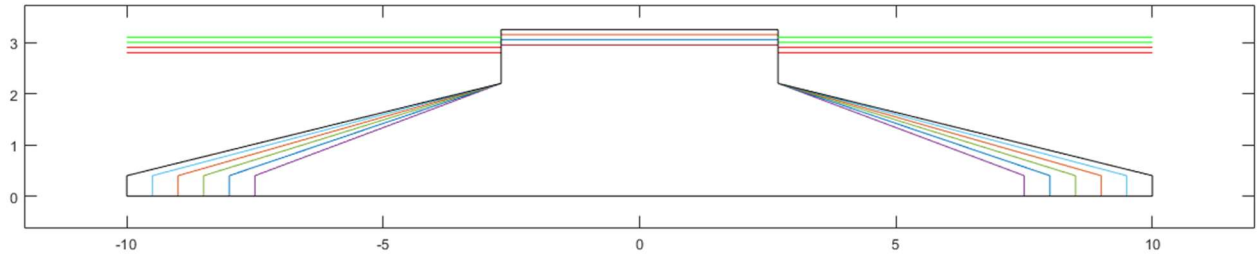

Figure 8.2 Foundation geometries generated in the d-RBD program execution

For comparison, if design input variability is in the high range and if the depth is maintained at 2.8 meters, the most economical foundation diameter determined through the d-RBD process is 19 meters which corresponds to a concrete volume of 363 cubic meters. Table 8.3 shows the reliability indices of all diameters included in the run. As can be noted in this example, reducing design parameters variability from high to medium, an objective that can be attained through more geotechnical information, can reduce foundation diameter from 19 to 17 meters and results in concrete volume reduction of about 60 cubic meters, as well as all associated economies in

reinforcing steel, excavation volumes, labor, etc. In this example, cost of geotechnical uncertainty is obvious.

Table 8.2 Reliability indices for medium variability assumptions, $D = 2.8\text{m}$

Limit State	Foundation diameter, B (m)					
	15.0	16.0	17.0	18.0	19.0	20.0
Tilt, $\beta_T = 1.7$	3.71	>3.71	>3.71 ✓	>3.71	>3.71	>3.71
Dynamic stiffness, $\beta_T = 1.7$	2.13	2.40	2.63 ✓	2.81	2.96	3.11
Static stiffness, $\beta_T = 1.7$	0.76 ×	1.30 ×	1.97 ✓	2.69	3.00	3.50
Drained bearing capacity, $\beta_T = 3.3$	2.89 ×	3.47	>3.47 ✓	>3.47	>3.47	>3.47
Undrained bearing capacity, $\beta_T = 3.3$	1.78 ×	2.78 ×	3.44 ✓	>3.44	>3.44	>3.44
Optimal design: • Diameter $B = 17\text{m}$ • Volume of concrete: $V_f = 301\text{m}^3$						

If the geotechnical information confirms the high variability of design inputs, optimization is still possible by varying foundation depth. When d-RBD is used with high variability, depth ranging from 2.8 to 3.1 meters and diameter ranging from 15 to 20 meters, the optimal design is found to be 18 meters in diameter and 3.0 meters deep with a corresponding concrete volume of 335 cubic meters. Thus, for the high variability case, a choice is available between a 19-meter foundation that is 2.8 meters deep (363 cubic meters of concrete) and an 18-meter foundation that is 3.0 meters deep (335 cubic meters of concrete). Essentially, the choice in this case is between saving about 30 cubic meters of concrete and saving 20 centimeters of additional excavation. This example illustrates how the d-RBD method can be used as a design optimization (d-RBDO) tool.

Table 8.3 Reliability indices for high variability assumptions, $D = 2.8\text{m}$

Limit State	Foundation diameter, B (m)					
	15.0	16.0	17.0	18.0	19.0	20.0
Tilt, $\beta_T = 1.7$	2.67	2.81	2.90	3.06	3.17 ✓	3.33
Dynamic stiffness, $\beta_T = 1.7$	1.31 ×	1.45 ×	1.58 ×	1.74	1.88 ✓	2.01
Static stiffness, $\beta_T = 1.7$	0.60 ×	0.90 ×	1.27 ×	1.60 ×	1.97 ✓	2.31
Drained bearing capacity, $\beta_T = 3.3$	2.30 ×	2.90 ×	3.24 ×	3.54	3.81 ✓	>3.81
Undrained bearing capacity, $\beta_T = 3.3$	1.39 ×	2.09 ×	2.80 ×	3.50	3.64 ✓	>3.64
Optimal design: • Diameter $B = 19\text{m}$ • Volume of concrete: $V_f = 363\text{m}^3$						

8.1.1 Tilt Limit State

The reliability of the tilt limit state appears high. This may be due to the assumptions adopted in this assessment which are based on guidance from draft standard IEC61400-6, (IEC, 2016). This guidance includes assessing settlement at the S3 load level which corresponds to positive compression being maintained under the entire foundation. The formulation used in this assessment is for elastic deformations at the S3 load level. For sites where consolidation settlement is of concern, the computed reliability could be lower. However, the S3 level may not be an appropriate level for consolidation settlement to occur. Additionally, the tilt limits discussed in Section 2.8.2 suggest that there is a healthy tilt margin built into industry practice.

8.1.2 Rocking Stiffness Limit State

Experience within the industry indicates that foundation stiffness can often be a design driver. This is the case in this design example where the static stiffness reliability is very close to

the target value and that for the dynamic stiffness under the high variability scenario is not too far from the target reliability. Shear wave velocity and applied loading are the most influential parameters, but when bedrock is within a depth of influence, the variability in depth to bedrock becomes a significant design driver, making the case for diligent assessment of this depth to improve design reliability.

8.1.3 Bearing Capacity Limit State

The drained ($\phi' - c'$) bearing capacity limit state has a high level of reliability for the low and medium parameter variability cases and is at the target reliability level for the high variability case. As expected, the limit state based on undrained ($\phi = 0$) bearing capacity has less reliability and meets the target reliability level only for the low variability case. The practical takeaway from this finding is that, for fine grained soils, verification of undrained bearing capacity should take precedence and reducing uncertainty relative to the driving design parameter, namely undrained shear strength, should be a top priority. Overall and with respect to the bearing capacity limit state, reliability should be higher than what is computed here. This is because the effective area approach was deemed to be conservative compared to other methods as discussed for interaction curve methods in Section 2.8.2.

8.1.4 Applications of the d-RBD Method

The d-RBD design process, implemented here using MATLAB, is a powerful approach that can consider any number of limit states and can arrive at an optimal design that meets the target reliability levels of all limit states under consideration. This objective is achieved without use of partial factors of any kind and by relying on judgement and experience for the selection of the computational model and supplying the best information available on variability of design

parameters. This is a significant departure from current design practice but appears to be much less confusing and more powerful.

8.2 Future Work

With the advent of powerful and portable computing devices, performing the number of calculations required by the d-RBD process is a light and readily achievable task for equation-based verifications. Millions of d-RBD realizations can be generated and analyzed in minutes. However, implementing d-RBD in a finite element-based framework would be computationally more challenging. Below are some future work areas for improving the efficiency and scope of the d-RBD process.

8.2.1 Incorporating Spatial Variability

A key limitation of formula-based d-RBD is that it fails to model spatial variability of soils. One way to incorporate the effects of spatial variability, at least partially, is through homogenization studies. The approach of homogenization aims to obtain "spatially averaged" or "equivalent" parameters for soil masses (Fenton & Griffiths, 2003; Fenton *et al.*, 2003; Griffiths *et al.*, 2013; Ching, Hu*, et al.*, 2015). Another way is to perform limited RFEM analyses to determine worst-case spatial correlation lengths for the important design variables (Baecher & Ingra, 1981; Griffiths *et al.*, 2016; Zhu *et al.*, 2018). Once that is completed, a designer could simply verify that the spatial correlation length for the project site and for the specific design parameter is outside the critical range. In this case, the regular d-RBD procedure can be followed with the knowledge that, with respect to spatial variability, results would be on the safe side. Alternatively, RFEM-based d-RBD can also be carried out with a lighter computational load since spatial variability can conservatively be limited to a value on the safe side of the identified worst-

case spatial correlation lengths. The computational load can also be reduced through the techniques described in the following section.

8.2.2 Computational Load Reduction

The d-RBD method as proposed in this dissertation is a standard direct MCS technique. MCS is a sound framework but it can be computationally intensive because it must generate a sufficiently high number of realizations relying on the variability information of the design input variables to estimate often low probabilities of failure. There are several techniques that can drastically reduce the number of realizations and hence the computational load. These include Bayesian updating, Kriging, Markov Chain Monte Carlo (MCMC) algorithms, neural networks and subset simulation (e.g. Au & Beck, 2001; Robert & Casella, 2011; Ahmed & Soubra, 2012; Au & Wang, 2014; Wang & Cao, 2015; Au, 2016; Proppe, 2017).

Markov Chain Monte Carlo represents a large class of techniques for sampling from a probability distribution with the purpose of estimating an integrand region of interest. In reliability analysis, the integrand could be the performance function and the region of interest would be the failure region. The samples can be independent, such as in "random walk Monte Carlo" or correlated which weigh the sampling towards the trials that make greater contribution to the integrand. Subset simulation is a simulation method that focuses on the complementary cumulative density function (CCDF) of the response to estimate low failure probabilities and can use MCMC for efficient sampling (Au & Wang, 2014; Au, 2016). Subset simulation can be combined with neural networks as done by Giovanis *et al.* (2010) for efficient computation of structural failure probability. Future work in this area includes integration of such techniques to improve the computational efficiency and accuracy of the d-RBD approach so that lower probabilities of failures can be computed more efficiently. Wang & Cao (2015) provided sample integrations of

the “Expanded RBD” method with subset simulation and used Microsoft Excel to implement the more computationally efficient procedure in a drilled shaft design example and slope stability analysis example.

8.2.3 Incorporating Design Robustness

In the d-RBD procedure adopted in this dissertation, the optimal design is selected as that which is least cost (interpreted here as least concrete volume) and meets the reliability requirement; i.e., has a probability of failure less than the target probability of failure. While this selection would indeed be an optimal one, there could be other selections that have lower probability of failure with only minor adjustments to design dimensions and hence only slightly more cost. These selections are more robust designs. In quality engineering, robust designs are insensitive to “noise factors” or “hard-to-control” parameters and are achieved through, among other things, adjustments to geometry, dimensions and process settings. In Robust Geotechnical Design (RGD), the objective is to produce reliability-based designs that are robust; i.e., designs that are be less sensitive to uncertainty in geotechnical design parameters. Such designs can be obtained through careful adjustments to dimensions or construction techniques (e.g. Khoshnevisan *et al.*, 2017; Shrestha *et al.*, 2017).

8.2.4 Considering Other Applications

The d-RBD method is illustrated in this dissertation for the design of shallow wind turbine foundations. However, it is equally applicable to countless other design situations such as design of deep foundations, retaining structures, slope stability, and any formulation involving a limit state verification. Another extension of the d-RBD method can be made to fatigue limit states. Fatigue is typically not considered in geotechnical design problems for lack of soil fatigue models.

For shallow foundations, the closest aspect to geomaterial fatigue is the consideration of soil degradation. This consideration is limited to observing industry guidelines relative to no-gapping limits and reducing the elastic moduli to reflect the strain level. Such measures consider the soil type and its susceptibility to degradation. Soil or rock fatigue models could be envisioned for active (pre-tensioned) anchors. When such models are available, the d-RBD method would be a logical choice to verify fatigue limit states.

REFERENCES

AASHTO. (1994). LRFD Bridge Design Specifications, 1st Ed. In. Washington, DC: American Association of State Highway and Transportation Officials (AASHTO).

AASHTO. (2012). AASHTO LRFD Bridge Design Specifications. In. Washington, DC: American Association of State Highway and Transportation Officials (AASHTO).

ACI. (2016). ACI ITG-9R-16: Report on Design of Concrete Wind Towers. In (Vol. ITG-9R-16): American Concrete Institute.

Ahmed, A., & Soubra, A. H. (2012). Probabilistic Analysis of Strip Footings Resting on a Spatially Random Soil using Subset Simulation Approach. *Georisk - Assessment and Management of Risk for Engineering Systems and Geohazards, 6*(3).

AISC. (1989). Manual of Steel Construction - Allowable Stress Design, 9th Edition. In. Chicago, IL: American Institute of Steel Construction (AISC).

Aladejare, A. E., & Wang, Y. (2017). Evaluation of rock property variability. *Georisk: Assessment and Management of Risk for Engineered Systems and Geohazards, 11*(1), 22-41.

Andersen, L. (2010). Assessment of lumped-parameter models for rigid footings. *Computers and Structures, 88*, 1333-1347.

Anderson, N., Thitimakorn, T., Hoffman, D., Stephenson, R., & Luna, R. (2006). *A comparison of four geophysical methods for determining the shear wave velocity of soils*. 6th International Conference & Exposition on Petroleum Geophysics "Kolkata 2006" - Geophysics for Mitigating Exploration Risks, Science City, Kolkata 9-11 January 2006.

Ang, A. H.-S., & Tang, W. H. (2007). *Probability Concepts in Engineering : Emphasis on Applications to Civil and Environmental Engineering* (n. Edition Ed.). New York: John Wiley & Sons.

Apostolakis, G. (1990). The concept of probability in safety assessments of technological systems. *Science, 250*(4986), 1359-1364.

Arya, S. C., O'Neill, M. W., & Pincus, G. (1979). *Design of structures and foundations for vibrating machines*. Houston: Gulf Pub. Co., Books Division.

ASCE. (2017). ASCE 7-16: Minimum Design Loads and Associated Criteria for Buildings and Other Structures. In (Vol. ASCE 7-16): American Society of Civil Engineers.

Au, S. K. (2016). On MCMC algorithm for subset simulation. *Probabilistic Engineering Mechanics, 43*, 117-120.

Au, S. K., & Beck, J. L. (2001). Estimation of small failure probabilities in high dimensions by subset simulation. *Probabilistic Engineering Mechanics, 16*, 263-277.

Au, S. K., & Wang, Y. (2014). *Engineering Risk Assessment with Subset Simulation*. Singapore: John Wiley & Sons.

AWEA. (2013). *U.S. Wind Industry Annual Market Report Year Ending 2013* American Wind Energy Association

AWEA. (2017). *U.S. Wind Indusrty Fourth Quarter 2017 Market Report - Public Version* American Wind Energy Association

AWEA, & ASCE. (2011). *ASCE/AWEA RP2011: Recommended Practice for Compliance of Large Land-based Wind Turbine Support Structures* American Wind Energy Association and American Society of Civil Engineers

Baecher, G. B. (2017). *2nd Lacasse Lecture: Bayesian thinking in geotechnics*. Georisk 2017, Denver, Colorado.

Baecher, G. B., & Christian, J. T. (2003). *Reliability and Statistics in Geotechnical Engineering*. Chichester, England ; Hoboken, NJ: Wiley.

Baecher, G. B., & Christian, J. T. (2015). *Bayes factors and the observational method*. 5th International Symposium on Geotechnical Safety and Risk (ISGSR2015), Rotterdam, The Netherlands 13-16 October 2015.

Baecher, G. B., & Ingra, T. S. (1981). Stochastic finite element method in settlement prediction. *J. Geotech. Engrg. Div., 107*(4), 449-463.

Barnes, R. J. (1993). *Geostatistics for Subgrade Characterization* University of Minnesota

Bea, R. (2006). Reliability and Human Factors in Geotechnical Engineering. *Journal of Geotechnical and Geoenvironmental Engineering, 132*(5), 631-643.

Becker, D. E. (1996a). Eighteenth Canadian Geotechnical Colloquium: limit states design for foundations - Part II - development for the National Building Code of Canada. *Canadian Geotechnical Journal, 33*, 984-1007.

Becker, D. E. (1996b). Eighteenth Canadian Geotechnical Colloquium: Limit states design for foundations. Part I. an overview of the foundation design process. *Canadian Geotechnical Journal, 33*, 956-983.

Becker, D. E. (2003). *Limit States Foundation Design Code Development in Canada*. LSD2003: International Workshop on Limit State Design in Geotechnical Enegineering Practice, MIT, Cambridge, MA.

Belidor, B. F. (1729). *La science des ingenieurs dans conduite des travaux de fortifications et d'architecture civil* Jombert, Paris:

Bell, R. W. (1991). *The Analysis of Offshore Foundations Subjected to Combined Loading.* (Master of Science), Oxford University,

Ben-Hassine, J., & Griffiths, D. V. (2012). *Reliability based design of shallow foundations subjected to combined loading with application to wind turbine foundations*. CIMENICS 2012 - 11th International Congress on Numerical Methods in Engineering and Scientific Applications, Isla de Margarita, Venezuela 26-28 March 2012.

Ben-Hassine, J., & Griffiths, D. V. (2013). *Geotechnical exploration for wind energy projects.* Paper presented at the 18th International Conference on Soil Mechanics and Geotechnical Engineering, Paris, France.

Bentley. (2018). STAAD.Pro. Bentley Systems, Incorporated: Exton, PA.

Bolton, M. D. (1993). *What are partial factors for?* Proc. International Symposium on Limit State Design in Geotechnical Engineering - ISSMFE TC 23, Copenhagen May 3, 1993.

Borden, R. H., & Gupta, A. (1996). Dynamic properties of Piedmont residual soils. *J. Geotech. Engrg., 122*(10), 813-821.

Bossanyi, E. A. (2003). Individual blade pitch control for load reduction. *Wind Energy, 6*, 119-128.

Bowles, D. S. (2013). *What is ALARP and how can it improve dam saefty decisions*. ASDSO 2013 Conference on Dams, Providence, Rhode Island 8-12 September 2013.

Bowles, J. E. (1996). *Foundation Analysis and Design* (5th ed.). New York: McGraw-Hill.

Bransby, M. F. (2001). Failure envelopes and plastic potentials for eccentrically loaded surface footings on undrained soil. *International Journal for Numerical and Analytical Methods in Geomechanics, 25*, 18.

Bransby, M. F., & Randolph, M. F. (1997, 2-7 November 1997). *Shallow Foundations Subject to Combined Loadings.* Paper presented at the IACMAG '97: Ninth Int. Conf. of the International Association for Computer Methods and Advances in Geomechanics, Wuhan, China.

BSI. (1972). CP 110 : Code of Practice for the Structural Use of Concrete, Part 1 - Design, Materials and Workmanship. In. London: British Standards Institution.

Butterfield, R., & Gottardi, G. (1994). A complete three-dimensional failure envelope for shallow footings on sand. *Geotechnique, 44*(1), 181-184.

Butterfield, R., Houlsby, G. T., & Gottardi, G. (1997). Standard Sign Conventions and Notation for Generally Loaded Foundations. *Geotechnique, 47*(5), 1051-1054.

Canadian Geotechnical Society. (2006). *Canadian Foundation Engineering Manual* (4th ed.). Richmond, B.C.: Canadian Geotechnical Society.

Cao, Z.-J., Wang, Y., & Li, D.-Q. (2016). Site-specific characterization of soil properties using multiple measurements from different test procedures at different locations – A Bayesian sequential updating approach. *Engineering Geology, 211*, 150-161.

Cao, Z., & Zhang, Y. (2012). Bayesian approach for probabilistic site characterization using cone penetration tests. *Journal of Geotechnical and Geoenvironmental Engineering*.

Casagrande, A. (1965). The role of 'Calculated Risk' in earthwork and foundation engineering. *J. Soil Mech. Div. (ASCE), 91*(4), 1-40.

Caspeele, R. (2014). From quality control to structural reliability: where Bayesian statistics meets risk analysis. *Heron, 59*(2).

Cassidy, M. J., Airey, D. W., & Carter, J. P. (2005). Numerical Modeling of Circular Footings Subjected to Monotonic Inclined Loading on Uncemented and Cemented Calcareous Sands. *Journal of Geotechnical and Geoenvironmental Engineering, 131*(1), 52-63.

Cassidy, M. J., Uzielli, M., & Tian, Y. (2013). Probabilistic combined loading failure envelopes of a strip footing on spatially variable soil. *Computers and Geotechnics, 49*, 191-205.

CEB-FIP. (2013). *fib Model Code for Concrete Structures 2010*. Berlin, Germany: Ernst & Sohn.

CEN. (2004). Eurocode 7: Geotechnical Design - Part 1: General Rules. In (Vol. EN 1997-1): European Committee for Standardization (CEN).

CEN. (2005). EN 1990: Eurocode - Basis of Structural Design. In (Vol. EN 1990:2002+A1). Brussels, Beligium.

Cherubini, C. (1997). *Data and considerations on the variability of geotechnical properties of soils*. International Conference on Safety and Reliability (ESREL) 97, Lisbon 17-20 June 1997.

Ching, J., Chen, J., Yeh, J., & Phoon, K. K. (2012). Updating uncertainties in friction angles of clean sands. *J. Geotech. Geoenviron. Eng., 138*(2), 217-229.

Ching, J., Hu, Y., & Phoon, K. K. (2015). *On the use of spatially averaged shear strength for the bearing capacity of a shallow foundation*. 12th International Conference on Applications of Statistics and Probability in Civil Engineering (ICASP12), Vancouver, Canada 12-15 July 2015.

Ching, J., & Phoon, K. K. (2011a). *Effective shear strengths of isotropic spatially variable soil masses*. First International Symposium on Uncertainty Modeling and Analysis and Management (ICVRAM 2011); and Fifth International Symposium on Uncertainty Modeling and Anaylsis (ISUMA), Hyattsville, Maryland, United States April 11-13, 2011.

Ching, J., & Phoon, K. K. (2011b). A quantile-based approach for calibrating reliability-based partial factors. *Structural Safety, 33*, 275-285.

Ching, J., & Phoon, K. K. (2012). *Probabilistic model for overall shear strengths of spatially variable soil masses*. GeoCongress 2012 - State of the Art and Practice in Geotechnical Engineering, Oakland, California, United States March 25-29, 2012.

Ching, J., & Phoon, K. K. (2013). Quantile value method versus design value method for calibration of reliability-based geotechnical codes. *Structural Safety, 44*, 47-58.

Ching, J., Phoon, K. K., & Yang, J. J. (2015). Role of redundancy in simplified geotechnical reliability-based design – A quantile value method perspective. *Structural Safety, 55*, 37-48.

Christian, J. T. (2007). LRFD for geotechnical applications. *Structure Magazine*(May 2007), 49-51.

Christian, J. T., & Baecher, G. B. (2002). The Point-Estimate Method with Large Numbers of Variables. *International Journal for Numerical and Analytical Methods in Geomechanics, 26*, 1515–1529.

Christian, J. T., & Baecher, G. B. (2011). *Unresolved problems in geotechnical risk and reliability*. GeoRisk 2011, Atlanta, GA.

Cornell, C. A. (1969). Probability-based structural code. *ACI Journal, 66*, 974-985.

Coulomb, C. A. (1773). Essai sur une application des regles de maximis et minimis a quelques problems de statique relatif a l'architecture. *Mem. Acad. Roy. Sciences, 7*, 343-382.

Dai, S. H., & Wang, M. O. (1992). *Reliability Analysis in Engineering Applications*. New York: Van Nostrand Reinhold.

Darendeli, M. B. (2001). *Development of a new family of normalized modulus reduction and material damping curves.* (Doctor of Philosophy), The University of Texas, Austin, Texas.

Das, B. M. (2007). *Principles of Foundation Engineering* (6th ed.). Pacific Grove, Calif.: PWS Pub.

DeMeo, E. (2017). *2016-2017 Status Assessment and Update on the Wind Vision Roadmap* (NREL/SR-6A20-69026).NREL

Denholm, P., Hand, M., Jackson, M., & Ong, S. (2009). *Land-Use Requirements of Modern Wind Power Plants in the United States* (NREL/TP-6A2-45834).National Renewable Energy Laboratory, US Department of Energy

Denver, H., & Ovesen, N. K. (1994). *Assessment of characteristic values of soil parameters for design*. XIII ICSMFE, New Delhi, India 5-10 January 1994.

Diamantidis, D. (2008). *Current safety acceptance criteria in codes and standards – A critical review* Structures 2008: Crossing Borders, Vancouver, British Columbia, Canada April 24-26, 2008.

Diaz-Rodriguez, J. A., & Lopez-Molina, J. A. (2008). *Strain thresholds in soil dynamics*. The 14th World Conference on Earthquake Engineering, Beijing, China October 12-17, 2008.

DIBt. (2012). Richtlinie für Windenergieanlagen (Guideline for Wind Turbines), Draft 12. In. Berlin: Deutschen Instituts für Bautechnik.

DNV-GL. (2016a). Loads and Site Conditions for Wind Turbines. In.

DNV-GL. (2016b). Support Structures for Wind Turbines, April 2016 Edition. In: DNV-GL.

DNV. (1992). *Classification Notes No. 30-4: Foundations* Det norske veritas

DNV/Riso. (2002). Guidelines for Design of Wind Turbines, 2nd Edition. In. Denmark: Det Norske Veritas / Riso.

DNV/Risø. (2002). Guidelines for Design of Wind Turbines, 2nd Edition. In. Denmark: Det Norske Veritas / Riso.

DNV/Risø. (2004). Design of Offshore Wind Turbine Structures. In: Det Norske Veritas (DNV).

Dobry, R. (2014). Simplified methods in soil dynamics. *Soil Dynamics and Earthquake Engineering, 61-62*, 246-268.

DOE. (2008). *20% Wind Energy by 2030 - Increasing Wind Energy's Contribution to the U.S. Electricity Supply* Energy Efficieny and Renewable Energy, U.S. Department of Energy

DOE. (2015). *Wind Vision: A New Era for Wind Power in the United States* US Department of Energy

DOE. (2017). *Wind Vision Detailed Roadmap Actions - 2017 Update* Department of Energy

Dong, Y., Lu, N., & McCartney, J. S. (2018). Scaling shear modulus from small to finite strain for unsaturated soils *J. Geotech. Geoenviron. Eng. , 144*(2), 04017110-04017111/04017111.

Doorn, N., & Hansson, S. O. (2011). Should probabilistic design replace safety factors? *Philos. Technol., 25*, 151-168.

Duncan, J. M. (2000). Factors of safety and reliability in geotechnical engineering. *Journal of Geotechnical and Geoenvironmental Engineering, 126*(4), 307-316.

Duncan, J. M., & Sleep, M. (2017). The need for judgement in geotechnical reliability studies. *Georisk - Assessment and Management of Risk for Engineering Systems and Geohazards, 11*(1), 70-74.

Ellingwood, B. (1980). *Development of a Probability Based Load Criterion for American National Standard A58: Building Code Requirements for Minimum Design Loads in Buildings and Other Structures*. [Washington, D.C.]: U.S. Dept. of Commerce, National Bureau of Standards : for sale by the Supt. of Docs., U.S. Govt. Print. Off.

Engström, S., Lyrner, T., Hassanzadeh, M., Stalin, T., & Johansson, J. (2010). *Tall Towers for Large Wind Turbines* Elforsk Electricity and Power Production Stockholm:

Ering, P., & Babu, S. G. (2017). A Bayesian framework for updating model parameters while considering spatial variability. *Georisk, 11*(4), 285-298.

Fahey, M., & Carter, J. P. (1993). A finite element study of the pressumeter test in sand using nonlinear elastic plastic model. *Canadian Geotechnical Journal, 30*(2), 348-362.

Fan, H., & Liang, R. (2012). *Application of Monte Carlo Simulation to Laterally Loaded Piles*. GeoCongress 2012, Oakland, CA.

Fenton, G. A., & Griffiths, D. V. (1993). Seepage beneath water retaining structures founded on spatially random soil. *Geotechnique, 43*(4).

Fenton, G. A., & Griffiths, D. V. (2003). Bearing capacity prediction of spatially random phi-c soils. *Canadian Geotechnical Journal, 40*(1), 54-65.

Fenton, G. A., & Griffiths, D. V. (2007). The random finite element method (RFEM) in bearing capacity analysis. In D. V. Griffiths & G. A. Fenton (Eds.), *Probabilistic Methods in Geotechnical Engineering* (pp. 295-315). New York: Springer Wien.

Fenton, G. A., & Griffiths, D. V. (2008). *Risk Assessment in Geotechnical Engineering*. Hoboken, N.J.: John Wiley & Sons.

Fenton, G. A., Griffiths, D. V., & Urquart, A. (2003). *A slope stability model for spatially random soils.* Paper presented at the ICASP9, Rotterdam, Netherlands.

Fenton, G. A., Naghibi, F., dundas, D., Bathurst, R. J., & Griffiths, D. V. (2016). Reliability-based geotechnical design in 2014 Canadian highway bridge design code. *Can. Geotech. J., 53*, 236-251.

Ferson, S., & Ginzburg, L. R. (1996). Different methods are needed to propagate ignorance and variability. *Reliability Engineering and System Safety, 54*, 133-144.

Fishman, G. S. (1995). *Monte Carlo: Concepts, Algorithms, and Applications*. New York: Springer-Verlag.

Foye, K. C., Salgado, R., & Scott, B. (2006). Assessment of variable uncertainties for reliability-based design of foundations. *Journal of Geotechnical and Geoenvironmental Engineering, 132*, 1197-1207.

Gazetas, G. (1975). *Dynamic Stiffness of Strip and Rectangular Footings on Layered Media.* (Master of Science), Massachusetts Institute of Technology,

Gazetas, G. (1983). Analysis of machine foundation vibrations: state of the art *Soil Dynamics and Earthquake Engineering, 2*(1), 2-42.

Gazetas, G. (1991). Formulas and charts for impedances of surface and embded foundations. *Journal of Geotechnical Engineering, 117*(9), 1363-1381.

Gazetas, G. (2013). *Soil-foundation-structure systems beyond conventional seismic failure thresholds*. Proceedings of the 18th International Conference on Soil Mechanics and Geotechnical Engineering, Paris, France 2-6 September 2013.

Gazetas, G. (2015). 4th Ishihara lecture: Soil-foundation-structure systems beyond conventional seismic failure thresholds. *Soil Dynamics and Earthquake Engineering, 68*, 23-39.

Gazetas, G., Anastasopoulos, I., Adamidis, O., & Kontoroupi, T. (2013). Nonlinear rocking stiffness of foundations. *Soil Dynamics and Earthquake Engineering, 47*, 83-91.

Gazetas, G., & Hatzikonstantinou, E. (1988). Elastic formulae for lateral displacement and rotation of arbitrarily-shaped embedded foundations. *Geotechnique, 38*(3), 439-444.

Giovanis, D. G., Papadopoulos, V., Lagaros, N. D., & Papadrakakis, M. (2010). *Structural reliability analysis using subset simulation and neural networks*. 10th International Conference on Structural Safety and Reliability (ICOSSAR2009), Osaka, Japan 13-17 September 2009.

GL. (2003). *Guideline for the Certification of Wind Turbines* Germanisher Lloyd WindEnergie

GL. (2010). Guideline for the Certification of Wind Turbines, Edition 2010. In. Hamburg, Germany: Germanischer Lloyd Industrial Services GmbH.

Goh, A. T. C., & Kulhawy, F. H. (2006). *Reliability Assessment of Geotechnical Serviceability State Using Neural Networks*.

Goh, T. C., Kulhawy, F. H., & Chua, C. G. (2005). Bayesian neural network analysis of undrained side resistance of drilled shafts. *Journal of Geotechnical and Geoenvironmental Engineering, 131*(1), 84-93.

Goldsworthy, J. S., Jaksa, M. B., Fenton, G. A., Griffiths, D. V., Kaggwa, W. S., & Poulos, H. G. (2007). *Measuring the risk of geotechnical site investigations*. Probabilistic Applications in Geotechnical Engineering. Geotechnical Special Publication No. 170. Proceedings of the Geo-Denver 2007 Symposium, Denver, CO.

Gottardi, G., & Butterfield, R. (1993). On the bearing capacity of surface footings on sand under general planar loads. *Soils and Foundations, 33*(4), 68-79.

Gottardi, G., Houlsby, G. T., & Butterfield, R. (1997). *The Plastic Response of Circular Footings on Sand under General Planar Loading* University of Oxford Oxford:

Greco, V. R. (2016). Variability and correlation of strength parameters inferred from direct shear tests. *Geotechnical and Geological Engineering, 34*, 585–603.

Griffiths, D. V. (1980). *Finite element analyses of footings, walls and slopes* Paper presented at the Computer Applications to Geotechnical Problems in Highway Engineering, Cambridge.

Griffiths, D. V. (2015). Observations on load and strength factors in bearing capacity analysis. *J Geotech Geoenv Eng, 141*(7), 1-4.

Griffiths, D. V., & Fenton, G. A. (2007a). *Probabilistic Methods in Geotechnical Engineering*. Wien ; New York: Springer Verlag.

Griffiths, D. V., & Fenton, G. A. (2007b). The random finite element method (RFEM) in slope stability analysis. In D. V. Griffiths & G. A. Fenton (Eds.), *Probabilistic*

Methods in Geotechnical Engineering (pp. 317-346). New York: Springer Wien.

Griffiths, D. V., Fenton, G. A., & Ziemann, H. R. (2006). *Seeking out failure: the random finite element method (RFEM) in probabilistic geotechnical analysis*. GeoCongress 2006 - Mini-Symposium on Numerical Modeling and Analysis (Probabilistic Modeling and Design), Atlanta, GA.

Griffiths, D. V., Paiboon, J., Huang, J., & Fenton, G. A. (2013). *Homogenization of geomaterials using the random finite element method*. 4th International Symposium on Geotechnical Safety and Risk (Geotechnical Safety and Risk IV), Hong Kong 4-6 December 2013.

Griffiths, D. V., Zhu, D., Huang, J., & Fenton, G. A. (2016). *Observations on probabilistic slope stability analysis*. 6th Asian-Pacific Symposium on Structural Reliability and its Applications, Shanghai, China 28-30 May 2016.

Guerreiro, P., Kontoe, S., & Taborda , D. (2012). *Comparative study of stiffness reduction and damping curves*. 15th World Conference in Earthquake Engineering, Lisbon, Portugal September 24-28, 2012.

GWEC. (2017). *Global Wind Report - Annual Market Update 2017* Global Wind Energy Council

Halim, I. S., & Tang, W. H. (1993). Site exploration strategy for geologic anomaly characterization. *ASCE J Geotech Eng, 119*(2), 195-213.

Hansen, J. B. (1953). *Earth Pressure Calculation*. Copenhagen: Danish Technical Press.

Hansen, J. B. (1970). A revised and extended formula for bearing capacity. *Geotechnical Institute Bulletin, Copenhagen, 28*.

Hardin, B. O., & Drnevich, V. P. (1972). Shear modulus and damping in soils: design equations and curves. *J. Soil Mech. and Found. Div. (ASCE), 98*(SM7), 667-692.

Harr, M. E. (1987). *Reliability-based design in civil engineering*. New York: McGraw-Hill.

Hasofer, A. M., & Lind, N. C. (1974). An exact and invariant second moment code format. *Journal of Engineering Mechanics, 100*, 111-121.

Holicky, M. (2009). *Reliability Analysis for Structural Design*. Stellenbosch, South Africa: Sun Press.

Holický, M., Diamantidis, D., & Sykora, M. (2015). *Determination of target safety for structures*. 12th International Conference on Applications of Statistics and Probability in Civil Engineering (ICASP12), Vancouver, Canada 12-15 July 2015.

Honjo, Y. (2011). *Challenges in geotechnical reliability based design* ISGSR 2011.

Horgan, C. (2013). Using Energy Payback Time to Optimise Onshore and Offshore Wind Turbine Foundations. *Renewable Energy, 53*, 287-298.

Houlsby, G. T., & Purzin, A. M. (1999). The Bearing Capacity of a Strip Footing on Clay under Combined Loading. *Proceedings of the Royal Society a-Mathematical Physical and Engineering Sciences, 455*, 893-916.

Huang, J., Griffiths, D. V., & Fenton, G. A. (2010). System reliability of slopes by RFEM. *Soils and Foundations, 50*(3), 343-353.

Huang, K., Cao, Z., & Wang, Y. (2013). *CPT-based Bayesian identification of underground soil stratigraphy*. Geotechnical Safety and Risk IV, Hong Kong.

Huber, M. (2013). *Soil Variability and its Consequences in Geotechnical Engineering.* University of Stuttgart, Stuttgart, Germany.

Hutchinson, P. J., & Beird, M. H. (2016a). 3D mapping with MASW. *The Leading Edge (Society of Exploration Geophysics), 35*(4), 350-352.

Hutchinson, P. J., & Beird, M. H. (2016b). A comparison of surface and standard penetration test-derived shear wave velocity. *Environmental and Engineering Geoscience, XXII*(1), 27-36.

ICC. (2018). International Building Code 2018. In: International Code Council.

IEA. (2013). *Technology Roadmap - Wind Energy* International Energy Agency

IEC. (2008). IEC 61400-1 Ed.3: Wind turbines - Part 1: Design requirements. In. Geneva, Switzerland: International Electrotechnical Commission.

IEC. (2016). IEC 61400-6: Wind turbines – Part 6: Tower and foundation design requirements (standard under active development, Edition 1 Committee Draft). In: International Electrotechnical Commission.

ISO. (2007). ISO 19902: Petroleum and Natural Gas Industries — Fixed Steel Offshore Structures. In (Vol. ISO 19902): ISO.

ISO. (2015). ISO 2394: General Principles on Reliability for Structures, 4th Edition. In (pp. 120): International Standards Organization.

Jaksa, M. B., Goldsworthy, J. S., Fenton, G. A., Kaggwa, W. S., Griffiths, D. V., Kuo, Y. L., & Poulos, H. G. (2005). Towards reliable and effective site investigations. *Geotechnique, 55*(2), 109-121.

JCSS. (2000). Probabilistic Model Code. Part 3: Material Properties. In: Joint Committee on Structural Safety.

JCSS. (2001a). Probabilistic Model Code. Part 1: Basis of Design, 12th Draft. In: Joint Committee on Structural Safety.

JCSS. (2001b). Probabilistic Model Code. Part 2: Load Models, 12th Draft. In: Joint Committee on Structural Safety.

JCSS. (2008). *Risk Assessment in Engineering: Principles, System Representation & Risk Criteria* (M. H. Faber Ed.): Joint Committee on Structural Safety.

Jones, A. L., Kramer, S. L., & Arduino, P. (2002). *Estimation of Uncertainty in Geotechnical Properties for Performance-based Earthquake Engineering* Pacific Earthquake Engineering Research Center (PEER)

Jonkman, S. N., Steenbergen, R. D. J. M., Morales-Nápoles, O., Vrouwenvelder, A. C. W. M., & Vrijling, J. K. (2015). *Probabilistic Design: Risk and Reliability Analysis in Civil Engineering*: Delft University of Technology.

JSCE. (2010). Guideline for Design of Wind Turbine Support Structure and Foundation, Japan. In. Japan: Japan Society of Civil Engineers.

Kaldellis, J. K., & Zafirakis, D. (2011). The wind energy (r)evolution: a short review of a long history. *Renewable Energy, 36*, 1887-1901.

Kalos, M. H., & Whitlock, P. A. (2008). *Monte Carlo Methods* (2nd ed.). Weinheim: Wiley-VCH.

Khoshnevisan, S., Wang, L., & Hsein Juang, C. (2017). Response surface-based robust geotechnical design of supported excavation – spreadsheet-based solution. *Georisk - Assessment and Management of Risk for Engineering Systems and Geohazards, 11*(1), 90-102.

Kondner, R. L. (1963a). *A hyperbolic stress-strain formulation for sands* Northwestern University

Kondner, R. L. (1963b). A hyperbolic stress-strain response: cohesive soils. *Journal of the Soil Mechanics and Foundations Division, 89*(1), 115-143.

Kondner, R. L., & Zelasko, J. S. (1963). *A hyperbolic stress–strain formulation of sands*. 2nd Pan Am. Conf. on Soil Mech. and Found. Engrg., Silo Paulo, Brazil.

Kourkoulis, R., Gelagoti, F., & Anastasopoulos, I. (2012). Rocking isolation of frames on isolated footings: design insights and limitations. *Journal of Earthquake Engineering, 16*(3), 374-400.

Krebs Ovesen, N. (1981). Towards a European code for foundation engineering. *Ground Engineering*(October 1981).

Kroese, D. P., Taimre, T., & Botev, Z. I. (2011). *Handbook of Monte Carlo Methods*. New York: John Wiley and Sons.

Krumbein, W. C., & Grayhill, F. A. (1965). *An Introduction to Statistical Models in Geolog*. New York: McGraw Hill.

Kulhawy, F. H. (1992). *On the Evaluation of Soil Properties*: ASCE.

Kulhawy, F. H. (1996). From Casagrande's "Calculated Risk" to reliability-based design in foundation engineering: the Sixth Arthur Casagrande Memorial Lecture. *Civil Engineering Practice (Journal of the Boston Society of Civil Engineers Section / ASCE), 11*(2), 43-56.

Kulhawy, F. H., & Mayne, P. W. (1990). *Manual on Estimating Soil Properties for Foundation Design* Cornell University

Lacasse, S., & Nadim, F. (1997). *Uncertainties in Characterizing Soil Properties* Norwegian Geotechnical Institute Oslo, Norway:

Lacasse, S., Nadim, F., & Hoeg, K. (2012). Risk Assessment and Mitigation in Geo-Practice. In (Vol. Geotechnical Engineering State of the Art and Practice): ASCE.

Lamb, H. (1904). On the propagation of tremors over the surface of an elastic solid. *Philosophical Transactions - The R.oyal Society, London, 203*(359-371), 1-42.

Lantz, E., Wiser, R., & Hand, M. (2012). *The Past and Future Cost of Wind Energy* NREL

Lee, I. K., White, W., & Ingles, O. G. (1983). *Geotechnical Engineering*: Pitman.

Leimeister, M., & Kolios, A. (2018). A review of reliability-based methods for risk analysis and their application in the offshore wind industry. *Renewable and Sustainable Energy Reviews, 91*, 1065-1076.

Li, D.-Q., Zhang, F.-P., Cao, Z.-J., Tang, X.-S., & Au, S.-K. (2018). Reliability sensitivity analysis of geotechnical monitoring variables using Bayesian updating. *Engineering Geology, 245*, 130-140.

Li, K. S., & Lumb, P. (1987). Probabilistic design of slopes. *Can. Geotech. J., 24*, 520-535.

Louie, J. N. (2001). Faster, better, shear-wave velocity to 100 meters depth from refraction microtremor arrays. *Bulletin Seismological Society of America, 85*, 900-922.

Loukidis, D., Chakraborty, T., & Salgado, R. (2008). Bearing capacity of strip footings on purely frictional soil under eccentric and inclined Loads. *Canadian Geotechnical Journal, 45*, 768-787.

Low, B. K. (2006). *Practical reliability approach in geotechnical engineering*. GeoCogress 2006, Atlanta, GA. February 26 - March 1, 2006.

Lumb, P. (1970). Safety factors and probability distribution of soil strength. *Can. Geotech. J., 7*(3), 225-242.

Lumb, P. (1974). Application of Statistics in Soil Mechanics. In I. K. Lee (Ed.), *Soil Mechanics: New Horizons* (pp. 44-111). London: Newnes-Butterworth.

Madhav, M. R., & Poorooshasb, H. B. (2001). *Rotation of tall structures founded on in-elastic ground*. 15th ICSMGE, Istanbul, Turkey August 2001.

Martin, C. M. (2005). *Exact bearing capacity calculations using the method of characteristics*. 11th Inter. Conf. of IACMAG, Torino, Italy 19-24 June 2005.

Matasovic, N., & Vucetic, M. (1993). Cyclic characterization of liquefiable sands. *J. Geotech. Eng., 119*(11), 1805-1822.

MathWorks. (2016). MATLAB. The MathWorks, Inc.: Natick, MA.

Mayne, P. W. (2001). *Stress-strain-strength-flow parameters from enhanced in-situ tests*. International Conference on In-Situ Measurement of Soil Properties & Case Histories (In-Situ 2001), Bali, Indonesia May 21-24, 2001.

Menezes, E. J. N., Araujo, A. M., & da Silva, N. S. B. (2018). A review on wind turbine control and its associated methods. *Journal of Cleaner Production, 174*, 945-953.

Meyerhof, G. G. (1953). *The bearing capacity of foundation under eccentric and inclined loads.* Paper presented at the 3rd International Conference on Soil Mechanics and Foundation Engineering, Zurich.

Microsoft. (2018). Micosoft Excel. Microsoft Corporation: Redmond, WA.

Moe, A. J. (1936). *The Factor of Safety of Reinforced Concrete Structures* Copenhagen:

Mone, C., Hand, M., Bolinger, M., Rand, J., Heimiller, D., & Ho, J. (2017). *2015 Cost of Wind Energy Review* Department of Energy

Morgan, M. G., & Henrion, M. (1999). *Uncertainty: a Guide to Dealing with Uncertainty in Quantitative Risk and Policy Analysis*. Cambridge: Cambridge University Press.

Mott, P. H., & Roland, C. M. (2013). Limits to Poisson's ratio in isotropic materials - general result for arbitrary deformation. *Physica Scripta, 87*(5), 1-6.

Murff, J. D. (1994). *Limit Analysis of Multi-footing Foundation Systems.* Paper presented at the 8th International Conference on Computer Methods and Advances in Geomechanics, Rotterdam.

Murthy, V. N. S. (2002). *Geotechnical Engineering - Principles and Practices of Soil Mechanics and Foundation Engineering*: CRC Press.

Nadim, F. (2007). Tools and strategies for dealing with uncertainty in geotechnics. In D. V. Griffiths & G. A. Fenton (Eds.), *Probabilistic Methods in Geotechnical Engineering* (pp. 71-95). New York: SpringerWien.

Nathwani, J. S., Lind, N. C., & Pandey, M. D. (1997). *Affordable Safety by Choice : The Life Quality Method* University of Waterloo Waterloo, Ontario:

Nazarian, S. (2012). Shear Wave Velocity Profiling with Surface Wave Methods. In (Vol. Geotechnical Engineering State of the Art and Practice): ASCE.

Neal, R. M. (1992). *Bayesian Training of Back-propagation Networks by the Hybrid Monte Carlo Method* University of Toronto Toronto:

Njiri, J. G., & Soffker, D. (2016). State-of-the-art in wind turbine control: trends and challenges. *Renewable and Sustainable Energy Reviews, 60*, 377-393.

Nowak, A. S. (1983). Risk Analysis for Code Calibration. *Structural Safety, 1*, 15.

NRC. (1995). *Probabilistic Methods in Geotechnical Engineering*. Washington, DC: The National Academies Press.

Ntambakwa, E., Yu, H., Guzman, C., & Rogers, M. (2016). *Geotechnical design considerations for onshore wind turbine shallow foundations* Geotechnical and Structural Engineering Congress 2016, Phoenix, AZ.

Orr, T. L. L. (2017). Defining and selecting characteristic values of geotechnical parameters for designs to Eurocode 7. *Georisk - Assessment and Management of Risk for Engineering Systems and Geohazards, 11*(1), 103-115.

Paikowsky, S. G., Canniff, M. C., Lesny, K., Kisse, A., Amatya, S., & Muganga, R. (2010). *NCHRP Report 651 - LRFD Design and Construction of Shallow Foundations for Highway Bridge Structures* National Cooperative Highway Research Program - Transportation Research Board Washington, DC:

Pais, A., & Kausel, E. (1988). Approximate formulas for dynamic stiffnesses of rigid foundations. *Soil Dynamics and Earthquake Engineering, 7*(4), 213-227.

Papaioannou, I., & Straub, D. (2017). Learning soil parameters and updating geotechnical reliability estimates under

spatial variability – theory and application to shallow foundations. *Georisk - Assessment and Management of Risk for Engineering Systems and Geohazards, 11*(1), 116-128.

Park, C. B., Miller, R. D., & Xia, J. (1999). Multichannel analysis of surface waves. *Geophysics, 64*(3), 800-808.

Phoon, K. K., & Ching, J. (2015). *Is there anything better than LRFD for simplified geotechnical RBD?* Fifth International Symposium on Geotechnical Safety and Risk (ISGSR2015), Rotterdam, The Netherlands 13-16 October 2015.

Phoon, K. K., & Kulhawy, F. H. (1999a). Characterization of geotechnical variability. *Canadian Geotechnical Journal, 36*, 13.

Phoon, K. K., & Kulhawy, F. H. (1999b). Evaluation of Geotechnical Property Variability. *Canadian Geotechnical Journal, 36*, 15.

Phoon, K. K., & Kulhawy, F. H. (2008). Serviceability limit state reliability-based design (Chapter 9). In *Reliability-based Design in Geotechnical Engineering: Computations and Applications* (pp. 344-383): Taylor & Francis, UK.

Poulos, H. G. (2018). *Estimation of geotechnical deformation parameters from small-strain shear modulus*. 2018 International Foundations Congress and Equipment Expo (IFCEE 2018), Orlando, FL.

Poulos, H. G., & Davis, E. H. (1974). *Elastic Solutions for Soil and Rock Mechanics*. New York: John Wiley & Sons.

Prandtl, L. (1920). Concerning the hardness of plastic bodies. *Nachr. Ges. Wiss. Gottingen*, 74-85.

Prandtl, L. (1921). Über die Eindringungsfestigkeit (Härte) plastischer Baustoffe und die Festigkeit von Schneiden" (On the Penetrating Strengths (Hardness) of Plastic Construction Materials and the Strength of Cutting Edges). *Zeit. Angew. Math. Mech., 1*(1), 15-20.

Proppe, C. (2017). Markov Chain Monte Carlo Simualtion methods for structural reliability analysis. *Procedia Engineering, 199*, 1122-1127.

PTC. (2018). MathCAD 15. PTC: Needham, MA.

Reddy, M. V., Grandhi, R. V., & Hopkins, D. A. (1994). Reliability-based structural optimization - a simplified safety index approach. *Computers & Structures, 53*(6), 1407-1418.

Reissner, E. (1936). Stationäre, axialsymmetrishe durch eine Schüttelnde Masse erregte Schwingungen eines homogenen elastischen Halbraumes. *Ingenieur-Archiv., 7*(Part 6), 381-396.

Richart, F. E., Jr., & Whitman, R. V. (1967). Comparison of footing vibration tests with theory, 93(6),. *J. Soil Mech. and Found. Div. (ASCE), 93*(6), 143-168.

Robert, C., & Casella, G. (2011). A short history of Markov Chain Monte Carlo: subjective recollections from incomplete data. *Statistical Science, 26*(1), 102–115.

Robert, C. P., & Casella, G. (1999). *Monte Carlo Statistical Methods* (2nd ed.): Springer.

Robertson, P. K., Campanella, R. G., & Gillespie, D. (1986). Seismic CPT to measure in-situ shear wave velocity. *Geotechnical Engineering Journal, 112*(791-804), 8.

Roscoe, K. H., & Schofield, A. N. (1957). The Stability of Short Pier Foundations on Sand. Discussion. *British Welding Journal*, 12-18.

Rosenblueth, E. (1975). Point estimates for probability moments. *Proceedings of the National Academy of Science, 72*(10), 3812-3814.

Rosenblueth, E. (1981). Two-point estimates in probabilitties. *Appl. Math. Modelling, 5*, 329-335.

Schneider, H. R. (1999). *Definition and determination of characteristic soil properties*. Fourteenth Int. Conf. on Soil Mech. and Foundation Engineering, Hamburg.

Schultze, E. (1971). Frequency distributions and correlations of soil properties. In P. Lumb (Ed.), *Statistics and Probability in Civil Engineering* (pp. 371-388): Hong Kong University Press.

Selvam, K. (2007). *Individual Pitch Control for Large Scale Wind Turbines - Multivariable Control Approach.* (Master's Thehis), TU Delft,

Shen, Z., Feng, X., & Gouvernec, S. (2016). Undrained capacity of surface foundations with zero-tension interface under planar V-H-M loading. *Computers and Geotechnics, 73*, 47-57.

Shi, J., & Asimaki, D. (2017). From stiffness to strength: formulation and validation of a hybrid hyperbolic nonlinear soil model for site-response analyses. *Bulletin of the Seismological Society of America, 107*(3), 1336-1355.

Shrestha, S., Ravichandran, N., & Rahbari, P. (2017). *Robust geotechnical design of piled-raft foundations for tall onshore wind turbines*. Geotechnical Frontiers 2017, Orlando, Florida March 12–15, 2017.

Sills, G. L., Vroman, N. D., Wahl, R. E., & Schanz, N. T. (2008). Overview of New Orleans Levee Failures: Lessons Learned and the Impact on National Levee Design and Assessment. *Journal of Geotechnical and Geoenvironmental Engineering, 134*(5), 556-565.

Snedecor, G. W., & Cochran, W. G. (1964). *Statistical Methods*: Univ of Iowa Press.

Sorensen, J. D., & Toft, H. S. (2014). *Safety Factors - IEC 61400-1 ed.4 - Background Document* DTU

Stokoe, K. H., & Hoar, R. J. (1981). *Crosshole measurement and analysis of shear waves*. 10th International Conference on Soil Mechanics and Foundation Engineering

Stockholm 15-19 June 1981.

Stokoe, K. H., & Woods, R. D. (1972). In-situ shear wave velocity by cross-hole method. *ASCE J Soil Mech Found Div, 98*(SM5), 443-460.

Stokoe, K. H. I., & Santamarina, J. C. (2000). *Seismic-wave-based testing in geotechnical engineering*. GeoEng 2000, Melbourne, Australia.

Taipodia, J., Babu, K. P., Kiran, B., & Dey, A. (2013). Subsurface characterization using MASW: preliminary experimentation and analysis. *International Journal of Innovative Research in Science, Engineering and Technology (IJIRSET), 3*(4 - Special Issue on National Conference on Recent Advances in Civil Engineering: NCRACE-2013), 129-138.

Tang, C., Phoon, K. K., & Toh, K.-C. (2015). Effect of footing width on N-gamma and failure envelope of eccentrically and obliquely loaded strip footings on sand. *Can. Geotech. J., 52*, 694-707.

Taylor, R. W. (1967). *Design of spread footings for earthquake loadings*. 5th Australia-New Zealand Conference on SMFE.

Tegen, S., Lantz, E., Hand, M., Maples, B., Smith, A., & Schwabe, P. (2011). *2011 Cost of Wind Energy Review* National Renewable Energy Laboratory (NREL)

Terzaghi, K. (1943). *Theoretical Soil Mechanics*. New York: John Wiley and Sons.

Terzaghi, K. (1955). Evaluation of Coefficient of Subgrade Reaction. *Geotechnique, 5*(4), 297-326.

Terzaghi, K., & Peck, R. P. (1948). *Soil Mechanics in Engineering Practice, 1st ed.* New York: John Wiley & Sons, Inc.

Terzaghi, K., & Peck, R. P. (1967). *Soil Mechanics in Engineering Practice, 2nd ed.* New York: John Wiley & Sons, Inc.

Tettinek, W., & Matl, F. (1953). *A contribution to calculating the inclination of eccentrically loaded foundations*. 3rd ICSMFE, Zurich.

Tippett, L. H. C. (1925). On the extreme individuals and the range of samples taken from a normal population. *Biometrika, 17*(3/4), 364-387.

Toro, G. R. (1996). Probabilistic Models of Site Velocity Profiles for Generic and Site-Specific Ground Motion Amplification Studies. In W. J. Silva, A. N., G. Toro, & C. Costantino (Eds.), *Description and Validation of the Stochastic Ground Motion Model* (Vol. Contract No. 770573): Brookhaven National Laboratory, Associated Universities, Inc. Upton, New York 11973, .

Trbojevic, V. M. (2005). *Risk criteria in EU*. 25th European Safety and Reliability Conference (ESREL'05), Poland 27-30 June 2005.

Trbojevic, V. M. (2009). Another look at risk and structural reliability criteria. *Structural Safety, 31*, 245 - 250.

USCOE. (2014). *Safety of Dams - Policy and Procedures*. (ER-1110-2-1156). Washington, DC: USACE.

Uzielli, M., Lacasse, S., Nadim, F., & Phoon, K. K. (2006). *Soil variability analysis for geotechnical practice*. 2nd International Workshop on Characterisation and Engineering Properties of Natural Soils, Singapore December 2006.

Vali, M., van Wingerden, J.-W., & Kuhn, M. (2016). *Optimal multivariable individual pitch control for load reduction of large wind turbines*. 2016 American Control Conference, Boston, MA 6-8 July 2016.

Vardanega, P. J., & Bolton, M. D. (2011, 31 August - 3 September 2011). *Practical methods to estimate the non-linear shear stiffness of fine grained soils* Paper presented at the Proceedings 5th International Conference on the deformation of Geomaterials, Seoul, Korea.

Veletsos, A. S., & Wei, Y. T. (1971). Lateral and rocking vibrations of footings. *Journal of the SoilMechanics and Foundations Division (ASCE), 97*(9), 1227-1248.

Vesic, A. S. (1975). Bearing Capacity of Shallow Foundations. In W. H.F. & H. Y. Fang (Eds.), *Foundation Engineering Handbook* (pp. 121-147). New York: Van Nostrand.

Vick, S. G. (2002). *Degrees of Belief: Subjective Probability and Engineering Judgement*: ASCE Press.

Wang, L., & Grandhi, R. V. (1994). Efficient safety index calculation for structural reliability analysis. *Computers and Structures, 52*(1), 103-111.

Wang, P., Lu, Z., & Tang, Z. (2013). An application of the Kriging method in global sensitivity analysis with parameter uncertainty. *Applied Mathematical Modelling, 37*, 6543-6555.

Wang, P., Zhang, J., Zhai, H., & Qiu, J. (2017). A new structural reliability index based on uncertainty theory. *Chinese Journal of Aeronautics, 30*(4), 1451-1458.

Wang, Y. (2011). Reliability-Based Design of Spread Foundations by Monte Carlo Simulations. *Geotechnique, 61*(8), 9.

Wang, Y., Akeju, O. V., & Cao, Z. (2016). Bayesian Equivalent Sample Toolkit (BEST): an Excel VBA program for probabilistic characterisation of geotechnical properties from limited observation data. *Georisk - Assessment and Management of Risk for Engineering Systems and Geohazards, 10*(4), 251-268.

Wang, Y., Au, S. K., & Kulhawy, F. H. (2011). Expanded reliability based design approach for drilled shafts. *Journal of Geotechnical and Geoenvironmental Engineering, 137*(2), 140-149.

Wang, Y., & Cao, Z. (2015). Practical reliability analysis and design by Monte Carlo Simulation in Spreadsheet. In K. K. Phoon & J. Ching (Eds.), *Risk and Reliability in Geotechnical Engineering* (pp. 301-335). Boca Raton: CRC Press.

Whitman, R. V. (1984). Evaluating calculated risk in geotechnical engineering. *Journal of Geotechnical Engineering, 110*(2).

Whitman, R. V. (2000). Organizing and evaluating uncertainty in geotechnical engineering. *Journal of Geotechnical and Geoenvironmental Engineering, 126*(7), 583-593.

Whitman, R. V., & Richart, F. E. J. (1967). *Design Procedures for Dynamically Loaded Foundations* The University of Michigan

Wiser, R., & Bolinger, M. (2014). *2013 Wind Technologies Market Report* U. S. Department of Energy

Wolf, J. P. (1994). *Foundation Vibration Analysis using Simple Physical Models*. NJ: Englewood Cliffs - Prentice Hall.

Wolff, T. F., Demsky, E. C., Schauer, J., & Perry, E. (1996). *Reliability assessment of dike and levee embankments.* Paper presented at the Uncertainty in the Geologic Environment, From Theory to Practice, Proceeding of Uncertainty '96 - Geotechnical Special Publication No. 58.

Xia, J., Miller, C. B., & Park, J. A. (1999). Estimation of near-surface shear-wave velocity by inversion of Rayleigh wave. *Geophysics, 64*(3), 691-700.

Yilmaz, M., Schubert, S., Tinjum, J. M., & Fratta, D. (2014). *Foundation soil response to wind turbine generator loading*. Geo-Congress 2014, Atlanta, GA February 23-26, 2014.

Yucemen, M. S., Tang, W. H., & Ang, A. H.-S. (1973). *A Probabilistic Study of Safety and Design of Earth Slopes* University of Illinois

Zhang, J. (2017). *Bayesian Method: a Natural Tool for Processing Geotechnical Information - 2017 Final Report of the Joint TC205/TC304 Working Group on "Discussion of statistical/reliability methods for Eurocodes"* ISSMGE

Zhang, J., Huang, H. W., Juang, C. H., & Su, W. W. (2014). Geotechnical reliability analysis with limited data: Consideration of model selection uncertainty. *Engineering Geology, 181*, 27-37.

Zhang, L., Li, D.-Q., Tang, X.-S., Cao, Z.-J., & Phoon, K. K. (2018). Bayesian model comparison and characterization of bivariate distribution for shear strength parameters of soil. *Computers and Geotechnics, 95*, 110-118.

Zhang, L., Lu, Z., & Wang, P. (2015). Efficient structural reliability analysis method based on advanced Kriging model. *Applied Mathematical Modelling, 39*, 781-793.

Zhang, L., Tang, W., Zhang, L., & Zheng, J. (2004). Reducing uncertainty of prediction from empirical correlations. *J. Geotech. Geoenviron. Eng., 130*(5), 526-534.

Zhang, Q. (2008). Failure Mode of Foundation under Combined Loadings. *Electronic Journal of Geotechnical Engineering, 13*.

Zhao, Y.-G., & Ono, T. (2000). New point estimates for probability moments. *Journal of Engineering Mechanics, 126*(4), 433-436.

Zhu, D., Griffiths, D. V., & Fenton, G. A. (2018). Worst case spatial correlation length in probabilistic slope stability analysis. *Geotechnique*.

APPENDIX A

MathCAD – DETERMINISTIC CALCULATIONS

DETERMINISTIC COMPUTATIONS AT RANDOM VARIABLE MEANS

Introduction

Deterministic compuations for the three limit states (tilt, rocking stiffness and bearing capacity) are included in this Appendix. The compuattions are carried out at the mean values of random variables and for the example problem included in the main body of this dissertation. The main objectives of these computations are:

- to get an idea on the expected value of the performance function,
- to verify all calculations are correct and
- to verify that all units are used properly.

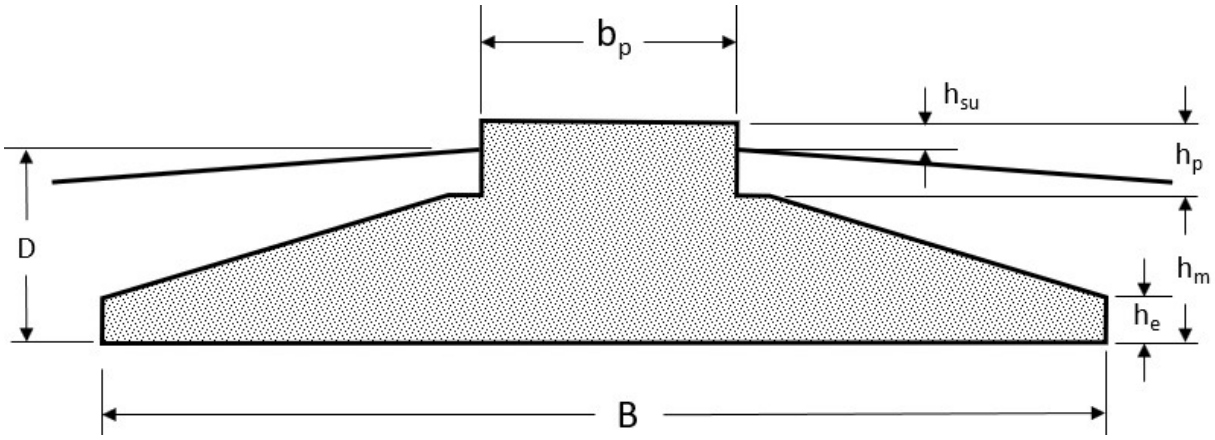

Tilt Limit State (SLS)

Foundation diameter: $B := 17m$

Moment (S3 level): $M_{S3} := 20000kN \cdot m$

In-situ soil density: $\rho := 1750 \frac{kg}{m^3}$

Shear wave velocity: $V_s := 200 \frac{m}{s}$

Poisson's ratio: $\nu := 0.35$

Correction factor: $I_\theta := 4.16$

Shear strain level: $\gamma := 5 \cdot 10^{-4}$

Curvature parameter: $\alpha := 0.9$

Shear strength: $\tau_{max} := 100kPa$

Maximum tilt: $\theta_{max} := 0.17deg$

Tilt angle:
$$\theta := \operatorname{atan}\left[M_{S3} \cdot \frac{(1-\nu)\cdot\left[1+\left(\frac{\gamma\cdot\rho\cdot V_s^{\,2}}{\tau_{max}}\right)^{\alpha}\right]}{2\cdot\rho\cdot V_s^{\,2}\cdot B^3} \cdot I_\theta \right] = 6.25613\times10^{-3}\cdot deg$$

Factor of safety:
$$FS_{tilt} := \frac{\theta_{max}}{\theta} = 27.173$$

Tilt perfromance function at the means:

$$G_{tilt} := \tan\left(\theta_{max}\right) - M_{S3}\cdot\frac{(1-\nu)\cdot\left[1+\left(\frac{\gamma\cdot\rho\cdot V_s^{\,2}}{\tau_{max}}\right)^{\alpha}\right]}{2\cdot\rho\cdot V_s^{\,2}\cdot B^3}\cdot I_\theta = 2.858\times10^{-3}$$

Verify by Computation of Intermediate Quantities:

Small strain shear modulus: $G_0 := \rho\cdot V_s^{\,2} = 70\cdot MPa$

Reference strain: $\gamma_{ref} := \frac{\tau_{max}}{G_0} = 1.429\times10^{-3}$

Shear modulus ratio: $\lambda := \frac{1}{1+\left(\frac{\gamma}{\gamma_{ref}}\right)^{\alpha}} = 0.72$

Degraded shear modulus: $G_r := \lambda\cdot G_0 = 50.405\cdot MPa$

Degraded Young's modulus: $E_r := 2\cdot(1+\nu)\cdot G_r = 136.094\cdot MPa$

Tilt angle: $\theta_{verify} := \operatorname{atan}\left(M_{S3}\cdot\frac{1-\nu^2}{E_r\cdot B^3}\cdot I_\theta\right) = 6.25613\times10^{-3}\cdot deg$

Dynamic Rocking Stiffness

Foundation depth: $D := 2.8m$

Minimum dynamic stiffness: $K_{dmin} := 50\frac{GN\cdot m}{rad}$

Distance to deep bedrock: $H_{bd} := 200m$

Distance to shallow bedrock: $H_{bs} := 8.5m$

Foundation radius: $R_f := 0.5\cdot B = 8.5\,m$

Dynamic stiffness for deep bedrock:

$$K_{ddb} := \frac{8\cdot\rho\cdot V_s^{\,2}\cdot R_f^{\,3}}{3\cdot(1-\nu)}\cdot\left(1+2\cdot\frac{D}{R_f}\right)\cdot\left(1+0.7\cdot\frac{D}{H_{bd}}\right)\cdot\left(1+\frac{R_f}{6\cdot H_{bd}}\right) = 297.517\cdot GN\cdot\frac{m}{rad}$$

Performance function at the means: $G_{kddb} := K_{ddb} - K_{dmin} = 247.517\cdot GN\cdot\frac{m}{rad}$

Factor of safety: $FS_{kddb} := \frac{K_{ddb}}{K_{dmin}} = 5.95$

Dynamic stiffness for bedrock within zone of influence:

$$K_{dsb} := \frac{8 \cdot \rho \cdot V_s^{\,2} \cdot R_f^{\,3}}{3 \cdot (1 - \nu)} \cdot \left(1 + 2 \cdot \frac{D}{R_f}\right) \cdot \left(1 + 0.7 \cdot \frac{D}{H_{bs}}\right) \cdot \left(1 + \frac{R_f}{6 \cdot H_{bs}}\right) = 420.02 \cdot GN \cdot \frac{m}{rad}$$

Performance function at the means: $G_{kdsb} := K_{dsb} - K_{dmin} = 370.02 \cdot GN \cdot \frac{m}{rad}$

Factor of safety: $FS_{kdsb} := \frac{K_{dsb}}{K_{dmin}} = 8.4$

Static Rocking Stiffness

Minimum static stiffness: $K_{smin} := 10 \frac{GN \cdot m}{rad}$

For static stiffness, the following is recommended per IEC61400-6 (Draft):

- Shear modulus must be reduced for the appropriate level of shear strain.
- Effective area should be used. To compute the effective width, the DNV effective area approach can be used.
- To compute effective dimensions, WTG self-weight, as well as foundation geometry and backfill unit weight are all needed.

Turbine self-weight: $P_{wtg} := 2275kN$

Moment (S1 level): $M_{S1} := 50000kN \cdot m$

Unit weight of concrete: $\gamma_c := 23.5 \frac{kN}{m^3}$

Unit weight of backfill: $\gamma_b := 17.0 \frac{kN}{m^3}$

Foundation Geometry:

Pedestal diameter: $B_p := 5.4m$

Backfill crossfall rate (1/n):: $n_{cf} := 33$

Slab edge thickness: $h_e := 0.4m$

Pedestal stickup: $h_{su} := 0.15m$

Slab middle thickness: $h_m := 2.2m$

Pedestal height: $h_p := D + h_{su} - h_m = 0.75\,m$

Height of upper (tapered) portion of base: $h_{tp} := D + h_{su} - h_p - h_e = 1.8\,m$

Footing area: $A_f := 0.25\cdot\pi\cdot B^2$

Pedestal area: $A_p := 0.25\cdot\pi\cdot B_p{}^2$

Volume of tapered portion of footing: $V_{tap} := \frac{1}{3}\left(A_p + \sqrt{A_p\cdot A_f} + A_f\right)\cdot h_{tp}$

Volume of footing: $V_f := A_p\cdot h_p + A_f\cdot h_e + V_{tap} = 301.158\cdot m^3$

Weight of footing: $P_{ftg} := V_f\cdot\gamma_c = 7.077\times 10^3\cdot kN$

Volume of backfill: $V_{soil} := A_f\cdot\left(h_{tp} + h_p - h_{su}\right) - A_p\cdot\left(h_p - h_{su}\right) - V_{tap} = 337.822\cdot m^3$

Weight of backfill: $P_{soil} := V_{soil}\cdot\gamma_b = 5.743\times 10^3\cdot kN$

Total vertical load: $P := P_{wtg} + P_{ftg} + P_{soil} = 1.51\times 10^4\cdot kN$

Computation of Effective Dimensions:

Load eccentricity: $ec := \frac{M_{S1}}{P} = 3.312\,m$

Effective area: $A_{eff} := 2\cdot\left(R_f{}^2\,\text{acos}\left(\frac{ec}{R_f}\right) - ec\cdot\sqrt{R_f{}^2 - ec^2}\right) = 117.28\,m^2$

Major axis dimensions:

$b_e := 2\cdot\left(R_f - ec\right) = 10.375\,m$ $\qquad l_e := 2\cdot R_f\cdot\sqrt{1 - \left(1 - \frac{b_e}{2\cdot R_f}\right)^2} = 15.656\,m$

Effective dimensions: $l_{eff} := \sqrt{A_{eff}\cdot\frac{l_e}{b_e}} = 13.303\,m$ $\qquad b_{eff} := \frac{l_{eff}}{l_e}\cdot b_e = 8.816\,m$

Computation of Static Stiffness:

Static stiffness for deep bedrock:

$$K_{sdb} := \frac{\rho\cdot V_s{}^2\cdot b_{eff}{}^3}{3\cdot(1-\nu)\cdot\left[1 + \left(\frac{\gamma\cdot\rho\cdot V_s{}^2}{\tau_{max}}\right)^{\alpha}\right]}\cdot\left(1 + 4\cdot\frac{D}{b_{eff}}\right)\cdot\left(1 + 0.7\cdot\frac{D}{H_{bd}}\right)\cdot\left(1 + \frac{b_{eff}}{12\cdot H_{bd}}\right)$$

$$K_{sdb} = 40.756 \cdot GN \cdot \frac{m}{rad}$$

Performance function at the means: $G_{ksdb} := K_{sdb} - K_{smin} = 30.756 \cdot GN \cdot \frac{m}{rad}$

Factor of safety: $FS_{ksdb} := \frac{K_{sdb}}{K_{smin}} = 4.076$

Static stiffness for bedrock within zone of influence:

$$K_{ssb} := \frac{\rho \cdot V_s^{\,2} \cdot b_{eff}^{\,3}}{3 \cdot (1 - \nu) \cdot \left[1 + \left(\frac{\gamma \cdot \rho \cdot V_s^{\,2}}{\tau_{max}} \right)^{\alpha} \right]} \cdot \left(1 + 4 \cdot \frac{D}{b_{eff}} \right) \cdot \left(1 + 0.7 \cdot \frac{D}{H_{bs}} \right) \cdot \left(1 + \frac{b_{eff}}{12 \cdot H_{bs}} \right)$$

$$K_{ssb} = 53.762 \cdot GN \cdot \frac{m}{rad}$$

Performance function at the means: $G_{kssb} := K_{ssb} - K_{smin} = 43.762 \cdot GN \cdot \frac{m}{rad}$

Factor of safety: $FS_{kssb} := \frac{K_{ssb}}{K_{smin}} = 5.376$

Drained Bearing Capacity

Effective dimensions are as computed for the static rocking stiffness.

Horizontal load component: $H_c := 660kN$

Effective soil unit weight: $\gamma' := 17.5 \frac{kN}{m^3}$

Effective friction angle: $\phi' := 25deg$

Effective cohesion: $c' := 50kPa$

Total vertical load: $P = 1.51 \times 10^4 \cdot kN$

Effective stress at bearing depth: $q_0 := \gamma' \cdot D = 4.9 \times 10^4 \, Pa$

Bearing Capacity Coefficients (N_c , N_q and N_γ):

$$N_q := e^{\pi \cdot \tan(\phi')} \cdot \frac{1 + \sin(\phi')}{1 - \sin(\phi')} = 10.662 \qquad N_c := \left(N_q - 1 \right) \cdot \cot(\phi') = 20.721$$

$$N_\gamma := \frac{3}{2} \cdot \left(N_q - 1 \right) \cdot \tan(\phi') = 6.758$$

N_c Correction Terms:

$$s_c := 1 + 0.2 \cdot \frac{b_{eff}}{l_{eff}} = 1.133 \qquad d_c := 1 + 0.4 \cdot \frac{D}{b_{eff}} = 1.127$$

$$i_c := \left(1 - \frac{H_c}{P + A_{eff} \cdot c' \cdot \cot(\phi')}\right)^2 = 0.953$$

N_q Correction Terms:

$$s_q := 1 + 0.2 \cdot \frac{b_{eff}}{l_{eff}} = 1.133 \qquad i_q := \left(1 - \frac{H_c}{P + A_{eff} \cdot c' \cdot \cot(\phi')}\right)^2 = 0.953$$

$$d_q := 1 + 1.2 \cdot \frac{D}{b_{eff}} \cdot (1 - \sin(\phi'))^2 \cdot \tan((\phi')) = 1.059$$

N_q Correction Terms:

$$s_\gamma := 1 - 0.4 \cdot \frac{b_{eff}}{l_{eff}} = 0.735 \qquad d_\gamma := 1.0 \qquad i_\gamma := \left(1 - \frac{H_c}{P + A_{eff} \cdot c' \cdot \cot(\phi')}\right)^4 = 0.908$$

Ultimate Bearing Capacity:

$$q_{ult} := c' \cdot N_c \cdot s_c \cdot d_c \cdot i_c + q_0 \cdot N_q \cdot s_q \cdot d_q \cdot i_q + \frac{1}{2} \cdot \gamma' \cdot b_{eff} \cdot N_\gamma \cdot s_\gamma \cdot d_\gamma \cdot i_\gamma = 2.205 \times 10^6 \, Pa$$

Applied Bearing: $q := \frac{P}{A_{eff}} = 1.287 \times 10^5 \, Pa$

Perfomance function mean: $gmean_{bcd} := q_{ult} - q = 2.076 \times 10^6 \, Pa$

Factor of safety: $FS_{drained} := \frac{q_{ult}}{q} = 17.133$

Undrained Bearing Capacity

Undrained shear strength: $s_u := \tau_{max} = 1 \times 10^5\,Pa$

$N_{c0} := 5.14$

$s_{c0} := 1 + 0.2 \cdot \frac{b_{eff}}{l_{eff}} = 1.133$

$i_{c0} := \frac{1}{2} + \frac{1}{2} \cdot \sqrt{1 - \frac{H_c}{A_{eff} \cdot s_u}} = 0.986$

$d_{c0} := 1.0$

$q_{ultu} := s_u \cdot N_{c0} \cdot s_{c0} \cdot d_{c0} \cdot i_{c0} + q_0 = 6.228 \times 10^5\,Pa$

Factor of safety: $FS_{undrained} := \frac{q_{ultu}}{q} = 4.839$

APPENDIX B

MATLAB SOURCE CODE AND OUTPUT

B.1 Medium Variability Case

B.1.1 Source Code

```
%% d-RBD of Gravity-base WTG Foundations
% All limit states in one loop
%
% Possible limit states are:
%   TLT = Tilt
%   DYS = Dynamic stiffness
%   STS = Static stiffness
%   DBC = Drained bearing capacity
%   UBC = Undrained bearing capacity
%
% Possibe distributions
%      NR = Normal
%      LN = Lognormal
%      TH = Tanh (bounded)
%      DT = Deterministic
% NOTES:
% 1. Always use consistent units: kg, m, s, N, Pa, J
% 2. Do not use NR PDF for any variable with COV>0.25 as the PDF will
%    likely produce meaningless negative numbers.
% 3. To study parameter rankings, run program from one combination of
%    design decision parameters.
% 4. The number of realizations can be adjusted by adjusting the COV on the
%    probability of failure. A COV of 0.3 or 0.4 could be used for
%    preliminary runs. For final runs, the COV should 0.1 or less.
%
clear all;                          % Clear all
fileID = fopen('dRBD_MV.txt','w');   % Change output file name, if desired.
fprintf(fileID,'%-73s\r\n', ...
  '~~~~~~~~~~~~~~~~~~~~~~~~~~~~~~~~~~~~~~~~~~~~~~~~~~~~~~~~~~~~~~~~~~~~~~~~~~~~');
fprintf(fileID,'%-73s\r\n', ...
  '---------------------- Details of dRBD Run Results ========--------------');
fprintf(fileID,'%-73s\r\n', ...
  '~~~~~~~~~~~~~~~~~~~~~~~~~~~~~~~~~~~~~~~~~~~~~~~~~~~~~~~~~~~~~~~~~~~~~~~~~~~~');
fprintf(fileID,'\r\n%73s\r\n', ...
  '                                                                         ');
fprintf(fileID,'%-73s\r\n', ...
  'This output file contains details of the d-RBD run and its results.      ');
fprintf(fileID,'%-73s\r\n', ...
  'All input is embedded into the MATLAB program and is echoed here for     ');
fprintf(fileID,'%-73s\r\n', ...
  'record, verification and documentation.');
fprintf(fileID,'%-73s\r\n\r\n', ...
  'All quantities are in consistent units: kg, m, s, N, Pa, J');


%% Main simulation parameters
Title="Medium Variability Case";     % Descriptive design case title
PLS=["TLT" "DYS" "STS" "DBC" "UBC"]; % Possible limit states
LSO=[    1     1     1     1     1]; % 1=verify, 0=do not verify
LST=[    1     1     1     2     2]; % Limit state type: 1=SLS,2=ULS,3-FLS
nrvmax=10;              % Maximum number of random variables in any limit state
```

```
B=15:1:20;              % Foundation diameter(s)
D=2.8:0.1:3.1;          % Foundation depth(s)
btsls=1.7;              % Target reliabilty index for SLS
btuls=3.3;              % Target reliability index for ULS
pfCOV=0.15;             % Desired COV of probability of failure
%% Computation of some prelimnary parameters
nls=nnz(LSO);           % Number of limit states in this run
nb=length(B);           % Number of foundation diameters
nd=length(D);           % Number of foundation depths
LS=strings(nls,1);LT=zeros(nls,1);YN=strings(nls,nb,nd);eg=zeros(nls,nb,nd);
nbdt=zeros(nb,nd);Xmuf=zeros(nls,nb,nd,nrvmax);
Voptls=zeros(nls,1);bols=zeros(nls,1);dols=zeros(nls,1);

nf=zeros(nls,nb,nd);pf=zeros(nls,nb,nd);ri=zeros(nls,nb,nd);
jp=0;
for ip=1:length(PLS)
  if LSO(ip)==1
    jp=jp+1;
    LS(jp,1)=PLS(ip);
    LT(jp)=LST(ip);
  end
end
% Compute tagert probabilities of failures (for SLS and ULS)
if btsls<2.6
  pftsls=1.2*exp(-2.06*btsls);
elseif (btsls>=2.6)&&(btsls<=4.8)
  pftsls=196*exp(-4.0*btsls);
else
  pftsls=1000000*exp(-5.8*btsls);
end
if btuls<2.6
  pftuls=1.2*exp(-2.06*btuls);
elseif (btuls>=2.6)&&(btuls<=4.8)
  pftuls=196*exp(-4.0*btuls);
else
  pftuls=1000000*exp(-5.8*btuls);
end
pftsls
pftuls
nr1=10*nb*nd/pftsls;             % Minimum number of realizations - Estimate 1
nr2=(1/pftsls-1)*nb*nd/pfCOV^2;  % Minimum number of realizations - Estimate 2
nrsls=round(max([nr1 nr2]));     % Number of realizations - SLS
nr1=10*nb*nd/pftuls;             % Minimum number of realizations - Estimate 1
nr2=(1/pftuls-1)*nb*nd/pfCOV^2;  % Minimum number of realizations - Estimate 2
nruls=round(max([nr1 nr2]));     % Number of realizations - ULS
nrmax=max(nruls,nrsls)
%nrmax=2000;
nrsls=nrmax;nruls=nrmax;ptot=zeros(nrmax,1);r=zeros(nrmax,1);
g=zeros(nls,nrmax);aeff=zeros(nls,nrmax);ecc=zeros(nls,nrmax);
%% Print results to output text file
fprintf(fileID,'%40s %-40s\r\n','Design case title.....................:', ...
  Title);
fprintf(fileID,'%40s %7.2f\r\n','Target reliabilty index for SLS........:', ...
  btsls);
fprintf(fileID,'%40s %7.4f\r\n','Target probability of failure for SLS..:', ...
  pftsls);
fprintf(fileID,'%40s %7.2f\r\n','Target reliabilty index for ULS........:', ...
  btuls);
fprintf(fileID,'%40s %7.5f\r\n','Target probability of failure for ULS..:', ...
  pftuls);
fprintf(fileID,'%40s %s\r\n','Foundation diameters...................:', ...
  sprintf('%5.1f ', B));
fprintf(fileID,'%40s %s\r\n','Foundation depths.....................:', ...
```

```
  sprintf('%5.1f ', D));
fprintf(fileID,'%40s %7i\r\n','Number of realizations all combinations:', ...
  nrmax);
fprintf(fileID,'%40s %7i\r\n','Number of design decision combinations.:', ...
  nb*nd);
fprintf(fileID,'%40s %7i\r\n','Number of realizations per combination.:', ...
  round(nrmax/(nb*nd)));

%% Fixed dimensions, other deterministic parameters & derived quantities
%
% Fixed dimensions and parameters
%
he=0.4;               % Base edge height
hm=2.2;               % Base middle height
hsu=0.15;             % Pedestal stickup
bp=5.4;               % Pedestal diameter
bb=5.4;               % Base top diameter
gconc=23500;          % Unit weight of concrete
gbsoil=17000;         % Unit weight of backfill soil
Pwtg=2.275e6;         % Weight of WTG
%
% Derived quantities
%
hp=zeros(nd,1);Af=zeros(nb,1);Vb1=zeros(nb,1);Vb2=zeros(nb,1);Vp=zeros(nd,1);
Vf=zeros(nb,nd);htp=zeros(nd);Vsoil=zeros(nb,nd);Pc=zeros(nb,nd);
Ps=zeros(nb,nd);Ptot=zeros(nb,nd);
ncomb=zeros(nb,nd);beta=zeros(nb,nd);
Ap=0.25*pi*bp^2;                          % Pedestal area
Ab=0.25*pi*bb^2;                          % Base top area
for ib=1:nb
  for id=1:nd
    hp(id)=D(id)+hsu-hm;                  % Pedestal height
    Af(ib)=0.25*pi*B(ib)^2;               % Footing area
    Vb1(ib)=Af(ib)*he;                    % Volume of lower portion of base
    Vb2(ib)=(Ab+(Ab*Af(ib))^0.5+ ...      % Volume of tapered portion of base
    Af(ib))*(hm-he)/3;
    Vp(id)=Ap*hp(id);                     % Pedestal volume
    Vf(ib,id)=Vb1(ib)+Vb2(ib)+Vp(id);     % Foundation volume
    htp(id)=D(id)+hsu-hp(id)-he;          % Height of tapered portion of footing
    Vsoil(ib,id)=Af(ib)*(htp(id)+ ...
    hp(id)-hsu)-Ap*(hp(id)-hsu)-Vb2(ib);  % Volume of backfill soil
    Pc(ib,id)=Vf(ib,id)*gconc;            % Weight of foundation concrete
    Ps(ib,id)=Vsoil(ib,id)*gbsoil;        % Weight of backfill soil
    Ptot(ib,id)=Pwtg+Pc(ib,id)+Ps(ib,id); % Total vertical load
  end
end
fprintf(fileID,'\r\n %-45s\r\n','Fixed quantities & Foundation Dimensions:');
fprintf(fileID,'%-35s %8.2f\r\n','Pedestal diameter.................:',bp);
fprintf(fileID,'%-35s %8.2f\r\n','Base top diameter.................:',bb);
fprintf(fileID,'%-35s %8.2f\r\n','Pedestal stick-up.................:',hsu);
fprintf(fileID,'%-35s %8.2f\r\n','Base middle thickness.............:',hm);
fprintf(fileID,'%-35s %8.2f\r\n','Base edge thickness...............:',he);
fprintf(fileID,'%-35s %8.1f\r\n','Concrete unit weight..............:',gconc);
fprintf(fileID,'%-35s %8.1f\r\n','Backfill soil unit weight.........:',gbsoil);
fprintf(fileID,'%-35s %5.2e\r\n','Self weight of WTG................:',Pwtg);
fprintf(fileID,'\r\n %-22s\r\n\r\n', ...
  'Foundation Volumes for all B-D Combinations:');
fprintf(fileID,'%-40s\r\n','        Foundation Diameter');
fprintf(fileID,'%6s %s\r\n\r\n',' Depth',sprintf('%7.2f ', B));
for id=1:nd
  fprintf(fileID,'%6.2f %s\r\n',D(id), ...
    sprintf('%7.2f ',Vf(:,id)));
end
```

```
fprintf(fileID,'\r\n');

%% Plot possible foundation geometries
color=["r" "g" "b" "m" "c" "k"];
figure('name', 'Foundation Geometries');
 for ib=1:nb
    for id=1:nd
     clr=color(randi(6));
     xf=[-B(ib)/2 -B(ib)/2 -bb/2 -bp/2 ...
       -bp/2 bp/2 bp/2 bb/2 0.5*B(ib) B(ib)/2 -B(ib)/2];
     yf=[0 he hm hm hm+hp(id) hm+hp(id) hm hm he 0 0];
     xgl=[-B(ib)/2 -bp/2];
     xgr=[bp/2 B(ib)/2];
     yg=[D(id) D(id)];
     plot(xf,yf)
     daspect([1 1 1])
     hold on
     plot(xgl,yg,clr)
     plot(xgr,yg,clr)
    end
 end
set(gca,'xlim',[-B(nb)/2-B(nb)/10 B(nb)/2+B(nb)/10])
set(gca,'ylim',[-0.2*D(nd) 1.2*D(nd)])
hold off

% Generate design decision variable values (uniform distribution)
b=B(randi(nb,nrmax,1));
d=D(randi(nd,nrmax,1));
for ir=1:nrmax
    r(ir)=0.5*b(ir);
    for ib=1:nb
      for id=1:nd
        if (b(ir)==B(ib))&&(d(ir)==D(id))
          nbdt(ib,id)=nbdt(ib,id)+1;
          ptot(ir)=Ptot(ib,id);
        end
      end
    end
end
%
% Loop on selected limit states
for ils=1:nls

%% Tilt limit state
  if LS(ils)=="TLT"
    tiltmax=0.17; tiltmaxr=tiltmax*pi/180.;       % Maximum allowed tilt
    etilt=zeros(nb,nd);
    % Random Variables
    %
    RV   = ["Mmnt"   "Dens"   "prat" "  Vs"   "sstn"   "tmax" "alpha"  "Itha"];
    Xdis = [  "LN"     "NR"     "NR"   "LN"     "LN"     "LN"    "LN"    "LN"];
    Xmu  = [2.0e+7   1750.0     0.35  200.0   0.0005   1.0e+5     0.9    4.16];
    Xcov = [  0.20     0.05     0.05    0.4     0.20     0.25     0.1    0.05];
    Xmin = [   0.0      0.0     0.25    0.0      0.0      0.0     0.0     0.0];
    Xmax = [   0.0      0.0     0.45    0.0      0.0      0.0     0.0     0.0];
    % Size arrays
    nrv=length(RV);L=zeros(nrv,nrv);cmut=zeros(nrv,nrv);cm=zeros(nrv,nrv);
    Z=zeros(nrv,1);RVS=strings(nrv,1);Xsig=zeros(nrv,1);p=zeros(nrv);
    q=zeros(nrv);
    %
    fprintf(fileID,'\r\n %-45s\r\n','Tilt Limit State:');
    fprintf(fileID,'%-35s %7.2f\r\n','Maximum allowed tilt (degrees)...:', ...
      tiltmax);
```

```
fprintf(fileID,'\r\n %-12s %s\r\n','Variable',sprintf(' %8s  ', RV));
fprintf(fileID,'%-12s %s\r\n','Distribution',sprintf(' %8s  ', Xdis));
fprintf(fileID,'%-12s %s\r\n','Mean Value',sprintf(' %5.2e  ', Xmu));
fprintf(fileID,'%-12s %s\r\n','COV',sprintf(' %8.2f  ', Xcov));
fprintf(fileID,'\r\n');
% Parameters of underlying normal PDF's
for irv=1:nrv
 Xsig(irv)=Xmu(irv)*Xcov(irv);
 if Xdis(irv)=="LN"
   q(irv)=sqrt(log(1+Xcov(irv)^2));
   p(irv)=log(Xmu(irv))-0.5*q(irv)^2;
 elseif Xdis(irv)=="TH"
   p(irv)=2.*pi/(0.46^2*(Xmax(irv)-Xmin(irv)^2-Xsig(irv)^2))^0.5;
   q(irv)=0;
 end
end
% Tilt value at the means
M      = Xmu(1);
den    = Xmu(2);
pr     = Xmu(3);
Vs     = Xmu(4);
ss     = Xmu(5);
tmax   = Xmu(6);
alpha  = Xmu(7);
itheta = Xmu(8);
for ib=1:nb
  for id=1:nd
    etilt(ib,id)  = atan(M*(1-pr)*(1+(ss*den*Vs^2/tmax)^alpha)* ...
      itheta/(2*den*Vs^2*B(ib)^3))*180./pi;
    eg(ils,ib,id) = tan(tiltmaxr)-M*(1-pr)*(1+(ss*den*Vs^2/tmax)^alpha)* ...
      itheta/(2*den*Vs^2*B(ib)^3);
  end
end
%    etilt
%    eg(ils,:,:)
%
% Define cross-correlation matrix [nrv x nrv]
icopt="No";
% For simplicity, enter upper triangular only
% Ignore the cross correlation matrix if icopt="No"
cmut=[1.0 0.0 0.0 0.0 0.0 0.0 0.0 0.0;
      0.0 1.0 0.0 0.0 0.0 0.0 0.0 0.0;
      0.0 0.0 1.0 0.0 0.0 0.0 0.0 0.0;
      0.0 0.0 0.0 1.0 0.0 0.0 0.0 0.0;
      0.0 0.0 0.0 0.0 1.0 0.0 0.0 0.0;
      0.0 0.0 0.0 0.0 0.0 1.0 0.0 0.0;
      0.0 0.0 0.0 0.0 0.0 0.0 1.0 0.0;
      0.0 0.0 0.0 0.0 0.0 0.0 0.0 1.0];
cm=cmut+transpose(cmut)-eye(nrv);
L = chol(cm,'lower');

% Generate standard normal variable values & apply cross-correlation
% (if applicable) & scale back up to appropriate PDF
crvsn=zeros(nrmax,nrv);crv=zeros(nrmax,nrv);
rvsn=normrnd(0,1,nrmax,nrv);
for ir=1:nrmax
  if icopt=="Yes"
    crvsn(ir,:)=transpose(rvsn(ir,:)*transpose(L));
  else
    crvsn(ir,:)=rvsn(ir,:);
  end
  % Scale back up to appropriate PDF
  for irv=1:nrv
```

```
      if Xdis(irv)=="NR"
        crv(ir,irv)=Xsig(irv)*crvsn(ir,irv)+Xmu(irv);
      elseif Xdis(irv)=="LN"
        crv(ir,irv)=exp(q(irv)*crvsn(ir,irv)+p(irv));
      elseif Xdis(irv)=="TH"
        x=p(irv)*1/(2*pi);     %Fix this. It needs to be G variate
        crv(ir,irv)=Xmin(irv)+0.5*(Xmax(irv)-Xmin(irv))*(1+tanh(x));
      end
    end
  end
%
%   Loop on realizations
%
  for ir=1:nrmax
    % Apply cross-correlations
    % Evaluate Performance function for each realizations, ir
    M        = crv(ir,1);
    den      = crv(ir,2);
    pr       = crv(ir,3);
    Vs       = crv(ir,4);
    ss       = crv(ir,5);
    tmax     = crv(ir,6);
    alpha    = crv(ir,7);
    itheta   = crv(ir,8);

    g(ils,ir)   = tan(tiltmaxr)-M*(1-pr)*(1+(ss*den*Vs^2/tmax)^alpha)* ...
                  itheta/(2*den*Vs^2*b(ir)^3);
    for ib=1:nb
      for id=1:nd
        if (b(ir)==B(ib))&&(d(ir)==D(id))&&(g(ils,ir)<=0)
          nf(ils,ib,id)=nf(ils,ib,id)+1;
          for irv=1:nrv
            Xmuf(ils,ib,id,irv)=Xmuf(ils,ib,id,irv)+crv(ir,irv);
          end
        end
      end
    end
  end
%
% Parameter ranking
%
  if nb*nd==1
    for ib=1:nb
      for id=1:nd
        for irv=1:nrv
          Xmuf(ils,ib,id,irv)=Xmuf(ils,ib,id,irv)/nf(ils,ib,id);
          Z(irv)=abs(Xmu(irv)-Xmuf(ils,ib,id,irv))/(Xsig(irv)/ ...
            sqrt(nf(ils,ib,id)));
        end
        [ZS,IS]=sort(Z);
        NZS=ZS/norm(Z);
        for irv=1:nrv;RVS(irv)=RV(IS(irv));end
      end
    end
    RVS
    NZS
  end
%% Dynamic stiffness limit state
 elseif LS(ils)=="DYS"
  Kdynmin=5e10;               % Minimum stiffness (Nm/rad)
  eKdyn=zeros(nb,nd);
  %
  % Random Variables
```

```
%
RV   = [ "Dens"    "Prat"    "  Vs" "Hbed"];
Xdis = [   "NR"      "NR"     "LN"   "LN"];
Xmu  = [ 1750.0      0.35    200.0    8.5];
Xcov = [   0.05      0.05     0.40   0.30];
Xmin = [    0.0       0.0      0.0    0.0];
Xmax = [    0.0       0.0      0.0    0.0];
% Size arrays
nrv=length(RV);L=zeros(nrv,nrv);cmut=zeros(nrv,nrv);cm=zeros(nrv,nrv);
Z=zeros(nrv,1);RVS=strings(nrv,1);Xsig=zeros(nrv,1);p=zeros(nrv);
q=zeros(nrv);
%
fprintf(fileID,'\r\n %-45s\r\n','Dynamic Stiffness Limit State:');
fprintf(fileID,'%-35s %7.2e\r\n','Minimum required stiffness........:', ...
  Kdynmin);
fprintf(fileID,'\r\n %-12s %s\r\n','Variable',sprintf(' %8s  ', RV));
fprintf(fileID,'%-12s %s\r\n','Distribution',sprintf(' %8s  ', Xdis));
fprintf(fileID,'%-12s %s\r\n','Mean Value',sprintf(' %5.2e  ', Xmu));
fprintf(fileID,'%-12s %s\r\n','COV',sprintf(' %8.2f  ', Xcov));
fprintf(fileID,'\r\n');

% Parameters of underlying normal PDF's
for irv=1:nrv
 Xsig(irv)=Xmu(irv)*Xcov(irv);
 if Xdis(irv)=="LN"
   q(irv)=sqrt(log(1+Xcov(irv)^2));
   p(irv)=log(Xmu(irv))-0.5*q(irv)^2;
 elseif Xdis(irv)=="TH"
   p(irv)=2.*pi/(0.46^2*(Xmax(irv)-Xmin(irv)^2-Xsig(irv)^2))^0.5;
   q(irv)=0;
 end
end
% Tilt value at the means
den    = Xmu(1);
pr     = Xmu(2);
Vs     = Xmu(3);
Hb     = Xmu(4);
for ib=1:nb
  for id=1:nd
    R=0.5*B(ib);
    eKdyn(ib,id)=8.*den*Vs^2*R^3*(1+2*D(id)/R)* ...
      (1+0.7*D(id)/Hb)*(1+R/(6*Hb))/(3*(1-pr));
    eg(ils,ib,id)  = eKdyn(ib,id)-Kdynmin;
  end
end
%   eKdyn
%   eg(ils,:,:)
%
% Define cross-correlation matrix [nrv x nrv]
icopt="No";
% For simplicity, enter upper triangular only
% Ignore the cross correlation matrix if icopt="No"
cmut=[1.0 0.0 0.0 0.0;
      0.0 1.0 0.0 0.0;
      0.0 0.0 1.0 0.0;
      0.0 0.0 0.0 1.0];
cm=cmut+transpose(cmut)-eye(nrv);
L = chol(cm,'lower');

% Generate standard normal variable values & apply cross-correlation
% (if applicable) & scale back up to appropriate PDF
crvsn=zeros(nrmax,nrv);crv=zeros(nrmax,nrv);
rvsn=normrnd(0,1,nrmax,nrv);
```

```
    for ir=1:nrmax
      if icopt=="Yes"
        crvsn(ir,:)=transpose(rvsn(ir,:)*transpose(L));
      else
        crvsn(ir,:)=rvsn(ir,:);
      end
      % Scale back up to appropriate PDF
      for irv=1:nrv
        if Xdis(irv)=="NR"
          crv(ir,irv)=Xsig(irv)*crvsn(ir,irv)+Xmu(irv);
        elseif Xdis(irv)=="LN"
          crv(ir,irv)=exp(q(irv)*crvsn(ir,irv)+p(irv));
        elseif Xdis(irv)=="TH"
          x=p(irv)*1/(2*pi);     %Fix this. It needs to be G variate
          crv(ir,irv)=Xmin(irv)+0.5*(Xmax(irv)-Xmin(irv))*(1+tanh(x));
        end
      end
    end
%
%   Loop on realizations
%
    for ir=1:nrmax
      % Apply cross-correlations
      % Evaluate Performance function for each realizations, ir
      den      = crv(ir,1);
      pr       = crv(ir,2);
      Vs       = crv(ir,3);
      Hb       = crv(ir,4);
      R=0.5*b(ir);
      g(ils,ir)   = 8.0*den*Vs^2*R^3*(1+2*d(ir)/R)* ...
                 (1+0.7*d(ir)/Hb)*(1+R/(6*Hb))/(3*(1-pr))-Kdynmin;
      for ib=1:nb
        for id=1:nd
          if (b(ir)==B(ib))&&(d(ir)==D(id))&&(g(ils,ir)<=0)
            nf(ils,ib,id)=nf(ils,ib,id)+1;
            for irv=1:nrv
              Xmuf(ils,ib,id,irv)=Xmuf(ils,ib,id,irv)+crv(ir,irv);
            end
          end
        end
      end
    end
%
% Parameter ranking
%
    if nb*nd==1
      for ib=1:nb
        for id=1:nd
          for irv=1:nrv
            Xmuf(ils,ib,id,irv)=Xmuf(ils,ib,id,irv)/nf(ils,ib,id);
            Z(irv)=abs(Xmu(irv)-Xmuf(ils,ib,id,irv))/(Xsig(irv)/ ...
              sqrt(nf(ils,ib,id)));
          end
          [ZS,IS]=sort(Z);
          NZS=ZS/norm(Z);
          for irv=1:nrv;RVS(irv)=RV(IS(irv));end
        end
      end
      RVS
      NZS
    end
%% Static stiffness limit state
   elseif LS(ils)=="STS"
```

```
    Kstamin=1e10;         % Minimum stiffness (Nm/rad)
    eKsta=zeros(nb,nd);
    %
    % Random Variables
    %
    RV   = ["Momt"  "Dens"  "  Vs" "Tmax" "sstn" "Alfa" "Hbed" "Prat"];
    Xdis = [  "LN"    "NR"    "LN"   "LN"   "LN"   "NR"   "LN"   "NR"];
    Xmu  = [  5.0e7 1750.0   200.0  1.0e5  5.e-4   0.90    8.5   0.35];
    Xcov = [   0.20   0.05    0.40   0.25    0.2   0.10   0.30   0.05];
    Xmin = [    0.0    0.0     0.0    0.0    0.0    0.0    0.0    0.0];
    Xmax = [    0.0    0.0     0.0    0.0    0.0    0.0    0.0    0.0];
    % Size arrays
    nrv=length(RV);L=zeros(nrv,nrv);cmut=zeros(nrv,nrv);cm=zeros(nrv,nrv);
    Z=zeros(nrv,1);RVS=strings(nrv,1);Xsig=zeros(nrv,1);p=zeros(nrv);
    q=zeros(nrv);
    %
    fprintf(fileID,'\r\n %-45s\r\n','Static Stiffness Limit State:');
    fprintf(fileID,'%-35s %7.2e\r\n','Minimum required stiffness.........:', ...
      Kstamin);
    fprintf(fileID,'\r\n %-12s %s\r\n','Variable',sprintf(' %8s  ', RV));
    fprintf(fileID,'%-12s %s\r\n','Distribution',sprintf(' %8s  ', Xdis));
    fprintf(fileID,'%-12s %s\r\n','Mean Value',sprintf(' %5.2e  ', Xmu));
    fprintf(fileID,'%-12s %s\r\n','COV',sprintf(' %8.2f  ', Xcov));
    fprintf(fileID,'\r\n');

    % Parameters of underlying normal PDF's
    for irv=1:nrv
     Xsig(irv)=Xmu(irv)*Xcov(irv);
     if Xdis(irv)=="LN"
       q(irv)=sqrt(log(1+Xcov(irv)^2));
       p(irv)=log(Xmu(irv))-0.5*q(irv)^2;
     elseif Xdis(irv)=="TH"
       p(irv)=2.*pi/(0.46^2*(Xmax(irv)-Xmin(irv)^2-Xsig(irv)^2))^0.5;
       q(irv)=0;
     end
    end
    % Static stiffness values at the means
    M     = Xmu(1);
    den   = Xmu(2);
    Vs    = Xmu(3);
    Tmax  = Xmu(4);
    sstrn = Xmu(5);
    alfa  = Xmu(6);
    Hb    = Xmu(7);
    pr    = Xmu(8);
    for ib=1:nb
      for id=1:nd
        R=0.5*B(ib);
        ec=M/Ptot(ib,id);
        Aeff=2*(R^2*acos(min(1,ec/R))-ec*sqrt(R^2-ec^2));
        be=2*(R-ec);
        le=2*R*sqrt(1-(1-be/(2*R))^2);
        leff=sqrt(Aeff*le/be);
        beff=leff*be/le;
        eKsta(ib,id)=den*Vs^2*beff^3*(1+4*D(id)/beff)*(1+0.7*D(id)/Hb)* ...
          (1+beff/12/Hb)/(3*(1-pr)*(1+(sstrn*den*Vs^2/Tmax)^alfa));
        eg(ils,ib,id)=eKsta(ib,id)-Kstamin;
      end
    end
%    eKsta
%    eg(ils,:,:)
    %
    % Define cross-correlation matrix [nrv x nrv]
```

```
    icopt="No";
    % For simplicity, enter upper triangular only
    % Ignore the cross correlation matrix if icopt="No"
    cmut=[1.0 0.0 0.0 0.0 0.0 0.0 0.0 0.0;
          0.0 1.0 0.0 0.0 0.0 0.0 0.0 0.0;
          0.0 0.0 1.0 0.0 0.0 0.0 0.0 0.0;
          0.0 0.0 0.0 1.0 0.0 0.0 0.0 0.0;
          0.0 0.0 0.0 0.0 1.0 0.0 0.0 0.0;
          0.0 0.0 0.0 0.0 0.0 1.0 0.0 0.0;
          0.0 0.0 0.0 0.0 0.0 0.0 1.0 0.0;
          0.0 0.0 0.0 0.0 0.0 0.0 0.0 1.0];
    cm=cmut+transpose(cmut)-eye(nrv);
    L = chol(cm,'lower');

    % Generate standard normal variable values & apply cross-correlation
    % (if applicable) & scale back up to appropriate PDF
    crvsn=zeros(nrmax,nrv);crv=zeros(nrmax,nrv);
    rvsn=normrnd(0,1,nrmax,nrv);
    for ir=1:nrmax
      if icopt=="Yes"
        crvsn(ir,:)=transpose(rvsn(ir,:)*transpose(L));
      else
        crvsn(ir,:)=rvsn(ir,:);
      end
      % Scale back up to appropriate PDF
      for irv=1:nrv
        if Xdis(irv)=="NR"
          crv(ir,irv)=Xsig(irv)*crvsn(ir,irv)+Xmu(irv);
        elseif Xdis(irv)=="LN"
          crv(ir,irv)=exp(q(irv)*crvsn(ir,irv)+p(irv));
        elseif Xdis(irv)=="TH"
          x=p(irv)*1/(2*pi);     %Fix this. It needs to be G variate
          crv(ir,irv)=Xmin(irv)+0.5*(Xmax(irv)-Xmin(irv))*(1+tanh(x));
        end
      end
    end
%
%   Loop on realizations
%
    for ir=1:nrmax
      % Apply cross-correlations
      % Evaluate Performance function for each realizations, ir
        M     = crv(ir,1);
        den   = crv(ir,2);
        Vs    = crv(ir,3);
        Tmax  = crv(ir,4);
        sstrn = crv(ir,5);
        alfa  = crv(ir,6);
        Hb    = crv(ir,7);
        pr    = crv(ir,8);
        R     = r(ir);
        ecc(ils,ir)=min(M/ptot(ir),0.9*R);
        EC=ecc(ils,ir);
        aeff(ils,ir)=2*(R^2*acos(min(1,EC/R))-EC*sqrt(R^2-EC^2));
        be=2*(R-EC);
        le=2*R*sqrt(1-(1-be/(2*R))^2);
        leff=sqrt(aeff(ils,ir)*le/be);
        beff=leff*be/le;
        g(ils,ir)=den*Vs^2*beff^3*(1+4*d(ir)/beff)*(1+0.7*d(ir)/Hb)* ...
          (1+beff/12/Hb)/(3*(1-pr)*(1+(sstrn*den*Vs^2/Tmax)^alfa))-Kstamin;
      for ib=1:nb
        for id=1:nd
          if (b(ir)==B(ib))&&(d(ir)==D(id))&&(g(ils,ir)<=0)
```

```
            nf(ils,ib,id)=nf(ils,ib,id)+1;
            for irv=1:nrv
              Xmuf(ils,ib,id,irv)=Xmuf(ils,ib,id,irv)+crv(ir,irv);
            end
          end
        end
      end
    end
%
% Parameter ranking
%
    if nb*nd==1
      for ib=1:nb
        for id=1:nd
          for irv=1:nrv
            Xmuf(ils,ib,id,irv)=Xmuf(ils,ib,id,irv)/nf(ils,ib,id);
            Z(irv)=abs(Xmu(irv)-Xmuf(ils,ib,id,irv))/(Xsig(irv)/sqrt(nf(ils,ib,id)));
          end
          [ZS,IS]=sort(Z);
          NZS=ZS/norm(Z);
          for irv=1:nrv;RVS(irv)=RV(IS(irv));end
        end
      end
      RVS
      NZS
    end

%% Drained bearing capacity limit state
   elseif LS(ils)=="DBC"
    %
    % Random Variables
    %
    RV =   ["Momt"  "Horz"  "eDen"  "ePhi"         "eCoh"];
    Xdis = [  "LN"    "LN"    "NR"    "LN"           "LN"];
    Xmu  = [  5.0e7  6.6e5  17500.    25.0*pi/180.  5.0e4];
    Xcov = [   0.20   0.20    0.05    0.30           0.20];
    Xmin = [    0.0    0.0     0.0     0.0            0.0];
    Xmax = [    0.0    0.0     0.0     0.0            0.0];
    % Size arrays
    nrv=length(RV);L=zeros(nrv,nrv);cmut=zeros(nrv,nrv);cm=zeros(nrv,nrv);
    Z=zeros(nrv,1);RVS=strings(nrv,1);Xsig=zeros(nrv,1);p=zeros(nrv);
    q=zeros(nrv);
    %
    fprintf(fileID,'\r\n %-45s\r\n','Drained Bearing Capacity Limit State:');
    fprintf(fileID,'%-12s %s\r\n','Variable',sprintf(' %8s  ', RV));
    fprintf(fileID,'%-12s %s\r\n','Distribution',sprintf(' %8s  ', Xdis));
    fprintf(fileID,'%-12s %s\r\n','Mean Value',sprintf(' %5.2e  ', Xmu));
    fprintf(fileID,'%-12s %s\r\n','COV',sprintf(' %8.2f  ', Xcov));
    fprintf(fileID,'\r\n');

    % Parameters of underlying normal PDF's
    for irv=1:nrv
     Xsig(irv)=Xmu(irv)*Xcov(irv);
     if Xdis(irv)=="LN"
       q(irv)=sqrt(log(1+Xcov(irv)^2));
       p(irv)=log(Xmu(irv))-0.5*q(irv)^2;
     elseif Xdis(irv)=="TH"
       p(irv)=2.*pi/(0.46^2*(Xmax(irv)-Xmin(irv)^2-Xsig(irv)^2))^0.5;
       q(irv)=0;
     end
    end
    % Static stiffness values at the means
    M    = Xmu(1);
```

```
    H    = Xmu(2);
    eDen = Xmu(3);
    ePhi = Xmu(4);
    eCoh = Xmu(5);
    for ib=1:nb
      for id=1:nd
        R=0.5*B(ib);
        ec=M/Ptot(ib,id);
        Aeff=2*(R^2*acos(min(1,ec/R))-ec*sqrt(R^2-ec^2));
        be=2*(R-ec);
        le=2*R*sqrt(1-(1-be/(2*R))^2);
        leff=sqrt(Aeff*le/be);
        beff=leff*be/le;
        nq=exp(pi*tan(ePhi))*(1+sin(ePhi))/(1-sin(ePhi));
        nc=(nq-1)*cot(ePhi);
        ng=1.5*(nq-1)*tan(ePhi);
        sc=1+0.2*beff/leff;
        dc=1+0.4*D(id)/beff;
        ic=(1-H/(Ptot(ib,id)+Aeff*eCoh*cot(ePhi)))^2;
        sq=1+0.2*beff/leff;
        dq=1+1.2*(D(id)/beff)*tan(ePhi)*(1.-sin(ePhi))^2;
        iq=ic;
        sg=1-0.4*beff/leff;
        dg=1.0;
        ig=ic^2;
        eg(ils,ib,id)=eCoh*nc*sc*dc*ic+eDen*D(id)*nq*sq*dq*iq+ ...
          0.5*eDen*beff*ng*sg*dg*ig-Ptot(ib,id)/Aeff;
      end
    end
%    eg(ils,:,:)
    %
    % Define cross-correlation matrix [nrv x nrv]
    icopt="No";
    % For simplicity, enter upper triangular only
    % Ignore the cross correlation matrix if icopt="No"
    cmut=[1.0 0.0 0.0 0.0 0.0;
          0.0 1.0 0.0 0.0 0.0;
          0.0 0.0 1.0 0.0 0.0;
          0.0 0.0 0.0 1.0 0.0;
          0.0 0.0 0.0 0.0 1.0];
    cm=cmut+transpose(cmut)-eye(nrv);
    L = chol(cm,'lower');

    % Generate standard normal variable values & apply cross-correlation
    % (if applicable) & scale back up to appropriate PDF
    crvsn=zeros(nrmax,nrv);crv=zeros(nrmax,nrv);
    rvsn=normrnd(0,1,nrmax,nrv);
    for ir=1:nrmax
      if icopt=="Yes"
        crvsn(ir,:)=transpose(rvsn(ir,:)*transpose(L));
      else
        crvsn(ir,:)=rvsn(ir,:);
      end
      % Scale back up to appropriate PDF
      for irv=1:nrv
        if Xdis(irv)=="NR"
          crv(ir,irv)=Xsig(irv)*crvsn(ir,irv)+Xmu(irv);
        elseif Xdis(irv)=="LN"
          crv(ir,irv)=exp(q(irv)*crvsn(ir,irv)+p(irv));
        elseif Xdis(irv)=="TH"
          x=p(irv)*1/(2*pi);     %Fix this. It needs to be G variate
          crv(ir,irv)=Xmin(irv)+0.5*(Xmax(irv)-Xmin(irv))*(1+tanh(x));
        end
```

```
      end
    end
%
%   Loop on realizations
%
    for ir=1:nrmax
      % Apply cross-correlations
      % Evaluate Performance function for each realizations, ir
      M    = crv(ir,1);
      H    = crv(ir,2);
      eDen = crv(ir,3);
      ePhi = crv(ir,4);
      eCoh = crv(ir,5);
      R=r(ir);
      ecc(ils,ir)=min(M/ptot(ir),0.9*R);
      EC=ecc(ils,ir);
      aeff(ils,ir)=2*(R^2*acos(min(1,EC/R))-EC*sqrt(max(0,R^2-EC^2)));
      be=2*(R-EC);
      le=2*R*sqrt(1-(1-be/(2*R))^2);
      leff=sqrt(aeff(ils,ir)*le/be);
      beff=leff*be/le;

      nq=exp(pi*tan(ePhi))*(1+sin(ePhi))/(1-sin(ePhi));
      nc=(nq-1)*cot(ePhi);
      ng=1.5*(nq-1)*tan(ePhi);
      sc=1+0.2*beff/leff;
      dc=1+0.4*D(id)/beff;
      ic=(1-H/(ptot(ir)+aeff(ils,ir)*eCoh*cot(ePhi)))^2;
      sq=1+0.2*beff/leff;
      dq=1+1.2*(d(ir)/beff)*tan(ePhi)*(1.-sin(ePhi))^2;
      iq=ic;
      sg=1-0.4*beff/leff;
      dg=1.0;
      ig=ic^2;
      g(ils,ir)=eCoh*nc*sc*dc*ic+eDen*d(ir)*nq*sq*dq*iq+ ...
          0.5*eDen*beff*ng*sg*dg*ig-ptot(ir)/aeff(ils,ir);

      for ib=1:nb
        for id=1:nd
          if (b(ir)==B(ib))&&(d(ir)==D(id))&&(g(ils,ir)<=0)
            nf(ils,ib,id)=nf(ils,ib,id)+1;
            for irv=1:nrv
              Xmuf(ils,ib,id,irv)=Xmuf(ils,ib,id,irv)+crv(ir,irv);
            end
          end
        end
      end
    end
%
% Parameter ranking
%
    if nb*nd==1
      for ib=1:nb
        for id=1:nd
          for irv=1:nrv
            Xmuf(ils,ib,id,irv)=Xmuf(ils,ib,id,irv)/nf(ils,ib,id);
            Z(irv)=abs(Xmu(irv)-Xmuf(ils,ib,id,irv))/(Xsig(irv)/ ...
              sqrt(nf(ils,ib,id)));
          end
          [ZS,IS]=sort(Z);
          NZS=ZS/norm(Z);
          for irv=1:nrv;RVS(irv)=RV(IS(irv));end
        end
```

```
      end
      RVS
      NZS
    end
%
%% Undrained bearing capacity limit state
   elseif LS(ils)=="UBC"
    %
    % Random Variables
    %
    RV   = ["Momt"  "Horz"  "  Su"  "tDen"];
    Xdis = [  "LN"    "LN"    "LN"    "NR"];
    Xmu  = [  5.0e7  6.6e5   1.0e5 17500.0];
    Xcov = [   0.20   0.20    0.25    0.05];
    Xmin = [    0.0    0.0     0.0     0.0];
    Xmax = [    0.0    0.0     0.0     0.0];
    % Size arrays
    nrv=length(RV);L=zeros(nrv,nrv);cmut=zeros(nrv,nrv);cm=zeros(nrv,nrv);
    Z=zeros(nrv,1);RVS=strings(nrv,1);Xsig=zeros(nrv,1);p=zeros(nrv);
    q=zeros(nrv);
    %
    fprintf(fileID,'\r\n %-45s\r\n','Undrained Bearing Capacity Limit State:');
    fprintf(fileID,'%-12s %s\r\n','Variable',sprintf(' %8s  ', RV));
    fprintf(fileID,'%-12s %s\r\n','Distribution',sprintf(' %8s  ', Xdis));
    fprintf(fileID,'%-12s %s\r\n','Mean Value',sprintf(' %5.2e  ', Xmu));
    fprintf(fileID,'%-12s %s\r\n','COV',sprintf(' %8.2f  ', Xcov));
    fprintf(fileID,'\r\n');
    % Parameters of underlying normal PDF's
    for irv=1:nrv
     Xsig(irv)=Xmu(irv)*Xcov(irv);
     if Xdis(irv)=="LN"
       q(irv)=sqrt(log(1+Xcov(irv)^2));
       p(irv)=log(Xmu(irv))-0.5*q(irv)^2;
     elseif Xdis(irv)=="TH"
       p(irv)=2.*pi/(0.46^2*(Xmax(irv)-Xmin(irv)^2-Xsig(irv)^2))^0.5;
       q(irv)=0;
     end
    end
    % Static stiffness values at the means
    M    = Xmu(1);
    H    = Xmu(2);
    Su   = Xmu(3);
    tDen = Xmu(4);
    for ib=1:nb
      for id=1:nd
        R=0.5*B(ib);
        ec=M/Ptot(ib,id);
        Aeff=2*(R^2*acos(min(1,ec/R))-ec*sqrt(max(0,R^2-ec^2)));
        be=2*(R-ec);
        le=2*R*sqrt(1-(1-be/(2*R))^2);
        leff=sqrt(Aeff*le/be);
        beff=leff*be/le;
        nc0=5.14;
        sc0=1+0.2*beff/leff;
        ic0=0.5+0.5*sqrt(max(0,1-H/(Aeff*Su)));
        eg(ils,ib,id)=Su*nc0*sc0*ic0+tDen*D(id)-Ptot(ib,id)/Aeff;
      end
    end
%    eg(ils,:,:)
    %
    % Define cross-correlation matrix [nrv x nrv]
    icopt="No";
    % For simplicity, enter upper triangular only
```

```
    % Ignore the cross correlation matrix if icopt="No"
    cmut=[1.0 0.0 0.0 0.0;
          0.0 1.0 0.0 0.0;
          0.0 0.0 1.0 0.0;
          0.0 0.0 0.0 1.0];
    cm=cmut+transpose(cmut)-eye(nrv);
    L = chol(cm,'lower');

    % Generate standard normal variable values & apply cross-correlation
    % (if applicable) & scale back up to appropriate PDF
    crvsn=zeros(nrmax,nrv);crv=zeros(nrmax,nrv);
    rvsn=normrnd(0,1,nrmax,nrv);
    for ir=1:nrmax
      if icopt=="Yes"
        crvsn(ir,:)=transpose(rvsn(ir,:)*transpose(L));
      else
        crvsn(ir,:)=rvsn(ir,:);
      end
      % Scale back up to appropriate PDF
      for irv=1:nrv
        if Xdis(irv)=="NR"
          crv(ir,irv)=Xsig(irv)*crvsn(ir,irv)+Xmu(irv);
        elseif Xdis(irv)=="LN"
          crv(ir,irv)=exp(q(irv)*crvsn(ir,irv)+p(irv));
        elseif Xdis(irv)=="TH"
          x=p(irv)*1/(2*pi);     %Fix this. It needs to be G variate
          crv(ir,irv)=Xmin(irv)+0.5*(Xmax(irv)-Xmin(irv))*(1+tanh(x));
        end
      end
    end
%
%   Loop on realizations
%
    for ir=1:nrmax
      % Apply cross-correlations
      % Evaluate Performance function for each realizations, ir
      M    = crv(ir,1);
      H    = crv(ir,2);
      Su   = crv(ir,3);
      tDen = crv(ir,4);
      R=r(ir);
      ecc(ils,ir)=min(M/ptot(ir),0.8*R);
      EC=ecc(ils,ir);
      aeff(ils,ir)=2*(R^2*acos(min(1,EC/R))-EC*sqrt(max(0,R^2-EC^2)));
      be=2*(R-EC);
      le=2*R*sqrt(1-(1-be/(2*R))^2);
      leff=sqrt(aeff(ils,ir)*le/be);
      beff=leff*be/le;
      nc0=5.14;
      sc0=1+0.2*beff/leff;
      ic0=0.5+0.5*sqrt(max(0,1-H/(aeff(ils,ir)*Su)));
      g(ils,ir)=Su*nc0*sc0*ic0+tDen*d(ir)-ptot(ir)/aeff(ils,ir);

      for ib=1:nb
        for id=1:nd
          if (b(ir)==B(ib))&&(d(ir)==D(id))&&(g(ils,ir)<=0)
            nf(ils,ib,id)=nf(ils,ib,id)+1;
            for irv=1:nrv
              Xmuf(ils,ib,id,irv)=Xmuf(ils,ib,id,irv)+crv(ir,irv);
            end
          end
        end
      end
```

```
    end
%
% Parameter ranking
%
    if nb*nd==1
      for ib=1:nb
        for id=1:nd
          for irv=1:nrv
            Xmuf(ils,ib,id,irv)=Xmuf(ils,ib,id,irv)/nf(ils,ib,id);
            Z(irv)=abs(Xmu(irv)-Xmuf(ils,ib,id,irv))/(Xsig(irv)/ ...
              sqrt(nf(ils,ib,id)));
          end
          [ZS,IS]=sort(Z);
          NZS=ZS/norm(Z);
          for irv=1:nrv;RVS(irv)=RV(IS(irv));end
        end
      end
      RVS
      NZS
    end
   else
    status="Not supposed to be here"
   end
end
for ils=1:nls
  for ib=1:nb
    for id=1:nd
      pf(ils,ib,id)=nf(ils,ib,id)*nb*nd/nrmax;
        if pf(ils,ib,id)>0.006
          ri(ils,ib,id)=log(1.2/pf(ils,ib,id))/2.06;
        elseif (pf(ils,ib,id)<=0.006)&&(pf(ils,ib,id)>=10^-6)
          ri(ils,ib,id)=log(196/pf(ils,ib,id))/4.0;
        else
          ri(ils,ib,id)=log(1000000/pf(ils,ib,id))/5.8;
        end
      if LT(ils)==1
        if ri(ils,ib,id)<=btsls
          YN(ils,ib,id)="N";
        else
          YN(ils,ib,id)="Y";
        end
      else
        if ri(ils,ib,id)<=btuls
          YN(ils,ib,id)="N";
        else
          YN(ils,ib,id)="Y";
        end
      end
    end
  end
end
nf
pf
ri
YN
for ils=1:nls
%  Voptls(ils)=max(Vf,[],'all');
  Voptls(ils)=max(max(Vf));
  bols(ils)=B(nb);
  dols(ils)=D(nd);
  for ib=nb:-1:1
    for id=nd:-1:1
      if (YN(ils,ib,id)=="Y")&&(Vf(ib,id)<Voptls(ils))
```

```
        Voptls(ils)=Vf(ib,id);
        bols(ils)=B(ib);
        dols(ils)=D(id);
      end
    end
  end
end
Vopt=min(Voptls);
for ils=1:nls
  if Voptls(ils)>Vopt
    Vopt=Voptls(ils);
    bo=bols(ils);
    do=dols(ils);
  end
end
%Voptls
%bols
%dols
Vopt
bo
do

%hold off
%for ils=1:nls
%  figure('name', 'Histogram g');
%  daspect auto
%  histogram(g(ils,:))
%end
fprintf(fileID,'\r\n %-22s\r\n\r\n','Probabilities of Failure');
fprintf(fileID,'%12s %6s %s\r\n\r\n',' Limit State',' Depth', ...
  sprintf('%7.2f ', B));
for ils=1:nls
  for id=1:nd
    fprintf(fileID,'%12s %6.2f %s\r\n',LS(ils),D(id), ...
      sprintf('%6.1e ',pf(ils,:,id)));
  end
  fprintf(fileID,'\r\n');
end
fprintf(fileID,'\r\n %-22s\r\n\r\n','Reliability Indices');
fprintf(fileID,'%12s %6s %s\r\n\r\n',' Limit State',' Depth', ...
  sprintf('%6.2f ', B));
for ils=1:nls
  for id=1:nd
    fprintf(fileID,'%12s %6.2f %s\r\n',LS(ils),D(id), ...
      sprintf('%6.2f ',ri(ils,:,id)));
  end
  fprintf(fileID,'\r\n');
end
fprintf(fileID,'\r\n %-22s\r\n\r\n','Acceptable/Unacceptable (Y/N) Analysis');
fprintf(fileID,'%12s %6s %s\r\n\r\n',' Limit State',' Depth', ...
  sprintf('%6.2f ', B));
for ils=1:nls
  for id=1:nd
    fprintf(fileID,'%12s %6.2f %s\r\n',LS(ils),D(id), ...
      sprintf('%6s ',YN(ils,:,id)));
  end
  fprintf(fileID,'\r\n');
end
fprintf(fileID,'\r\n %-22s\r\n\r\n','Optimal Design:');
fprintf(fileID,'%-25s %6.2f\r\n','Foundation diameter....:',bo);
fprintf(fileID,'%-25s %6.2f\r\n','Foundation depth.......:',do);
fprintf(fileID,'%-25s %6.2f\r\n','Foundation volume......:',Vopt);
fclose(fileID);
```

B.1.2 Output

```
~~~~~~~~~~~~~~~~~~~~~~~~~~~~~~~~~~~~~~~~~~~~~~~~~~~~~~~~~~~~~~~~~~~~~~~~~~~~
----------------------- Details of dRBD Run Results ========--------------
~~~~~~~~~~~~~~~~~~~~~~~~~~~~~~~~~~~~~~~~~~~~~~~~~~~~~~~~~~~~~~~~~~~~~~~~~~~~


This output file contains details of the d-RBD run and its results.
All input is embedded into the MATLAB program and is echoed here for
record, verification and documentation.
All quantities are in consistent units: kg, m, s, N, Pa, J

Design case title.....................: Medium Variability Case
Target reliabilty index for SLS.......:    1.70
Target probability of failure for SLS..:  0.0362
Target reliabilty index for ULS.......:    3.30
Target probability of failure for ULS..: 0.00036
Foundation diameters..................:  15.0  16.0  17.0  18.0  19.0  20.0
Foundation depths.....................:   2.8   2.9   3.0   3.1
Number of realizations all combinations: 2939695
Number of design decision combinations.:      24
Number of realizations per combination.:  122487

 Fixed quantities & Foundation Dimensions:
Pedestal diameter.................:     5.40
Base top diameter.................:     5.40
Pedestal stick-up.................:     0.15
Base middle thickness.............:     2.20
Base edge thickness...............:     0.40
Concrete unit weight..............:  23500.0
Backfill soil unit weight.........:  17000.0
Self weight of WTG................: 2.28e+06

 Foundation Volumes for all B-D Combinations:

        Foundation Diameter
 Depth   15.00   16.00   17.00   18.00   19.00   20.00

  2.80  245.80  272.69  301.16  331.19  362.80  395.97
  2.90  248.09  274.99  303.45  333.48  365.09  398.26
  3.00  250.38  277.28  305.74  335.77  367.38  400.55
  3.10  252.67  279.57  308.03  338.06  369.67  402.84


 Tilt Limit State:
Maximum allowed tilt (degrees)...:     0.17

 Variable          Mmnt       Dens       prat         Vs       sstn       tmax      alpha
Itha
Distribution        LN         NR         NR         LN         LN         LN         LN
LN
Mean Value    2.00e+07   1.75e+03   3.50e-01   2.00e+02   5.00e-04   1.00e+05   9.00e-
01   4.16e+00
COV               0.20       0.05       0.05       0.40       0.20       0.25       0.10
0.05


 Dynamic Stiffness Limit State:
Minimum required stiffness.........: 5.00e+10

 Variable          Dens       Prat         Vs       Hbed
Distribution        NR         NR         LN         LN
```

```
Mean Value    1.75e+03   3.50e-01   2.00e+02   8.50e+00
COV               0.05       0.05       0.40       0.30

 Static Stiffness Limit State:
Minimum required stiffness.........: 1.00e+10

 Variable          Momt       Dens         Vs       Tmax       sstn       Alfa       Hbed
Prat
Distribution        LN         NR         LN         LN         LN         NR         LN
NR
Mean Value    5.00e+07   1.75e+03   2.00e+02   1.00e+05   5.00e-04   9.00e-01   8.50e+00
3.50e-01
COV               0.20       0.05       0.40       0.25       0.20       0.10       0.30
0.05


 Drained Bearing Capacity Limit State:
Variable          Momt       Horz       eDen       ePhi       eCoh
Distribution        LN         LN         NR         LN         LN
Mean Value    5.00e+07   6.60e+05   1.75e+04   4.36e-01   5.00e+04
COV               0.20       0.20       0.05       0.30       0.20


 Undrained Bearing Capacity Limit State:
Variable          Momt       Horz         Su       tDen
Distribution        LN         LN         LN         NR
Mean Value    5.00e+07   6.60e+05   1.00e+05   1.75e+04
COV               0.20       0.20       0.25       0.05


 Probabilities of Failure

 Limit State  Depth   15.00   16.00   17.00   18.00   19.00   20.00

         TLT   2.80 4.1e-05 0.0e+00 8.2e-06 0.0e+00 0.0e+00 0.0e+00
         TLT   2.90 8.2e-05 1.6e-05 8.2e-06 0.0e+00 0.0e+00 0.0e+00
         TLT   3.00 4.9e-05 2.4e-05 0.0e+00 0.0e+00 0.0e+00 0.0e+00
         TLT   3.10 6.5e-05 8.2e-06 8.2e-06 8.2e-06 0.0e+00 0.0e+00

         DYS   2.80 1.7e-02 8.7e-03 5.1e-03 2.7e-03 1.5e-03 8.6e-04
         DYS   2.90 1.5e-02 8.8e-03 4.4e-03 2.3e-03 1.2e-03 7.3e-04
         DYS   3.00 1.3e-02 8.3e-03 4.4e-03 2.3e-03 1.0e-03 6.9e-04
         DYS   3.10 1.3e-02 7.2e-03 4.1e-03 2.2e-03 1.2e-03 5.3e-04

         STS   2.80 2.8e-01 8.8e-02 2.3e-02 5.2e-03 1.0e-03 2.4e-04
         STS   2.90 2.4e-01 7.3e-02 1.7e-02 3.9e-03 7.8e-04 1.8e-04
         STS   3.00 2.0e-01 5.9e-02 1.4e-02 2.9e-03 6.8e-04 1.8e-04
         STS   3.10 1.7e-01 4.5e-02 1.0e-02 2.1e-03 4.2e-04 8.2e-05

         DBC   2.80 1.8e-03 9.0e-05 1.6e-05 0.0e+00 0.0e+00 0.0e+00
         DBC   2.90 1.3e-03 5.7e-05 0.0e+00 0.0e+00 0.0e+00 0.0e+00
         DBC   3.00 1.3e-03 6.5e-05 0.0e+00 0.0e+00 0.0e+00 0.0e+00
         DBC   3.10 6.6e-04 0.0e+00 0.0e+00 0.0e+00 0.0e+00 0.0e+00

         UBC   2.80 3.3e-02 3.5e-03 2.7e-04 8.2e-06 0.0e+00 0.0e+00
         UBC   2.90 2.7e-02 2.6e-03 1.7e-04 0.0e+00 0.0e+00 0.0e+00
         UBC   3.00 2.1e-02 1.9e-03 1.2e-04 8.2e-06 0.0e+00 0.0e+00
         UBC   3.10 1.7e-02 1.7e-03 4.9e-05 0.0e+00 0.0e+00 0.0e+00


 Reliability Indices

 Limit State  Depth  15.00  16.00  17.00  18.00  19.00  20.00
```

TLT	2.80	3.85	Inf	4.25	Inf	Inf	Inf
TLT	2.90	3.67	4.08	4.25	Inf	Inf	Inf
TLT	3.00	3.80	3.97	Inf	Inf	Inf	Inf
TLT	3.10	3.73	4.25	4.25	4.25	Inf	Inf
DYS	2.80	2.08	2.39	2.64	2.80	2.95	3.08
DYS	2.90	2.11	2.39	2.67	2.84	3.00	3.12
DYS	3.00	2.18	2.41	2.67	2.84	3.04	3.14
DYS	3.10	2.20	2.48	2.70	2.85	3.01	3.20
STS	2.80	0.71	1.27	1.92	2.64	3.05	3.41
STS	2.90	0.78	1.36	2.07	2.70	3.11	3.48
STS	3.00	0.86	1.47	2.17	2.78	3.14	3.48
STS	3.10	0.95	1.60	2.32	2.86	3.27	3.67
DBC	2.80	2.90	3.65	4.08	Inf	Inf	Inf
DBC	2.90	2.98	3.76	Inf	Inf	Inf	Inf
DBC	3.00	2.98	3.73	Inf	Inf	Inf	Inf
DBC	3.10	3.15	Inf	Inf	Inf	Inf	Inf
UBC	2.80	1.74	2.73	3.37	4.25	Inf	Inf
UBC	2.90	1.84	2.81	3.49	Inf	Inf	Inf
UBC	3.00	1.97	2.88	3.57	4.25	Inf	Inf
UBC	3.10	2.05	2.91	3.80	Inf	Inf	Inf

Acceptable/Unacceptable (Y/N) Analysis

Limit State	Depth	15.00	16.00	17.00	18.00	19.00	20.00
TLT	2.80	Y	Y	Y	Y	Y	Y
TLT	2.90	Y	Y	Y	Y	Y	Y
TLT	3.00	Y	Y	Y	Y	Y	Y
TLT	3.10	Y	Y	Y	Y	Y	Y
DYS	2.80	Y	Y	Y	Y	Y	Y
DYS	2.90	Y	Y	Y	Y	Y	Y
DYS	3.00	Y	Y	Y	Y	Y	Y
DYS	3.10	Y	Y	Y	Y	Y	Y
STS	2.80	N	N	Y	Y	Y	Y
STS	2.90	N	N	Y	Y	Y	Y
STS	3.00	N	N	Y	Y	Y	Y
STS	3.10	N	N	Y	Y	Y	Y
DBC	2.80	N	Y	Y	Y	Y	Y
DBC	2.90	N	Y	Y	Y	Y	Y
DBC	3.00	N	Y	Y	Y	Y	Y
DBC	3.10	N	Y	Y	Y	Y	Y
UBC	2.80	N	N	Y	Y	Y	Y
UBC	2.90	N	N	Y	Y	Y	Y
UBC	3.00	N	N	Y	Y	Y	Y
UBC	3.10	N	N	Y	Y	Y	Y

Optimal Design:

Foundation diameter....: 17.00
Foundation depth.....: 2.80
Foundation volume.....: 301.16

B.2 High Variability Case

B.2.1 Source Code

```
%% d-RBD of Gravity-base WTG Foundations
% All limit states in one loop
%
% Possible limit states are:
%   TLT = Tilt
%   DYS = Dynamic stiffness
%   STS = Static stiffness
%   DBC = Drained bearing capacity
%   UBC = Undrained bearing capacity
%
% Possibe distributions
%      NR = Normal
%      LN = Lognormal
%      TH = Tanh (bounded)
%      DT = Deterministic
% NOTES:
% 1. Always use consistent units: kg, m, s, N, Pa, J
% 2. Do not use NR PDF for any variable with COV>0.25 as the PDF will
%    likely produce meaningless negative numbers.
% 3. To study parameter rankings, run program from one combination of
%    design decision parameters.
% 4. The number of realizations can be adjusted by adjusting the COV on the
%    probability of failure. A COV of 0.3 or 0.4 could be used for
%    preliminary runs. For final runs, the COV should 0.1 or less.
%
clear all;                          % Clear all
fileID = fopen('dRBD_HV.txt','w');   % Change output file name, if desired.
fprintf(fileID,'%-73s\r\n', ...
  '~~~~~~~~~~~~~~~~~~~~~~~~~~~~~~~~~~~~~~~~~~~~~~~~~~~~~~~~~~~~~~~~~~~~~~~~~~~~');
fprintf(fileID,'%-73s\r\n', ...
  '------------------------ Details of dRBD Run Results ========--------------');
fprintf(fileID,'%-73s\r\n', ...
  '~~~~~~~~~~~~~~~~~~~~~~~~~~~~~~~~~~~~~~~~~~~~~~~~~~~~~~~~~~~~~~~~~~~~~~~~~~~~');
fprintf(fileID,'\r\n%73s\r\n', ...
  '                                                                         ');
fprintf(fileID,'%-73s\r\n', ...
  'This output file contains details of the d-RBD run and its results.      ');
fprintf(fileID,'%-73s\r\n', ...
  'All input is embedded into the MATLAB program and is echoed here for     ');
fprintf(fileID,'%-73s\r\n', ...
  'record, verification and documentation.');
fprintf(fileID,'%-73s\r\n\r\n', ...
  'All quantities are in consistent units: kg, m, s, N, Pa, J');


%% Main simulation parameters
Title="High Variability Case";     % Descriptive design case title
PLS=["TLT" "DYS" "STS" "DBC" "UBC"]; % Possible limit states
LSO=[    1     1     1     1     1]; % 1=verify, 0=do not verify
LST=[    1     1     1     2     2]; % Limit state type: 1=SLS,2=ULS,3-FLS
nrvmax=10;              % Maximum number of random variables in any limit state
B=15:1:20;              % Foundation diameter(s)
D=2.8:0.1:3.1;          % Foundation depth(s)
btsls=1.7;              % Target reliabilty index for SLS
btuls=3.3;              % Target reliability index for ULS
pfCOV=0.15;             % Desired COV of probability of failure
```

```
%% Computation of some prelimnary parameters
nls=nnz(LSO);           % Number of limit states in this run
nb=length(B);           % Number of foundation diameters
nd=length(D);           % Number of foundation depths
LS=strings(nls,1);LT=zeros(nls,1);YN=strings(nls,nb,nd);eg=zeros(nls,nb,nd);
nbdt=zeros(nb,nd);Xmuf=zeros(nls,nb,nd,nrvmax);
Voptls=zeros(nls,1);bols=zeros(nls,1);dols=zeros(nls,1);

nf=zeros(nls,nb,nd);pf=zeros(nls,nb,nd);ri=zeros(nls,nb,nd);
jp=0;
for ip=1:length(PLS)
  if LSO(ip)==1
    jp=jp+1;
    LS(jp,1)=PLS(ip);
    LT(jp)=LST(ip);
  end
end
% Compute tagert probabilities of failures (for SLS and ULS)
if btsls<2.6
  pftsls=1.2*exp(-2.06*btsls);
elseif (btsls>=2.6)&&(btsls<=4.8)
  pftsls=196*exp(-4.0*btsls);
else
  pftsls=1000000*exp(-5.8*btsls);
end
if btuls<2.6
  pftuls=1.2*exp(-2.06*btuls);
elseif (btuls>=2.6)&&(btuls<=4.8)
  pftuls=196*exp(-4.0*btuls);
else
  pftuls=1000000*exp(-5.8*btuls);
end
pftsls
pftuls
nr1=10*nb*nd/pftsls;             % Minimum number of realizations - Estimate 1
nr2=(1/pftsls-1)*nb*nd/pfCOV^2;  % Minimum number of realizations - Estimate 2
nrsls=round(max([nr1 nr2]));     % Number of realizations - SLS
nr1=10*nb*nd/pftuls;             % Minimum number of realizations - Estimate 1
nr2=(1/pftuls-1)*nb*nd/pfCOV^2;  % Minimum number of realizations - Estimate 2
nruls=round(max([nr1 nr2]));     % Number of realizations - ULS
nrmax=max(nruls,nrsls)
%nrmax=2000;
nrsls=nrmax;nruls=nrmax;ptot=zeros(nrmax,1);r=zeros(nrmax,1);
g=zeros(nls,nrmax);aeff=zeros(nls,nrmax);ecc=zeros(nls,nrmax);
%% Print results to output text file
fprintf(fileID,'%40s %-40s\r\n','Design case title.....................:', ...
  Title);
fprintf(fileID,'%40s %7.2f\r\n','Target reliabilty index for SLS........:', ...
  btsls);
fprintf(fileID,'%40s %7.4f\r\n','Target probability of failure for SLS..:', ...
  pftsls);
fprintf(fileID,'%40s %7.2f\r\n','Target reliabilty index for ULS........:', ...
  btuls);
fprintf(fileID,'%40s %7.5f\r\n','Target probability of failure for ULS..:', ...
  pftuls);
fprintf(fileID,'%40s %s\r\n','Foundation diameters...................:', ...
  sprintf('%5.1f ', B));
fprintf(fileID,'%40s %s\r\n','Foundation depths......................:', ...
  sprintf('%5.1f ', D));
fprintf(fileID,'%40s %7i\r\n','Number of realizations all combinations:', ...
  nrmax);
fprintf(fileID,'%40s %7i\r\n','Number of design decision combinations.:', ...
  nb*nd);
```

```
fprintf(fileID,'%40s %7i\r\n','Number of realizations per combination.:', ...
  round(nrmax/(nb*nd)));

%% Fixed dimensions, other deterministic parameters & derived quantities
%
% Fixed dimensions and parameters
%
he=0.4;               % Base edge height
hm=2.2;               % Base middle height
hsu=0.15;             % Pedestal stickup
bp=5.4;               % Pedestal diameter
bb=5.4;               % Base top diameter
gconc=23500;          % Unit weight of concrete
gbsoil=17000;         % Unit weight of backfill soil
Pwtg=2.275e6;         % Weight of WTG
%
% Derived quantities
%
hp=zeros(nd,1);Af=zeros(nb,1);Vb1=zeros(nb,1);Vb2=zeros(nb,1);Vp=zeros(nd,1);
Vf=zeros(nb,nd);htp=zeros(nd);Vsoil=zeros(nb,nd);Pc=zeros(nb,nd);
Ps=zeros(nb,nd);Ptot=zeros(nb,nd);
ncomb=zeros(nb,nd);beta=zeros(nb,nd);
Ap=0.25*pi*bp^2;                          % Pedestal area
Ab=0.25*pi*bb^2;                          % Base top area
for ib=1:nb
  for id=1:nd
    hp(id)=D(id)+hsu-hm;                  % Pedestal height
    Af(ib)=0.25*pi*B(ib)^2;               % Footing area
    Vb1(ib)=Af(ib)*he;                    % Volume of lower portion of base
    Vb2(ib)=(Ab+(Ab*Af(ib))^0.5+ ...      % Volume of tapered portion of base
    Af(ib))*(hm-he)/3;
    Vp(id)=Ap*hp(id);                     % Pedestal volume
    Vf(ib,id)=Vb1(ib)+Vb2(ib)+Vp(id);     % Foundation volume
    htp(id)=D(id)+hsu-hp(id)-he;          % Height of tapered portion of footing
    Vsoil(ib,id)=Af(ib)*(htp(id)+ ...
    hp(id)-hsu)-Ap*(hp(id)-hsu)-Vb2(ib);  % Volume of backfill soil
    Pc(ib,id)=Vf(ib,id)*gconc;            % Weight of foundation concrete
    Ps(ib,id)=Vsoil(ib,id)*gbsoil;        % Weight of backfill soil
    Ptot(ib,id)=Pwtg+Pc(ib,id)+Ps(ib,id); % Total vertical load
  end
end
fprintf(fileID,'\r\n %-45s\r\n','Fixed quantities & Foundation Dimensions:');
fprintf(fileID,'%-35s %8.2f\r\n','Pedestal diameter.................:',bp);
fprintf(fileID,'%-35s %8.2f\r\n','Base top diameter.................:',bb);
fprintf(fileID,'%-35s %8.2f\r\n','Pedestal stick-up.................:',hsu);
fprintf(fileID,'%-35s %8.2f\r\n','Base middle thickness.............:',hm);
fprintf(fileID,'%-35s %8.2f\r\n','Base edge thickness...............:',he);
fprintf(fileID,'%-35s %8.1f\r\n','Concrete unit weight..............:',gconc);
fprintf(fileID,'%-35s %8.1f\r\n','Backfill soil unit weight.........:',gbsoil);
fprintf(fileID,'%-35s %5.2e\r\n','Self weight of WTG................:',Pwtg);
fprintf(fileID,'\r\n %-22s\r\n\r\n',...
  'Foundation Volumes for all B-D Combinations:');
fprintf(fileID,'%-40s\r\n','        Foundation Diameter');
fprintf(fileID,'%6s %s\r\n\r\n',' Depth',sprintf('%7.2f ', B));
for id=1:nd
  fprintf(fileID,'%6.2f %s\r\n',D(id), ...
    sprintf('%7.2f ',Vf(:,id)));
end
fprintf(fileID,'\r\n');


%% Plot possible foundation geometries
color=["r" "g" "b" "m" "c" "k"];
```

```
figure('name', 'Foundation Geometries');
 for ib=1:nb
    for id=1:nd
     clr=color(randi(6));
     xf=[-B(ib)/2 -B(ib)/2 -bb/2 -bp/2 ...
       -bp/2 bp/2 bp/2 bb/2 0.5*B(ib) B(ib)/2 -B(ib)/2];
     yf=[0 he hm hm hm+hp(id) hm+hp(id) hm hm he 0 0];
     xgl=[-B(ib)/2 -bp/2];
     xgr=[bp/2 B(ib)/2];
     yg=[D(id) D(id)];
     plot(xf,yf)
     daspect([1 1 1])
     hold on
     plot(xgl,yg,clr)
     plot(xgr,yg,clr)
    end
 end
set(gca,'xlim',[-B(nb)/2-B(nb)/10 B(nb)/2+B(nb)/10])
set(gca,'ylim',[-0.2*D(nd) 1.2*D(nd)])
hold off

% Generate design decision variable values (uniform distribution)
b=B(randi(nb,nrmax,1));
d=D(randi(nd,nrmax,1));
for ir=1:nrmax
    r(ir)=0.5*b(ir);
    for ib=1:nb
      for id=1:nd
        if (b(ir)==B(ib))&&(d(ir)==D(id))
          nbdt(ib,id)=nbdt(ib,id)+1;
          ptot(ir)=Ptot(ib,id);
        end
      end
    end
end
%
% Loop on selected limit states
for ils=1:nls

%% Tilt limit state
  if LS(ils)=="TLT"
    tiltmax=0.17; tiltmaxr=tiltmax*pi/180.;       % Maximum allowed tilt
    etilt=zeros(nb,nd);
    % Random Variables
    %
    RV   = ["Mmnt"   "Dens"   "prat" "  Vs"   "sstn"   "tmax" "alpha"  "Itha"];
    Xdis = [  "LN"     "NR"     "NR"   "LN"     "LN"     "LN"    "LN"    "LN"];
    Xmu  = [2.0e+7   1750.0     0.35  200.0   0.0005   1.0e+5     0.9    4.16];
    Xcov = [  0.25     0.10     0.10    0.6     0.30     0.50     0.2    0.10];
    Xmin = [   0.0      0.0     0.25    0.0      0.0      0.0     0.0     0.0];
    Xmax = [   0.0      0.0     0.45    0.0      0.0      0.0     0.0     0.0];
    % Size arrays
    nrv=length(RV);L=zeros(nrv,nrv);cmut=zeros(nrv,nrv);cm=zeros(nrv,nrv);
    Z=zeros(nrv,1);RVS=strings(nrv,1);Xsig=zeros(nrv,1);p=zeros(nrv);
    q=zeros(nrv);
    %
    fprintf(fileID,'\r\n %-45s\r\n','Tilt Limit State:');
    fprintf(fileID,'%-35s %7.2f\r\n','Maximum allowed tilt (degrees)...:', ...
      tiltmax);
    fprintf(fileID,'\r\n %-12s %s\r\n','Variable',sprintf(' %8s  ', RV));
    fprintf(fileID,'%-12s %s\r\n','Distribution',sprintf(' %8s  ', Xdis));
    fprintf(fileID,'%-12s %s\r\n','Mean Value',sprintf(' %5.2e  ', Xmu));
    fprintf(fileID,'%-12s %s\r\n','COV',sprintf(' %8.2f  ', Xcov));
```

```
    fprintf(fileID,'\r\n');
    % Parameters of underlying normal PDF's
    for irv=1:nrv
     Xsig(irv)=Xmu(irv)*Xcov(irv);
     if Xdis(irv)=="LN"
       q(irv)=sqrt(log(1+Xcov(irv)^2));
       p(irv)=log(Xmu(irv))-0.5*q(irv)^2;
     elseif Xdis(irv)=="TH"
       p(irv)=2.*pi/(0.46^2*(Xmax(irv)-Xmin(irv)^2-Xsig(irv)^2))^0.5;
       q(irv)=0;
     end
    end
    % Tilt value at the means
    M      = Xmu(1);
    den    = Xmu(2);
    pr     = Xmu(3);
    Vs     = Xmu(4);
    ss     = Xmu(5);
    tmax   = Xmu(6);
    alpha  = Xmu(7);
    itheta = Xmu(8);
    for ib=1:nb
      for id=1:nd
        etilt(ib,id)  = atan(M*(1-pr)*(1+(ss*den*Vs^2/tmax)^alpha)* ...
          itheta/(2*den*Vs^2*B(ib)^3))*180./pi;
        eg(ils,ib,id) = tan(tiltmaxr)-M*(1-pr)*(1+(ss*den*Vs^2/tmax)^alpha)* ...
          itheta/(2*den*Vs^2*B(ib)^3);
      end
    end
%    etilt
%    eg(ils,:,:)
    %
    % Define cross-correlation matrix [nrv x nrv]
    icopt="No";
    % For simplicity, enter upper triangular only
    % Ignore the cross correlation matrix if icopt="No"
    cmut=[1.0 0.0 0.0 0.0 0.0 0.0 0.0 0.0;
          0.0 1.0 0.0 0.0 0.0 0.0 0.0 0.0;
          0.0 0.0 1.0 0.0 0.0 0.0 0.0 0.0;
          0.0 0.0 0.0 1.0 0.0 0.0 0.0 0.0;
          0.0 0.0 0.0 0.0 1.0 0.0 0.0 0.0;
          0.0 0.0 0.0 0.0 0.0 1.0 0.0 0.0;
          0.0 0.0 0.0 0.0 0.0 0.0 1.0 0.0;
          0.0 0.0 0.0 0.0 0.0 0.0 0.0 1.0];
    cm=cmut+transpose(cmut)-eye(nrv);
    L = chol(cm,'lower');

    % Generate standard normal variable values & apply cross-correlation
    % (if applicable) & scale back up to appropriate PDF
    crvsn=zeros(nrmax,nrv);crv=zeros(nrmax,nrv);
    rvsn=normrnd(0,1,nrmax,nrv);
    for ir=1:nrmax
      if icopt=="Yes"
        crvsn(ir,:)=transpose(rvsn(ir,:)*transpose(L));
      else
        crvsn(ir,:)=rvsn(ir,:);
      end
      % Scale back up to appropriate PDF
      for irv=1:nrv
        if Xdis(irv)=="NR"
          crv(ir,irv)=Xsig(irv)*crvsn(ir,irv)+Xmu(irv);
        elseif Xdis(irv)=="LN"
          crv(ir,irv)=exp(q(irv)*crvsn(ir,irv)+p(irv));
```

```
        elseif Xdis(irv)=="TH"
          x=p(irv)*1/(2*pi);     %Fix this. It needs to be G variate
          crv(ir,irv)=Xmin(irv)+0.5*(Xmax(irv)-Xmin(irv))*(1+tanh(x));
        end
      end
    end
%
%   Loop on realizations
%
    for ir=1:nrmax
      % Apply cross-correlations
      % Evaluate Performance function for each realizations, ir
      M        = crv(ir,1);
      den      = crv(ir,2);
      pr       = crv(ir,3);
      Vs       = crv(ir,4);
      ss       = crv(ir,5);
      tmax     = crv(ir,6);
      alpha    = crv(ir,7);
      itheta   = crv(ir,8);

      g(ils,ir)   = tan(tiltmaxr)-M*(1-pr)*(1+(ss*den*Vs^2/tmax)^alpha)* ...
                  itheta/(2*den*Vs^2*b(ir)^3);
      for ib=1:nb
        for id=1:nd
          if (b(ir)==B(ib))&&(d(ir)==D(id))&&(g(ils,ir)<=0)
            nf(ils,ib,id)=nf(ils,ib,id)+1;
            for irv=1:nrv
              Xmuf(ils,ib,id,irv)=Xmuf(ils,ib,id,irv)+crv(ir,irv);
            end
          end
        end
      end
    end
%
% Parameter ranking
%
    if nb*nd==1
      for ib=1:nb
        for id=1:nd
          for irv=1:nrv
            Xmuf(ils,ib,id,irv)=Xmuf(ils,ib,id,irv)/nf(ils,ib,id);
            Z(irv)=abs(Xmu(irv)-Xmuf(ils,ib,id,irv))/(Xsig(irv)/ ...
              sqrt(nf(ils,ib,id)));
          end
          [ZS,IS]=sort(Z);
          NZS=ZS/norm(Z);
          for irv=1:nrv;RVS(irv)=RV(IS(irv));end
        end
      end
      RVS
      NZS
    end
%% Dynamic stiffness limit state
   elseif LS(ils)=="DYS"
    Kdynmin=5e10;               % Minimum stiffness (Nm/rad)
    eKdyn=zeros(nb,nd);
    %
    % Random Variables
    %
    RV   = [ "Dens"    "Prat"    "  Vs" "Hbed"];
    Xdis = [   "NR"      "NR"     "LN"   "LN"];
    Xmu  = [ 1750.0      0.35    200.0    8.5];
```

```
    Xcov = [   0.10      0.10     0.60   0.30];
    Xmin = [    0.0       0.0      0.0    0.0];
    Xmax = [    0.0       0.0      0.0    0.0];
    % Size arrays
    nrv=length(RV);L=zeros(nrv,nrv);cmut=zeros(nrv,nrv);cm=zeros(nrv,nrv);
    Z=zeros(nrv,1);RVS=strings(nrv,1);Xsig=zeros(nrv,1);p=zeros(nrv);
    q=zeros(nrv);
    %
    fprintf(fileID,'\r\n %-45s\r\n','Dynamic Stiffness Limit State:');
    fprintf(fileID,'%-35s %7.2e\r\n','Minimum required stiffness.........:', ...
      Kdynmin);
    fprintf(fileID,'\r\n %-12s %s\r\n','Variable',sprintf(' %8s  ', RV));
    fprintf(fileID,'%-12s %s\r\n','Distribution',sprintf(' %8s  ', Xdis));
    fprintf(fileID,'%-12s %s\r\n','Mean Value',sprintf(' %5.2e  ', Xmu));
    fprintf(fileID,'%-12s %s\r\n','COV',sprintf(' %8.2f  ', Xcov));
    fprintf(fileID,'\r\n');

    % Parameters of underlying normal PDF's
    for irv=1:nrv
     Xsig(irv)=Xmu(irv)*Xcov(irv);
     if Xdis(irv)=="LN"
       q(irv)=sqrt(log(1+Xcov(irv)^2));
       p(irv)=log(Xmu(irv))-0.5*q(irv)^2;
     elseif Xdis(irv)=="TH"
       p(irv)=2.*pi/(0.46^2*(Xmax(irv)-Xmin(irv)^2-Xsig(irv)^2))^0.5;
       q(irv)=0;
     end
    end
    % Tilt value at the means
    den    = Xmu(1);
    pr     = Xmu(2);
    Vs     = Xmu(3);
    Hb     = Xmu(4);
    for ib=1:nb
      for id=1:nd
        R=0.5*B(ib);
        eKdyn(ib,id)=8.*den*Vs^2*R^3*(1+2*D(id)/R)* ...
          (1+0.7*D(id)/Hb)*(1+R/(6*Hb))/(3*(1-pr));
        eg(ils,ib,id)  = eKdyn(ib,id)-Kdynmin;
      end
    end
%    eKdyn
%    eg(ils,:,:)
    %
    % Define cross-correlation matrix [nrv x nrv]
    icopt="No";
    % For simplicity, enter upper triangular only
    % Ignore the cross correlation matrix if icopt="No"
    cmut=[1.0 0.0 0.0 0.0;
          0.0 1.0 0.0 0.0;
          0.0 0.0 1.0 0.0;
          0.0 0.0 0.0 1.0];
    cm=cmut+transpose(cmut)-eye(nrv);
    L = chol(cm,'lower');

    % Generate standard normal variable values & apply cross-correlation
    % (if applicable) & scale back up to appropriate PDF
    crvsn=zeros(nrmax,nrv);crv=zeros(nrmax,nrv);
    rvsn=normrnd(0,1,nrmax,nrv);
    for ir=1:nrmax
      if icopt=="Yes"
        crvsn(ir,:)=transpose(rvsn(ir,:)*transpose(L));
      else
```

```
        crvsn(ir,:)=rvsn(ir,:);
      end
      % Scale back up to appropriate PDF
      for irv=1:nrv
        if Xdis(irv)=="NR"
          crv(ir,irv)=Xsig(irv)*crvsn(ir,irv)+Xmu(irv);
        elseif Xdis(irv)=="LN"
          crv(ir,irv)=exp(q(irv)*crvsn(ir,irv)+p(irv));
        elseif Xdis(irv)=="TH"
          x=p(irv)*1/(2*pi);     %Fix this. It needs to be G variate
          crv(ir,irv)=Xmin(irv)+0.5*(Xmax(irv)-Xmin(irv))*(1+tanh(x));
        end
      end
    end
%
%   Loop on realizations
%
    for ir=1:nrmax
      % Apply cross-correlations
      % Evaluate Performance function for each realizations, ir
      den      = crv(ir,1);
      pr       = crv(ir,2);
      Vs       = crv(ir,3);
      Hb       = crv(ir,4);
      R=0.5*b(ir);
      g(ils,ir)   = 8.0*den*Vs^2*R^3*(1+2*d(ir)/R)* ...
                  (1+0.7*d(ir)/Hb)*(1+R/(6*Hb))/(3*(1-pr))-Kdynmin;
      for ib=1:nb
        for id=1:nd
          if (b(ir)==B(ib))&&(d(ir)==D(id))&&(g(ils,ir)<=0)
            nf(ils,ib,id)=nf(ils,ib,id)+1;
            for irv=1:nrv
              Xmuf(ils,ib,id,irv)=Xmuf(ils,ib,id,irv)+crv(ir,irv);
            end
          end
        end
      end
    end
%
% Parameter ranking
%
    if nb*nd==1
      for ib=1:nb
        for id=1:nd
          for irv=1:nrv
            Xmuf(ils,ib,id,irv)=Xmuf(ils,ib,id,irv)/nf(ils,ib,id);
            Z(irv)=abs(Xmu(irv)-Xmuf(ils,ib,id,irv))/ ...
              (Xsig(irv)/sqrt(nf(ils,ib,id)));
          end
          [ZS,IS]=sort(Z);
          NZS=ZS/norm(Z);
          for irv=1:nrv;RVS(irv)=RV(IS(irv));end
        end
      end
      RVS
      NZS
    end
%% Static stiffness limit state
   elseif LS(ils)=="STS"
    Kstamin=1e10;         % Minimum stiffness (Nm/rad)
    eKsta=zeros(nb,nd);
    %
    % Random Variables
```

```
%
RV   = ["Momt"  "Dens"  "  Vs" "Tmax" "sstn" "Alfa" "Hbed" "Prat"];
Xdis = [  "LN"    "NR"    "LN"   "LN"   "LN"   "NR"   "LN"   "NR"];
Xmu  = [  5.0e7 1750.0   200.0  1.0e5  5.e-4   0.90    8.5   0.35];
Xcov = [   0.25   0.10    0.60   0.50    0.3   0.20   0.30   0.10];
Xmin = [    0.0    0.0     0.0    0.0    0.0    0.0    0.0    0.0];
Xmax = [    0.0    0.0     0.0    0.0    0.0    0.0    0.0    0.0];
% Size arrays
nrv=length(RV);L=zeros(nrv,nrv);cmut=zeros(nrv,nrv);cm=zeros(nrv,nrv);
Z=zeros(nrv,1);RVS=strings(nrv,1);Xsig=zeros(nrv,1);p=zeros(nrv);
q=zeros(nrv);
%
fprintf(fileID,'\r\n %-45s\r\n','Static Stiffness Limit State:');
fprintf(fileID,'%-35s %7.2e\r\n','Minimum required stiffness........:' ...
  ,Kstamin);
fprintf(fileID,'\r\n %-12s %s\r\n','Variable',sprintf(' %8s  ', RV));
fprintf(fileID,'%-12s %s\r\n','Distribution',sprintf(' %8s  ', Xdis));
fprintf(fileID,'%-12s %s\r\n','Mean Value',sprintf(' %5.2e  ', Xmu));
fprintf(fileID,'%-12s %s\r\n','COV',sprintf(' %8.2f  ', Xcov));
fprintf(fileID,'\r\n');

% Parameters of underlying normal PDF's
for irv=1:nrv
 Xsig(irv)=Xmu(irv)*Xcov(irv);
 if Xdis(irv)=="LN"
   q(irv)=sqrt(log(1+Xcov(irv)^2));
   p(irv)=log(Xmu(irv))-0.5*q(irv)^2;
 elseif Xdis(irv)=="TH"
   p(irv)=2.*pi/(0.46^2*(Xmax(irv)-Xmin(irv)^2-Xsig(irv)^2))^0.5;
   q(irv)=0;
 end
end
% Static stiffness values at the means
M     = Xmu(1);
den   = Xmu(2);
Vs    = Xmu(3);
Tmax  = Xmu(4);
sstrn = Xmu(5);
alfa  = Xmu(6);
Hb    = Xmu(7);
pr    = Xmu(8);
for ib=1:nb
  for id=1:nd
    R=0.5*B(ib);
    ec=M/Ptot(ib,id);
    Aeff=2*(R^2*acos(min(1,ec/R))-ec*sqrt(R^2-ec^2));
    be=2*(R-ec);
    le=2*R*sqrt(1-(1-be/(2*R))^2);
    leff=sqrt(Aeff*le/be);
    beff=leff*be/le;
    eKsta(ib,id)=den*Vs^2*beff^3*(1+4*D(id)/beff)*(1+0.7*D(id)/Hb)* ...
      (1+beff/12/Hb)/(3*(1-pr)*(1+(sstrn*den*Vs^2/Tmax)^alfa));
    eg(ils,ib,id)=eKsta(ib,id)-Kstamin;
  end
end
%  eKsta
%  eg(ils,:,:)
%
% Define cross-correlation matrix [nrv x nrv]
icopt="No";
% For simplicity, enter upper triangular only
% Ignore the cross correlation matrix if icopt="No"
cmut=[1.0 0.0 0.0 0.0 0.0 0.0 0.0 0.0;
```

```
      0.0 1.0 0.0 0.0 0.0 0.0 0.0 0.0;
      0.0 0.0 1.0 0.0 0.0 0.0 0.0 0.0;
      0.0 0.0 0.0 1.0 0.0 0.0 0.0 0.0;
      0.0 0.0 0.0 0.0 1.0 0.0 0.0 0.0;
      0.0 0.0 0.0 0.0 0.0 1.0 0.0 0.0;
      0.0 0.0 0.0 0.0 0.0 0.0 1.0 0.0;
      0.0 0.0 0.0 0.0 0.0 0.0 0.0 1.0];
cm=cmut+transpose(cmut)-eye(nrv);
L = chol(cm,'lower');

% Generate standard normal variable values & apply cross-correlation
% (if applicable) & scale back up to appropriate PDF
crvsn=zeros(nrmax,nrv);crv=zeros(nrmax,nrv);
rvsn=normrnd(0,1,nrmax,nrv);
for ir=1:nrmax
  if icopt=="Yes"
    crvsn(ir,:)=transpose(rvsn(ir,:)*transpose(L));
  else
    crvsn(ir,:)=rvsn(ir,:);
  end
  % Scale back up to appropriate PDF
  for irv=1:nrv
    if Xdis(irv)=="NR"
      crv(ir,irv)=Xsig(irv)*crvsn(ir,irv)+Xmu(irv);
    elseif Xdis(irv)=="LN"
      crv(ir,irv)=exp(q(irv)*crvsn(ir,irv)+p(irv));
    elseif Xdis(irv)=="TH"
      x=p(irv)*1/(2*pi);     %Fix this. It needs to be G variate
      crv(ir,irv)=Xmin(irv)+0.5*(Xmax(irv)-Xmin(irv))*(1+tanh(x));
    end
  end
end
%
%   Loop on realizations
%
for ir=1:nrmax
  % Apply cross-correlations
  % Evaluate Performance function for each realizations, ir
    M     = crv(ir,1);
    den   = crv(ir,2);
    Vs    = crv(ir,3);
    Tmax  = crv(ir,4);
    sstrn = crv(ir,5);
    alfa  = crv(ir,6);
    Hb    = crv(ir,7);
    pr    = crv(ir,8);
    R     = r(ir);
    ecc(ils,ir)=min(M/ptot(ir),0.9*R);
    EC=ecc(ils,ir);
    aeff(ils,ir)=2*(R^2*acos(min(1,EC/R))-EC*sqrt(R^2-EC^2));
    be=2*(R-EC);
    le=2*R*sqrt(1-(1-be/(2*R))^2);
    leff=sqrt(aeff(ils,ir)*le/be);
    beff=leff*be/le;
    g(ils,ir)=den*Vs^2*beff^3*(1+4*d(ir)/beff)*(1+0.7*d(ir)/Hb)* ...
      (1+beff/12/Hb)/(3*(1-pr)*(1+(sstrn*den*Vs^2/Tmax)^alfa))-Kstamin;
  for ib=1:nb
    for id=1:nd
      if (b(ir)==B(ib))&&(d(ir)==D(id))&&(g(ils,ir)<=0)
        nf(ils,ib,id)=nf(ils,ib,id)+1;
        for irv=1:nrv
          Xmuf(ils,ib,id,irv)=Xmuf(ils,ib,id,irv)+crv(ir,irv);
        end
```

```
          end
        end
      end
    end
%
% Parameter ranking
%
    if nb*nd==1
      for ib=1:nb
        for id=1:nd
          for irv=1:nrv
            Xmuf(ils,ib,id,irv)=Xmuf(ils,ib,id,irv)/nf(ils,ib,id);
            Z(irv)=abs(Xmu(irv)-Xmuf(ils,ib,id,irv))/ ...
              (Xsig(irv)/sqrt(nf(ils,ib,id)));
          end
          [ZS,IS]=sort(Z);
          NZS=ZS/norm(Z);
          for irv=1:nrv;RVS(irv)=RV(IS(irv));end
        end
      end
      RVS
      NZS
    end

%% Drained bearing capacity limit state
   elseif LS(ils)=="DBC"
    %
    % Random Variables
    %
    RV =   ["Momt"  "Horz"  "eDen"  "ePhi"          "eCoh"];
    Xdis = [  "LN"    "LN"    "NR"    "LN"            "LN"];
    Xmu  = [  5.0e7  6.6e5  17500.    25.0*pi/180.  5.0e4];
    Xcov = [   0.25   0.25    0.10    0.45           0.30];
    Xmin = [    0.0    0.0     0.0     0.0            0.0];
    Xmax = [    0.0    0.0     0.0     0.0            0.0];
    % Size arrays
    nrv=length(RV);L=zeros(nrv,nrv);cmut=zeros(nrv,nrv);cm=zeros(nrv,nrv);
    Z=zeros(nrv,1);RVS=strings(nrv,1);Xsig=zeros(nrv,1);p=zeros(nrv);
    q=zeros(nrv);
    %
    fprintf(fileID,'\r\n %-45s\r\n','Drained Bearing Capacity Limit State:');
    fprintf(fileID,'%-12s %s\r\n','Variable',sprintf(' %8s  ', RV));
    fprintf(fileID,'%-12s %s\r\n','Distribution',sprintf(' %8s  ', Xdis));
    fprintf(fileID,'%-12s %s\r\n','Mean Value',sprintf(' %5.2e  ', Xmu));
    fprintf(fileID,'%-12s %s\r\n','COV',sprintf(' %8.2f  ', Xcov));
    fprintf(fileID,'\r\n');

    % Parameters of underlying normal PDF's
    for irv=1:nrv
     Xsig(irv)=Xmu(irv)*Xcov(irv);
     if Xdis(irv)=="LN"
       q(irv)=sqrt(log(1+Xcov(irv)^2));
       p(irv)=log(Xmu(irv))-0.5*q(irv)^2;
     elseif Xdis(irv)=="TH"
       p(irv)=2.*pi/(0.46^2*(Xmax(irv)-Xmin(irv)^2-Xsig(irv)^2))^0.5;
       q(irv)=0;
     end
    end
    % Static stiffness values at the means
    M    = Xmu(1);
    H    = Xmu(2);
    eDen = Xmu(3);
    ePhi = Xmu(4);
```

```
    eCoh = Xmu(5);
    for ib=1:nb
      for id=1:nd
        R=0.5*B(ib);
        ec=M/Ptot(ib,id);
        Aeff=2*(R^2*acos(min(1,ec/R))-ec*sqrt(R^2-ec^2));
        be=2*(R-ec);
        le=2*R*sqrt(1-(1-be/(2*R))^2);
        leff=sqrt(Aeff*le/be);
        beff=leff*be/le;
        nq=exp(pi*tan(ePhi))*(1+sin(ePhi))/(1-sin(ePhi));
        nc=(nq-1)*cot(ePhi);
        ng=1.5*(nq-1)*tan(ePhi);
        sc=1+0.2*beff/leff;
        dc=1+0.4*D(id)/beff;
        ic=(1-H/(Ptot(ib,id)+Aeff*eCoh*cot(ePhi)))^2;
        sq=1+0.2*beff/leff;
        dq=1+1.2*(D(id)/beff)*tan(ePhi)*(1.-sin(ePhi))^2;
        iq=ic;
        sg=1-0.4*beff/leff;
        dg=1.0;
        ig=ic^2;
        eg(ils,ib,id)=eCoh*nc*sc*dc*ic+eDen*D(id)*nq*sq*dq*iq+ ...
          0.5*eDen*beff*ng*sg*dg*ig-Ptot(ib,id)/Aeff;
      end
    end
%    eg(ils,:,:)
    %
    % Define cross-correlation matrix [nrv x nrv]
    icopt="No";
    % For simplicity, enter upper triangular only
    % Ignore the cross correlation matrix if icopt="No"
    cmut=[1.0 0.0 0.0 0.0 0.0;
          0.0 1.0 0.0 0.0 0.0;
          0.0 0.0 1.0 0.0 0.0;
          0.0 0.0 0.0 1.0 0.0;
          0.0 0.0 0.0 0.0 1.0];
    cm=cmut+transpose(cmut)-eye(nrv);
    L = chol(cm,'lower');

    % Generate standard normal variable values & apply cross-correlation
    % (if applicable) & scale back up to appropriate PDF
    crvsn=zeros(nrmax,nrv);crv=zeros(nrmax,nrv);
    rvsn=normrnd(0,1,nrmax,nrv);
    for ir=1:nrmax
      if icopt=="Yes"
        crvsn(ir,:)=transpose(rvsn(ir,:)*transpose(L));
      else
        crvsn(ir,:)=rvsn(ir,:);
      end
      % Scale back up to appropriate PDF
      for irv=1:nrv
        if Xdis(irv)=="NR"
          crv(ir,irv)=Xsig(irv)*crvsn(ir,irv)+Xmu(irv);
        elseif Xdis(irv)=="LN"
          crv(ir,irv)=exp(q(irv)*crvsn(ir,irv)+p(irv));
        elseif Xdis(irv)=="TH"
          x=p(irv)*1/(2*pi);     %Fix this. It needs to be G variate
          crv(ir,irv)=Xmin(irv)+0.5*(Xmax(irv)-Xmin(irv))*(1+tanh(x));
        end
      end
    end
%
```

```
%   Loop on realizations
%
    for ir=1:nrmax
      % Apply cross-correlations
      % Evaluate Performance function for each realizations, ir
      M    = crv(ir,1);
      H    = crv(ir,2);
      eDen = crv(ir,3);
      ePhi = crv(ir,4);
      eCoh = crv(ir,5);
      R=r(ir);
      ecc(ils,ir)=min(M/ptot(ir),0.9*R);
      EC=ecc(ils,ir);
      aeff(ils,ir)=2*(R^2*acos(min(1,EC/R))-EC*sqrt(max(0,R^2-EC^2)));
      be=2*(R-EC);
      le=2*R*sqrt(1-(1-be/(2*R))^2);
      leff=sqrt(aeff(ils,ir)*le/be);
      beff=leff*be/le;

      nq=exp(pi*tan(ePhi))*(1+sin(ePhi))/(1-sin(ePhi));
      nc=(nq-1)*cot(ePhi);
      ng=1.5*(nq-1)*tan(ePhi);
      sc=1+0.2*beff/leff;
      dc=1+0.4*D(id)/beff;
      ic=(1-H/(ptot(ir)+aeff(ils,ir)*eCoh*cot(ePhi)))^2;
      sq=1+0.2*beff/leff;
      dq=1+1.2*(d(ir)/beff)*tan(ePhi)*(1.-sin(ePhi))^2;
      iq=ic;
      sg=1-0.4*beff/leff;
      dg=1.0;
      ig=ic^2;
      g(ils,ir)=eCoh*nc*sc*dc*ic+eDen*d(ir)*nq*sq*dq*iq+ ...
          0.5*eDen*beff*ng*sg*dg*ig-ptot(ir)/aeff(ils,ir);

      for ib=1:nb
        for id=1:nd
          if (b(ir)==B(ib))&&(d(ir)==D(id))&&(g(ils,ir)<=0)
            nf(ils,ib,id)=nf(ils,ib,id)+1;
            for irv=1:nrv
              Xmuf(ils,ib,id,irv)=Xmuf(ils,ib,id,irv)+crv(ir,irv);
            end
          end
        end
      end
    end
%
% Parameter ranking
%
    if nb*nd==1
      for ib=1:nb
        for id=1:nd
          for irv=1:nrv
            Xmuf(ils,ib,id,irv)=Xmuf(ils,ib,id,irv)/nf(ils,ib,id);
            Z(irv)=abs(Xmu(irv)-Xmuf(ils,ib,id,irv))/ ...
              (Xsig(irv)/sqrt(nf(ils,ib,id)));
          end
          [ZS,IS]=sort(Z);
          NZS=ZS/norm(Z);
          for irv=1:nrv;RVS(irv)=RV(IS(irv));end
        end
      end
      RVS
      NZS
```

```
    end
%
%% Undrained bearing capacity limit state
   elseif LS(ils)=="UBC"
    %
    % Random Variables
    %
    RV   = ["Momt"  "Horz"  "  Su"  "tDen"];
    Xdis = [  "LN"    "LN"    "LN"    "NR"];
    Xmu  = [  5.0e7  6.6e5   1.0e5 17500.0];
    Xcov = [   0.25   0.25    0.40    0.10];
    Xmin = [    0.0    0.0     0.0     0.0];
    Xmax = [    0.0    0.0     0.0     0.0];
    % Size arrays
    nrv=length(RV);L=zeros(nrv,nrv);cmut=zeros(nrv,nrv);cm=zeros(nrv,nrv);
    Z=zeros(nrv,1);RVS=strings(nrv,1);Xsig=zeros(nrv,1);p=zeros(nrv);
    q=zeros(nrv);
    %
    fprintf(fileID,'\r\n %-45s\r\n','Undrained Bearing Capacity Limit State:');
    fprintf(fileID,'%-12s %s\r\n','Variable',sprintf(' %8s  ', RV));
    fprintf(fileID,'%-12s %s\r\n','Distribution',sprintf(' %8s  ', Xdis));
    fprintf(fileID,'%-12s %s\r\n','Mean Value',sprintf(' %5.2e  ', Xmu));
    fprintf(fileID,'%-12s %s\r\n','COV',sprintf(' %8.2f  ', Xcov));
    fprintf(fileID,'\r\n');
    % Parameters of underlying normal PDF's
    for irv=1:nrv
     Xsig(irv)=Xmu(irv)*Xcov(irv);
     if Xdis(irv)=="LN"
       q(irv)=sqrt(log(1+Xcov(irv)^2));
       p(irv)=log(Xmu(irv))-0.5*q(irv)^2;
     elseif Xdis(irv)=="TH"
       p(irv)=2.*pi/(0.46^2*(Xmax(irv)-Xmin(irv)^2-Xsig(irv)^2))^0.5;
       q(irv)=0;
     end
    end
    % Static stiffness values at the means
    M    = Xmu(1);
    H    = Xmu(2);
    Su   = Xmu(3);
    tDen = Xmu(4);
    for ib=1:nb
      for id=1:nd
        R=0.5*B(ib);
        ec=M/Ptot(ib,id);
        Aeff=2*(R^2*acos(min(1,ec/R))-ec*sqrt(max(0,R^2-ec^2)));
        be=2*(R-ec);
        le=2*R*sqrt(1-(1-be/(2*R))^2);
        leff=sqrt(Aeff*le/be);
        beff=leff*be/le;
        nc0=5.14;
        sc0=1+0.2*beff/leff;
        ic0=0.5+0.5*sqrt(max(0,1-H/(Aeff*Su)));
        eg(ils,ib,id)=Su*nc0*sc0*ic0+tDen*D(id)-Ptot(ib,id)/Aeff;
      end
    end
%    eg(ils,:,:)
    %
    % Define cross-correlation matrix [nrv x nrv]
    icopt="No";
    % For simplicity, enter upper triangular only
    % Ignore the cross correlation matrix if icopt="No"
    cmut=[1.0 0.0 0.0 0.0;
          0.0 1.0 0.0 0.0;
```

```
      0.0 0.0 1.0 0.0;
      0.0 0.0 0.0 1.0];
  cm=cmut+transpose(cmut)-eye(nrv);
  L = chol(cm,'lower');

  % Generate standard normal variable values & apply cross-correlation
  % (if applicable) & scale back up to appropriate PDF
  crvsn=zeros(nrmax,nrv);crv=zeros(nrmax,nrv);
  rvsn=normrnd(0,1,nrmax,nrv);
  for ir=1:nrmax
    if icopt=="Yes"
      crvsn(ir,:)=transpose(rvsn(ir,:)*transpose(L));
    else
      crvsn(ir,:)=rvsn(ir,:);
    end
    % Scale back up to appropriate PDF
    for irv=1:nrv
      if Xdis(irv)=="NR"
        crv(ir,irv)=Xsig(irv)*crvsn(ir,irv)+Xmu(irv);
      elseif Xdis(irv)=="LN"
        crv(ir,irv)=exp(q(irv)*crvsn(ir,irv)+p(irv));
      elseif Xdis(irv)=="TH"
        x=p(irv)*1/(2*pi);     %Fix this. It needs to be G variate
        crv(ir,irv)=Xmin(irv)+0.5*(Xmax(irv)-Xmin(irv))*(1+tanh(x));
      end
    end
  end
%
%   Loop on realizations
%
  for ir=1:nrmax
    % Apply cross-correlations
    % Evaluate Performance function for each realizations, ir
    M    = crv(ir,1);
    H    = crv(ir,2);
    Su   = crv(ir,3);
    tDen = crv(ir,4);
    R=r(ir);
    ecc(ils,ir)=min(M/ptot(ir),0.8*R);
    EC=ecc(ils,ir);
    aeff(ils,ir)=2*(R^2*acos(min(1,EC/R))-EC*sqrt(max(0,R^2-EC^2)));
    be=2*(R-EC);
    le=2*R*sqrt(1-(1-be/(2*R))^2);
    leff=sqrt(aeff(ils,ir)*le/be);
    beff=leff*be/le;
    nc0=5.14;
    sc0=1+0.2*beff/leff;
    ic0=0.5+0.5*sqrt(max(0,1-H/(aeff(ils,ir)*Su)));
    g(ils,ir)=Su*nc0*sc0*ic0+tDen*d(ir)-ptot(ir)/aeff(ils,ir);

    for ib=1:nb
      for id=1:nd
        if (b(ir)==B(ib))&&(d(ir)==D(id))&&(g(ils,ir)<=0)
          nf(ils,ib,id)=nf(ils,ib,id)+1;
          for irv=1:nrv
            Xmuf(ils,ib,id,irv)=Xmuf(ils,ib,id,irv)+crv(ir,irv);
          end
        end
      end
    end
  end
%
% Parameter ranking
```

```
%
    if nb*nd==1
      for ib=1:nb
        for id=1:nd
          for irv=1:nrv
            Xmuf(ils,ib,id,irv)=Xmuf(ils,ib,id,irv)/nf(ils,ib,id);
            Z(irv)=abs(Xmu(irv)-Xmuf(ils,ib,id,irv))/(Xsig(irv)/ ...
              sqrt(nf(ils,ib,id)));
          end
          [ZS,IS]=sort(Z);
          NZS=ZS/norm(Z);
          for irv=1:nrv;RVS(irv)=RV(IS(irv));end
        end
      end
      RVS
      NZS
    end
   else
    status="Not supposed to be here"
   end
end
for ils=1:nls
  for ib=1:nb
    for id=1:nd
      pf(ils,ib,id)=nf(ils,ib,id)*nb*nd/nrmax;
        if pf(ils,ib,id)>0.006
          ri(ils,ib,id)=log(1.2/pf(ils,ib,id))/2.06;
        elseif (pf(ils,ib,id)<=0.006)&&(pf(ils,ib,id)>=10^-6)
          ri(ils,ib,id)=log(196/pf(ils,ib,id))/4.0;
        else
          ri(ils,ib,id)=log(1000000/pf(ils,ib,id))/5.8;
        end
      if LT(ils)==1
        if ri(ils,ib,id)<=btsls
          YN(ils,ib,id)="N";
        else
          YN(ils,ib,id)="Y";
        end
      else
        if ri(ils,ib,id)<=btuls
          YN(ils,ib,id)="N";
        else
          YN(ils,ib,id)="Y";
        end
      end
    end
  end
end
nf
pf
ri
YN
for ils=1:nls
%  Voptls(ils)=max(Vf,[],'all');
  Voptls(ils)=max(max(Vf));
  bols(ils)=B(nb);
  dols(ils)=D(nd);
  for ib=nb:-1:1
    for id=nd:-1:1
      if (YN(ils,ib,id)=="Y")&&(Vf(ib,id)<Voptls(ils))
        Voptls(ils)=Vf(ib,id);
        bols(ils)=B(ib);
        dols(ils)=D(id);
```

```
      end
    end
  end
end
Vopt=min(Voptls);
for ils=1:nls
  if Voptls(ils)>Vopt
    Vopt=Voptls(ils);
    bo=bols(ils);
    do=dols(ils);
  end
end
%Voptls
%bols
%dols
Vopt
bo
do

%hold off
%for ils=1:nls
%  figure('name', 'Histogram g');
%  daspect auto
%  histogram(g(ils,:))
%end
fprintf(fileID,'\r\n %-22s\r\n\r\n','Probabilities of Failure');
fprintf(fileID,'%12s %6s %s\r\n\r\n',' Limit State',' Depth', ...
  sprintf('%7.2f ', B));
for ils=1:nls
  for id=1:nd
    fprintf(fileID,'%12s %6.2f %s\r\n',LS(ils),D(id), ...
      sprintf('%6.1e ',pf(ils,:,id)));
  end
  fprintf(fileID,'\r\n');
end
fprintf(fileID,'\r\n %-22s\r\n\r\n','Reliability Indices');
fprintf(fileID,'%12s %6s %s\r\n\r\n',' Limit State',' Depth', ...
  sprintf('%6.2f ', B));
for ils=1:nls
  for id=1:nd
    fprintf(fileID,'%12s %6.2f %s\r\n',LS(ils),D(id), ...
      sprintf('%6.2f ',ri(ils,:,id)));
  end
  fprintf(fileID,'\r\n');
end
fprintf(fileID,'\r\n %-22s\r\n\r\n','Acceptable/Unacceptable (Y/N) Analysis');
fprintf(fileID,'%12s %6s %s\r\n\r\n',' Limit State',' Depth', ...
  sprintf('%6.2f ', B));
for ils=1:nls
  for id=1:nd
    fprintf(fileID,'%12s %6.2f %s\r\n',LS(ils),D(id), ...
      sprintf('%6s ',YN(ils,:,id)));
  end
  fprintf(fileID,'\r\n');
end
fprintf(fileID,'\r\n %-22s\r\n\r\n','Optimal Design:');
fprintf(fileID,'%-25s %6.2f\r\n','Foundation diameter....:',bo);
fprintf(fileID,'%-25s %6.2f\r\n','Foundation depth.......:',do);
fprintf(fileID,'%-25s %6.2f\r\n','Foundation volume......:',Vopt);
fclose(fileID);
```

B.2.2 Output

```
~~~~~~~~~~~~~~~~~~~~~~~~~~~~~~~~~~~~~~~~~~~~~~~~~~~~~~~~~~~~~~~~~~~~~~~~~~~~
----------------------- Details of dRBD Run Results ========--------------
~~~~~~~~~~~~~~~~~~~~~~~~~~~~~~~~~~~~~~~~~~~~~~~~~~~~~~~~~~~~~~~~~~~~~~~~~~~~


This output file contains details of the d-RBD run and its results.
All input is embedded into the MATLAB program and is echoed here for
record, verification and documentation.
All quantities are in consistent units: kg, m, s, N, Pa, J

Design case title.....................: High Variability Case
Target reliabilty index for SLS.......:    1.70
Target probability of failure for SLS..:  0.0362
Target reliabilty index for ULS.......:    3.30
Target probability of failure for ULS..: 0.00036
Foundation diameters..................:  15.0  16.0  17.0  18.0  19.0  20.0
Foundation depths.....................:   2.8   2.9   3.0   3.1
Number of realizations all combinations: 2939695
Number of design decision combinations.:      24
Number of realizations per combination.:  122487

 Fixed quantities & Foundation Dimensions:
Pedestal diameter.................:     5.40
Base top diameter.................:     5.40
Pedestal stick-up.................:     0.15
Base middle thickness.............:     2.20
Base edge thickness...............:     0.40
Concrete unit weight..............:  23500.0
Backfill soil unit weight.........:  17000.0
Self weight of WTG................: 2.28e+06

 Foundation Volumes for all B-D Combinations:

        Foundation Diameter
 Depth   15.00   16.00   17.00   18.00   19.00   20.00

  2.80  245.80  272.69  301.16  331.19  362.80  395.97
  2.90  248.09  274.99  303.45  333.48  365.09  398.26
  3.00  250.38  277.28  305.74  335.77  367.38  400.55
  3.10  252.67  279.57  308.03  338.06  369.67  402.84


 Tilt Limit State:
Maximum allowed tilt (degrees)...:     0.17

 Variable          Mmnt       Dens       prat         Vs       sstn       tmax      alpha
Itha
Distribution        LN         NR         NR         LN         LN         LN         LN
LN
Mean Value    2.00e+07   1.75e+03   3.50e-01   2.00e+02   5.00e-04   1.00e+05   9.00e-
01   4.16e+00
COV               0.25       0.10       0.10       0.60       0.30       0.50       0.20
0.10


 Dynamic Stiffness Limit State:
Minimum required stiffness.........: 5.00e+10

 Variable          Dens       Prat         Vs       Hbed
Distribution        NR         NR         LN         LN
```

```
Mean Value    1.75e+03   3.50e-01   2.00e+02   8.50e+00
COV               0.10       0.10       0.60       0.30

 Static Stiffness Limit State:
Minimum required stiffness.........: 1.00e+10

 Variable          Momt       Dens         Vs       Tmax       sstn       Alfa       Hbed
Prat
Distribution        LN         NR         LN         LN         LN         NR         LN
NR
Mean Value    5.00e+07   1.75e+03   2.00e+02   1.00e+05   5.00e-04   9.00e-01   8.50e+00
3.50e-01
COV               0.25       0.10       0.60       0.50       0.30       0.20       0.30
0.10

 Drained Bearing Capacity Limit State:
Variable          Momt       Horz       eDen       ePhi       eCoh
Distribution        LN         LN         NR         LN         LN
Mean Value    5.00e+07   6.60e+05   1.75e+04   4.36e-01   5.00e+04
COV               0.25       0.25       0.10       0.45       0.30


 Undrained Bearing Capacity Limit State:
Variable          Momt       Horz         Su       tDen
Distribution        LN         LN         LN         NR
Mean Value    5.00e+07   6.60e+05   1.00e+05   1.75e+04
COV               0.25       0.25       0.40       0.10


 Probabilities of Failure

 Limit State  Depth   15.00   16.00   17.00   18.00   19.00   20.00

         TLT   2.80 5.4e-03 2.9e-03 1.7e-03 1.1e-03 6.8e-04 3.4e-04
         TLT   2.90 5.0e-03 3.0e-03 1.7e-03 1.2e-03 6.6e-04 4.1e-04
         TLT   3.00 5.2e-03 3.1e-03 1.7e-03 1.1e-03 6.4e-04 5.5e-04
         TLT   3.10 5.2e-03 2.8e-03 1.7e-03 1.1e-03 6.6e-04 3.6e-04

         DYS   2.80 8.9e-02 6.7e-02 4.9e-02 3.7e-02 2.8e-02 2.0e-02
         DYS   2.90 8.6e-02 6.4e-02 4.8e-02 3.6e-02 2.7e-02 2.0e-02
         DYS   3.00 8.4e-02 6.2e-02 4.6e-02 3.3e-02 2.6e-02 1.9e-02
         DYS   3.10 8.1e-02 6.0e-02 4.5e-02 3.4e-02 2.4e-02 1.8e-02

         STS   2.80 3.9e-01 2.1e-01 1.0e-01 4.6e-02 2.2e-02 1.1e-02
         STS   2.90 3.6e-01 1.8e-01 8.7e-02 4.0e-02 2.0e-02 9.4e-03
         STS   3.00 3.3e-01 1.6e-01 7.5e-02 3.5e-02 1.7e-02 8.3e-03
         STS   3.10 3.0e-01 1.5e-01 6.6e-02 3.2e-02 1.4e-02 7.6e-03

         DBC   2.80 1.0e-02 1.8e-03 2.1e-04 2.4e-05 4.1e-05 1.6e-05
         DBC   2.90 8.3e-03 1.4e-03 1.8e-04 1.6e-05 8.2e-06 8.2e-06
         DBC   3.00 6.5e-03 1.2e-03 1.6e-04 2.4e-05 3.3e-05 1.6e-05
         DBC   3.10 5.3e-03 6.9e-04 6.5e-05 2.4e-05 8.2e-06 0.0e+00

         UBC   2.80 7.3e-02 1.8e-02 3.2e-03 4.4e-04 9.0e-05 0.0e+00
         UBC   2.90 6.5e-02 1.4e-02 2.5e-03 3.0e-04 4.9e-05 0.0e+00
         UBC   3.00 5.5e-02 1.2e-02 2.2e-03 2.2e-04 4.9e-05 0.0e+00
         UBC   3.10 4.7e-02 1.0e-02 1.6e-03 1.6e-04 2.4e-05 0.0e+00


 Reliability Indices

 Limit State  Depth  15.00  16.00  17.00  18.00  19.00  20.00
```

TLT	2.80	2.62	2.78	2.91	3.03	3.14	3.31
TLT	2.90	2.65	2.77	2.91	3.00	3.15	3.27
TLT	3.00	2.64	2.76	2.91	3.03	3.16	3.20
TLT	3.10	2.63	2.79	2.91	3.02	3.15	3.30
DYS	2.80	1.26	1.40	1.55	1.69	1.83	1.99
DYS	2.90	1.28	1.43	1.56	1.70	1.85	2.00
DYS	3.00	1.29	1.44	1.58	1.75	1.87	2.02
DYS	3.10	1.31	1.46	1.60	1.73	1.90	2.04
STS	2.80	0.54	0.86	1.21	1.58	1.95	2.29
STS	2.90	0.59	0.91	1.27	1.65	2.00	2.36
STS	3.00	0.63	0.97	1.35	1.72	2.08	2.41
STS	3.10	0.68	1.02	1.41	1.77	2.16	2.45
DBC	2.80	2.31	2.90	3.43	3.97	3.85	4.08
DBC	2.90	2.41	2.96	3.48	4.08	4.25	4.25
DBC	3.00	2.53	3.00	3.51	3.97	3.90	4.08
DBC	3.10	2.63	3.14	3.73	3.97	4.25	Inf
UBC	2.80	1.36	2.04	2.75	3.25	3.65	Inf
UBC	2.90	1.42	2.15	2.81	3.35	3.80	Inf
UBC	3.00	1.49	2.22	2.85	3.42	3.80	Inf
UBC	3.10	1.57	2.32	2.93	3.51	3.97	Inf

Acceptable/Unacceptable (Y/N) Analysis

Limit State	Depth	15.00	16.00	17.00	18.00	19.00	20.00
TLT	2.80	Y	Y	Y	Y	Y	Y
TLT	2.90	Y	Y	Y	Y	Y	Y
TLT	3.00	Y	Y	Y	Y	Y	Y
TLT	3.10	Y	Y	Y	Y	Y	Y
DYS	2.80	N	N	N	N	Y	Y
DYS	2.90	N	N	N	N	Y	Y
DYS	3.00	N	N	N	Y	Y	Y
DYS	3.10	N	N	N	Y	Y	Y
STS	2.80	N	N	N	N	Y	Y
STS	2.90	N	N	N	N	Y	Y
STS	3.00	N	N	N	Y	Y	Y
STS	3.10	N	N	N	Y	Y	Y
DBC	2.80	N	N	Y	Y	Y	Y
DBC	2.90	N	N	Y	Y	Y	Y
DBC	3.00	N	N	Y	Y	Y	Y
DBC	3.10	N	N	Y	Y	Y	Y
UBC	2.80	N	N	N	N	Y	Y
UBC	2.90	N	N	N	Y	Y	Y
UBC	3.00	N	N	N	Y	Y	Y
UBC	3.10	N	N	N	Y	Y	Y

Optimal Design:

Foundation diameter....: 18.00
Foundation depth.....: 3.00
Foundation volume.....: 335.77

APPENDIX C

SUPPLEMENTAL ELECTRONIC FILES

This appendix lists electronic files used in this dissertation and provided in source format. MATLAB is needed to run the MATLAB files. MathCAD 15 is needed to run the MathCAD file.

File Name	Description
dRBD_GBF_MV.m	Gravity-base foundation source MATLAB d-RBD program for the medium variability case.
dRBD_MV.txt	Output file for the medium variability case.
dRBD_GBF_HV.m	Gravity-base foundation source MATLAB d-RBD program for the high variability case.
dRBD_HV.txt	Output file for the high variability case.
Appendix A - Deterministic Computations.xmcd	MathCAD file containing deterministic computations for the limit states considered in this dissertation.